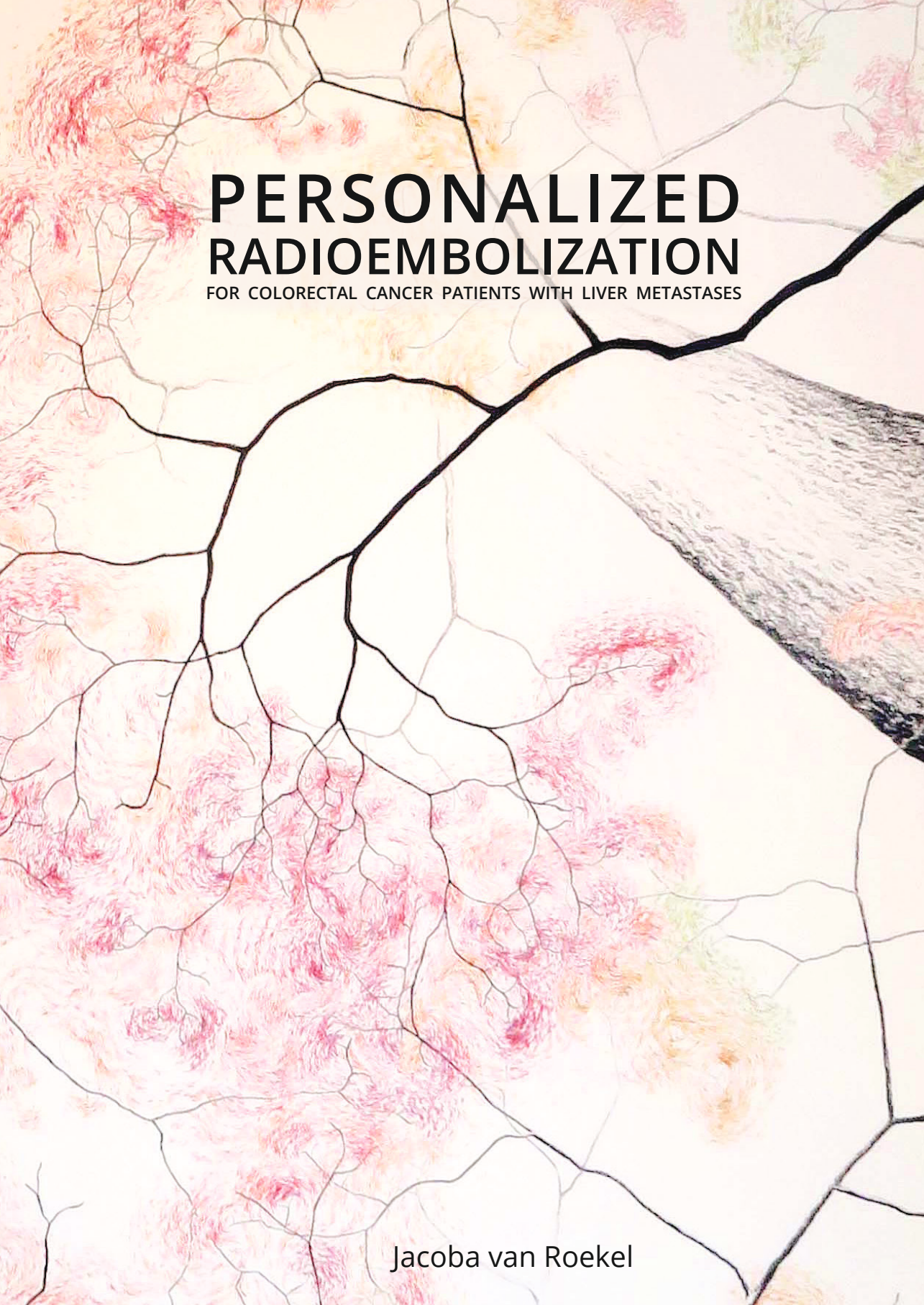

PERSONALIZED RADIOEMBOLIZATION

FOR COLORECTAL CANCER PATIENTS WITH LIVER METASTASES

Jacoba van Roekel

Personalized radioembolization for colorectal cancer patients with liver metastases

Jacoba van Roekel

Colofon

Personalized radioembolization for colorectal cancer patients with liver metastases
PhD thesis, Utrecht University, The Netherlands

ISBN: 978-90-393-7341-5

Cover: De afbeelding op de voorzijde is gemaakt door Sigrid Nora van der Mersch, waarvoor veel dank!
Layout: Lara Leijtens, persoonlijkproefschrift.nl
Printing: Ridderprint, www.ridderprint.nl

Publication of this thesis was financially supported by:
Quirem Medical B.V.
Chipsoft
RMG B.V.
Nederlandse Vereniging voor Interventieradiologie

Personalized radioembolization for colorectal cancer patients with liver metastases

Gepersonaliseerde behandeling met radioembolisatie voor patiënten met levermetastasen van colorectaalcarcinoom
(met een samenvatting in het Nederlands)

Proefschrift

ter verkrijging van de graad van doctor aan de
Universiteit Utrecht
op gezag van de
rector magnificus, prof.dr. H.R.B.M. Kummeling,
ingevolge het besluit van het college voor promoties
in het openbaar te verdedigen op

dinsdag 24 november 2020 des middags te 12.45 uur

door

Jacoba van Roekel

geboren op 21 oktober 1990
te Tiel

Promotoren:

Prof. dr. M.G.E.H. Lam
Prof. dr. M.A.A.J. van den Bosch

Copromotoren:

Dr. M.L.J. Smits
Dr. A.J.A.T. Braat

TABLE OF CONTENTS

General introduction

Although there are many treatment options for colorectal cancer patients with liver metastases, colorectal cancer still remains the second most common type of cancer death worldwide (1).

There is a wide variety in colorectal cancer incidence rates: the disease can be considered a marker of socioeconomic development and is more prevalent in countries with a high human development index. In developing countries, such as Russia and China, there is an increase in both incidence and mortality. In long-term developed countries, such as the United Kingdom and Denmark, there is an increase in incidence but a decrease in mortality. In other countries, such as France and the United States, a decrease in both incidence and mortality is seen. The rises in incidence can be explained by a change in dietary patterns (processed meat and alcohol drinks) and lifestyle factors (a sedentary lifestyle), as well as a consequence of screening programs that lead to early detection. The decreases in mortality are due to improved treatment strategies in developed countries (1).

The incidence rate increases with age, with the median age worldwide being 66 years. Although the incidence and mortality rates decline for almost all age groups, in high-income countries, they are increasing for individuals younger than 50 years. This is likely due to the change in diet and lifestyle over the past decades, which is first reflected in incidence rates in young age groups. In this patient group, most patients present with advanced-stage disease. For patients with distant-stage disease, the five-year survival rate is only 14% (2). The first site of metastasis is the liver and up to 30% of patients with colorectal cancer develops hepatic metastases (3). For these patients, improved treatment strategies are needed.

One of these improved treatment strategies is radioembolization. Radioembolization is a treatment option for patients with primary or secondary liver tumors. The treatment principle consists of the delivery of millions of tiny radioactive microspheres that are injected into the hepatic vasculature via a microcatheter. As hepatic malignancies are fed mainly by arterial blood, the microspheres lodge in small tumor arterioles and selectively irradiate the tumors, while relatively sparing the healthy liver tissue. Treatment is always preceded by a preparatory angiography to map the vascular anatomy and to

assess the distribution of the treatment particles by means of the injection of a scout dose. Yttrium-90 (^{90}Y)-based microspheres are the most widely used particles in radioembolization, but in the UMC Utrecht, holmium-166 (^{166}Ho)-based microspheres were developed as an alternative. A detailed overview of radioembolization is provided in the next chapter of this thesis (Chapter 2).

Although radioembolization is a promising treatment strategy for colorectal cancer patients with liver metastases and does lead to improved survival rates (4), many patients still experience early progressive disease (5, 6). With a personalized treatment strategy, patient outcomes could be improved (7). The aim of this thesis was to investigate different aspects of ^{166}Ho-radioembolization that can be used to develop a tailored treatment approach for individual patients.

An individualized treatment approach is based on two major principles: selection and planning. Selection comes down to using patient characteristics determining who is a good candidate for treatment with radioembolization. An example of patient characteristics that may be used for selection is the location of the primary tumor: patients with a right-sided primary tumor generally have a much worse prognosis than patients with a left-sided primary tumor, and poorly respond to treatment with cetuximab (8). Similar patient characteristics are important for radioembolization as well. In patients with unfavorable prognostic characteristics , treatment with radioembolization may do more harm than good. As trivial as this may seem, these prognostic characteristics are not always accounted for in routine clinical practice. For example, the distribution of the scout dose can be used for patient selection: in case of an unfavorable activity distribution with a high parenchymal-absorbed dose and a low tumor-absorbed dose, it may be better to withhold patients from radioembolization.

Besides selection, the distribution of the scout dose can also be used in a very important aspect of treatment planning. After the right patients are selected, treatment may be optimized for each individual patient, based on scout dose distribution as a simulation of the treatment itself. The most important factor in treatment planning is personalized activity calculation: this should be done based on known thresholds for safety and efficacy (i.e. the maximum

tolerable dose on the parenchyma and the minimum tumor-absorbed dose required for response). This is of vital importance to obtain the best possible response for each patient while maintaining safety. The first aspect of ^{166}Ho-radioembolization that can be used to develop a tailored treatment approach that was investigated in this thesis was the quality of life after radioembolization (Chapter 3). Quality of life is especially important in patients of advanced age, with a shortened life expectancy. Therefore, the impact of treatment strategies on quality of life should be known before making a treatment decision.

The second aspect comprised of the logistics of radioembolization: should the preparatory angiography and the treatment procedure be performed on a single day, which could be beneficial for patients with highly progressive disease, or is it better to separate the preparatory angiography from the treatment procedure (Chapter 4)?

Also, the outcome after radioembolization was assessed. If the type of progression is known, which can be either based on growth of existing intra- or extrahepatic lesions, or on new intra- or extrahepatic lesions, this could possibly be linked to prognostic characteristics and be used for patient selection (Chapter 5).

A key assumption for treatment planning is the existence of a dose-response relationship. This was investigated first in a mixed-tumor type cohort (Chapter 6) and secondly in colorectal cancer patients only (Chapter 7). In this last group, the dose-toxicity relationship was also investigated. The results of these studies, specifically the obtained dose thresholds, will be used for future patients.

Finally, the impact of catheter-related techniques on treatment outcomes were assessed. First, the efficacy of coil-embolization to obtain intrahepatic redistribution was analyzed (Chapter 8). Secondly, the impact of an anti-reflux catheter on treatment outcomes was assessed in a prospective trial (Chapter 9). The hypothesis of the use of an anti-reflux catheter was that this may lead to a higher tumor- to non-tumor activity concentration ratio: (partial) obstruction of the vascular lumen induces a decreased downstream pressure, possibly leading to a better tumor targeting (9-14).

Altogether, these aspects could be used for a personalized treatment approach in radioembolization. In this respect, it is important to make a distinction between patient selection (selecting the right candidates for this type of treatment) and treatment planning (optimizing treatment outcomes for each individual patient).

REFERENCES

1. Bray F, Ferlay J, Soerjomataram I, Siegel RL, Torre LA, Jemal A. Global cancer statistics 2018: GLOBOCAN estimates of incidence and mortality worldwide for 36 cancers in 185 countries. CA Cancer J Clin. 2018;68(6):394-424.

2. Siegel RL, Miller KD, Goding Sauer A, Fedewa SA, Butterly LF, Anderson JC, et al. Colorectal cancer statistics, 2020. CA Cancer J Clin. 2020.

3. Engstrand J, Nilsson H, Stromberg C, Jonas E, Freedman J. Colorectal cancer liver metastases - a population-based study on incidence, management and survival. BMC Cancer. 2018;18(1):78.

4. Kennedy A, Cohn M, Coldwell DM, Drooz A, Ehrenwald E, Kaiser A, et al. Updated survival outcomes and analysis of long-term survivors from the MORE study on safety and efficacy of radioembolization in patients with unresectable colorectal cancer liver metastases. J Gastrointest Oncol. 2017;8(4):614-24.

5. Martin LK, Cucci A, Wei L, Rose J, Blazer M, Schmidt C, et al. Yttrium-90 radioembolization as salvage therapy for colorectal cancer with liver metastases. Clin Colorectal Cancer. 2012;11(3):195-9.

6. Bester L, Meteling B, Pocock N, Pavlakis N, Chua TC, Saxena A, et al. Radioembolization versus standard care of hepatic metastases: comparative retrospective cohort study of survival outcomes and adverse events in salvage patients. J Vasc Interv Radiol. 2012;23(1):96-105.

7. Salem R, Padia SA, Lam M, Bell J, Chiesa C, Fowers K, et al. Clinical and dosimetric considerations for Y90: recommendations from an international multidisciplinary working group. Eur J Nucl Med Mol Imaging. 2019;46(8):1695-704.

8. Wang Z, Wang X, Zhang Z, Wang X, Chen M, Lu L, et al. Association between Primary Tumor Location and Prognostic Survival in Synchronous Colorectal Liver Metastases after Surgical Treatment: A Retrospective Analysis of SEER Data. J Cancer. 2019;10(7):1593-600.

9. van den Hoven AF, Lam MG, Jernigan S, van den Bosch MA, Buckner GD. Innovation in catheter design for intra-arterial liver cancer treatments results in favorable particle-fluid dynamics. J Exp Clin Cancer Res. 2015;34:74.

10. van den Hoven AF, Prince JF, Samim M, Arepally A, Zonnenberg BA, Lam MG, et al. Posttreatment PET-CT-confirmed intrahepatic radioembolization performed without coil embolization, by using the antireflux Surefire Infusion System. CardioVasc Interv Radiol. 2014;37(2):523-8.

11. Rose SC, Kikolski SG, Chomas JE. Downstream hepatic arterial blood pressure changes caused by deployment of the surefire antireflux expandable tip. CardioVasc Interv Radiol. 2013;36(5):1262-9.

12. Rose SC, Narsinh KH, Newton IG. Quantification of Blood Pressure Changes in the Vascular Compartment When Using an Anti-Reflux Catheter during Chemoembolization versus Radioembolization: A Retrospective Case Series. J Vasc Interv Radiol. 2017;28(1):103-10.

13. Arepally A, Chomas J, Kraitchman D, Hong K. Quantification and reduction of reflux during embolotherapy using an antireflux catheter and tantalum microspheres: ex vivo analysis. J Vasc Interv Radiol. 2013;24(4):575-80.

14. Rose SC, Narsinh KH, Isaacson AJ, Fischman AM, Golzarian J. The Beauty and Bane of Pressure-Directed Embolotherapy: Hemodynamic Principles and Preliminary Clinical Evidence. Am J Rontg. 2019;212(3):686-95.

Radioembolization

Caren van Roekel, Arthur J.A.T. Braat, Maarten L.J. Smits, Rutger C.G. Bruijnen, Bart de Keizer, Marnix G.E.H. Lam

Clinical Nuclear Medicine 2020

ABSTRACT

Radioembolization is a therapy during which radioactive microspheres are injected into the hepatic artery. A microcatheter is placed in the hepatic arterial vasculature and millions of microspheres are administered. Hepatic malignancies are fed mainly by arterial blood and because of preferential arterial flow, the microspheres lodge in small tumor arterioles. There, they emit high-energy β-radiation to induce cell death. This way, the hepatic tumors are selectively irradiated and the healthy liver tissue is relatively spared.

The essential steps for radioembolization include [1] visceral angiography to map tumor-perfusing vessels, embolize collateral vessels and assess portal vein patency, [2] assessment of pulmonary and gastrointestinal shunts by intra-arterial administration of a scout dose, and [3] determination of the optimal therapeutic activity, e.g. dosimetry (1).

Key words: radioembolization, microspheres, hepatic tumors, yttrium-90, holmium-166, angiography, dosimetry

1. BASIC PRINCIPLES AND INDICATIONS

1.1. Radioembolization

Also known as Selective Internal Radiation Therapy (SIRT), radioembolization is a therapy during which radioactive microspheres are injected into the hepatic artery. A microcatheter is placed in the hepatic arterial vasculature and millions of microspheres are administered. Hepatic malignancies are fed mainly by arterial blood and because of preferential arterial flow, the microspheres lodge in small tumor arterioles. There, they emit high-energy β-radiation to induce cell death. In this way, the hepatic tumors are selectively irradiated and the healthy liver tissue is relatively spared, which is a great advantage over conventional external beam radiation therapy (EBRT) (2). Radioembolization is a fast developing field of expertise and therefore, in this chapter, we will confine ourselves to the basics.

The essential steps for radioembolization include [1] visceral angiography to map tumor-feeding vessels, embolize collateral vessels and assess portal vein patency, [2] assessment of pulmonary and gastrointestinal shunts by intra-arterial administration of a scout dose, and [3] determination of the optimal therapeutic activity, e.g. dosimetry (1).

1.2. Types of microspheres

Ideal properties of radiolabelled micro-particles for sufficient intra-arterial therapy are (3-5):

- The microspheres should be easily labelled and resistant to elution of the radioactive label, macrophage removal or radiolysis.
- Uniform microsphere size (i.e. greater than microcapillary diameter of around 8 micron and small enough to lodge as distal as possible) and density comparable to that of blood are necessary to prevent settling and ensure uniform distribution.
- For efficacy, the radionuclide label must be a high-energy β-emitter with sufficient range and an intermediate half-life of a few days.
- The microspheres should be visible by PET (positron emission), SPECT (γ-emission), CT (sufficient density), or MRI (paramagnetic properties), to assess distribution.

- The microspheres can be based on polymers, polymeric resins, albumin or inorganic materials.

Currently, three different types of radioactive microspheres are commercially available. The type of microspheres can be divided based on the embedded radioactive isotope (yttrium-90 (^{90}Y) or holmium-166 (^{166}Ho)) or microsphere material (resin, glass or poly-L-lactic acid).

1.2.1. ^{90}Y microspheres

^{90}Y is a pure (99.99%) β^--emitter that decays to stable zirconium-90 (^{90}Zr) with an average β-energy of 0.9 MeV and a half-life of 64.2 hours (6, 7). ^{90}Y can either be produced by neutron bombardment of stable yttrium-89 (^{89}Y) in a commercial reactor or by chemical separation from the parent isotope strontium-90 (^{90}Sr), a fission product of uranium (7). The mean tissue penetration is approximately 2.5 mm and the maximum range in tissue is 1.1 cm (8, 9). Imaging of ^{90}Y is possible by using either the bremsstrahlung for bremsstrahlung-single photon emission computed tomography/computed tomography (SPECT/CT) (10, 11) or the emitted positrons (32 positrons per 1 million decays) for positron emission tomography/computed tomography (PET/CT) imaging (6).

Two commercially available ^{90}Y-labelled microspheres are currently on the market:

- Glass microspheres (TheraSphere®, BTG international Medicine)
- Resin microspheres (SIR-Spheres®, SIRTEX Medical Limited)

1.2.1.1. TheraSphere®

^{90}Y is permanently embedded in the glass. Each glass sphere has a diameter of 20-30 µm. ^{89}Y yttriumoxide is stable incorporated. For labelling, the microspheres are irradiated with neutrons in a nuclear reactor (12). TheraSphere® has a high specific gravity and density (3.3 g/cm^3). A typical injected activity ranges from 3–5 million microspheres with a high specific activity of 2500 Bq/sphere. An extended shelf-life activity ranges from 5-10 million microspheres with a high specific activity of approximately 1250 Bq/sphere. The standard activity of TheraSphere® in water for injection is 5 GBq per patient; activities of 3 GBq up to 20 GBq are available.

1.2.1.2. SIR-Spheres®

^{90}Y is permanently embedded in an acrylic polymer resin (13). Each resin microsphere has a diameter of 20-60 μm. The microspheres are labelled with ^{90}Y via cation-exchange with sufficiently strong binding. ^{90}Y is a decay product of ^{90}Sr obtained from a generator. SIR-Spheres® have a low specific gravity and density (1.4 g/cm^3) and a specific activity of 50 Bq/sphere. A typical injected activity ranges from 40–80 million microspheres. The standard activity of SIR-Spheres® is 3 GBq per patient in 5 ml water for injection.

1.2.2. ^{166}Ho microspheres (QuiremSpheres®)

^{166}Ho is a high-energy beta-emitting isotope for therapeutic use and emits primary gamma photons. The maximum energy of the beta particles is 1.85 MeV (50.0%) and 1.77 MeV (48.7%) with a half-life of 26.8 hours. The maximum range of emissions of the beta particles in tissue is 9 mm (mean 3.2 mm). They were developed by the University Medical Center Utrecht (the Netherlands) and are commercialized under the name QuiremSpheres® (Quirem Medical, Diepenveen, the Netherlands).

Just like ^{90}Y microspheres, ^{166}Ho emits an electron to reach a stable state (beta radiation). Furthermore, it emits gamma photons (81 keV, 6%), which are useful for SPECT/CT imaging (14). ^{166}Ho is part of the metallic chemical elements known as lanthanides, which have paramagnetic properties, so magnetic resonance imaging (MRI) can also be used to image the distribution in the liver and quantify the dose in the tumors (15, 16).

^{166}Ho microspheres decay is faster due to a shorter half-life (26.8 vs 64.2 hour), but deposit less energy than ^{90}Y microspheres per decay (16 vs 49 J/GBq). This results in a higher administered activity to reach the same dose deposition. As a result, a higher dose rate is achieved.

Microspheres loaded with Ho are irradiated per patient-dose in one of the pre-determined neutron reactors with a suitable irradiation profile: the reactor must have a high neutron flux without being accompanied by extensive gamma heating, as this detriments the structural integrity of ^{166}Ho microspheres (17). In the current commercially available product, the specific activity is 450 Bq/sphere with a density of 1.4 g/mL.

1.3. Patient selection

Currently, radioembolization is mainly indicated in a palliative setting for unresectable, chemorefractory primary and secondary hepatic malignancies (2). Several studies investigate(d) the role of radioembolization combined with systemic therapy in the first and second line treatment of colorectal cancer liver metastases (18) (19).

Work-up for radioembolization includes clinical status, hematologic and biochemical status, anatomic assessment with CT/MR imaging and, when appropriate, molecular imaging with SPECT/CT or PET/CT. Indications and contraindications for radioembolization are listed in Table 1, according to Braat et al. (2). Since a higher age has no influence on prognosis, age is not a contraindication (20). In patients with hepatocellular carcinoma (HCC), radioembolization is reserved for patients with intermediate and early advanced disease stages (with Barcelona Clinic Liver Cancer [BCLC] stage B-C, liver-dominant disease, Eastern Cooperative Oncology Group [ECOG] status 1-2, and a portal vein tumor thrombus [PVT]). Patients with a Child-Pugh score >B7 and a main portal vein tumor thrombus tend to have a limited potential survival benefit after radioembolization, thus patient selection should be done carefully (2). It should be noted that, as clinical experience accumulates over the years, indications and contraindications may change over time.

2. WORKUP

2.1. Clinical investigations

During clinical investigation, a detailed medical history of the patient should be obtained. Previous treatments, current use of medication, chronic diseases, allergies and recent periods of acute illness should be recorded. Also, the performance status (as defined by the World Health Organization(WHO)/ECOG (21)) should be defined: 0 – asymptomatic, 1 – symptomatic but completely ambulatory, 2 – symptomatic and <50% of time in bed, 3 – symptomatic and >50% of time in bed but not bedbound, 4 – bedbound, 5 – dead. A performance status >2 is considered an exclusion criterion for radioembolization.

TABLE 1. Common indications and relative and absolute contraindications for radioembolization

Indication	Relative contraindication	Absolute contraindication
Disease not amenable to surgical resection, liver transplantation, or curative ablative strategies	Portal vein thrombosis of main branch (no contraindication in HCC)	Extensive and untreated portal hypertension
Disease not amenable to or refractory to chemotherapeutic alternatives, or patient not willing to receive these alternatives	Abnormalities of bile ducts or stents; exceptions: papillotomy and cholecystectomy	Life expectancy < 3 months
Compensated or early decompensated liver cirrhosis (Child-Pugh ≤B7)	Serum bilirubin >34.2 µmol/L (2 mg/dL)	Active hepatitis
Performance state (ECOG) ≤2	Leukocytes <2x10^9/L or platelet count <50x10^9/L	
Liver-only or liver-dominant disease	Glomerular filtration rate <35 mL/min	Uncorrectable gastrointestinal microsphere deposition; expected lung dose >30 Gy (or 50 Gy cumulative)
Preoperative indications, such as downstaging before surgery or the inducement of contralateral hypertrophy before surgery	INR (internationalized normalized ratio) >1.5	Active use of antiangiogenic agents (bevacizumab, aflibercept)
	Celiac axis and superior mesenteric artery occluded	Occluded intrahepatic arterial network
	Interval since last dose of systemic therapy < 4 weeks	

2.2. Laboratory investigations

The laboratory investigations are needed to assess hepatobiliary function (aspartate aminotransferase, alanine aminotransferase, alkaline phosphatase, gamma-glutamyl transferase, total bilirubin, lactate dehydrogenase and albumin), renal function (creatinine, estimated glomerular filtration ratio), hematological function (white cell count, hemoglobin and hematocrit) and coagulation status (internationalized normalized ratio, thrombin time, prothrombin time, activated partial thromboplastin time and platelet count).

2.3 Imaging

Before treatment, it is essential to perform cross-sectional imaging of the patient, to identify all sites of (metastatic) disease and to assess the vascular anatomy. For this purpose, various imaging modalities can be used.

2.3.1. Liver CT/MRI and ^{18}F-FDG-PET

In general, three-phase CT images are made: late arterial phase for the detection of hypervascular tumors, a portal venous phase for the detection of hypovascular tumors and a late venous phase for the detection of wash-out (22). An early arterial phase may be preferable for vascular evaluation in the work-up for radioembolization. Compared to the late arterial phase, the contrast-to-noise ratio of the hepatic artery relative to the portal vein is higher in this early arterial phase (23).

MRI is superior to CT in terms of soft tissue contrast, but inferior regarding the detection of small arteries, due to the higher resolution of CT. Dynamic contrast-enhanced sequences can be used to assess tumor hypervascularity and washout in a large number of phases. Diffusion weighted and T2-weighted imaging provide options for high sensitivity tumor detection.

The added value of ^{18}F-FDG-PET-imaging in the workup for radioembolization is widely accepted. The most important benefit in the workup is the visualization of extrahepatic disease. The study of Rosenbaum et al. have found a change of management in 17% of patients with metastatic colorectal carcinoma, based on imaging with ^{18}F-FDG-PET (24). Metastases from uveal melanoma, breast cancer, colorectal carcinoma are generally FDG-avid. HCC, however, accumulates FDG to varying degrees, limiting the sensitivity of PET for primary tumors (25). Despite this lower sensitivity, the studies of Nagaoka et al. and Cho et al. show that ^{18}F-FDG-PET does have a role in initial staging of hepatocellular carcinoma (26, 27). Well-differentiated HCC lesions show very little uptake on ^{18}F-FDG-PET imaging, whereas poorly differentiated HCCs show much more uptake. Park et al. have reported that patients with ^{18}F-FDG-positive tumors have lower survival compared to patients with ^{18}F-FDG-negative tumors (28). Thus, ^{18}F-FDG-PET may be useful for characterization of cancer biology(29).

Over 90% of gastroenteropancreatic neuroendocrine tumors have high concentrations of somatostatin receptors. A 68-gallium-labelled somatostanin

receptor analog (i.e. DOTATATE/DOTATOC/DOTANOC) PET/CT is the most sensitive imaging modality to detect neuroendocrine tumors and metastases (30, 31).

2.3.2. Vascular anatomy

The functional anatomy of the liver is based on the branching pattern of the portal vein. According to the Couinaud model of segmental anatomy, eight liver segments can be distinguished with a distinct vascularization and biliary drainage (Figure 1).

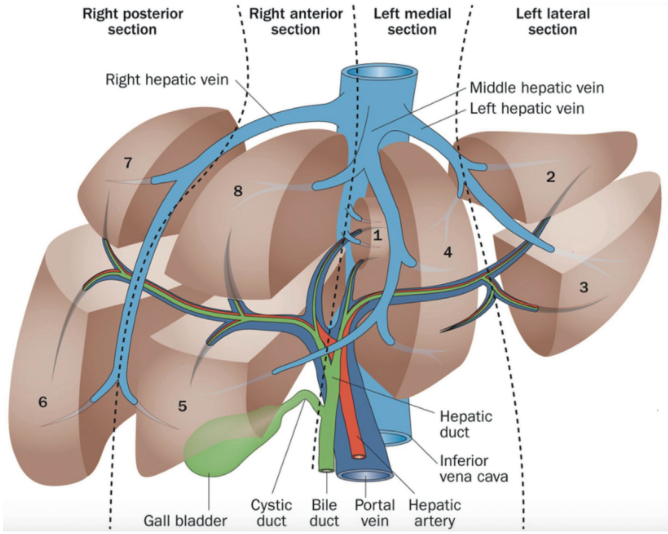

FIGURE 1. Segmental hepatic anatomy according to Couinaud.

The standard arterial anatomy of the adult liver is described as a common hepatic artery (CHA) originating from a celiac trifurcation that gives off the gastroduodenal artery branch (GDA) and then continues as the proper hepatic artery (PHA). The PHA then splits into the left hepatic artery (LHA), vascularizing segment 2-4, and the right hepatic artery (RHA), vascularizing segment 5-8.

However, in as much as 21-45% of patients, there are anatomic variants of the hepatic arterial configuration (32-35). The vascularization of the caudate lobe (segment 1 according to Couinaud) is particularly varied, with a range of 1-5 arteries supplying this lobe. Most often, this segment is supplied by two branches, originating from the RHA and LHA. Although resection of caudate lobe tumors is associated with high complication and mortality rates and techniques such as radiofrequency

ablation (RFA) are hindered by the nearby large vessels, radioembolization is a good alternative for treatment of caudate lobe tumors (36).

Van den Hoven et al. have described as many as sixteen different hepatic arterial segmental vascularization patterns, differing by the presence of accessory or replaced hepatic arteries, their respective vascular territory, and the origin of the artery vascularizing liver segment 4 (37). An accessory hepatic artery is an aberrant hepatic artery that vascularizes the left (segment 2) or right hemi-liver partially (any segments), existing in addition to a normally derived LHA and RHA. A replaced hepatic artery is an (aberrant) hepatic artery with a different origin (not the PHA) that vascularizes the left (segments 2-3 or segments 2-4) or right hemi-liver (segments 5-8). Timely assessment of the anatomy enables the establishment of a personalized treatment strategy ahead of time, including coil embolization of aberrant arteries, planning the number of injection positions and pretreatment activity calculation (37, 38). It is important to localize the segment 4 artery: it can be decided to use the segment 4 artery as a separate site of administration, include it in a more proximal injection position or coil-embolize it to induce intrahepatic redistribution of blood flow (39, 40). Knowledge of the location of the segment 4 artery can also be used in pretreatment activity calculation and avoidance of over- or underdosing of segment 4 (23).

3. PREPARATORY ANGIOGRAPHY AND INTRAPROCEDURAL IMAGING

Before treatment, a preparatory angiography is performed for several reasons: [1] to map the arterial anatomy, [2] to assess the necessity of coil embolization of arterial branches, [3] to determine optimal catheter positioning and [4] to administer a simulation scout tracer. Traditionally, a transcutaneous transfemoral approach using the Seldinger technique was mostly used to gain intra-arterial access. Recently, there has been a rapid increase in the use of the radial artery as access site. Bishay et al. have found that the transradial approach is a safe and feasible access option for radioembolization and that it is associated with a low complication rate (41).

After securing the access site, a pre-shaped catheter is used to enter the source of the hepatic arterial vasculature (usually the celiac axis). A standard end-

hole microcatheter is advanced over an atraumatic microguidewire for further selectively catheterization (Figure 2a,b).

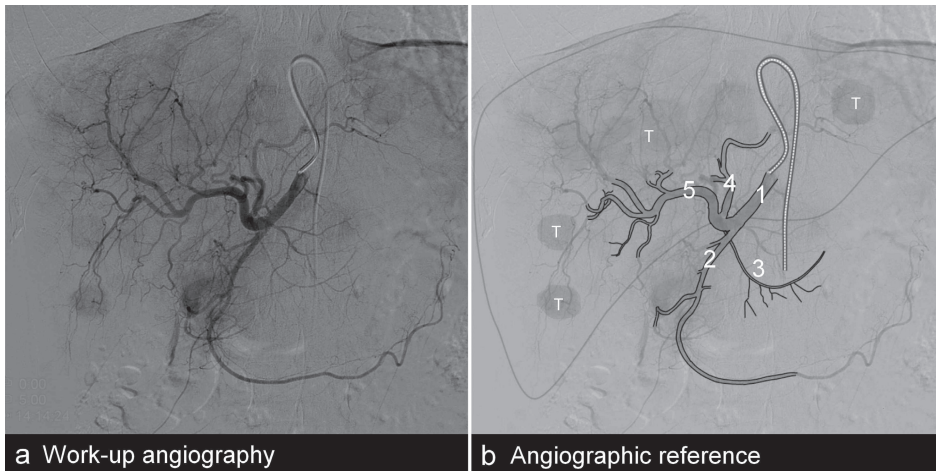

FIGURE 2A AND B. Figure 2a shows a digital subtraction angiography with contrast injection in the common hepatic artery. Figure 2b shows the angiographic reference: 1. Common hepatic artery; 2. Gastroduodenal artery; 3. Right gastric artery; 4. Left hepatic artery; 5. Right hepatic artery. Image reproduced from angiofellow.com, with permission from M. Smits.

3.1. Intraprocedural imaging

During angiography, digital subtraction angiography (DSA) is performed (Figure 3). DSA provides two-dimensional images of the vasculature at a high spatial resolution. Moreover, it is possible to acquire cinematic DSA images during high rate contrast administration with a power injector. The study of Theysohn et al. shows that with DSA as much as 6.5% of extrahepatic shunt vessels is missed, leading to possible extrahepatic deposition of the microspheres. Therefore, other imaging modalities are needed in the work-up for radioembolization (42).

Cone beam computed tomography (CBCT) is a relatively new imaging modality that has been integrated into the angiography suite and that provides 3D images. CBCT is based on the rotational movement of a C-arm equipped with a flat panel detector around the patient (43). It can be used to acquire, reconstruct and display 3D images of selective contrast-enhanced vessels and the surrounding soft-tissue. During radioembolization, CBCT is used to map the hepatic arterial anatomy, to identify extrahepatic branches and to rule out extrahepatic shunting

or non-perfusion of a target volume (44). There are various CBCT protocols. The CBCT acquisitions in the liver are mostly obtained following intravascular contrast administration through a catheter that is placed in the vessel of interest. Several types of 3D images can be obtained: unenhanced, angiographic, and images of the liver parenchyma during arterial, portal venous and delayed phases(43). Van den Hoven et al. have developed an acquisition protocol for CBCT imaging that provides a combination of these images. In their study, a continuous infusion of contrast agent, a variable scan delay based on the time to parenchymal enhancement on DSA, and a 10-second high-dose scan setting resulted in images that contain both contrast enhancement of the arterial tree and liver parenchyma. They also show gastrointestinal shunting and provide sufficient contrast between perfused and non-perfused liver territories (44).

The study of Grözinger et al. has shown that the CBCT approach is superior to the angiographic determination of vascular supply of specific segments, mainly segments 1 and 4 (45).

The main limitation of CBCT is the limited field of view compared to conventional CT. Other limitations are the greater risk of motion artifacts and the increased procedural time (43).

FIGURE 3. Work-up procedure in the angiography suite. Image reproduced from angiofellow.com, with permission from M. Smits.

3.2. Coil embolization of culprit vessels

Since extrahepatic deposition of radioactive microspheres may cause serious complications, it should be assessed whether arterial branches pose a risk. The 3 most common culprit vessels that cause extrahepatic deposition are the gastroduodenal artery, the cystic artery and the right gastric artery. Previously, it was advised to preventively coil-embolize these arteries. However, there are quite some disadvantages to coil-embolization: there is an increased radiation dose and an increase of procedure time and complexity, potential vessel damage and complications of coil deployment. Moreover, in the time between the preparatory angiography and treatment, new collateral vessels may develop. Nowadays, most centers try to avoid coil embolization unless extrahepatic deposition of activity is found on pretreatment simulation scout dose SPECT/CT. Sometimes, a more distal injection position or the use of an antireflux catheter can provide a safe treatment procedure without the need for coil embolization (2).

4. SCOUT DOSE IMAGING AND PRETREATMENT DOSIMETRY

4.1. ^{99m}Tc-MAA

Worldwide, pretreatment simulation of radioembolization with ^{90}Y is currently based on ^{99m}Tc-MAA planar imaging and SPECT/CT for assessment of extrahepatic depositions and lung shunting.

MAA are biodegradable particles. Their size is not well-calibrated, estimated at between 10 and 150 µm, with 90% of the particles falling between 10 and 40 µm, and 1 to 2% below 15 µm (46). Typically, between 150 and 250 MBq of ^{99m}Tc-MAA are injected into the hepatic artery for therapy simulation, with around 1.5x10^6 MAA particles (47). As a comparison, normally around 3-5x10^6 spheres for 3 GBq of glass microspheres are injected, and around 40-80x10^6 spheres for 1.5 GBq of resin microspheres.

The size, density and number of injected particles differs between ^{99m}Tc-MAA particles and glass/resin microspheres. Thus far, ^{99m}Tc-MAA particles are the only particles used for the pretreatment simulation of radioembolization with ^{90}Y, but there are controversies regarding the predictive value. Wondergem et al. have studied the relation between pre-treatment ^{99m}Tc-MAA distribution and post-treatment ^{90}Y distribution. They found a difference of >10% in 68% of the

hepatic segments analysed(48). Haste et al. have evaluated the value of ^{99m}Tc-MAA in predicting subsequent ^{90}Y glass microspheres distribution in patients with hepatocellular carcinoma. ^{99m}Tc-MAA was found to be a poor surrogate to quantitatively predict the tumor absorbed dose of ^{90}Y, but there was a correlation between ^{99m}Tc-MAA and ^{90}Y in the distribution in normal liver tissue (49). Ilhan et al. have analyzed the predictive value of ^{99m}Tc-MAA SPECT for radioembolization with ^{90}Y resin microspheres, by comparing uptake on pretherapeutic ^{99m}Tc-MAA SPECT with uptake on posttherapeutic ^{90}Y bremsstrahlung SPECT. They analyzed 502 patients who underwent radioembolization for primary and secondary liver tumors. They found a significant but quite low correlation between the ^{99m}Tc-MAA and ^{90}Y-microsphere tumor-to-background ratio (50). Another study, however, evaluated the agreement between ^{99m}Tc-MAA SPECT/CT-based predictive dosimetry and posttreatment ^{90}Y PET/CT-based dosimetry in patients with hepatocellular carcinoma, treated with both glass and resin spheres. They found that predictive dosimetry based on ^{99m}Tc-MAA SPECT/CT provides good estimates of absorbed doses as calculated on posttreatment ^{90}Y PET/CT, for tumor and nontumor tissues (51). However, the majority of the treatments analysed (25/27) was selective, which may have led to more positive results and a better correlation between ^{99m}Tc-MAA and ^{90}Y.

Not only the size, density and number of the injected particles play a role in the different distributions of ^{99m}Tc-MAA and ^{90}Y –microspheres. Other confounding factors are tumor type, tumor vascularization, tumor size, prior therapy, ^{99m}Tc-MAA injection parameters and angiographic considerations such as catheter position and vasoactive arterial status. There are large differences in ^{99m}Tc-MAA uptake between hepatocellular carcinomas that are generally large and hypervascular and liver metastases such as colorectal cancer liver metastases, which are often smaller and hypovascular. Prior therapy can also have an influence, because it can induce arterial disorders and weaknesses. There is no established protocol for the injection of ^{99m}Tc-MAA, but guidelines indicate that the injection time should be 20-30 seconds. This is quite comparable to a bolus injection, which is significantly different from the pulsing method used during the actual administration of resin- and ^{166}Ho-microspheres.

The most important factor is the injection position of the catheter during ^{99m}Tc-MAA infusion and ^{90}Y-microsphere infusion. This catheter position

should be exactly the same, with the same distance to bifurcations and the same orientation in the vascular lumen (48). Another important factor is the vasoactive status of the hepatic arteries at the time of injection, since vasospasm may occur during radioembolization procedures and they may impact the distribution of microspheres (46).

Because of the discrepancies between ^{99m}Tc-MAA and ^{90}Y-microsphere distribution, several alternatives to ^{99m}Tc-MAA are currently under investigation (52).

4.2. ^{166}Ho scout dose

When planning radioembolization with ^{166}Ho, a small batch of ^{166}Ho-microspheres with limited radioactivity (200-250 MBq) can be used as a scout dose, instead of ^{99m}Tc-MAA. This ^{166}Ho scout dose is sufficient to be visualized and quantified on SPECT imaging, but limited enough not to cause tissue damage in case of shunting to the gastrointestinal organs or the lungs. To prevent embolization of the arteries before treatment, only 60 mg is administered, whereas a treatment dose consists of 540-600 mg of microspheres. Because the same particles are used, lung shunting can be estimated more accurately (53). The safety of the ^{166}Ho scout dose has been established recently by Braat et al (54). Figure 4 shows a microscopic image of ^{99m}Tc-MAA particles and ^{166}Ho-microspheres.

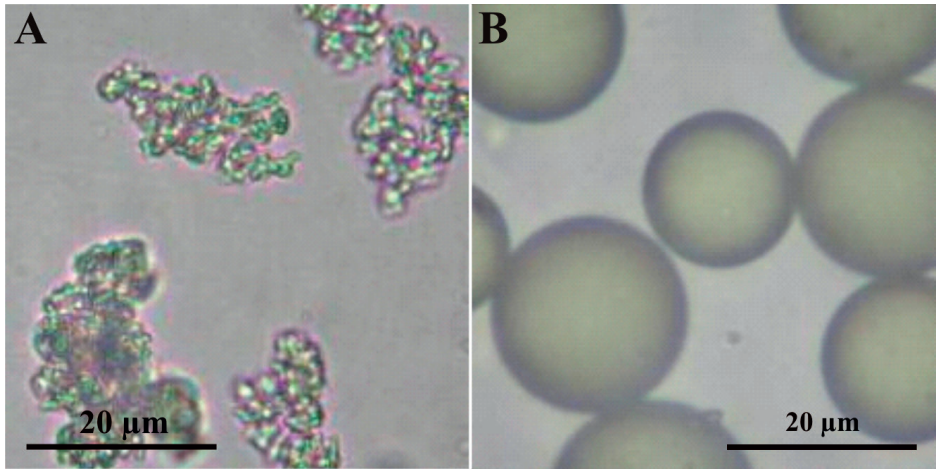

FIGURE 4. Figure 4a shows a microscopic image of ^{99m}Tc-MAA particles. Figure 4b shows a microscopic image of ^{166}Ho-microspheres.

4.3. Lung shunt calculation

Lung shunting is caused by arteriovenous anastomoses or shunts in the liver parenchyma or in a tumor. Excessive activity deposition in the lungs can result in radiation pneumonitis after radioembolization. Based on experience with external beam radiation therapy (EBRT), the highest tolerable lung shunt was defined as 30 Gy after a single treatment and a cumulative dose of 50 Gy after repeated treatments (2).

The lung shunt fraction (LSF) is defined as:

$$LSF = \frac{\sqrt{lungs_{anterior} * lungs_{posterior}}}{\sqrt{lungs_{anterior} * lungs_{posterior}}) + \sqrt{liver_{anterior} * liver_{posterior}}}$$

(1, 46). Planar imaging can be used to calculate the lung shunt after administration of ^{99m}Tc-MAA (Figure 5). However, Elschot et al. and Yu et al. have demonstrated that the lung absorbed doses are significantly overestimated by pretreatment ^{99m}Tc-MAA imaging (53, 55).

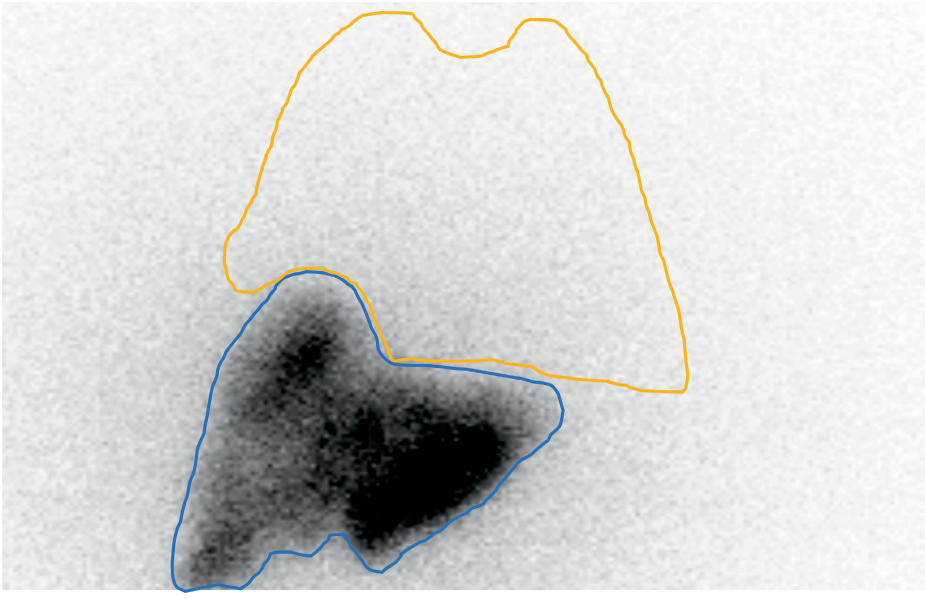

FIGURE 5. Figure 5 shows a planar scan with lung and liver ROIs to calculate lung shunt. In this example, there was visually no lung shunt and calculation showed 9%.

There are several factors that may have an influence on LSF calculation. LSF estimation without attenuation correction gives a large overestimation with respect to attenuation-corrected evaluations. There is reduced photon attenuation in the lungs compared to the photon attenuation in the abdomen. Another factor is scatter correction, which should be applied in order to avoid overestimations of the LSF. Moreover, ^{99m}Tc-MAA degrades after several hours, which increases the LSF. Therefore, it is important to perform the image acquisition as soon as possible after administration of ^{99m}Tc-MAA (1, 46). The studies of Yu et al. and Kao et al. have proven that SPECT/CT leads to more accurate calculation of lung shunt absorbed dose than planar imaging (55, 56).

However, lung shunting differs significantly between different tumor types. Gaba et al. have published a study of 141 patients with primary and secondary hepatic malignancies who underwent radioembolization. The LSF was calculated for every patient and LSF>20% occurred much more often in HCC patients than in patients with other tumor types (14% versus 3%). In HCC patients, a high LSF was associated with infiltrative morphologic structure, tumor burden >50%, portal vein invasion and arterioportal shunting. In other tumor types, such as colorectal carcinoma metastases, neuroendocrine tumors and cholangiocarcinomas, a larger tumor size and greater tumor burden were associated with lung shunting (57). In patients with these factors, care should be taken to avoid deposition of radioactive microspheres in the lungs.

4.4. Extrahepatic activity and nontumor dose in the liver

Pretreatment simulation with ^{99m}Tc-MAA is not only useful to establish the LSF, but also to give an impression of the total absorbed radiation dose in the healthy liver parenchyma: the non-tumor dose. It is widely known that with an increasing non-tumor dose the risk of complications such as radioembolization-induced liver disease (REILD) is higher, but the maximum tolerable non-tumor dose is not well established. It is dependent on the type of tumor, the condition of the liver, prior treatments (e.g. bevacizumab) and the distribution of radiation within the non-tumor volume. With radioembolization, the absorbed dose in the liver is never uniform, which makes higher average absorbed doses tolerable. A non-tumor dose limit of <70 Gy in normal liver tissue and a non-tumor dose limit of <50 Gy in cirrhotic livers is proposed, but this is highly dependent on microspheres used and the number of microspheres administered (2, 46).

Thresholds for an acceptable average normal liver absorbed dose have yet to be established.

4.5. Pretreatment dosimetry

Different methods for pretreatment activity calculations for the different types of microspheres have been proposed. The first method that was used was the so-called 'empirical' method, based on the tumor burden. The used activity ranged between 2 and 3 GBq. This method was abandoned because it was associated with unacceptable clinical toxicity (58).

For resin microspheres, the Body Surface Area (BSA) method is mostly used. This method adjusts the prescribed activity for the patient's BSA and the fractional tumor burden. The formula for BSA in square meter is:

$$BSA = 0.2024 * height(m)^{0,725} * weight(kg)^{0,425}$$

The formula for the injected activity (IA) is:

$$IA_{(GBq)} = (BSA - 0,2) + \frac{tumor\ volume}{(tumor\ volume + liver\ volume)}$$ (1, 2).

The prescribed activity is reduced in case of lung shunting, depending on the percentage of lung shunting: 20% activity reduction with 10-15% LSF, 40% activity reduction with 15-20% LSF and no treatment with >20% LSF (52). The BSA method assumes a correlation between BSA and liver weight. However, this is not necessarily true and may result in an undertreatment of small patients with large livers, and an overtreatment of large patients with small livers. Another limitation of this method is that it does not take into account the degree of tumor uptake (1, 2).

For glass microspheres, Salem et al. have developed the Medical Internal Radiation Dose (MIRD) method (59-61). With this method, the prescribed activity is determined by calculating the activity required to achieve a desired absorbed dose (between 80-150 Gy). The MIRD method assumes a homogenous intrahepatic microsphere distribution throughout the treated portion of the liver, and an assumed yield of 50 Gy per GBq ^{90}Y per kilogram of liver tissue. This method also does not take into account the degree of tumor uptake, nor does it account for fractional or total tumor burden. The formula for the IA is:

$$IA_{(GBq)} = \frac{\left(Desired\ average\ absorbed\ dose\ (Gy) * M_{Target}(kg)\right)}{50\left(\frac{J}{GBq}\right)}$$

where M_{Target} is the mass of the target volume. The MIRD method is especially useful for radiation segmentectomy, where a large absorbed dose (e.g. 200 Gy) is administered to a limited target volume in order to ablate both the tumorous and non-tumorous liver tissue within that target volume, while sparing the untreated part of the liver (52).

For ^{166}Ho, a method comparable to the MIRD method for ^{90}Y is currently used. Based on findings of the HEPAR I trial, a phase I dose escalation study, a maximum tolerable absorbed dose for the whole liver is set at 60 Gy (62). The absorbed dose in Gy delivered by 1 GBq in 1 kg tissue is 15.87 Gy for ^{166}Ho, under the assumption of homogenous distribution in the target volume and absorption of all energy within that volume. The formula for the IA is:

$$IA_{(MBq)} = liver\ weight\ (kg) * 3780\ \left(\frac{MBq}{kg}\right)$$

Another method, that can be used for pretreatment dosimetry for both resin and glass spheres, is the partition model. In general, the tumor and healthy liver tissue are delineated on anatomical imaging modalities. The anticipated activity in these delineated compartments is calculated on ^{99m}Tc-MAA SPECT/CT. The tumor to nontumor (T/N) ratio on MAA is calculated as:

$$\frac{T}{N} = \frac{\frac{Activity_{tumor}(GBq)}{Mass_{tumor}(kg)}}{\frac{Activity_{liver}(Gbq)}{Mass_{liver}(kg)}}$$

The formula for the IA is:

$$A(GBq) = \frac{Dose\ (Gy) * \left(\left[\frac{T}{N} * Mass_{tumor}(kg)\right] + Mass_{tumor}(kg)\right)}{49{,}670 * (1 - lung\ shunt\ fraction)}$$

The partition method does correct for the difference in tumor and nontumor dose. Limitations of this model are that it is more time-consuming and that it

is problematic in patients with ill-defined tumors (2, 52). Furthermore, nor the acceptable absorbed dose in the healthy liver, neither the effective absorbed tumor-dose are defined yet.

Recently, Chiesa et al. have developed a method for activity calculation that does take non-uniformity of the absorbed dose into account. In a cohort of 52 patients with HCC, treated with glass microspheres, they studied lesion and parenchyma absorbed dose at voxel level on ^{99m}Tc-MAA SPECT images. The biodistribution of the ^{99m}Tc-MAA and ^{90}Y-microspheres was assumed to be identical. The degree of agreement between clinical observations of response and several dosimetric variables was compared. A dosimetric variable that accounts for both non-uniformity of absorbed dose deposition and the dose-rate effect was found to be the best variable to predict response of a lesion. The 50% tumor control probability was different for small (<10 cc) and large (>10cc) lesions, with much higher absorbed doses needed for larger lesions, which weakens the predictive power of planning on lesions. There was a high tolerance of the healthy liver tissue to glass microspheres. The best prediction method was found to be the parenchyma mean dose, with a limit of 75 Gy at a 15% toxicity risk (63). Drawbacks of a voxel-based dosimetry approach can be divided in physical factors, such as attenuation, scatter, noise, and partial-volume effects, and in clinical factors, such as respiration. Corrections for these factors should be implemented in the reconstruction protocol (64).

5. TREATMENT

5.1. Treatment angiography

Usually, within two weeks after the scout procedure, the treatment procedure takes place. Similar to the angiography procedure for the scout dose administration, intra-arterial access is obtained via the femoral artery. Before infusion of the microspheres, the vascular tree should be investigated carefully. The exact same injection position as during the scout procedure should be chosen to avoid a different intrahepatic distribution. Wondergem et al. have found a relative difference of >30% in absorbed activity per milliliter in as many as 24 of 68 analyzed segments, due to a difference in injection position of >5 mm (48). It is important to make sure that no new hepaticoenteric collaterals have been recruited in the time interval between the scout and therapy procedures.

In a study of 122 patients with primary and metastatic hepatic tumors, Abdelmaksoud et al. investigated the development of new hepatoenteric collaterals. These patients underwent a preparatory angiography before treatment with radioembolization, during which hepaticoenteric collaterals were embolized. At the time of radioembolization, new collaterals had developed in 42 patients (34.4%), requiring adjunctive embolization. The mean time interval between the preparatory and treatment angiography in this subgroup was 14.7 days (range 1-72) (40). In 2007, one of the official recommendations of the radioembolization brachytherapy oncology consortium was that 'all extrahepatic vessels originating from the hepatic arteries that supply the gastrointestinal tract should, under most circumstances, be embolized to exclude extrahepatic deposition of the ^{90}Y microspheres' (65). However, the rapid development of new hepaticoenteric collaterals opposes this so-called skeletonization and brings it benefit into question. In a review, Borggreve et al. looked into the evidence supporting prophylactic embolization. They found that refraining from embolization of the GDA, right gastric artery (RGA) and the cystic artery (CA) is justified when the catheter tip can be placed distal to the origin of these arteries (66). It is recommended to use a more distal injection position, already during the scout procedure.

5.2. Medication

During treatment, it is common practice to monitor vital signs (blood pressure, pulse and saturation). Recently, a large study was published on adjuvant medications that improve survival after locoregional therapy, such as radioembolization. The medications were taken at the time of embolization. Beta-blockers and aspirin were associated with improved survival in HCC patients. These medications were not associated with improved survival when taken by patients with neuroendocrine tumors or colorectal cancer liver metastases (67). The authors provided the following hypotheses for the mechanisms behind this survival benefit: (1) aspirin inhibits hypoxia-induced angiogenesis, which might prevent radioembolization-induced ischemia from promoting angiogenesis and growth of the residual viable tumor. It also inhibits glycolysis, which may make tumor cells less likely to survive radioembolization-induced ischemia. Furthermore, aspirin is a COX inhibitor and COX-2 inhibition promotes an antitumor immune response. (2) Beta-blockers decrease blood flow in the portal vein, which is associated with improved response after

radioembolization of colorectal cancer liver metastases. Moreover, beta-blockers can reduce stress hormone-mediated invasion of tumor cells (67).

Besides beta-blockers and aspirin, proton-pump inhibitors are often given during the first week before and continued up to a month after treatment, as prophylaxis for gastrointestinal ulcer formation. Heparin, according to local guidelines in interventional radiology, is given for thrombosis prophylaxis during treatment. If a vasospasm occurs during the procedure, it is indicated to give a vasodilator intra-arterially.

Neuro-endocrine tumors can rapidly release a large amount of vasoactive substances after radioembolization. This may lead to a carcinoid crisis with flushing, hypertension and tachycardia, followed by hypotension and possibly death (68). To prevent a carcinoid crisis, somatostatin analog prophylaxis intravenously may be indicated.

When patients are in pain, intravenous analgesia should be considered during the procedure, according to local interventional radiology guidelines.

5.3. Dose administration

All three types of microspheres are provided in a vial. The administration systems are quite different from each other, but they all have two lines: one that connects the vial with the microcatheter, and one through which the nuclear physician can inject a diluting solution in the vial (i.e. saline, sterile water or 5% glucose) (9, 69, 70).

There are significant differences in administration techniques between ^{90}Y resin microspheres, ^{90}Y glass microspheres and ^{166}Ho microspheres.

^{90}Y resin microspheres should be administered very carefully with a flow rate of no more than 5 mL per minute, to allow for optimal distribution in the tumor microvasculature. The administration usually takes up to 20 minutes. While administrating, the interventional radiologist should check for slow flow or stasis, by administrating small aliquots of contrast fluid and microspheres alternately. When stasis occurs, the procedure should be terminated to prevent reflux (9). It was hypothesized that sterile water, which was injected

with the microspheres, caused a temporary change in the osmolality of the blood, leading to vascular endothelial injury and vasospasm, causing stasis. Two studies have been published regarding the replacement of sterile water with glucose 5% water (G5W). Ahmadzadehfar et al. report about 78 patients treated with resin microspheres. Fifty procedures were performed with sterile water and 54 procedures were performed with G5W. A significantly higher proportion of the calculated activity was administered with G5W (96.1% versus 77.4%), there was a significantly lower incidence of stasis (28% versus 11%) and significantly less abdominal pain during the procedure (1.8% versus 44%) (70). The findings of Paprottka et al. confirm the positive effects of using G5W as a diluting solution, as they also showed a significantly reduced need for periprocedural analgesia (71). ^{90}Y glass microspheres are less prone to stasis because the number of microspheres is much lower. Administration of ^{90}Y glass microspheres is much faster, because they are injected in one bolus (69). To prevent high injection pressures, a small pressure relief valve is included in the administration set, limiting the injection pressure to 30 pound-force per square inch (PSI) (69).

^{166}Ho microspheres are administered in the same way as ^{90}Y resin microspheres: carefully with a low flow rate in a pulsatile manner, to avoid stasis and reflux (72). However, simultaneous injection with a diluted contrast agent is possible.

5.4. Possible side effects and adverse events

In the literature, controversy exists on the term 'toxicity' after radioembolization. It is graded in multiple ways on diverse time points after treatment. To compare data on toxicity, it is essential this is graded according to the same definition. Most often, side effects after treatment are scored according to the Common Terminology Criteria for Adverse Events (CTCAE) version 4.0. Adverse events (AEs) are defined as 'any unfavorable and unintended sign, symptom, or disease temporally associated with the use of a medical treatment or procedure that may or may not be considered related to the medical treatment or procedure'. Five grades are used to classify the adverse events, referring to the severity of the AEs, with grade 1 being mild and grade 5 indicating death related to the AE (73).

Hepatotoxicity is the most important adverse event after radioembolization, but a clear definition is often lacking. Braat et al have proposed the following grading for hepatotoxicity after radioembolization (74):

- Grade 0: no liver toxicity (i.e. no CTCAE toxicity grade changes over baseline)
- Grade 1: minor liver toxicity, limited to increased aspartate aminotransferase, alanine aminotransferase, alkaline phosphatase, and/or γ-glutamyl transpeptidase levels (all not exceedingly newly developed grade 1 CTCAE toxicity)
- Grade 2: moderate liver toxicity, with a self-limiting course. No medical intervention necessary.
- Grade 3: REILD, manageable with noninvasive treatments such as diuretics, ursodeoxycholic acid, and steroids
- Grade 4: REILD necessitating invasive medical treatment such as paracentesis, transfusions, hemodialysis or a transjugular intrahepatic portosystemic shunt
- Grade 5: fatal REILD

The most frequent side effect of radioembolization is the post-embolization syndrome, which consists of fatigue, nausea, vomiting, anorexia, fever and abdominal pain. These effects are usually mild and self-limiting within two weeks. The post-embolization syndrome occurs in up to 55% of patients (75). Another common side effect is a transient elevation of liver enzymes (75). In a retrospective analysis of 58 patients with diverse hepatic malignancies, Roberson et al. found that a decreased pretreatment albumin and an elevated pretreatment INR were associated with the development of severe liver toxicity after radioembolization (76). Gabrielson et al. evaluated toxicity after radioembolization in patients with hepatocellular carcinoma. They found that a pretreatment elevation of bilirubin and an elevation of the transaminases (ALT/AST) were associated with a higher risk of a decline in liver function after treatment (77).

Laboratory abnormalities usually go without associated clinical side effects (78). However, when laboratory toxicities are associated with ascites, this may be a sign of a much more serious complication: radioembolization- induced liver disease (REILD) (Figure 6).

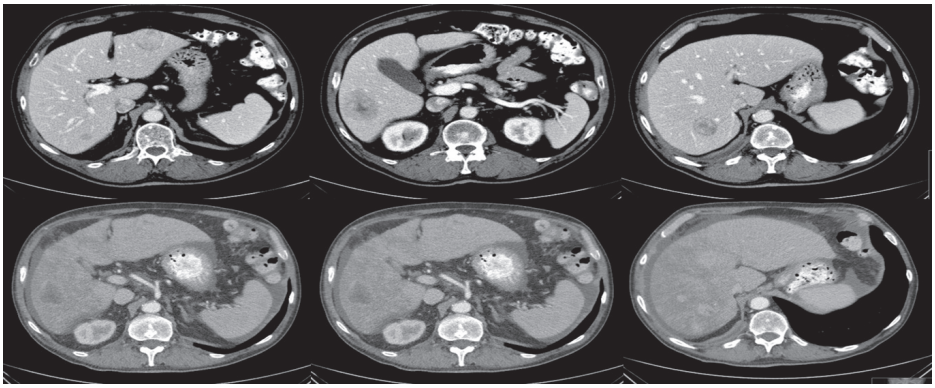

FIGURE 6. The upper row shows contrast-enhanced CT images of a 60-year-old woman with hepatic metastases of a neuro-endocrine carcinoma, before treatment with radioembolization. The lower row shows contrast-enhanced CT images after treatment with ^{166}Ho-radioembolization, with the development of REILD (impaired hepatic function and ascites).

REILD is usually defined as : 'a symptomatic post-radioembolization deterioration in the ability of the liver to maintain its (normal or preprocedural) synthetic, excretory and detoxifying functions. It is characterized by jaundice and the development of or increase in ascites, hyperbilirubinemia and hypoalbuminemia developing at least two weeks – four months after radioembolization, in the absence of tumor progression or biliary obstruction' (74). Histopathologically, REILD is characterized by veno-occlusive disease with congestion of the central veins and sinusoids (78). The incidence of REILD is reported to be 0-5.4%. The natural course of REILD is highly variable: it can either result in fulminant hepatic failure and death, or it can be transient and self-limiting. Reported risk factors for REILD include previous liver-directed therapies, such as chemotherapy, external beam radiation therapy (EBRT), radioembolization and other intra-arterial therapies. Furthermore, a high absorbed dose and single-session whole liver treatment also increase the risk of hepatotoxicity (74). Other risk factors are exposure to chemotherapy within 2 months after radioembolization, a liver volume <1.5 L, and increased baseline bilirubin and aspartate aminotransferase (79). Treatment options consist mainly of supportive measures, such as the reduction of ascites or pleural effusion and the avoidance of hepatotoxic drugs (74). To reduce the excessive extravascular volume, diuretics (spironolactone 100 mg and/or furosemide 40 mg daily) can be tried. When liver function

starts to decline, 10 mg/day defibrotide intravenously or oral steroids can be considered. If medical treatment is ineffective, a transjugular intrahepatic portosystemic stent-shunt (TIPS) could be placed. Based on an expert panel and literature review, prevention of REILD can be pursued by excluding patients with poor liver functional reserve (such as total bilirubin >2 mg/dL or ascites) from radioembolization. Furthermore, it is recommended to adapt the calculated activity in patients with steatosis, steatohepatitis, hepatitis, cirrhosis, a liver volume <1.5 L and with multiple lines of prior chemotherapy. Also, sequential lobar treatment may improve liver tolerance to radioembolization (79). Since a high absorbed dose is an important cause of hepatotoxicity, a personalized dosimetric approach, as proposed by Chiesa et al., should be implemented in clinical practice, especially in patients with known risk factors. The most vital aspect in the prevention of REILD should be the healthy-liver tissue absorbed dose. Therefore, the parenchymal mean dose should be taken into account in treatment planning (63).

Another relatively uncommon complication of radioembolization is gastrointestinal ulceration, caused by non-target delivery of microspheres (75). Gastrointestinal ulceration usually presents 2-6 weeks after treatment with symptoms of acute epigastric pain, nausea, vomiting, dyspepsia and anorexia. The incidence is about 2-3%. Symptoms can last up to 10 months despite adequate treatment with proton pump inhibitors. Normally, full recovery occurs. Prevention of ulceration by using proton pump inhibitors around treatment is often advocated but lacks scientific evidence (79). Lam et al. have performed a root cause analysis to identify risk factors for the development of gastrointestinal ulceration. In their cohort of 278 treatments in 247 patients, the following risk factors were identified: stasis, proximal administration site, young age and distal origin of the GDA. To prevent gastrointestinal ulceration, it is advised to administer microspheres exclusively distally (80). Although much attention is paid to its prevention by calculating lung shunt, radiation pneumonitis is rarely seen. It is characterized by exertional dyspnea, dry cough, restrictive ventilator dysfunction and bilateral lung infiltrates. The lung shunt is estimated based on the fraction of ^{99m}Tc-MAA that is deposited in the lung vasculature after the pretreatment work-up. However, Elschot et al. have shown that ^{99m}Tc-MAA usually overestimates the lung shunt, with an absolute error range of 9.4-12.1 Gy (53). The manufacturer of resin microspheres recommends

dose reductions of 20%, 40% and 100% if the LSF exceeds 10%, 15% or 20% (79). A maximum tolerated dose of 30 Gy in one treatment or 50 Gy in sequential treatments to the lungs is widely used, but due to the very low incidence of radiation pneumonitis, it is difficult to establish an endorsed threshold. Sangro et al. propose to refrain from treatment with radioembolization if the LSF is ≥15%, rather than adjusting the amount of injected activity. However, since lung shunt doses are often overestimated, this would result in withholding patients from what can be their last treatment option. Radiation pneumonitis is characterized by bilateral symmetric ill-defined patchy opacities and ground-glass nodularities on CT (Figure 7a-d). Treatment consists of steroids and supportive measures (79).

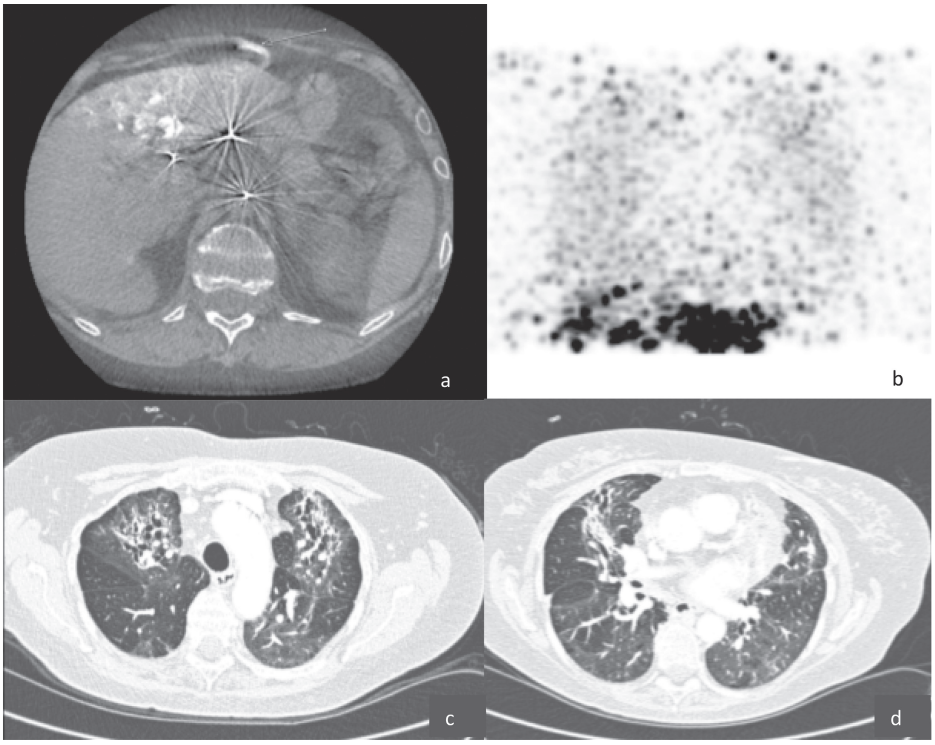

FIGURE 7A-D. Figure 7a: cone-beam CT of 65-year old woman with HCC, with arteriovenous shunt (arrow). Figure 7b shows the lung shunt on ^{90}Y-PET. Figure 7c-d show high-resolution CT images of the lungs with ground-glass nodularities and fibrosis.

Other complications that may arise are portal hypertension and biliary tree damage. Portal hypertension can develop months to years after

radioembolization. Symptoms consist of an increased spleen volume and possibly gastro-oesofageal varices. Bile duct necrosis and strictures are often asymptomatic and seen in about 2-4% of patients (79).

Furthermore, radiation cholecystitis is occasionally reported. The incidence ranges from 0-7%. It is characterized by upper right quadrant abdominal pain, nausea, vomiting, malaise and occasional fever (81). The diagnosis is confirmed by the presence of a thickened, hyperenhanced gallbladder wall with pericholecystic fluid, intramural gas or hydrops, seen on ultrasound, CT or MRI. The mainstay of treatment is analgetic treatment. However in severe cases, a cholecystectomy can be considered (79). Prince et al. propose the following strategies for gallbladder protection during radioembolization: if possible, placing the microcatheter distal to the cystic artery, or adjustment of the catheter position to alter the direction of blood flow. It is advised not to apply temporarily or permanently occluding of the cystic artery, since this can lead to ischemic cholecystitis (81).

In some patients, extrahepatic deposition is seen in the falciform ligament, due to a patent hepatic falciform artery (HFA). Theoretically, this could cause radiation dermatitis or abdominal pain. However, this is rarely seen and only a few cases have been described. In a review of 410 radioembolization treatments, Braat et al. have found only 16 cases of extrahepatic deposition in the falciform ligament. None of these patients experienced symptoms compatible with the extrahepatic deposition. These results show that there is no need for prophylactic measures or even exclusion from therapy of patients with a patent HFA (82).

5.5 Long-term hepatic changes

Su et al. have investigated the long-term hepatotoxicity after radioembolization in patients with NENs. The median follow-up time was 3.5 years. Twenty-six of 54 evaluated patients developed cirrhosis-like morphology after a median time of 1.8 years, but only 5 of them exhibited clinical symptoms that were attributable to radioembolization. Splenic volume increased by 64.7% in patients treated with whole-liver radioembolization and by 21.9% in patients treated with unilobar radioembolization. Findings of portal hypertension, such as ascites and varices, also developed more frequently in patients who received

a whole-liver treatment (83). This study shows that the long-term hepatotoxicity is mild. Long-term hepatotoxicity will become more and more important, since in the future, (combination) treatment with radioembolization may be applied in first- or second line settings.

6. POST-TREATMENT IMAGING AND DOSIMETRY

Post-treatment imaging

Currently, post-treatment imaging serves two purposes: the evaluation of technical success and the prediction of treatment efficacy. Technical success is evaluated by checking for extrahepatic deposition of microspheres and assessing the intrahepatic distribution.

The heterogeneity of microsphere distribution within a lesion and the absorbed radiation dose within a lesion can be obtained. By evaluating dose-response relationships, treatment efficacy can be predicted (84).

6.1. ^{90}Y imaging

^{90}Y decays without emission of gamma photons. Bremsstrahlung x-rays are emitted along a continuous decreasing energy spectrum ranging up to 2.3 MeV. Positron emission, which produces two annihilation gamma rays, happens only in 32 out of one million decays.

Thus, the quantitative imaging is limited to bremsstrahlung SPECT/CT and PET/CT.

6.1.1. ^{90}Y SPECT/CT

The emitted bremsstrahlung x-rays have energies that can range up to 2.3 MeV. The maximal energy usable by a gamma camera with a mechanical collimator is approximately 0.5 MeV. As a result, all acquisitions are corrupted by high energy x-rays scattering down into the acquisition window.

There are five different image-degrading effects: scattering inside the patient body, penetration through collimator septa, scattering from a collimator septa, the lead fluorescence K_α and K_β emissions and the back-scattering from the photo multiplier tube, electronic boards and lead housing of the camera (85).

The shape and magnitude of these effects depend on photon energy, tissue composition, collimator and detector characteristics, the distance between the source and the collimator, and the energy window settings (86). Elschot et al. have developed a new method for ^{90}Y SPECT reconstruction. This Monte Carlo-based reconstruction algorithm compensates for scatter and attenuation effects and improves the quantitative accuracy of bremsstrahlung SPECT images (86). Because of the wide range of photon energy, the energy window for bremsstrahlung SPECT/CT should be wide. However, because of the high focal uptake in the liver after radioembolization, a single-window approach is sufficient (87). Reported ranges in the literature are 105-195 keV and 50-250 keV (86-88). A high-energy collimator is proven to be better than a medium energy collimator by Elschot et al (14). The specifications of the SPECT/CT are defined by Elschot et al.: a radius of rotation of camera of 260 mm, 120 projections/360°, 40-minute acquisition time, 256x256 matrix size and 1.6x1.6 mm^2 pixel size (88, 89).

A largely neglected issue in clinical SPECT is respiratory motion. Bastiaannet et al. have shown that respiratory motion has a very large effect on dosimetry on the spatial scale of individual tumors, with an average decrease in activity recovery and tumor to non-tumor ratio from 90% to 66%. Thus, respiratory motion leads to an underestimation of tumor dose. This can partially be solved by using retrospective gating schemes (90).

6.1.2. ^{90}Y PET/CT

Although annihilation photon pairs are produced about 700 times less often than bremsstrahlung photons, ^{90}Y PET/CT was found to be superior over bremsstrahlung SPECT/CT for the assessment of the microsphere distribution after radioembolization (88, 91). One of the first post-infusion clinical ^{90}Y PET/CT scans was performed in 2009. Since then, many studies have described results from both patient and phantom imaging. There are two major issues in ^{90}Y PET/CT imaging: the low true-coincidence rate and the high singles rate due to bremsstrahlung x-rays. The first issue may result in noisy images, long scan times and background noise from scintillator-decay. The singles-count rate from bremsstrahlung is much higher than the positron emission rate and may cause saturation of the detector, leading to a limited quantitative accuracy (84). However, this latter issue has not been found in recent investigations

(92). Regarding the first problem: the full-width at half maximum (FWHM) of ^{90}Y PET/CT is around 5 mm, and scan times of about 20 minutes are enough for dosimetry. The background noise is worse in organs were the ^{90}Y activity concentration is lower (84).

Due to the higher intrinsic resolution of ^{90}Y PET/CT compared to ^{90}Y SPECT/CT, intrahepatic distribution is more accurately visualized by ^{90}Y PET/CT imaging.

In the next generation PET/CT systems, the photomultiplier tubes are replaced with solid-state digital photon counting detectors. Wright et al have shown that detection of internal pair production is feasible with this digital photon counting (dPET) technology. dPET images provided increased contrast and allow for more precise localization of microsphere distribution (93). There is no guideline as to when patients should undergo ^{90}Y PET/CT imaging. Due to the limited sensitivity, it is advised to perform these scans the day of treatment or one day later.

6.1.3. ^{90}Y PET/MRI

The next development in ^{90}Y imaging is PET/MRI. PET/MRI provides a better soft tissue contrast than PET/CT. The first clinical study of ^{90}Y radioembolization with post-treatment PET/MRI imaging was conducted by Fowler et al. Twenty-four patients with tumors of diverse origin were treated with radioembolization with either glass or resin microspheres. Images were qualitatively assessed for microsphere distribution and the absorbed doses per lesion were calculated, as well as dose volume histograms, to measure the dose distribution within a tumor. The duration of PET/MR imaging ranged from 42-60 minutes. They found that the average dose per lesion, as well as the minimum dose to 70% of the lesion, were significant predictors of response (94).

Simultaneous PET/MRI offers the opportunity to directly image liver motion due to respiration during the PET acquisition and correct for it during the PET reconstruction. Eldib et al. have performed phantom experiments with PET/MRI. They found that motion resulted in a large loss of contrast recovery, but this was successfully corrected by MR-based data correction (95).

6.2. ^{166}Ho imaging

Because ^{166}Ho emits gamma photons, is paramagnetic and has a high attenuation coefficient, it can be detected during and after administration. While radioactive, the gamma photons emitted by ^{166}Ho can be measured using single-photon emission computed tomography (SPECT) (Figure 8a-c). Independent of radioactivity, holmium is a lanthanide and with its paramagnetic properties allows visualization and quantification using MR imaging, while the high atom weight attenuates X-rays (15, 16).

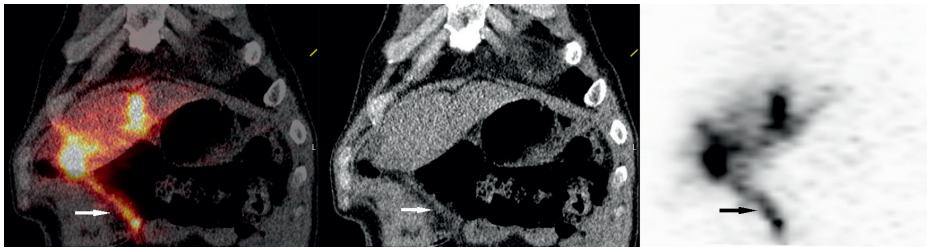

FIGURE 8A-C. Figure a-c show extrahepatic deposition in the falciform ligament (arrows) in a 53-year old patient with hepatic metastases of a neuro-endocrine neoplasm who was treated with ^{166}Ho-radioembolization. Figures 8a-c show the ^{166}Ho SPECT/CT, the low dose CT and a planar image of the ^{166}Ho SPECT/CT.

6.2.1. ^{166}Ho SPECT/CT

Upon decay, ^{166}Ho emits several gamma photons, most of which are 81 keV (abundance 6.7%), 1379 keV (0.9%) or 1581 keV (0.2%). To quantify ^{166}Ho accurately, the SPECT detector has to be set to register photons with an energy window of 7.5% around the photon peak of 81 keV (14). However, the bremsstrahlung photons and other photons with high energies scatter and become part of the photo peak window, limiting accurate quantification. Also, the higher keV gamma photons from ^{166}Ho decay interact with the patient and the detector. Both these effects are partially corrected for by a downscatter window of 118±6% keV, as well as the use of a medium energy collimator. Furthermore, attenuation of the patient's body causes a decrease in the photons. A Monte Carlo simulation compensates for attenuation, scatter and collimator-detector response, and has been developed to improve quantification (86).

Acquisition of a ^{166}Ho SPECT/CT takes about 30 minutes. When all ^{166}Ho has decayed to erbium, there are no more gamma photons to image, so there is a

time constraint on the imaging procedure. Conversely, just after administration of ^{166}Ho, the gamma photons are so abundant, that they invoke detector dead-time; the recorded photon produces a pulse of a certain duration during which no second pulse can be detected. Detector dead-time is seen when the activity in the scanner is greater than 1420 MBq (14). In practice, patients undergo a SPECT when the activity of their ^{166}Ho microspheres is between 250-500 MBq, between 3 and 6 days after treatment, depending on the infused activity.

6.2.2. ^{166}Ho MRI

Quantification of ^{166}Ho using MR techniques is possible because of the local field inhomogeneities it induces. It allows for imaging of higher resolution, is independent of radioactivity, and can be combined with anatomical scans of different kinds to show tumor boundaries and deposition of microspheres, but its application is limited to tissue without air (i.e., not in lungs and gastrointestinal organs) and metal (staples from prior hepatectomies).

In MR imaging, the nuclear magnetic moment of the nuclei of hydrogen atoms is aligned along a constantly applied magnetic field, after which a radiofrequency pulse disturbs its alignment. The resulting realignment of the nuclei after this pulse induces an electrical current in the receiver coil, which can be reconstructed to form an image. The realignment can be separated in a longitudinal (expressed in T_1) and a transversal vector (T_2). The T_2 vector from tissue decays quickly (several milliseconds) which is accelerated by the presence of Ho, while its effect on the T_1 is little to none. The decrease in T_2* invokes a lower signal on gradient echo MR images; the microspheres show up as dark areas on these images. A linear relation has been shown between the disturbance in the T_2 signal decay and the concentration of Ho present (16). This relationship, called the relaxivity (R_2*), depends on the strength of the main magnetic field of the scanner and the Ho content.

A calibration phantom with known Ho microspheres concentrations enables the translation of the differences in R_2* into units of microsphere concentrations, which convert into local activity using the activity per sphere.

As MR imaging of Ho is independent of radioactivity, it is possible during or immediately after infusion, but also after several months. The first enables

real-time estimation of damage to tumors or healthy liver, which could, in the future, lead to MR-guided radioembolization with simultaneous quantification for treatment optimization. The latter is useful for research into the dynamics and stability of implanted microspheres. The first human MR quantification was performed as part of the phase 1 HEPAR I trial (15). Of the injected mean total of 523 mg (range, 438-640 mg), MR quantification detected a mean of 431 mg (range, 236-666 mg) of microspheres in the liver, or 89±19%. As surgical clips distorted the quantification, the detection improved to 96±13% when these patients (5/14) were excluded. For this quantification, a map of T_2* values of the liver was made before and after radioembolization. After subtraction (with inherent registration errors), the amount of microspheres was computed.

7. FOLLOW-UP IMAGING AND RESPONSE IDENTIFICATION

7.1. Imaging with CT and MRI

After radioembolization, follow-up imaging is usually performed at three-month intervals (1). It is important to consider the changes in tumor appearance that may be a consequence of radioembolization treatment itself. For example, the tumor may increase shortly after therapy, due to acute necrosis, edema and hemorrhage. Also, inflammation and fibrosis adjacent to the tumor may be falsely interpreted. These changes may lead to a rim enhancement around the tumor, which resembles vital tumor. Furthermore, the presence of tumor necrosis has to be taken into account when measuring tumor size.

Because of these typical radioembolization-induced changes, CT and MRI protocols should at least include contrast-enhanced imaging, using an arterial and portal-venous contrast delay. Unenhanced images can be helpful to distinguish between hemorrhage and vital tumor tissue.

With MRI, different sequences add to the diagnosis of a lesion. T1 sequences allow for the detection of fat and other substances with a high T1 signal, such as hemorrhage. T2 sequences are used to distinguish between solid and cystic lesions. Diffusion weighted imaging (DWI) evaluates the free motility of water molecules. The mobility is restricted by cell membranes and tissues with different cellularity have differences in water molecule movement. Malignancies are generally highly cellular and water molecule motility is

restricted, so malignancies appear hyperintense on DWI. DWI can be quantified by apparent diffusion coefficient (ADC). Changes of DWI under therapy are applied for response evaluation and can be used as a surrogate for the degree of tumor necrosis: necrotic tissue reveals an increased ADC because the free water mobility is increased. However, drawbacks of DWI sequences are a lack of reproducibility and no uniform DWI protocol (96).

DWI can also be used as a prognostic factor: Schmeel et al. have investigated the prognostic value of the pretreatment mean ADC in predicting treatment response, progression-free survival and overall survival in 46 patients who underwent radioembolization for unresectable colorectal cancer liver metastases. The mean post-treatment ADC values were increased by 23% on average. Patients with progressive disease had significantly lower tumor ADC values than patients with tumor response ($p=0.04$). A cut-off value for distinguishing long- and short-term survivors was estimated to be a tumor ADC value of 935. The difference in survival between patients below and above this threshold was significant (3 months versus 5 months) (97). These findings seem to be of great potential, but they have to be confirmed in larger prospective series. Due to the absence of uniform DWI protocols, these results cannot be translated to DWI assessments in other centers.

Recently, the use of perfusion imaging has emerged. This is based on the assumption that tumors with a higher arterial flow would receive a greater number of microspheres and respond better to treatment. CT perfusion parameters are well correlated with histopathologically determined tumor vascularity. Morsbach et al. have analyzed 40 patients who underwent radioembolization for hepatic metastases of various tumors. They found a significant difference between responders and non-responders in arterial perfusion, with the latter being much higher in responders (98).

Using dynamic contrast-enhanced (DCE) sequences, tumor perfusion can also be quantified on MRI images (96). In a multivariate analysis of prognostic factors in 45 patients with neuroendocrine neoplasms, Sommer et al. found that the vascularization of hepatic metastases is of great prognostic significance, with hypervascularized metastases showing a significantly longer progression-free survival (99).

7.2. Functional imaging with ^{18}FDG-PET CT and somatostatin receptor analogue

Functional imaging modalities may overcome the drawbacks of morphologic based treatment assessment. The backbone of oncologic imaging is ^{18}F-FDG-PET. Most malignancies have a high FDG uptake and this can be assessed both qualitatively and quantitatively during follow up.

However, not all tumors show a high FDG uptake. Neuro-endocrine neoplasms G1/2 (Ki67<20%) are not well visualized by ^{18}F-FDG-PET imaging. These tumors express somatostatin receptors and this has led to the development of molecular imaging with radiolabelled somatostatin analogues. Gallium-68 is a positron-emitting isotope and a ^{68}Ga-somatostatin analogue (^{68}Ga-DOTATATE/-TOC/-NOC) PET scan is proven to be superior to ^{18}F-FDG-PET imaging in the detection and follow up of neuro-endocrine neoplasms (100, 101).

7.3. Response evaluation

There is a variety of established response criteria. Most are based on the change in size of lesions, but since the rise of functional imaging also quantitative response criteria have been determined. The most widely used criteria, the RECIST, mRECIST and PERCIST, will be briefly discussed.

7.3.1. RECIST 1.1.

The Response Evaluation Criteria In Solid Tumors (RECIST) have been developed in 2000 and were revised in 2009. The rationale behind these criteria is that objective response (shrinkage of the tumor) and time to progression are important endpoints in clinical trials. These endpoints are used to measure treatment effect, and tumor shrinkage is believed to positively influence overall survival.

At baseline, two target lesions per organ, with a maximum of five lesions in total, have to be chosen. The longest diameter of the lesions must be measured and the lesions should be at least 10 mm in size if the CT scan has a slice thickness ≤5 mm. Usually, the biggest and most well-defined lesions are chosen as target lesions.

The sum of diameters should be recorded and this parameter is used as a reference. At follow-up evaluation, the same target lesions must be evaluated. Complete response is defined as a disappearance of all target lesions. Partial response is classified as a ≥30% decrease in the sum of diameters of target lesions. Progressive disease is characterized by a ≥20% increase in the sum of diameters of target lesions. The sum must also demonstrate an absolute increase of ≥5 mm, and the appearance of a new lesion denotes progression as well. Stable disease, at last, is depicted by an increase in diameter of target lesions of <20% or a decrease of <30% (102).

Limitations of the RECIST criteria are that the thresholds for response and progression are arbitrarily chosen (sometimes a small change in size can already have quite some influence on overall survival) and that there is a large inter-observer variability (103). Furthermore, necrosis (i.e. an effect that regularly occurs after loco-regional treatments) is included in the target lesion, leading to an overestimation of remaining tumor load (104).

7.3.2. mRECIST

The modified RECIST (mRECIST) criteria have been developed for the evaluation of hepatocellular carcinoma (HCC). They take into account the tumor necrosis induced by treatment. Viable tumor shows an uptake of contrast agent in the arterial phase on contrast-enhanced CT or MRI.

Just as the RECIST criteria, target lesions are defined at baseline. An HCC lesion should be ≥10 mm, measurable, well-defined, and should have intratumoral arterial enhancement on contrast-enhanced CT or MRI. Response categories are defined like the RECIST response categories with the alteration that only the viable, enhancing part of the lesions should be measured. Not all HCC lesions show arterial enhancement or are well-defined. For those lesions, conventional RECIST criteria must be used (103, 105). mRECIST could also be used for other hypervascular tumors, like neuro-endocrine neoplasms, however need to be validated in future studies.

7.3.3. PERCIST 1.0

Metabolic tumor response can be assessed using the Positron Emission Tomography (PET) Response Criteria in Solid Tumors (PERCIST 1.0) criteria. At

baseline, measurement of the 'hottest' single tumor and background area is required. The background data are needed to establish the right threshold for the standardized uptake value (SUV) of a lesion at baseline. The SUV is corrected for lean body mass and abbreviated as 'SUL'. A single target lesion is chosen at each time point during follow-up, because the most metabolically active tumor focus corresponds to the most aggressive portion of the tumor. The tumor portion with the highest average SUL value, along with the activity in the surrounding 1 cm^3, is recorded as SULpeak. PERCIST 1.1. categories for response are a bit more elaborate than the RECIST response categories. Complete response is the complete resolution of FDG uptake of the target lesion, with the uptake of all other lesions returning to background values as well. Partial metabolic response is a decrease of ≥30% and of ≥0.8 SUL units between the most intense lesion at follow-up and the most intense lesion at baseline. This is not necessarily the same lesion. Furthermore, there should be no new lesions compared to baseline and no increase of ≥30% in size of a non-target lesion. Stable metabolic disease is defined as an increase or decrease in SULpeak of <30%. Progressive disease, finally, is characterized by an increase ≥30% and of ≥0.8 SUL units in a target lesion, or by the development of a new lesion (106).

7.3.4. Comparison of RECIST and PERCIST criteria

In a recent review, Min et al. have analyzed six studies that compared RECIST and PERCIST response criteria. Overall, there was moderate agreement of tumor response between the two criteria (linear weighted kappa=0.59, 95%CI = 0.52-0.66) and in almost 38% there was discordance in response category. Overall response rates were 35.1% by the RECIST and 54.1% by the PERCIST criteria. Thus, the PERCIST criteria significantly increased the overall tumor response rate. An example of a difference in response according to the RECIST and PERCIST criteria after radioembolization is depicted in Figure 9a-d. This figure shows images of an 80-year-old woman with metastases of an intrahepatic cholangiocarcinoma who was treated with radioembolization. According to the RECIST 1.1 criteria, the response to treatment would be characterized as SD (stable disease). According to the mRECIST and PERCIST criteria, however, the response to treatment would be characterized as CR (complete response) and CMR (complete metabolic response). Since functional imaging can detect metabolic changes when there are no morphological changes yet, response

evaluation using the PERCIST criteria may be a better mainstay for clinicians (107). However, PERCIST comes with several logistical challenges before allowing physicians to compare baseline and follow-up imaging (108).

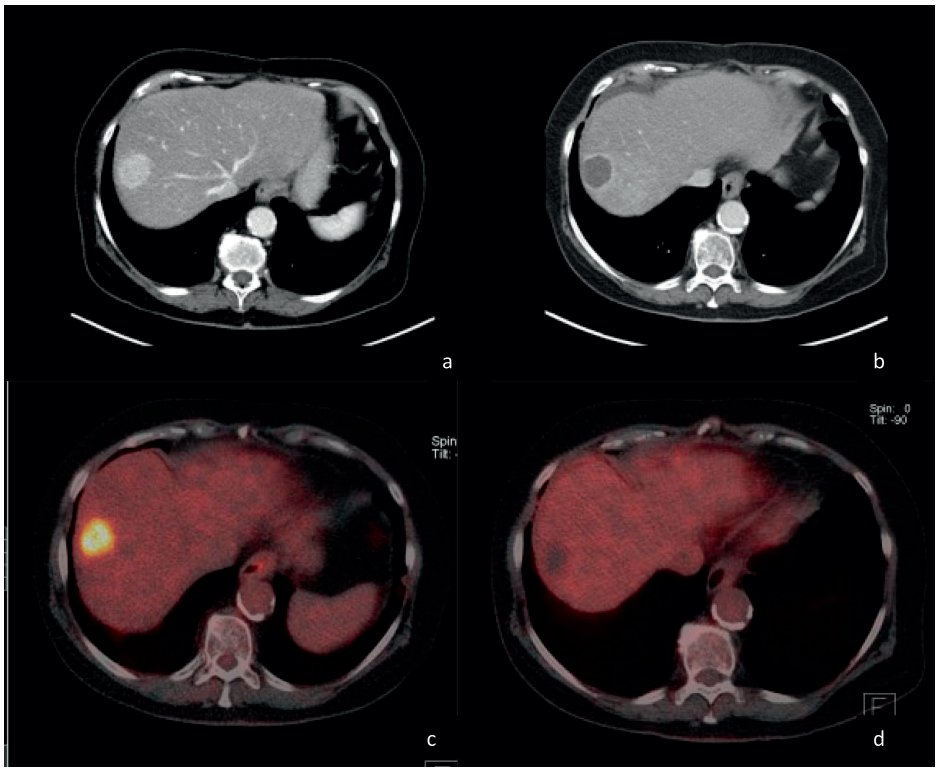

FIGURE 9A-D. Figure a shows a contrast-enhanced CT image of a metastasis of an intrahepatic cholangiocarcinoma in a 80-year-old woman. Figure b shows a contrast-enhanced CT image of the same metastasis 3 months later, after treatment with radioembolization (120 Gy Theraspheres). Figure c shows a baseline PET/CT image of the same metastases. Figure d shows a PET/CT image of the same metastasis 3 months after treatment.

8. RESPONSE

Hepatocellular carcinoma (HCC) is the fifth most common type of cancer and the third cancer-related cause of death worldwide. The incidence is highest in Asia and rising in the US. Risk factors of HCC are hepatitis C virus infection,

hepatitis B virus infection and alcohol abuse. These risk factors can cause chronic liver disease, possibly leading to the development of fibrosis and/or cirrhosis and HCC. (109)

Patients with HCC are classified according to the BCLC staging system. This system is divided in five categories: 0-D, based on performance status, liver function and tumor dimensions. Patients are treated according to the proposed treatment strategy for each BCLC stage (110). Although radioembolization is not incorporated in the treatment algorithm yet, several trials on radioembolization in HCC patients have been conducted. For selected patients, radioembolization could be positioned between TACE and sorafenib (Figure 10).

For patients with BCLC stage 0-A, ablation, resection or liver transplantation are the treatment options of choice. There is a possible role for radioembolization in these stages in the form of radiation segmentectomy. Padia et al. have described superselective radioembolization for patients with unresectable HCC, with a median dose to the treated segments of 254 Gy. Response rates were excellent, with 95% CR and 5% PR. There was no significant hepatoxicity (111). Recently, a retrospective analysis of Biederman et al. has been published. In a cohort of 121 patients with solitary HCC up to 3 cm, 41 patients were treated with radiation segmentectomy and 80 patients were treated with a combination of TACE and microwave ablation (MWA). Target lesion complete response was 87.5% in both groups. Median time to progression was 11.6 months in the TACE MWA group and 11.1 months in the radiation segmentectomy group (p=0.83). Overall progression and overall survival rates were similar in both groups. These findings show that radiation segmentectomy is just as effective as the combination of TACE and MWA in BCLC stage A patients (112).

Radioembolization can be used for down-staging or as a bridge to transplantation. Many patients do not meet the Milan criteria for transplantation (≤5 cm for single lesion or no more than 3 lesions with the largest measuring ≤ 3 cm) (113). Radioembolization can be used to induce a shrinkage of the lesions to render patients eligible for transplantation. Since waiting times for the transplantation list are long, many patients develop progressive disease and are no longer candidates for transplantation. To overcome this, radioembolization can be used to delay progression.

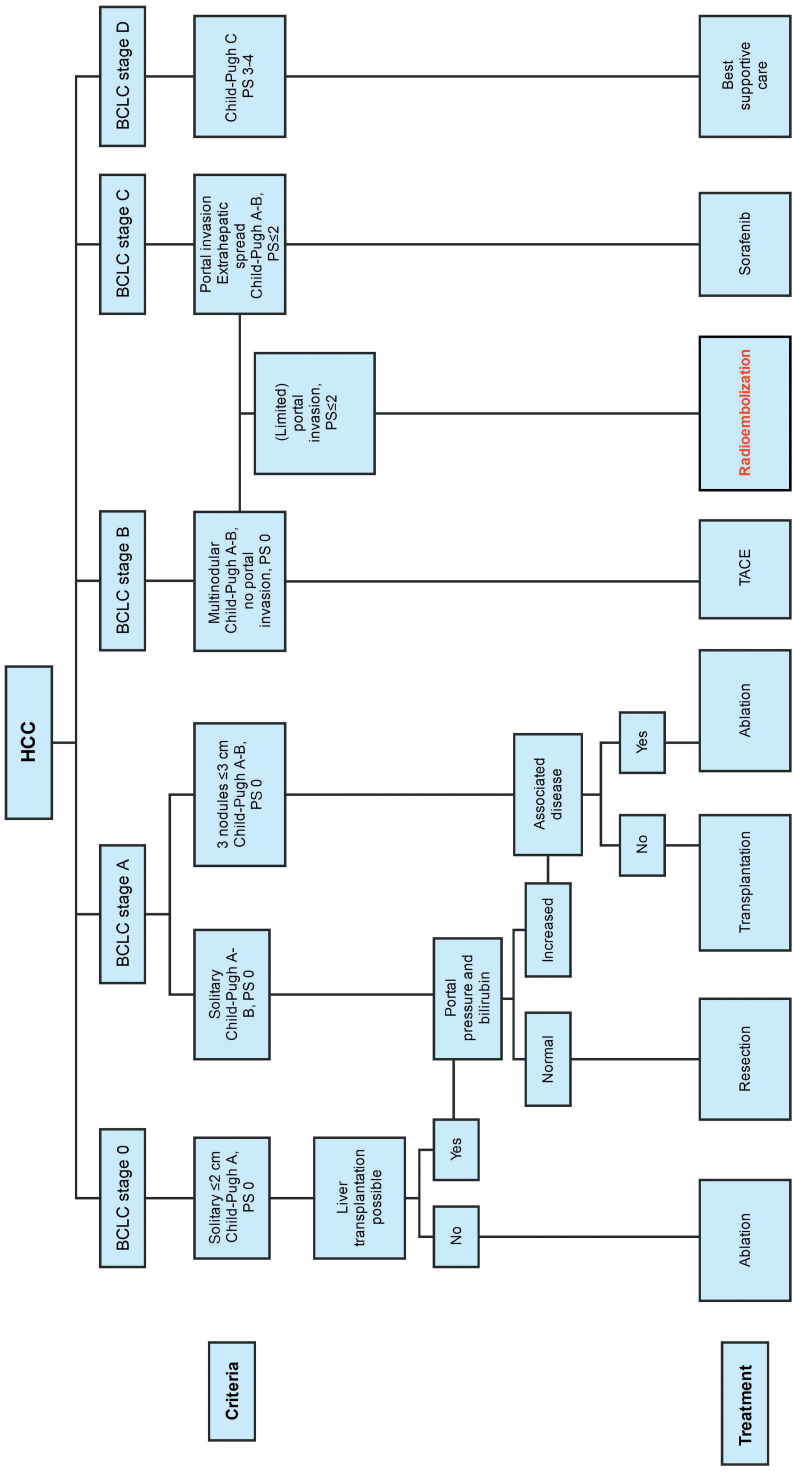

FIGURE 10. Barcelona Clinic Liver Cancer (BCLC) staging system with proposal for radioembolization in the treatment algorithm. PS = performance score.

Tohme et al. describe 20 patients with HCC who were treated with radioembolization as a bridge to transplantation. Radioembolization induced a complete or partial response in 9 of 16 evaluable patients. Histopathologic analysis of the explanted livers showed complete tumor necrosis in 5 cases, 50-99% necrosis in 6 cases and <50% necrosis in 9 cases. Median survival was 75.1 months and there were 4 patients with disease recurrence, of whom one had cancer in the new liver (113). Mohamed et al. have reported their center's experience in using several therapeutic modalities before liver transplantation. In comparison with stereotactic radiotherapy, TACE and RFA, treatment with radioembolization yielded the highest radiologic complete response rate (33% versus 25% for TACE, 8.6% for stereotactic radiotherapy and 22% for RFA) and also the highest proportion of pathologic necrosis (75%, versus 41% for TACE, 28.5% for stereotactic radiotherapy and 60% for RFA). There were 7 patients with disease recurrence after transplantation, but none of them was treated with radioembolization (114).

These findings show that radioembolization can enable patients to remain on the waiting list for transplantation by stabilizing or even down-staging their disease.

To date, several trials with radioembolization have been performed with BCLC stage B and C patients. Transarterial chemoembolization (TACE), the gold standard for BCLC stage B, is not always possible because of a large portal vein main branch tumor thrombus (BCLC stage C). However, this is not an absolute contra-indication for treatment with radioembolization. Furthermore, large tumor size (>10 cm) can be a contra-indication for TACE, whereas for radioembolization, it is not (2).

In a small randomized controlled trial, Kolligs et al. have compared the effectiveness of radioembolization versus TACE as first-line treatment. The disease control rates were slightly higher for radioembolization than for TACE: 76.9% versus 73.3%. The impact on quality of life was comparable (115). The PREMIERE trial is a prospective randomized phase 2 study of TACE versus radioembolization in HCC. Forty-five patients with BCLC stage A/B were included and randomly assigned to TACE (n=21) or radioembolization (n=24). Clinical toxicities and objective response rates were similar in both patient

groups. Median time to progression was 6.4 months in the TACE group and not reached in the radioembolization group (p=0.002). However, this significantly longer time to progression did not translate into a significant difference in overall survival (116).

Katsanos et al. have compared the effectiveness of different transarterial embolization therapies, alone or in combination with local ablative or adjuvant systemic treatments, in patients with HCC. They compared studies investigating bland transarterial embolization (TAE), TACE, chemoembolization with drug-eluting beads (DEB-TACE), TACE+radiotherapy, TACE+ablation, TACE+adjuvant, DEB-TACE+adjuvant and radioembolization with control series. TACE combined with external radiation therapy or percutaneous tumor ablation were found to be the most effective treatment strategies, in terms of overall survival. Radioembolization was proven to be the safest treatment modality with less adverse events and side effects than the other locoregional therapies. Median survival of patients treated with radioembolization was 24.3 months, compared to 13.9 months in the control series with best supportive treatment (117).

In BCLC stage C patients, a portal vein tumor thrombus (PVT) is present, which is a contraindication for surgery and chemoembolization, but not for radioembolization. In a retrospective cohort study of 41 patients, Garin et al. showed that good PVT targeting and a tumor dose ≥205 Gy are significantly correlated with overall survival. Using aimed absorbed dose intensification, a high response rate of 85% was obtained (118). Ali et al. have studied factors influencing survival in BCLC stage C patients treated with radioembolization. Three-hundred forty-five patients were included, of whom 223 had a performance status of 1 and 10 an ECOG performance score of 2. Ninety-six patients had a portal vein tumor thrombus (PVT) before therapy and 16 patients had extrahepatic metastases. The median OS was 10.7 months. Multivariate survival analysis showed that median OS was significantly longer for patients without PVT than for patients with PVT: 15.6 versus 7.3 months, $p<0.0001$. Extrahepatic disease at baseline also significantly influenced median OS: 7.4 versus 12.6 months for patients with and without extrahepatic metastases (119). The presence of PVT as a prognostic factor is confirmed by Floridi et al. who studied radioembolization in patients with mainly BCLC stage B. These patients had a longer median OS of 22.7 months after radioembolization (120).

Recently, two trials have compared radioembolization with sorafenib: the Study to Compare Selective Internal Radiation Therapy (SIRT) Versus Sorafenib in Locally Advanced Hepatocellular Carcinoma (SIRveNIB) and the SorAfenib Versus Radioembolization in Advanced Hepatocellular carcinoma (SARAH) trial (clinicaltrials.gov identifiers NCT01135056 and NCT01482442). The results of the SIRveNIB trial are not published yet, but they have been presented at an international congress. Both trials were developed to identify whether radioembolization improves OS compared to the standard treatment with sorafenib. The results from the SARAH trial showed no significant difference in OS (median OS 8.0 months for radioembolization and 9.9 months for sorafenib in the intention-to-treat groups, and median OS 9.9 months for radioembolization and 9.9 months for sorafenib in the per protocol analysis). Median progression-free survival was a bit longer for the radioembolization group (4.1 versus 3.7 months) but this was not significantly different. However, progression in the liver as first site was significantly lower in the radioembolization group (HR 0.72, 95% CI 0.56-0.93, p=0.01) and tumor response rate was significantly better (19% of evaluable patients in the radioembolization group achieved a complete or partial response, versus 12% of evaluable patients in the sorafenib group (p=0.04). Most important, the number of adverse events was lower with radioembolization and the quality of life over time was significantly better (Figure 11) (121).

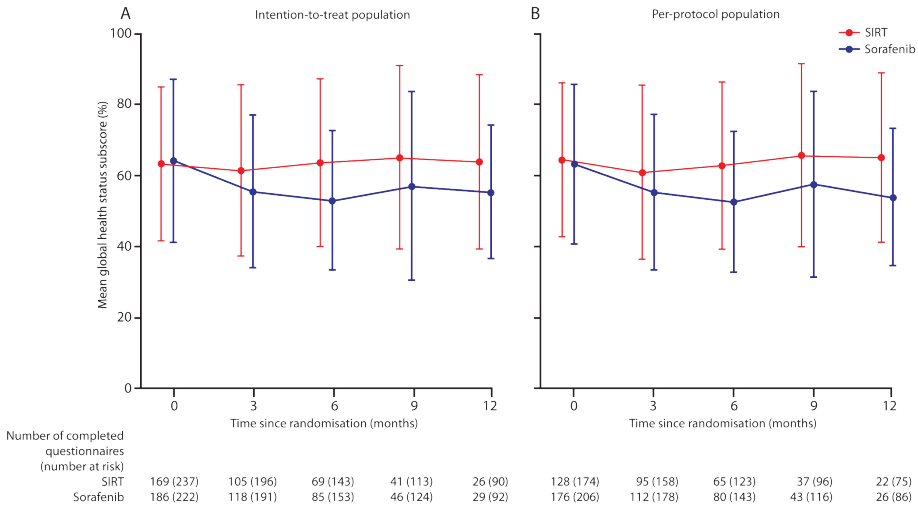

FIGURE 11. Quality of life (as depicted by the mean global health status subscore from the EORTC QLQ-C30 questionnaire) over time of patients treated in the SARAH trial. Reprinted with permission from Elsevier.

In the SIRveNIB trial, there was no significant difference in OS either. Median OS was 8.8 months for radioembolization and 10 months for sorafenib. Tumor-response rate was much better for the radioembolization group: 16.5% versus 1.7% ($p<0.001$) Like the SARAH trial, patients who received radioembolization had significantly fewer (serious) adverse events when compared with those treated with sorafenib (122).

Unfortunately, these trials are not without limitations. In both studies, a larger proportion of patients in radioembolization group did not receive the allocated intervention compared to the patients randomized to sorafenib (SARAH trial: 22.0% versus 4.6%; SIRveNIB trial: 28.6% versus 9.0%) (121, 122). Furthermore, in both studies, the BSA method was used for activity calculation. This method often leads to over- or underdosing and does not differentiate between tumorous and non-tumorous tissue, which may have led to suboptimal treatment outcomes. Also, time to progression in the liver was significantly longer in the radioembolization groups, but progression at any site was comparable or shorter in the radioembolization group. This is not unexpected when comparing a regional versus a systemic therapy and one may advocate the addition of a systemic therapy to radioembolization.

8.1. Metastatic colorectal carcinoma

The majority of patients with hepatic metastases of colorectal carcinoma is not suitable for surgical therapy. Resection of hepatic metastases is the only possible curative treatment option. The 5-year survival is only 10% for patients with unresectable disease. Treatment with radioembolization is possible even after several lines of chemotherapy.

To date, two randomized controlled trials have investigated the value of radioembolization in the salvage setting.

The first trial was published in 2001. This study looked at the added value of radioembolization to hepatic artery chemotherapy with floxuridine versus chemotherapy with floxuridine alone. Tumor response rate and progression free survival was significantly better in the combination group. Moreover, although not significantly different , the five-year survival rates in the combination and chemotherapy group were 3.5% versus 0% (58).

The second study was a phase III trial comparing intravenous fluorouracil infusion alone or with radioembolization in patients with liver-limited metastatic colorectal carcinoma (mCRC). Forty-four patients were treated and median time to liver progression was 2.1 months in the chemotherapy arm, versus 5.5 months in the combination arm. Median OS rates in the treatment arms were 7.3 and 10.0 months, respectively, but this was not significantly different (123).

The MORE study was a large retrospective study of mCRC patients treated with radioembolization. The main findings of this study were that radioembolization offered favorable survival benefits for patients with unresectable mCRC, even after several lines of chemotherapy (124).

Prognostic factors for poorer survival after radioembolization in this salvage setting were ECOG performance status ≥1, baseline extrahepatic metastases, elevated levels of carcinoembryonic antigen (CEA), high tumor to non-tumor ratio, increased lines of chemotherapy, ascites, impaired liver function, lymphovascular invasion of the primary tumor and KRAS mutation (67, 125, 126).

In the first-line setting, three trials investigating the role of radioembolization were performed. In the SIRFLOX, FOXFIRE and FOXFIRE-Global studies, the efficacy of combining first-line chemotherapy (FOLFOX with or without targeted therapy) with radioembolization was evaluated in a randomized setting. The studies were designed for combined analysis of overall survival. Five-hundred forty-nine patients were assigned to FOLFOX alone and 554 patients were assigned to the combination group. The patients that received the combination treatment had a significantly higher objective response (72% versus 63%, p=0.0012), however, this did not translate into a higher median OS. Median OS and overall progression-free survival were comparable between both groups. Therefore, early use of radioembolization in combination with chemotherapy in unselected patients with metastatic colorectal cancer cannot be recommended (127). However, a lot of factors contributing to the result of this combined analysis cannot be ignored, thus the result of these studies should interpreted with caution. The most important factor is the dosimetry. In their study, Wasan et al. have used the BSA method for activity calculation. However, this

method often leads to over- or underdosing. Furthermore, the BSA method does not differentiate between tumorous and non-tumorous tissue, leading to undetermined absorbed doses in these tissues. In the SIRFLOX-, FOXFIRE- and FOXFIRE-Global studies, the tumor-absorbed dose was not optimized, leading to an uncertainty about the true effect of radioembolization in the first-line setting (128).

8.2. Neuro-endocrine neoplasms

Neuro-endocrine neoplasms (NENs) metastasize to the liver in 50-95% of patients (83). Neuro-endocrine neoplasm metastases generally have a high arterial uptake and are therefore excellent candidates for radioembolization (99). To date, several studies about radioembolization for NEN metastases were published. A meta-analysis of 12 studies showed that median OS ranged from 14-70 months, with a median of 28.5 months. The pooled disease control rate was 86%. The wide range in OS may be due to the inclusion of pancreatic NENs in the analysis, because pancreatic NENs generally have a lower survival than NENs from other primary sites (129)Jia et al. have analyzed the outcome of radioembolization in 36 patients with hepatic metastases of NENs. At 3 months follow-up, overall disease control rate (CR, PR or SD) was 88.9%. There were 16 patients with carcinoid syndrome (flushing, diarrhea) and 15 of them experienced symptomatic improvement after treatment. Side effects were mild, with the exception of 2 patients who developed duodenal ulcers. Median OS was 41 months (130).

In a retrospective study, Chansanti et al. have analyzed the tumor-dose relationship in NENs. They included 15 patients with a total of 55 tumors. Primary tumors were located in the pancreas (n=8), the gastrointestinal tract (n=6) and in the lung (n=1). The majority of tumors were hypervascular (80%). Tumor-absorbed dose was estimated using the partition model, as predicted by uptake of ^{99m}Tc-MAA. Mean tumor-absorbed dose was 231.4 Gy and a cutoff value of ≥191 Gy predicted tumor response with 93% specificity. These results show that tumor-absorbed dose estimation based on ^{99m}Tc-MAA uptake is predictive of tumor response and that the partition model can be used for optimal treatment planning (131). Prognostic factors that may influence OS after radioembolization are ECOG score ≥1, higher tumor grade and tumor burden >50% (132).

8.3. Other tumor types

Radioembolization is also increasingly used for hepatic metastases of other primary tumors, such as intrahepatic cholangiocarcinoma, breast carcinoma, pancreatic adenocarcinoma, renal cell carcinoma and uveal melanoma. In all these tumor types, radioembolization shows promising results with limited toxicity (133-137).

9. FUTURE DIRECTIONS

9.1. Retreatment

Radioembolization is usually performed as a mono-therapy (i.e. one shot), after failure of other therapeutic options. However, sometimes there is an indication for repeated radioembolization. Patients may have an impaired liver function after a previous radioembolization treatment, which raises questions regarding safety. Two studies have investigated the safety of repeated radioembolization. Lam et al. describe 8 patients that underwent repeated treatment, defined as multiple treatments to the same target volume. The second procedure was done with a reduced radioactivity dose. The interval between treatments was 203-968 days. After the second treatment, 3 patients had stable disease, 4 patients partial response and 1 patient complete response. After the second radioembolization procedure, two patients developed REILD and deceased shortly after treatment. The authors concluded that a higher administered activity per target volume increased the risk of REILD (138).

Zarva et al. analyzed repeated radioembolization in 21 patients with HCC or hepatic metastases from different primary tumors. Sixteen patients received 3 lobar treatments, 4 patients received 4 lobar treatments and 1 patient received 5 lobar treatments. The interval between sessions was 4-6 weeks. The most frequent adverse events were ascites, elevation of bilirubin or liver enzymes and decrease of serum albumin levels. There were no grade IV or V toxicities. Median time to progression after the first treatment session was 3 months and median OS was 18 months (139).

Despite the possible increased risk of REILD, repeated radioembolization may be a good option for patients with progressive disease after radioembolization.

Careful patient selection should be applied and doses should be calculated with taking into account the administered activity per target volume.

9.2. Advances in dosimetry

The need for optimized dosimetry is more and more emphasized. A huge step forward from the BSA and the MIRD method was made with the invention of the partition method for activity calculation. This method takes into account the mass of the tumors and the liver. However, it does not correct for the difference in tumor and non-tumor expected absorbed dose. Another limitation is that it is difficult to delineate ill-defined tumors. As stated above, a voxel-based method for activity calculation is proposed by Chiesa et al (63). This method uses the ^{99m}Tc-MAA quantification as a surrogate of microsphere distribution and takes non-uniformity of the absorbed dose into account. However, limitations of this voxel-based approach are physical factors such as attenuation, scatter, noise and partial-volume effects, that should be corrected for (64). Garin et al. have developed a personalized dosimetry approach, with an aimed absorbed tumordose of ≥205 Gy. They evaluated the ^{99m}Tc-MAA volume of distribution in the injected liver and tumor and the total injected activity. The injected activities in the tumors and liver were calculated with the MIRD formula, with the end points of attaining a tumor-absorbed dose of ≥205 Gy, a healthy liver absorbed dose of <120 Gy and a lung absorbed dose of <30 Gy. Treatment intensification was performed when the estimated tumor dose would not reach 205 Gy as calculated with the MIRD method (118). In a study of 85 patients with HCC, this method was used for activity calculation. Response rate was 80.3% on lesion-based analysis and 77.5% on patient-based analysis. There was a clear dose-response relationship, with a response rate of 89.7% for tumors with an absorbed dose of ≥205 Gy versus a response rate of 9.1% in tumors with an absorbed dose <205 Gy. Tumor-absorbed dose was also significantly associated with overall survival (p=0.005 on multivariate analysis) (140).

A personalized dosimetric approach is advocated for the treatment of not only HCC patients but also for patients with hepatic metastases. Optimal tumor-absorbed doses and maximum tolerable dose to the healthy liver have to be defined for multiple tumor types.

9.3. Radioembolization as a bridge to surgery

Surgical resection of hepatic tumors offers the best chance of survival. Still, in many patients the future liver remnant (FLR) is deemed too small to preserve enough liver function, and often patients die because of liver failure. To overcome this hepatic failure, different strategies have been developed to increase the FLR, such as portal vein embolization (PVE). The FLR increases with 44-69% already 6-8 weeks after PVE. However, there are reports of patients developing tumors in the embolized and non-embolized lobes, which makes them ineligible for surgery.

Radioembolization also induces hypertrophy of the untreated liver lobe, but this develops at a slower pace. This slower pace allows for the discovery of possible new lesions in the treated lobe and new lesions in the FLR (i.e. biological test of time). Furthermore, contrary to PVE, there is a tumoricidal effect in the treated lobe (141). Goebel et al. have found a mean increase of 36% in FLR volume in a series of 27 patients with HCC. A lower tumor burden, lower Child Pugh score and lower age were associated with a larger increase in FLR volume (142). An example of a patient who underwent radioembolization to induce hypertrophy of the FLR is shown in Figure 12a-d.

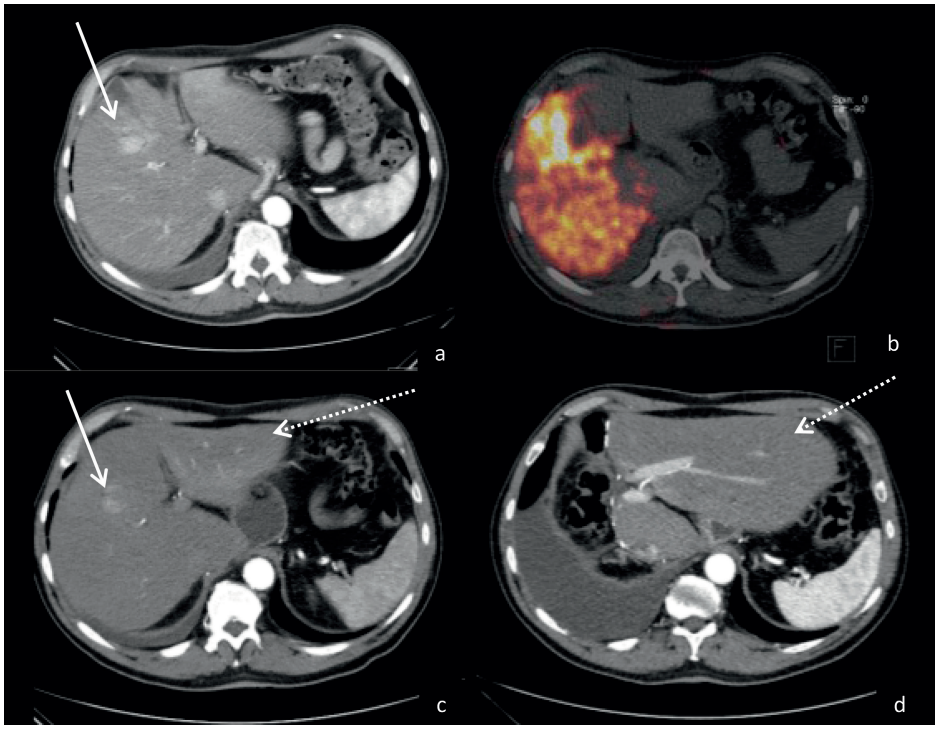

FIGURE 12A-D. Figure a shows a contrast-enhanced CT image of a 60-year old man with an HCC (white arrow). Figure b shows the ^{90}Y-PET CT after treatment with radioembolization of the right hemiliver (120 Gy, Theraspheres). Figure c shows a CT image of a hypertrophied left hemiliver (dotted white arrow), 3 months after radioembolization. Figure d shows a contrast-enhanced CT image of the left hemiliver (dotted white arrow) 4 months after right hemihepatectomy.

9.4. Single-day sessions

Currently, the standard radioembolization treatment algorithm is a work-up with ^{99m}Tc-MAA, followed by administration of the ^{90}Y-microspheres about 2 weeks later. This can be quite burdensome for patients, as they have to visit the hospital multiple times. Furthermore, it is expensive, since in most hospitals, radioembolization is not performed as an outpatient procedure so patients will have to stay the night after treatment.

Gates et al. described the outpatient single-session radioembolization with ^{90}Y-glass microspheres of 14 patients. Before the patients arrived, the hepatic volume and number of primary vessels supplying the treatment volume were

acquired using CT images. Activity vials were ordered assuming a 10% LSF for HCC and 5% LSF for metastatic disease. At the day of treatment, patients underwent the work-up angiographic procedure with administration of ^{99m}Tc-MAA. Within 2 hours, planar scintigraphy was performed and LSF was calculated. Activity was calculated according to the MIRD method and this was done between the scan and the transfer back to the angiography suite, where patients received treatment. Cone-beam CT was used for the evaluation of possible enterohepatic vessels. The mean total procedure time was 2.7 hours. This study shows that single-day treatment is feasible (143). In a letter to the editor, Van den Hoven et al. even advocate to eliminate the LSF calculation in patients with colorectal carcinoma metastases, since these patients seldom have a high LSF (144). However, if one leaves out this work-up procedure, personalized dosimetry based on the distribution of ^{99m}Tc-MAA becomes impossible.

Radioembolization with ^{166}Ho is always performed on a single day in the current clinical trials. Between the work-up procedure and the treatment procedure, the angiography suite is used for other treatments, to increase cost-effectiveness.

9.5. Technical advances

Another option to shorten treatment time is to use simultaneous x-ray and nuclear imaging. This would allow the intervention radiologist to directly identify possible extrahepatic deposition of the microspheres and render the possibility of e.g. adjusting the injection position. A prototype was built with a mobile C-arm and a gamma camera with a four-pinhole collimator (Figure 13). The x-ray detector, the x-ray tube and the gamma camera were all placed in one line to enable imaging of the same field-of-view. Measurements with this prototype have demonstrated the feasibility of simultaneous x-ray and nuclear imaging (145, 146).

Recently, much effort is being put into the development of different catheter types, such as anti-reflux catheters. Advantages of anti-reflux catheters, such as the Surefire catheters with an expandable tip or the Occlusafe catheters with an expandable balloon tip, are the anti-reflux capacities and the fixed catheter tip in the middle of the lumen(147, 148). The anti-reflux mechanism

may obliterate the need for coil-embolization of proximal branches, leading to a reduced procedure time, radiation dose and even costs (149, 150). Furthermore, by affecting the fluid-particle hemodynamics, the fixed catheter tip position may influence the distribution of the microspheres (151, 152).

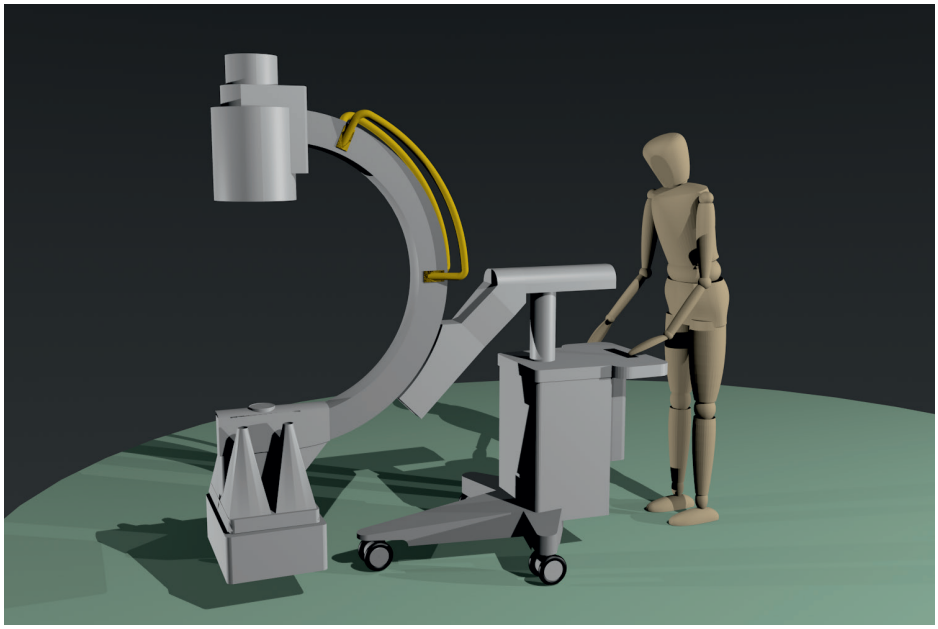

FIGURE 13. This image shows a prototype of the hybrid fluoroscopic and nuclear imaging device. With courtesy to Van der Velden et al.

CONCLUSION

Radioembolization is a minimal invasive therapy during which radioactive microspheres are injected into the hepatic artery. A microcatheter is placed in the hepatic arterial vasculature and millions of microspheres are administered, that selectively irradiate the tumors and relatively spare the healthy liver tissue. The essential steps for radioembolization are a visceral angiography to map the vascular anatomy, followed by a SPECT/CT after administration of a scout dose to assess lung shunt, exclude extrahepatic depositions and assess intrahepatic particle distribution, after which the optimal therapeutic activity is calculated and administered during a second visceral angiography.

Radioembolization is a safe and effective treatment and currently mainly indicated in a palliative setting for unresectable, chemorefractory primary and secondary hepatic malignancies.

Side effects of radioembolization are usually mild and self-limiting.

Within nuclear medicine and interventional oncology, radioembolization is a fast developing field of expertise.

ABBREVIATIONS

^{18}F-FDG	fluor-18 fluorodeoxyglucose
^{68}Ga	gallium-68
^{89}Y	yttrium-89
^{90}Y	yttrium-90
^{90}Sr	strontium-90
^{90}Zr	zirconium-90
^{99m}Tc-MAA	^{99m}Technetium macro-accregated albumin
^{166}Ho	holmium-166
ADC	apparent diffusion coefficient
AE	adverse event
BED_{ave}	biologically effective dose averaged over voxel values
BCLC	Barcelona Clinic Liver Cancer
Bq	Becquerel
BSA	body surface area
CA	cystic artery
CBCT	C-arm cone beam CT
CEA	carcinoembryonic antigen
CHA	common hepatic artery
CMR	complete metabolic response
CT	computed tomography
D	mean absorbed dose
DEB-TACE	chemoembolization with drug-eluting beads
DCE	dynamic contrast-enhanced
dPET	digital photon counting PET
DSA	digital subtraction angiography

DWI	diffusion weighted imaging
EBRT	external beam radiation therapy
ECOG performance status	Eastern Cooperative Oncology Group performance status
EUBED	equivalent uniform biologically effective dose
EUD	equivalent uniform dose
FLR	future liver remnant
FWHM	full-width at half maximum
G5W	glucose 5% water
GBq	Giga Becquerel
GDA	gastroduodenal artery
Gy	Gray
HCC	hepatocellular carcinoma
HFA	hepatic falciform artery
IA	injected activity
keV	kilo electron volt
LHA	left hepatic artery
LSF	lung shunt fraction
MBq	Mega Becquerel
mCRC	metastatic colorectal carcinoma
MeV	mega electron volt
MIRD	Medical Internal Radiation Dose
mRECIST	modified RECIST
MRI	magnetic resonance imaging
MWA	microwave ablation
NEN	neuro-endocrine neoplasm
OS	overall survival
PERCIST	Positron Emission Tomography Response Criteria in Solid Tumors
PET	positron emission tomography
PHA	proper hepatic artery
PSI	pound-force per square inch
PVE	portal vein embolization
PVT	portal vein thrombus
RECIST	Response Evaluation Criteria In Solid Tumors
REILD	radioembolization induced liver disease

RGA	right gastric artery
RHA	right hepatic artery
SIRT	selective internal radiation therapy
SPECT	single photon emission computed tomography
SUL	SUV corrected for lean body mass
SUV	standardized uptake value
TACE	transarterial chemoembolization
TAE	transarterial embolization
T/N ratio	tumor to nontumor ratio
WHO	World Health Organization

REFERENCES

1. Giammarile F, Bodei L, Chiesa C, Flux G, Forrer F, Kraeber-Bodere F, et al. EANM procedure guideline for the treatment of liver cancer and liver metastases with intra-arterial radioactive compounds. Eur J Nucl Med Mol Im. 2011;38(7):1393-406. Epub 2011/04/16.

2. Braat AJ, Smits ML, Braat MN, van den Hoven AF, Prince JF, de Jong HW, et al. (9)(0)Y Hepatic Radioembolization: An Update on Current Practice and Recent Developments. J Nucl Med. 2015;56(7):1079-87. Epub 2015/05/09.

3. Harbert J. Nuclear Medicine Diagnosis and Therapy. Harbert J, editor. New York: Thieme Medical Publishers, Inc.; 1996. 1141-55 p.

4. Wunderlich G, Drews A, Kotzerke J. A kit for labeling of [188Re] human serum albumin microspheres for therapeutic use in nuclear medicine. Applied radiation and isotopes. 2005;62(6):915-8. Epub 2005/04/01.

5. Wunderlich G, Pinkert J, Stintz M, Kotzerke J. Labeling and biodistribution of different particle materials for radioembolization therapy with 188Re. Applied radiation and isotopes. 2005;62(5):745-50. Epub 2005/03/15.

6. Gates VL, Esmail AA, Marshall K, Spies S, Salem R. Internal pair production of 90Y permits hepatic localization of microspheres using routine PET: proof of concept. J Nucl Med. 2011;52(1):72-6. Epub 2010/12/15.

7. Walker LA. Radioactive Yttrium 90: A review of its properties, biological behavior, and clinical uses. Acta Radiologica: Therapy, Physics, Biology. 1964;2(4):302-14.

8. Lewandowski RJ, Salem R. Yttrium-90 radioembolization of hepatocellular carcinoma and metastatic disease to the liver. Semin Intervent Radiol 2006;23(1).

9. Sirtex. SIR-Spheres Y-90 resin microspheres. Sirtex Medical Limited; 2017 [15-09-2017]; Available from: https://www.sirtex.com/media/155126/ssl-us-13.pdf.

10. Ahmadzadehfar H, Muckle M, Sabet A, Wilhelm K, Kuhl C, Biermann K, et al. The significance of bremsstrahlung SPECT/CT after yttrium-90 radioembolization treatment in the prediction of extrahepatic side effects. Eur J Nucl Med Mol Im. 2011. Epub 2011/10/07.

11. Wang XD, Yang RJ, Cao XC, Tan J, Li B. Dose delivery estimated by bremsstrahlung imaging and partition model correlated with response following intra-arterial radioembolization with 32P-glass microspheres for the treatment of hepatocellular carcinoma. J Gastrointest Surg. 2010;14(5):858-66. Epub 2010/03/13.

12. Andrews JC, Walker SC, Ackermann RJ, Cotton LA, Ensminger WD, Shapiro B. Hepatic radioembolization with yttrium-90 containing glass microspheres: preliminary results and clinical follow-up. J Nucl Med. 1994;35(10):1637-44. Epub 1994/10/01.

13. Gray B. Patent application WO 02/34300 A1. Polymer based radionuclide containing particulate material. 2002.

14. Elschot M, Nijsen JF, Dam AJ, De Jong HW. Quantitative evaluation of scintillation camera imaging characteristics of isotopes used in liver radioembolization. PloS One. 2011.

15. van de Maat GH, Seevinck PR, Elschot M, Smits ML, de Leeuw H, van Het Schip AD, et al. MRI-based biodistribution assessment of holmium-166 poly(L-lactic acid) microspheres after radioembolisation. Eur Radiol. 2013;23(3):827-35. Epub 2012/09/28.

16. Nijsen JF, Seppenwoolde JH, Havenith T, Bos C, Bakker CJ, van het Schip AD. Liver tumors: MR imaging of radioactive holmium microspheres--phantom and rabbit study. Radiology. 2004;231(2):491-9. Epub 2004/03/20.

17. Vente MA, Nijsen JF, de Roos R, van Steenbergen MJ, Kaaijk CN, Koster-Ammerlaan MJ, et al. Neutron activation of holmium poly(L-lactic acid) microspheres for hepatic arterial radio-embolization: a validation study. Biomedical microdevices. 2009;11(4):763-72. Epub 2009/02/26.

18. Virdee PS, Moschandreas J, Gebski V, Love SB, Francis EA, Wasan HS, et al. Protocol for Combined Analysis of FOXFIRE, SIRFLOX, and FOXFIRE-Global Randomized Phase III Trials of Chemotherapy +/- Selective Internal Radiation Therapy as First-Line Treatment for Patients With Metastatic Colorectal Cancer. JMIR research protocols. 2017;6(3):e43. Epub 2017/03/30.

19. van Hazel GA, Heinemann V, Sharma NK, Findlay MP, Ricke J, Peeters M, et al. SIRFLOX: Randomized Phase III Trial Comparing First-Line mFOLFOX6 (Plus or Minus Bevacizumab) Versus mFOLFOX6 (Plus or Minus Bevacizumab) Plus Selective Internal Radiation Therapy in Patients With Metastatic Colorectal Cancer. J Clin Oncol. 2016;34(15):1723-31. Epub 2016/02/24.

20. Golfieri R, Bilbao JI, Carpanese L, Cianni R, Gasparini D, Ezziddin S, et al. Comparison of the survival and tolerability of radioembolization in elderly vs. younger patients with unresectable hepatocellular carcinoma. J Hepatol. 2013;59:753-61.

21. Oken MM, Creech RH, Tormey DC, Horton J, Davis TE, McFadden ET, et al. Toxicity and response criteria of the Eastern Cooperative Oncology Group. Am J Clin Oncol. 1982;5(6):649-55.

22. American College of Radiology. CT/MRI LI-RADS v2018.

23. van den Hoven AF, Braat MN, Prince JF, van Doormaal PJ, van Leeuwen MS, Lam MG, et al. Liver CT for vascular mapping during radioembolisation workup: comparison of an early and late arterial phase protocol. Eur Radiol. 2017;27(1):61-9. Epub 2016/04/25.

24. Rosenbaum CE, van den Bosch MA, Veldhuis WB, Huijbregts JE, Koopman M, Lam MG. Added value of FDG-PET imaging in the diagnostic workup for yttrium-90 radioembolisation in patients with colorectal cancer liver metastases. Eur Radiol. 2013;23(4):931-7. Epub 2012/11/01.

25. Yoon KT, Kim JK, Kim DY, Ahn SH, Lee JD, Yun M, et al. Role of 18F-fluorodeoxyglucose positron emission tomography in detecting extrahepatic metastasis in pretreatment staging of hepatocellular carcinoma. Oncology. 2007;72 Suppl 1:104-10. Epub 2007/12/22.

26. Cho Y, Lee DH, Lee YB, Lee M, Yoo JJ, Choi WM, et al. Does 18F-FDG positron emission tomography-computed tomography have a role in initial staging of hepatocellular carcinoma? PloS One. 2014;9(8):e105679. Epub 2014/08/26.

27. Nagaoka S, Itano S, Ishibashi M, Torimura T, Baba K, Akiyoshi J, et al. Value of fusing PET plus CT images in hepatocellular carcinoma and combined hepatocellular and cholangiocarcinoma patients with extrahepatic metastases: preliminary findings. Liver international. 2006;26(7):781-8. Epub 2006/08/17.

28. Park JW, Kim JH, Kim SK, Kang KW, Park KW, Choi JI, et al. A prospective evaluation of 18F-FDG and 11C-acetate PET/CT for detection of primary and metastatic hepatocellular carcinoma. J Nucl Med. 2008;49(12):1912-21. Epub 2008/11/11.

29. Lam MG, Kwee TC, Basu S, Alavi A. Underestimated role of 18F-FDG PET for HCC evaluation and promise of 18F-FDG PET/MR imaging in this setting. J Nucl Med. 2013;54(8):1510-1. Epub 2013/06/20.

30. Sadowski SM, Millo C, Cottle-Delisle C, Merkel R, Yang LA, Herscovitch P, et al. Results of (68)Gallium-DOTATATE PET/CT Scanning in Patients with Multiple Endocrine Neoplasia Type 1. J Ame Coll Surg. 2015;221(2):509-17. Epub 2015/07/25.

31. Van Binnebeek S, Vanbilloen B, Baete K, Terwinghe C, Koole M, Mottaghy FM, et al. Comparison of diagnostic accuracy of (111)In-pentetreotide SPECT and (68)Ga-DOTATOC PET/CT: A lesion-by-lesion analysis in patients with metastatic neuroendocrine tumours. European Radiology. 2016;26(3):900-9. Epub 2015/07/15.

32. Michels NA. Newer anatomy of the liver and its variant blood supply and collateral circulation. Am J Surg. 1966;112(3):337-47.

33. Koops A, Wojciechowski B, Broering DC, Adam G, Krupski-Berdien G. Anatomic variations of the hepatic arteries in 604 selective celiac and superior mesenteric angiographies. SRA. 2004;26(3):239-44. Epub 2004/02/18.

34. Hiatt JR, Gabbay J, Busuttil RW. Surgical Anatomy of the Hepatic Arteries in 1000 Cases. Ann Surg. 1994;220(1):50-2.

35. Gruttadauria S, Foglienie S, Doria C, Luca A, Lauro A, Marino IR. The hepatic artery in liver transplantation and surgery: vascular anomalies in 701 cases. Clin Transplant. 2001;15:359-63.

36. Braat MN, van den Hoven AF, van Doormaal PJ, Bruijnen RC, Lam MG, van den Bosch MA. The Caudate Lobe: The Blind Spot in Radioembolization or an Overlooked Opportunity? Cardiovasc Interv Radiol. 2016;39(6):847-54. Epub 2016/03/24.

37. van den Hoven AF, van Leeuwen MS, Lam MG, van den Bosch MA. Hepatic arterial configuration in relation to the segmental anatomy of the liver; observations on MDCT and DSA relevant to radioembolization treatment. Cardiovasc Interv Radiol. 2015;38(1):100-11. Epub 2014/03/08.

38. van den Hoven AF, Smits ML, de Keizer B, van Leeuwen MS, van den Bosch MA, Lam MG. Identifying aberrant hepatic arteries prior to intra-arterial radioembolization. Cardiovasc Interv Radiol. 2014;37(6):1482-93. Epub 2014/01/29.

39. Spreafico C, Morosi C, Maccauro M, Romito R, Lanocita R, Civelli EM, et al. Intrahepatic flow redistribution in patients treated with radioembolization. Cardiovasc Interv Radiol. 2015;38(2):322-8. Epub 2014/06/15.

40. Abdelmaksoud MH, Hwang GL, Louie JD, Kothary N, Hofmann LV, Kuo WT, et al. Development of new hepaticoenteric collateral pathways after hepatic arterial skeletonization in preparation for yttrium-90 radioembolization. J Vasc Interv Radiol. 2010;21(9):1385-95. Epub 2010/08/07.

41. Bishay VL, Biederman DM, Ward TJ, van der Bom IMJ, Patel RS, Kim E, et al. Transradial Approach for Hepatic Radioembolization: Initial Results and Technique. Am J Roentgenol. 2016;207(5):1112-21.

42. Theysohn JM, Ruhlmann M, Muller S, Dechene A, Best J, Haubold J, et al. Radioembolization with Y-90 Glass Microspheres: Do We Really Need SPECT-CT to Identify Extrahepatic Shunts? PloS One. 2015;10(9):e0137587. Epub 2015/09/04.

43. Bapst B, Lagadec M, Breguet R, Vilgrain V, Ronot M. Cone Beam Computed Tomography (CBCT) in the Field of Interventional Oncology of the Liver. Cardiovasc Interv Radiol. 2016;39(1):8-20. Epub 2015/07/17.

44. van den Hoven AF, Prince JF, de Keizer B, Vonken EJ, Bruijnen RC, Verkooijen HM, et al. Use of C-Arm Cone Beam CT During Hepatic Radioembolization: Protocol Optimization for Extrahepatic Shunting and Parenchymal Enhancement. Cardiovasc Interv Radiol. 2016;39(1):64-73. Epub 2015/06/13.

45. Grozinger G, Kupferschlager J, Dittmann H, Maurer M, Grosse U, la Fougere C, et al. Assessment of the parenchymal blood volume by C-arm computed tomography for radioembolization dosimetry. Eur J Radiol. 2016;85(9):1525-31. Epub 2016/08/10.

46. Garin E, Rolland Y, Laffont S, Edeline J. Clinical impact of (99m)Tc-MAA SPECT/CT-based dosimetry in the radioembolization of liver malignancies with (90)Y-loaded microspheres. Eur J Nucl Med Mol Im. 2016;43(3):559-75. Epub 2015/09/05.

47. Van de Wiele C, Maes A, Brugman E, D'Asseler Y, De Spiegeleer B, Mees G, et al. SIRT of liver metastases: physiological and pathophysiological considerations. European journal of nuclear medicine and molecular imaging. 2012;39(10):1646-55. Epub 2012/07/18.

48. Wondergem M, Smits ML, Elschot M, de Jong HW, Verkooijen HM, van den Bosch MA, et al. 99mTc-macroaggregated albumin poorly predicts the intrahepatic distribution of 90Y resin microspheres in hepatic radioembolization. J Nucl Med. 2013;54(8):1294-301. Epub 2013/06/12.

49. Haste P, Tann M, Persohn S, LaRoche T, Aaron V, Mauxion T, et al. Correlation of Technetium-99m Macroaggregated Albumin and Yttrium-90 Glass Microsphere Biodistribution in Hepatocellular Carcinoma: A Retrospective Review of Pretreatment Single Photon Emission CT and Posttreatment Positron Emission Tomography/CT. J Vasc Interv Radiol. 2017;28(5):722-30 e1. Epub 2017/02/28.

50. Ilhan H, Goritschan A, Paprottka P, Jakobs TF, Fendler WP, Todica A, et al. Predictive Value of 99mTc-MAA SPECT for 90Y-Labeled Resin Microsphere Distribution in Radioembolization of Primary and Secondary Hepatic Tumors. J Nucl Med. 2015;56(11):1654-60. Epub 2015/09/01.

51. Gnesin S, Canetti L, Adib S, Cherbuin N, Silva Monteiro M, Bize P, et al. Partition Model-Based 99mTc-MAA SPECT/CT Predictive Dosimetry Compared with 90Y TOF PET/CT Posttreatment Dosimetry in Radioembolization of Hepatocellular Carcinoma: A Quantitative Agreement Comparison. J Nucl Med. 2016;57(11):1672-8. Epub 2016/11/03.

52. Smits ML, Elschot M, Sze DY, Kao YH, Nijsen JF, Iagaru AH, et al. Radioembolization dosimetry: the road ahead. Cardiovasc Interv Radiol. 2015;38(2):261-9. Epub 2014/12/30.

53. Elschot M, Nijsen JF, Lam MG, Smits ML, Prince JF, Viergever MA, et al. ((9)(9)m)Tc-MAA overestimates the absorbed dose to the lungs in radioembolization: a quantitative evaluation in patients treated with (1)(6)(6)Ho-microspheres. Eur J Nucl Med Mol Im. 2014;41(10):1965-75. Epub 2014/05/14.

54. Braat A, Prince JF, van Rooij R, Bruijnen RCG, van den Bosch M, Lam M. Safety analysis of holmium-166 microsphere scout dose imaging during radioembolisation work-up: A cohort study. Eur Radiol. 2017. Epub 2017/08/09.

55. Yu N, Srinivas SM, Difilippo FP, Shrikanthan S, Levitin A, McLennan G, et al. Lung dose calculation with SPECT/CT for (9)(0)Yittrium radioembolization of liver cancer. Int J Rad Oncol Biol Phys. 2013;85(3):834-9. Epub 2012/08/09.

56. Kao YH, Magsombol BM, Toh Y, Tay KH, Chow PKH, Goh ASW, et al. Personalized predictive lung dosimetry by technetium-99m macroaggregated albumin SPECT/CT for yttrium-90 radioembolization. EJNMMI research. 2014;4(33).

57. Gaba RC, Zivin SP, Dikopf MS, Parvinian A, Casadaban LC, Lu Y, et al. Characteristics of primary and secondary hepatic malignancies associated with hepatopulmonary shunting. Radiology. 2014;271(2):602-12.

58. Gray B, Van Hazel G, Hope M, Burton M, Moroz P, Anderson J, et al. Randomised trial of SIR-Spheres plus chemotherapy vs. chemotherapy alone for treating patients with liver metastases from primary large bowel cancer. Ann Oncol. 2001;12(12):1711-20.

59. Salem R, Thurston KG. Radioembolization with 90Yttrium microspheres: a state-of-the-art brachytherapy treatment for primary and secondary liver malignancies. Part 1: Technical and methodologic considerations. J Vasc Interv Radiol. 2006;17(8):1251-78. Epub 2006/08/23.

60. Salem R, Thurston KG. Radioembolization with 90yttrium microspheres: a state-of-the-art brachytherapy treatment for primary and secondary liver malignancies. Part 2: special topics. J Vasc Interv Radiol. 2006;17(9):1425-39. Epub 2006/09/23.

61. Salem R, Thurston KG. Radioembolization with yttrium-90 microspheres: a state-of-the-art brachytherapy treatment for primary and secondary liver malignancies: part 3: comprehensive literature review and future direction. J Vasc Interv Radiol. 2006;17(10):1571-93. Epub 2006/10/24.

62. Smits MLJ, Nijsen JFW, van den Bosch MAAJ, Lam MGEH, Vente MAD, Mali WPTM, et al. Holmium-166 radioembolisation in patients with unresectable, chemorefractory liver metastases (HEPAR trial): a phase 1, dose-escalation study. Lancet Oncol. 2012;13(10):1025-34.

63. Chiesa C, Mira M, Maccauro M, Spreafico C, Romito R, Morosi C, et al. Radioembolization of hepatocarcinoma with (90)Y glass microspheres: development of an individualized treatment planning strategy based on dosimetry and radiobiology. Eur J Nucl Med Mol Im. 2015;42(11):1718-38. Epub 2015/06/27.

64. Pacilio M, Ferrari M, Chiesa C, Lorenzon L, Mira M, Botta F, et al. Impact of SPECT corrections on 3D-dosimetry for liver transarterial radioembolization using the patient relative calibration methodology. Medical physics. 2016;43(7).

65. Kennedy A, Nag S, Salem R, Murthy R, McEwan AJ, Nutting C, et al. Recommendations for radioembolization of hepatic malignancies using yttrium-90 microsphere brachytherapy: a consensus panel report from the radioembolization brachytherapy oncology consortium. Int J Rad Oncol Biol Phys. 2007;68(1):13-23. Epub 2007/04/24.

66. Borggreve AS, Landman AJ, Vissers CM, De Jong CD, Lam MG, Monninkhof EM, et al. Radioembolization: Is Prophylactic Embolization of Hepaticoenteric Arteries Necessary? A Systematic Review. Cardiovasc Interv Radiol. 2016;39(5):696-704. Epub 2016/03/05.

67. Boas FE, Ziv E, Yarmohammadi H, Brown KT, Erinjeri JP, Sofocleous CT, et al. Adjuvant Medications That Improve Survival after Locoregional Therapy. J Vasc Interv Radiol. 2017;28(7):971-7 e4. Epub 2017/05/22.

68. Yarmohammadi H, Erinjeri JP, Brown KT. Embolization of metastatic neuroendocrine tumor resulting in clinical manifestations of syndrome of inappropriate secretion of antidiuretic hormone. J Vasc Interv Radiol. 2015;26(4):533-7. Epub 2015/03/26.

69. BTG. TheraSphere Yttrium-90 Glass Microspheres Instructions for Use. [15-09-2017]; Available from: https://www.btg-im.com/BTG/media/TheraSphere-Documents/PDF/10093509-Rev8_English-searchable.pdf.

70. Ahmadzadehfar H, Meyer C, Pieper CC, Bundschuh R, Muckle M, Gartner F, et al. Evaluation of the delivered activity of yttrium-90 resin microspheres using sterile water and 5 % glucose during administration. EJNMMI research. 2015;5(1):54. Epub 2015/10/16.

71. Paprottka KJ, Lehner S, Fendler WP, Ilhan H, Rominger A, Sommer W, et al. Reduced Periprocedural Analgesia After Replacement of Water for Injection with Glucose 5% Solution as the Infusion Medium for 90Y-Resin Microspheres. J Nucl Med. 2016;57(11):1679-84. Epub 2016/11/03.

72. Customer Kit and Delivery Set. QuiremSpheres; 2017 [09-15-2017]; Available from: http://www.quiremspheres.com/customer-kit.html.

73. Services UDoHaH. Common Terminology Criteria for Adverse Events (CTCAE) Version 4.0. . National Cancer Institute. 2010.

74. Braat MN, van Erpecum KJ, Zonnenberg BA, van den Bosch MA, Lam MG. Radioembolization-induced liver disease: a systematic review. Eur J Gastroent Hepatol. 2017;29(2):144-52. Epub 2016/12/08.

75. Mahnken AH. Current status of transarterial radioembolization. World J Radiol. 2016;8(5):449-59. Epub 2016/06/02.

76. Roberson Ii JD, McDonald AM, Baden CJ, Lin CP, Jacob R, Burnett Iii OL. Factors associated with increased incidence of severe toxicities following yttrium-90 resin microspheres in the treatment of hepatic malignancies. World J Gastroenterol. 2016;22(10):3006-14. Epub 2016/03/15.

77. Gabrielson A, Miller A, Banovac F, Kim A, He AR, Unger K. Outcomes and Predictors of Toxicity after Selective Internal Radiation Therapy Using Yttrium-90 Resin Microspheres for Unresectable Hepatocellular Carcinoma. Frontiers in oncology. 2015;5:292. Epub 2016/01/19.

78. Smits ML, van den Hoven AF, Rosenbaum CE, Zonnenberg BA, Lam MG, Nijsen JF, et al. Clinical and laboratory toxicity after intra-arterial radioembolization with (90)y-microspheres for unresectable liver metastases. PloS One. 2013;8(7):e69448. Epub 2013/07/31.

79. Sangro B, Martínez-Urbistondo D, Bester L, Bilbao JI, Coldwell DM, Flamen P, et al. Prevention and treatment of complications of selective internal radiation therapy: Expert guidance and systematic review. Hepatology. 2017;66(3).

80. Lam MG, Banerjee S, Louie JD, Abdelmaksoud MH, Iagaru AH, Ennen RE, et al. Root cause analysis of gastroduodenal ulceration after yttrium-90 radioembolization. Cardiovasc Interv Radiol. 2013;36(6):1536-47. Epub 2013/02/26.

81. Prince JF, van den Hoven AF, van den Bosch MA, Elschot M, de Jong HW, Lam MG. Radiation-induced cholecystitis after hepatic radioembolization: do we need to take precautionary measures? J Vasc Interv Radiol. 2014;25(11):1717-23. Epub 2014/12/03.

82. Braat A, Lam M. No need for prophylactic abdominal ice packing during radioembolization. Cardiovasc Interv Radiol. 2018; 41:200-201.

83. Su YK, Mackey RV, Riaz A, Gates VL, Benson AB, 3rd, Miller FH, et al. Long-Term Hepatotoxicity of Yttrium-90 Radioembolization as Treatment of Metastatic Neuroendocrine Tumor to the Liver. J Vasc Interv Radiol. 2017. Epub 2017/07/05.

84. Pasciak AS, Bourgeois AC, McKinney JM, Chang TT, Osborne DR, Acuff SN, et al. Radioembolization and the Dynamic Role of (90)Y PET/CT. Frontiers in oncology. 2014;4:38. Epub 2014/03/01.

85. Yue J, Mauxion T, Reyes D, Lodge M, Hobbs R, Rong X, et al. Comparison of quantitative Y-90 SPECT and non-time-of-flight PET imaging in post-therapy radioembolization of liver cancer. Medical physics. 2016;43(10):5779.

86. Elschot M, Lam MG, van den Bosch MA, Viergever MA, de Jong HW. Quantitative Monte Carlo-based 90Y SPECT reconstruction. J Nucl Med. 2013;54(9):1557-63. Epub 2013/08/03.

87. Dewaraja YK, Chun SY, Srinivasa RN, Kaza RK, Cuneo KC, Majdalany BS, et al. Improved quantitative 90Y bremsstrahlung SPECT/CT reconstruction with Monte Carlo scatter modeling. Medical physics. 2017;44(12):6364-76.

88. Elschot M, Vermolen BJ, Lam MG, de Keizer B, van den Bosch MA, de Jong HW. Quantitative comparison of PET and Bremsstrahlung SPECT for imaging the in vivo yttrium-90 microsphere distribution after liver radioembolization. PloS One. 2013;8(2):e55742. Epub 2013/02/14.

89. Takahashi A, Himuro K, Yamashita Y, Komiya I, Baba S, Sasaki M. Monte Carlo simulation of PET and SPECT imaging of 90Y. Medical Physics. 2015;42(4):1926-35. Epub 2015/04/04.

90. Bastiaannet R, Viergever MA, de Jong H. Impact of respiratory motion and acquisition settings on SPECT liver dosimetry for radioembolization. Medical Physics. 2017. Epub 2017/07/25.

91. Zade AA, Rangarajan V, Purandare NC, Shah SA, Agrawal AR, Kulkarni SS, et al. 90Y microsphere therapy: does 90Y PET/CT imaging obviate the need for 90Y Bremsstrahlung SPECT/CT imaging? Nucl Med Commun. 2013;34(11):1090-6. Epub 2013/08/15.

92. Willowson KP, Tapner M, Bailey DL. A multicentre comparison of quantitative (90)Y PET/CT for dosimetric purposes after radioembolization with resin microspheres : The QUEST Phantom Study. Eur J Nucl Med Mol Im. 2015;42(8):1202-22. Epub 2015/05/15.

93. Wright CL, Binzel K, Zhang J, Wuthrick EJ, Knopp MV. Clinical feasibility of 90Y digital PET/CT for imaging microsphere biodistribution following radioembolization. Eur J Nucl Med Mol Im. 2017;44(7):1194-7. Epub 2017/04/14.

94. Fowler KJ, Maughan NM, Laforest R, Saad NE, Sharma A, Olsen J, et al. PET/MRI of Hepatic 90Y Microsphere Deposition Determines Individual Tumor Response. Cardiovasc Interv Radiol. 2016;39(6):855-64. Epub 2016/01/02.

95. Eldib M, Oesingmann N, Faul DD, Kostakoglu L, Knesaurek K, Fayad ZA. Optimization of yttrium-90 PET for simultaneous PET/MR imaging: A phantom study. Medical Physics. 2016;43(8):4768. Epub 2016/08/05.

96. Donato H, Franca M, Candelaria I, Caseiro-Alves F. Liver MRI: From basic protocol to advanced techniques. Eur J Radiol. 2017;93:30-9. Epub 2017/07/03.

97. Schmeel FC, Simon B, Luetkens JA, Traber F, Meyer C, Schmeel LC, et al. Prognostic value of pretreatment diffusion-weighted magnetic resonance imaging for outcome prediction of colorectal cancer liver metastases undergoing 90Y-microsphere radioembolization. J Canc Res Clin Oncol. 2017;143(8):1531-41. Epub 2017/03/21.

98. Morsbach F, Sah BR, Spring L, Puippe G, Gordic S, Seifert B, et al. Perfusion CT best predicts outcome after radioembolization of liver metastases: a comparison of radionuclide and CT imaging techniques. Eur Radiol. 2014;24(7):1455-65. Epub 2014/05/13.

99. Sommer WH, Ceelen F, Garcia-Albeniz X, Paprottka PM, Auernhammer CJ, Armbruster M, et al. Defining predictors for long progression-free survival after radioembolisation of hepatic metastases of neuroendocrine origin. Eur Radiol. 2013;23(11):3094-103. Epub 2013/06/29.

100. Mojtahedi A, Thamake S, Tworowska I, Ranganathan D, Delpassand ES. The value of 68Ga DOTATATE PET/CT in diagnosis and management of neuroendocrine tumors compared to current FDA approved imaging modalities: a review of literature. . Am J Nucl Med Mol Imaging. 2014;4(5):426-34.

101. Kayani I, Bomanji JB, Groves A, Conway G, Gacinovic S, Win T, et al. Functional imaging of neuroendocrine tumors with combined PET/CT using 68Ga-DOTATATE (DOTA-DPhe1,Tyr3-octreotate) and 18F-FDG. Cancer. 2008;112(11):2447-55. Epub 2008/04/03.

102. Eisenhauer EA, Therasse P, Bogaerts J, Schwartz LH, Sargent D, Ford R, et al. New response evaluation criteria in solid tumours: revised RECIST guideline (version 1.1). Eur J Cancer. 2009;45(2):228-47. Epub 2008/12/23.

103. Fournier L, Ammari S, Thiam R, Cuenod CA. Imaging criteria for assessing tumour response: RECIST, mRECIST, Cheson. Diagn Interv Im. 2014;95(7-8):689-703. Epub 2014/06/22.

104. Tirkes T, Hollar MA, Tann M, Kohli MD, Akisik F, Sandrasegaran K. Response criteria in oncologic imaging: Review of traditional and new criteria. Radiographics. 2013;33:1323-41.

105. Lencioni R, Llovet JM. Modified RECIST (mRECIST) assessment for hepatocellular carcinoma. Seminars in liver disease. 2010;30(1):52-60. Epub 2010/02/23.

106. Hyun O, Lodge M, Wahl R. Practical PERCIST: A simplified guide to PET response criteria in solid tumors 1.0. Radiology. 2016;280(2):576-84.

107. Min SJ, Jang HJ, Kim JH. Comparison of the RECIST and PERCIST criteria in solid tumours: a pooled analysis and review. Oncotarget. 2016;7(19).

108. Hyun O, Lodge M, Wahl R. Practical PERCIST: a simplified guid to PET response criteria in solid tumors 1.0. Radiology. 2016;280(2):576-84.

109. Magistri P, Tarantino G, Ballarin R, Berretta M, Pecchi A, Ramacciato G, et al. The Evolving Role of Local Treatments for HCC in the Third Millennium. Anticancer research. 2017;37(2):389-401. Epub 2017/02/10.

110. Bruix J, Reig M, Sherman M. Evidence-Based Diagnosis, Staging, and Treatment of Patients With Hepatocellular Carcinoma. Gastroenterology. 2016;150(4):835-53. Epub 2016/01/23.

111. Padia SA, Kwan SW, Roudsari B, Monsky WL, Coveler A, Harris WP. Superselective yttrium-90 radioembolization for hepatocellular carcinoma yields high response rates with minimal toxicity. J Vasc Interv Radiol. 2014;25(7):1067-73. Epub 2014/05/20.

112. Biederman DM, Titano JJ, Bishay VL, Durrani RJ, Dayan E, Tabori N, et al. Radiation Segmentectomy versus TACE Combined with Microwave Ablation for Unresectable Solitary Hepatocellular Carcinoma Up to 3 cm: A Propensity Score Matching Study. Radiology. 2017;283(3):895-905.

113. Tohme S, Sukato D, Chen HW, Amesur N, Zajko AB, Humar A, et al. Yttrium-90 radioembolization as a bridge to liver transplantation: a single-institution experience. J Vasc Interv Radiol. 2013;24(11):1632-8. Epub 2013/10/29.

114. Mohamed M, Katz AW, Tejani MA, Sharma AK, Kashyap R, Noel MS, et al. Comparison of outcomes between SBRT, yttrium-90 radioembolization, transarterial chemoembolization, and radiofrequency ablation as bridge to transplant for hepatocellular carcinoma. Advances in radiation oncology. 2016;1(1):35-42. Epub 2015/12/29.

115. Kolligs FT, Bilbao JI, Jakobs T, Inarrairaegui M, Nagel JM, Rodriguez M, et al. Pilot randomized trial of selective internal radiation therapy vs. chemoembolization in unresectable hepatocellular carcinoma. Liver international 2015;35(6):1715-21. Epub 2014/12/03.

116. Gordon A, Lewandowski R, Hickey R, Kallini J, Gabr A, Sato K, et al. Prospective randomized phase 2 study of chemoembolization versus radioembolization in hepatocellular carcinoma: results from the PREMIERE trial. J Vasc Interv Radiol. 2016;27(3):S61-S2.

117. Katsanos K, Kitrou P, Spiliopoulos S, Maroulis I, Petsas T, Karnabatidis D. Comparative effectiveness of different transarterial embolization therapies alone or in combination with local ablative or adjuvant systemic treatments for unresectable hepatocellular carcinoma: A network meta-analysis of randomized controlled trials. PloS One. 2017;12(9):e0184597. Epub 2017/09/22.

118. Garin E, Rolland Y, Edeline J, Icard N, Lenoir L, Laffont S, et al. Personalized dosimetry with intensification using 90Y-loaded glass microsphere radioembolization induces prolonged overall survival in hepatocellular carcinoma patients with portal vein thrombosis. J Nucl Med. 2015;56(3):339-46. Epub 2015/02/14.

119. Ali R, Gabr A, Abouchaleh N, Al Asadi A, Mora RA, Kulik L, et al. Survival Analysis of Advanced HCC Treated with Radioembolization: Comparing Impact of Clinical Performance Status Versus Vascular Invasion/Metastases. Cardiovasc Interv Radiol. 2017. Epub 2017/09/08.

120. Floridi C, Pesapane F, Angileri SA, De Palma D, Fontana F, Caspani F, et al. Yttrium-90 radioembolization treatment for unresectable hepatocellular carcinoma: a single-centre prognostic factors analysis. Med Oncol. 2017;34(10):174. Epub 2017/09/07.

121. Vilgrain V, Pereira H, Assenat E, Guiu B, Ilonca AD, Pageaux G-P, et al. Efficacy and safety of selective internal radiotherapy with yttrium-90 resin microspheres compared with sorafenib in locally advanced and inoperable hepatocellular carcinoma (SARAH): an open-label randomised controlled phase 3 trial. Lancet Oncol. 2017.

122. Chow PK, Gandhi M. SIRveNIB Clinical Study ASCO Oral Abstract Presentation. 2017.

123. Hendlisz A, Van den Eynde M, Peeters M, Maleux G, Lambert B, Vannoote J, et al. Phase III trial comparing protracted intravenous fluorouracil infusion alone or with yttrium-90 resin microspheres radioembolization for liver-limited metastatic colorectal cancer refractory to standard chemotherapy. J Clin Oncol. 2010;28(23):3687-94. Epub 2010/06/23.

124. Kennedy A, Cohn M, Coldwell DM, Drooz A, Ehrenwald E, Kaiser A, et al. Updated survival outcomes and analysis of long-term survivors from the MORE study on safety and efficacy of radioembolization in patients with unresectable colorectal cancer liver metastases. J Gastrointest Oncol. 2017;8(4):614-24. Epub 2017/09/12.

125. Kennedy AS, Nutting C, Coldwell D, Gaiser J, Drachenberg C. Pathologic response and microdosimetry of (90) Y microspheres in man: review of four explanted whole livers. Int J Rad Oncol Biol Phys. 2004;60(5):1552-63. Epub 2004/12/14.

126. Sofocleous CT, Violari EG, Sotirchos VS, Shady W, Gonen M, Pandit-Taskar N, et al. Radioembolization as a Salvage Therapy for Heavily Pretreated Patients With Colorectal Cancer Liver Metastases: Factors That Affect Outcomes. Clin Colorect Cancer. 2015;14(4):296-305. Epub 2015/08/19.

127. Wasan HS, Gibbs P, Sharma NK, Taieb J, Heinemann V, Ricke J, et al. First-line selective internal radiotherapy plus chemotherapy versus chemotherapy alone in patients with liver metastases from colorectal cancer (FOXFIRE, SIRFLOX and FOXFIRE-Global): a combined analysis of three multicentre, randomised, phase 3 trials. Lancet Oncol. 2017.

128. Braat AJAT, Kappadath SC, Bruijnen RCG, van den Hoven AF, Mahvash A, de Jong HWAM, et al. Adequate SIRT activity dose is as important as adequate chemotherapy dose. Lancet Oncol. 2017;18(11):e636.

129. Devcic Z, Rosenberg J, Braat AJ, Techasith T, Banerjee A, Sze DY, et al. The efficacy of hepatic 90Y resin radioembolization for metastatic neuroendocrine tumors: a meta-analysis. J Nucl Med. 2014;55(9):1404-10. Epub 2014/07/12.

130. Jia Z, Paz-Fumagalli R, Frey G, Sella DM, McKinney JM, Wang W. Single-institution experience of radioembolization with yttrium-90 microspheres for unresectable metastatic neuroendocrine liver tumors. J Gastroenterol Hepatol. 2017;32(9):1617-23. Epub 2017/01/31.

131. Chansanti O, Jahangiri Y, Matsui Y, Adachi A, Geeratikun Y, Kaufman JA, et al. Tumor Dose Response in Yttrium-90 Resin Microsphere Embolization for Neuroendocrine Liver Metastases: A Tumor-Specific Analysis with Dose Estimation Using SPECT-CT. J Vasc Interv Radiol. 2017. Epub 2017/09/11.

132. Chen JX, Rose S, White SB, El-Haddad G, Fidelman N, Yarmohammadi H, et al. Embolotherapy for Neuroendocrine Tumor Liver Metastases: Prognostic Factors for Hepatic Progression-Free Survival and Overall Survival. Cardiovasc Interv Radiol. 2017;40(1):69-80. Epub 2016/10/16.

133. Jia Z, Jiang G, Zhu C, Wang K, Li S, Qin X. A systematic review of yttrium-90 radioembolization for unresectable liver metastases of melanoma. Eur J Radiol. 2017;92:111-5. Epub 2017/06/19.

134. Michl M, Haug AR, Jakobs TF, Paprottka P, Hoffmann RT, Bartenstein P, et al. Radioembolization with Yttrium-90 microspheres (SIRT) in pancreatic cancer patients with liver metastases: efficacy, safety and prognostic factors. Oncology. 2014;86(1):24-32. Epub 2014/01/10.

135. Kim AY, Unger K, Wang H, Pishvaian MJ. Incorporating Yttrium-90 trans-arterial radioembolization (TARE) in the treatment of metastatic pancreatic adenocarcioma: a single center experience. BMC cancer. 2016;16:492. Epub 2016/07/20.

136. Kis B, Shah J, Choi J, El-Haddad G, Sweeney J, Biebel B, et al. Transarterial Yttrium-90 Radioembolization Treatment of Patients with Liver-Dominant Metastatic Renal Cell Carcinoma. J Vasc Interv Radiol. 2017;28(2):254-9. Epub 2016/12/14.

137. Kuei A, Saab S, Cho SK, Kee ST, Lee EW. Effects of Yttrium-90 selective internal radiation therapy on non-conventional liver tumors. World J Gastroenterol. 2015;21(27):8271-83. Epub 2015/07/29.

138. Lam MG, Louie JD, Iagaru AH, Goris ML, Sze DY. Safety of repeated yttrium-90 radioembolization. Cardiovasc Interv Radiol. 2013;36(5):1320-8. Epub 2013/01/29.

139. Zarva A, Mohnike K, Damm R, Ruf J, Seidensticker R, Ulrich G, et al. Safety of repeated radioembolizations in patients with advanced primary and secondary liver tumors and progressive disease after first selective internal radiotherapy. J Nucl Med. 2014;55(3):360-6. Epub 2014/02/12.

140. Garin E, Rolland Y, Pracht M, Le Sourd S, Laffont S, Mesbah H, et al. High impact of macroaggregated albumin-based tumour dose on response and overall survival in hepatocellular carcinoma patients treated with (90) Y-loaded glass microsphere radioembolization. Liver International. 2017;37(1):101-10. Epub 2016/08/16.

141. Braat MN, Samim M, van den Bosch MA, Lam MG. The role of 90Y-radioembolization in downstaging primary and secondary hepatic malignancies: a systematic review. Clin Translat Im. 2016;4:283-95. Epub 2016/08/12.

142. Goebel J, Sulke M, Lazik-Palm A, Goebel T, Dechene A, Bellendorf A, et al. Factors associated with contralateral liver hypertrophy after unilateral radioembolization for hepatocellular carcinoma. PloS One. 2017;12(7):e0181488. Epub 2017/07/15.

143. Gates VL, Marshall KG, Salzig K, Williams M, Lewandowski RJ, Salem R. Outpatient single-session yttrium-90 glass microsphere radioembolization. J Vasc Interv Radiol. 2014;25(2):266-70. Epub 2013/12/18.

144. Van den Hoven AF, Prince JF, Van den Bosch MA, Lam MGEH. Hepatic radioembolization as a true single-session treatment. J Vasc Interv Radiol. 2014;25(7):1143-4.

145. Van der Velden S, Beijst C, Viergever MA, de Jong HW. Simultaneous fluoroscopic and nuclear imaging: impact of collimator choice on nuclear image quality. Medical Physics. 2017;44(1):249-61. Epub 2017/01/04.

146. Beijst C, Elschot M, Viergever MA, De Jong HWAM. Toward simultaneous real-time fluoroscopic and nuclear imaging in the intervention room. Radiology. 2015;278(1):232-8.

147. Occlusafe - Occlusive micro balloon catheter. Terumo Interventional Systems; [05-12-2017]; Available from: http://www.terumo-europe.com/en-emea/interventional-oncology/access-diagnostic-products/balloon-occlusive-catheter/occlusafe%C2%AE-occlusive-micro-balloon-catheter.

148. The Surefire Infusion System. Surefire Medical; [05-12-2017]; Available from: https://surefiremedical.com/products/.

149. Fischman AM, Ward TJ, Patel RS, Arepally A, Kim E, Nowakowski FS, et al. Prospective, randomized study of coil embolization versus Surefire infusion system during yttrium-90 radioembolization with resin microspheres. J Vasc Interv Radiol. 2014;25(11):1709-16. Epub 2014/09/23.

150. Morshedi MM, Bauman M, Rose SC, Kikolski SG. Yttrium-90 resin microsphere radioembolization using an antireflux catheter: an alternative to traditional coil embolization for nontarget protection. Cardiovasc Interv Radiol. 2015;38(2):381-8. Epub 2014/07/06.

151. van den Hoven AF, Lam MG, Jernigan S, van den Bosch MA, Buckner GD. Innovation in catheter design for intra-arterial liver cancer treatments results in favorable particle-fluid dynamics. J Exp Clin Cancer Res. 2015;34:74. Epub 2015/08/02.

152. Aramburu J, Anton R, Rivas A, Ramos JC, Sangro B, Bilbao JI. Computational particle-haemodynamics analysis of liver radioembolization pretreatment as an actual treatment surrogate. Int J Numer Method Biomed Eng. 2017;33(2). Epub 2016/04/03.

Quality of life in patients with liver tumors treated with holmium-166 radioembolization

Caren van Roekel, Maarten L.J. Smits, Jip F. Prince, Rutger C.G. Bruijnen, Maurice A.A.J. van den Bosch, Marnix G.E.H. Lam

Clinical & Experimental Metastasis 2020

ABSTRACT

Background

Holmium-166 radioembolization is a palliative treatment option for patients with unresectable hepatic malignancies. Its influence on quality of life has not been evaluated yet. Since quality of life is very important in the final stages of disease, the aim of this study was to evaluate the effect of holmium-166 radioembolization on quality of life.

Materials and Methods

Patients with hepatic malignancies were treated with holmium-166 radioembolization in the HEPAR I and II studies. The European Organization for Research and Treatment of Cancer QLQ-C30 and LMC21 questionnaires were used to evaluate quality of life at baseline, 1 week, 6 weeks and at 6, 9 and 12 months after treatment. The course of the global health status and symptom and functioning scales were analyzed using a linear mixed model.

Results

Quality of life was studied in a total of 53 patients with a compliance of 94%. Role functioning was the most affected functioning scale. Fatigue and pain were the most affected symptom scales. Changes in almost all categories were most notable at one week after treatment. A higher WHO performance score at baseline decreased global health status, physical functioning, role functioning and social functioning and it increased symptoms of fatigue, dyspnea and diarrhea.

Conclusion

Quality of life in salvage patients with liver metastases treated with holmium-166 radioembolization was not significantly affected over time, although a striking decline was seen during the first week post-treatment. A WHO performance score >0 at baseline significantly influenced quality of life.

Key words: radioembolization, holmium-166, quality of life, hepatic metastases

BACKGROUND

Radioembolizaton (RE) is an intra-arterial therapeutic option for patients with unresectable hepatic malignancies. Tumors within the liver receive their blood supply almost entirely from the hepatic artery whereas the normal liver is supplied mainly from the portal vein. Therefore, infusion of radiolabeled microspheres into the arterial system results in delivery of effective doses of radiation to the tumor without causing intolerable toxicity to the normal liver (1).

Holmium-166-poly(L-lactic acid) (^{166}Ho)-microspheres (QuiremSpheres®, Quirem Medical B.V., The Netherlands) have been developed as an alternative to yttrium-90 (^{90}Y) microspheres. The main advantage of ^{166}Ho-microspheres is the ability to be visualized in-vivo by SPECT and MRI, which enables quantitative biodistribution imaging (2). ^{166}Ho-microspheres have a mean diameter of 30 μm (range 15-60 μm). Overall, RE is safe and well tolerated, with primarily short-term toxicity. Mild clinical side effects of RE consist mainly of abdominal pain, nausea, vomiting, fatigue and fever and usually occur within 4-6 weeks after treatment (post-embolic syndrome) (3, 4). Palliative chemotherapy in the same setting, however, is known to be associated with substantial side effects (5). With the advances in cancer treatment and increased survival, quality of life (QoL) has become increasingly important (6). Tumor-specific therapy can potentially prolong life, but, due to its possible toxicity, may considerably reduce QoL (7). The majority of patients (82-95%) value the impact on QoL of the treatment at least as much as the survival benefit (8, 9). Factors known to influence QoL in cancer patients are, among others, age, gender, cancer type, performance status, and high symptom burden (10-13) In patients with hepatic malignancies, specifically, extrahepatic recurrence is of significant influence on QoL (14). To form an impression of the influence of RE on QoL, we performed a systematic review of the literature (See Figure S1 for the search strategies). The effect of Y90-RE on QoL was investigated in 14 studies (15-28). In most studies, QoL did not change significantly after Y90-RE (Table 1) (15, 17, 19-21, 23, 25, 27). In a minority, QoL either improved (16, 26) or worsened after ^{90}Y-RE (18, 24). The purpose of the current study was to evaluate the effect of ^{166}Ho-RE on QoL. Based on the literature, our hypothesis was that QoL would not be significantly affected by ^{166}Ho-RE, similar to what is known for ^{90}Y-RE. Furthermore, the hypothesis was that QoL may be impaired by the known short-term side-effects of ^{90}Y-RE, i.e. the post-embolization syndrome.

TABLE 1. Overview of literature

First author, year	Treatment arm	Control arm	n (Y-RE/ other)	Primary tumor(s)	RE approach	Questionnaires	Scale range	Timing	Outcome
					Solely Y-RE				
Cosimelli, 2010 (15)	Y-RE	-	14[a]	Colorectal	Whole liver, re-RE in 3 patients	QLQ-C30, QLQ-LMC21, QLQ-CR38	0-100	Baseline, 6 weeks	QoL was not adversely affected
Kalinowski, 2009 (16)	Y-RE	-	9	Neuroendocrine tumour	7 patients whole liver, 2 patients bilobar with re-RE	QLQ-C30, QLQ-LMC21	0-100	Baseline, 3-monthly (up to 44 months)	After 6 months, QoL significantly improved
Salem, 2013 (17)	Y-RE	TACE[b]	29/27	HCC[c]	20 patients lobar, 9 patients segmental	Fact-Hep	0-180	Baseline, 2 weeks, 4 weeks	No significant difference between arms
Steel, 2004 (18)	Y-RE	TACE	14/14	HCC	Whole liver	Fact-Hep	0-180	Baseline, 3 months, 6 months, 1 year	At 3 months, significantly higher QoL scores for Y-RE group than control group. No significant difference at 6 months
Kolligs, 2015 (19)	Y-RE	TACE	8/10[d]	HCC	5 patients lobar, 1 patient segmental, 7 patients whole liver	Fact-Hep	0-180	Baseline, 6 weeks, 12 weeks	No significant difference between groups

TABLE 1. Overview of literature (continued)

First author, year	Treatment arm	Control arm	n (Y-RE/ other)	Primary tumor(s)	RE approach	Questionnaires	Scale range	Timing	Outcome
Cramer, 2016 (23)	Y-RE	-	30	Neuroendocrine tumour	Lobar	Short Form-36 Health Survey Form	0-100	Baseline, 1,3,6,12,24 months	QoL was sustained for up to 24 months following treatment
Vilgrain, 2019 (28)	Y-RE	Sorafenib	184/206	HCC	205 lobar treatments, 81 segmental/ sector treatments	QLQ-C30, EORTC-HCC18	0-100	Baseline, 1 month, 3-monthly (up to 12 months)	Global health status was significantly better in the Y-RE group than in the sorafenib group
Kirchner, 2018 (25)	Y-RE	TACE	21/46	HCC	NR	QLQ-C30, EORTC-HCC18	0-100	Baseline, 2 weeks	QoL was not significantly affected and there was no significant difference between groups
Gill, 2018 (26)	Y-RE	TACE, sorafenib		HCC	NR	Online survey	NR	NR	QoL improved after RE and TACE compared to sorafenib
Xing, 2018 (27)	Y-RE	-	30	HCC	Lobar	Short Form-36 Health Survey Form	0-100	Baseline, 1, 3, 6 months	No significant changes in QoL
					Y-RE + chemo				
Gray, 2001 (20)	Y-RE & 5-FU	5-FU[e]	36/34	Colorectal	Whole liver	Self Assessment Scale		Baseline, 3-monthly (up to 18 months)	No significant difference, in both arms QoL tended to improve

TABLE 1. Overview of literature (continued)

First author, year	Treatment arm	Control arm	n (Y-RE/ other)	Primary tumor(s)	RE approach	Questionnaires	Scale range	Timing	Outcome
Van Hazel, 2004 (21)	Y-RE & 5-FU/LV	5-FU/LV[f]	11/10	Colorectal	Whole liver	FLIC questionnaire, Spitzer index		Baseline, 3-monthly (up to 36 months)	No significant difference between arms
Chow, 2014 (22)	Y-RE & sorafenib	-	29	HCC	20 patients whole liver, 9 patients lobar	EQ-5D Index		Baseline, every month until progression, 6-month intervals after progression	EQ-5D index in BCLC[g] stage B decreased over time, while it increased in BCLC Stage C
Wasan, 2017 (24)	Y-RE & FOLFOX	FOLFOX	554/549	Colorectal	NA[h]	EQ-5D-3L Index	0-1	Baseline, 2-3,6,12,24 months	EQ-5D-3L index decreased over time in both groups, no clinically meaningful differences

[a]: Of 50 included patients, 14 were evaluated for QoL. [b]: Transarterial chemoembolization. [c]: Hepatocellular carcinoma. [d]: 10 patients with missing baseline data were excluded from QoL analysis. [e]: 5-Fluorouracil. [f]: Leucovorin. [g]: Barcelona Clinic Liver Cancer. [h]: Not available.

MATERIALS AND METHODS

Patients and study design

QoL was evaluated in patients included in the HEPAR I and HEPAR II studies (clinicaltrials.gov identifier NCT01031784 and NCT01612325). The inclusion criteria for treatment were exactly the same and the patient population in both studies was comparable (Table S1). In these studies, patients with unresectable, chemorefractory liver metastases of any primary origin and cholangiocarcinoma were included. Patients were eligible if they were diagnosed with liver-dominant disease, had a life expectancy of >3 months, had measurable disease on CT, had adequate liver, renal and bone marrow function, and had a WHO performance score of ≤2. The institutional review board approved these studies and all patients provided written informed consent. The aim of the HEPAR I study was to assess the safety and the maximum tolerated radiation dose of ^{166}Ho-RE. The maximum tolerated dose was found to be 60 Gy and its safety and efficacy was established in the HEPAR II study. A more detailed description of the study designs and the main study results have been published elsewhere (29-31).

Treatment

Patients received a work-up angiography approximately 1 week before treatment in which extra-hepatic vessels were coil-embolized, if necessary. A scout dose of ^{99m}Tc-MAA (150 MBq, Technescan LyoMAA®; Mallinckrodt Medical B.V., Petten, The Netherlands) was administered to assess the extrahepatic and intra-hepatic distribution. After a 1-2 week interval, patients were scheduled for a second and third angiography. The second angiography was planned in the morning, during which patients received a scout dose of ^{166}Ho-microspheres, directly followed by SPECT and MRI. The treatment dose of ^{166}Ho-microspheres was administered that same afternoon and was followed by SPECT and MR image acquisition 3-5 days later (30, 31).

Quality of life assessment

QoL in patients was assessed using the validated European Organization for Research and Treatment of Cancer (EORTC) QLQ-C30 version 3.0 and QLQ-LMC21 questionnaires (32) (33). The EORTC QLQ-C30 contains 30 questions and the EORTC QLQ-LMC21 contains 21 items. They are composed of both multi-item scales and single-item measures: from the questionnaires, a Global Health Status/

Quality of Life (GHS), 5 functioning scales and 22 symptom scores were derived. All but two items are scored on 4-point Likert scales (1: not at all, 2: a little, 3: quite a bit, 4: very much). The two other items are scored on a 7-point linear analogue scale. The raw subscale scores are transformed to a 0-100 scale, where a high score in a functioning scale represents unimpaired functioning and high score in a symptom scale represents a high level of symptomatology. The functioning scales are: physical functioning (PF), role functioning (RF), emotional functioning (EF), cognitive functioning (CF) and social functioning (SF). The symptom scales are: fatigue (FA), nausea and vomiting (NV), pain (PA), dyspnea (DY), insomnia (SL), appetite loss (AP), constipation (CO), diarrhea (DI), financial difficulties (FI)(QLQ-C30); and eating (LMNutri), fatigue (LMCFati), pain (LMCPA), emotional problems (LMCEp), weight loss (LMCWL), taste (LMCTA), dry mouth (LMCDM), sore mouth/tongue (LMCSM), peripheral neuropathy (LMCPN), jaundice (LMCJ), contact with friends (LMCFr), talking about feelings (LMCFeelings), and sex life (LMCSx) (QLQ-LMC21).

Patients received the questionnaires at baseline, 6 weeks and 3 months after treatment. Follow-up in the HEPAR II study was longer, so those patients also received the questionnaires at 6, 9 and 12 months after treatment. The last included 26 patients of the HEPAR II study received an extra questionnaire 1 week after treatment to better reflect patients' transient symptoms shortly after treatment (30, 31).

Response assessment

Response assessment was based on contrast-enhanced CT at 3 months post-treatment, according to the Response Evaluation Criteria in Solid Tumours (RECIST) version 1.1 (34).

Scoring and statistical analysis

Scoring of the questionnaires was performed according to the scoring manual provided by the EORTC (EORTC scoring manual). Missing values were imputed using multiple imputation. Internal consistency of the multi-item scales was determined using Cronbach's alpha.

Kolmogrov-Smirnov and Shapiro-Wilk tests were carried out for all categories at the different time points and showed that the data were not normally distributed ($p \leq 0.001$).

Descriptive analyses were performed to summarize patient demographics and treatment characteristics. A linear mixed-effects regression model was fitted to evaluate the development of QoL, taking into account all available data (35). The influence of the following variables on QoL was tested, as these were believed to be of possible influence on QoL: gender (male versus female), previous treatments (systemic, locoregional, both or none), extrahepatic disease at baseline (yes/no), performance status at baseline (WHO score 0, 1 or 2), primary tumor type (colorectal carcinoma versus other), time and response category (complete response, partial response, stable disease or progressive disease). Random effects were tested based on Akaike's information criterion and fixed effects were tested using a backward stepwise approach.

A relatively conservative P-value ≤0.001 (instead of ≤0.05) was considered statistically significant in order to reduce type I errors (36). Statistical analyses were performed using R (version 3.5.1).

RESULTS

QoL was studied in a total of 53 patients treated with ^{166}Ho-RE between November 2009 and March 2015; 15 patients in the HEPAR I study and 38 patients in the HEPAR II study (Flowchart for study inclusions: Figure S2). Patient characteristics are listed in Table 2.

TABLE 2. Baseline characteristics of treated patients in the HEPAR I and II studies

Characteristic	**Value**
N	
	53
Age (years)	
Median (range)	66 (38-87)
Gender	
Male, %	31 (58%)
Primary tumour – no.	
Colorectal carcinoma	29
Ocular melanoma	8
Cholangiocarcinoma	6
Breast carcinoma	5

TABLE 2. Baseline characteristics of treated patients in the HEPAR I and II studies (continued)

Characteristic	Value
Neuroendocrine tumour	2
Pancreatic cancer	1
Gastric cancer	1
Thymoma	1
Administered activity (MBq)	
Median (range)	6210 (1615-13187)
Aimed whole liver dose (Gray) – no.	
20	6
40	3
60	41
80	3
Previous therapies	
Systemic treatment	43
Locoregional treatment	10
Treatment procedure	
Whole liver	48
Lobar	5
WHO performance status	
0	45
1	7
2	1
Extrahepatic metastases	
Bone	4
Lung	9
Lymph node	8
None	33

Due to the dose-escalating nature of the HEPAR I study, 9 patients received an aimed whole liver dose <60 Gy (i.e. 20 Gy [n=6], 40 Gy [n=3]). The other 44 patients received an aimed whole liver dose of ≥60 Gy. One patient was excluded from response analysis because this patient did not receive contrast at 3-month follow-up CT-scan. Based on 3-month follow-up CT (using the RECIST 1.1 evaluation), 8 patients had partial response and 14 patients had stable disease. The remaining 28 patients had progressive disease.

Compliance

Fifty of 53 patients (94%) filled out the baseline questionnaire and at least 1 follow-up questionnaire. Since patients were withdrawn from the HEPAR II study after diagnosis of progressive disease, there was quite some variability in follow-up time. Three patients failed to fill out the questionnaire at baseline and 3 months after treatment and were therefore excluded from analysis. Three patients failed to fill out a follow-up questionnaire (1 patient at 6 weeks and 2 patients at 6 months after treatment) and these questionnaires were pairwise excluded from analysis. Four patients left a question blank.

Development of QoL

Median and interquartile ranges of all categories at the different time points are listed in table S3 and graphically displayed in Figures 1 and 2 and supplemental figure S3a-d. Cronbach's alpha was determined for the multi-item scales at baseline and at 3 months follow-up and varied from 0.52-0.95 (Table S2).

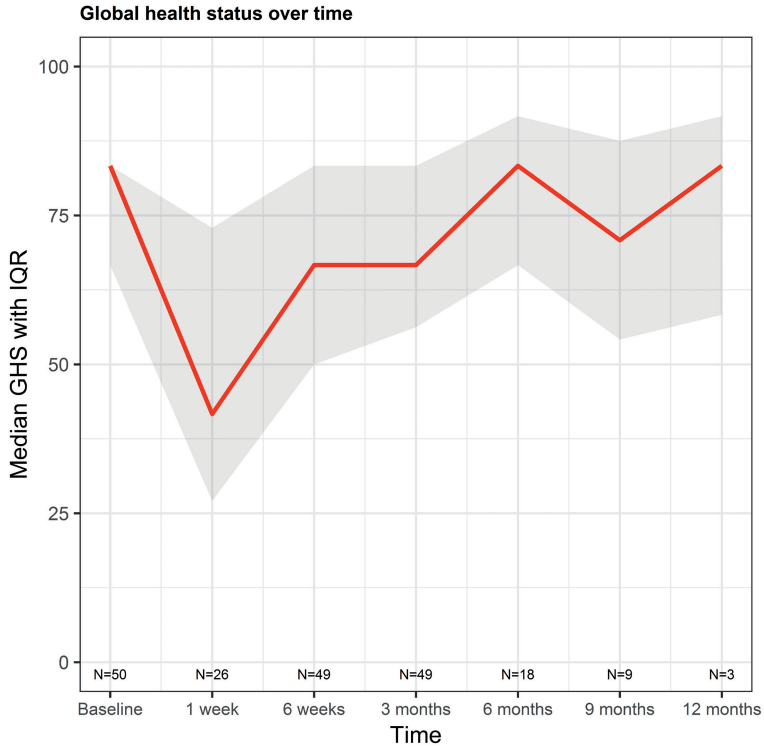

FIGURE 1. Median global health score over time with interquartile range (shaded area). A high score represents a good health score.

From the figures it can be depicted that changes in almost all categories were most notable at one week after treatment. Role functioning was the most affected functioning scale. Fatigue and pain were the most affected symptom scales. Although there were very few patients that filled in the questionnaires beyond three months follow-up, all categories seemed to stabilize over time. At every time point, there was a lot of variation between patients in all categories except FI, LMCSM, LMCJ and LMCFeelings.

The development of QoL was best explained by a linear mixed-effects regression model using a random intercept per patient, to allow for different starting points at baseline.

For GHS, as a general measure of quality of life, an increase of on average 0.55 points per time point was found. However, this was not significant ($p=0.48$) and there was quite some variation between patients, as can be seen in Figure 1. Still, there was a steep decline in functioning scores and rise of symptoms from baseline to 1 week. Patients with a higher WHO performance score had on average 20 points lower GHS ($p=0.0002$, 95% CI [-32.3;-8.8]). No other variables were of significant influence on the development of GHS. Figure 3 shows the development of GHS per patient for patients with WHO performance scores of 0 versus scores 1 or 2. Although there is a lot of variation between patients, patients with a lower WHO performance score have on average a higher QoL.

In functioning scales, PF, RF and SF were significantly influenced by WHO performance status, where a higher WHO performance status at baseline decreased functioning ($p<0.001$ in all categories).

In symptom scales, a higher WHO performance status increased mean symptom scores of FA, DY, DI, and LMCFati ($p<0.001$ in all categories). There were no other variables that had a significant influence on the various symptom scores. Both within and between patients, there was a lot of variation in scores.

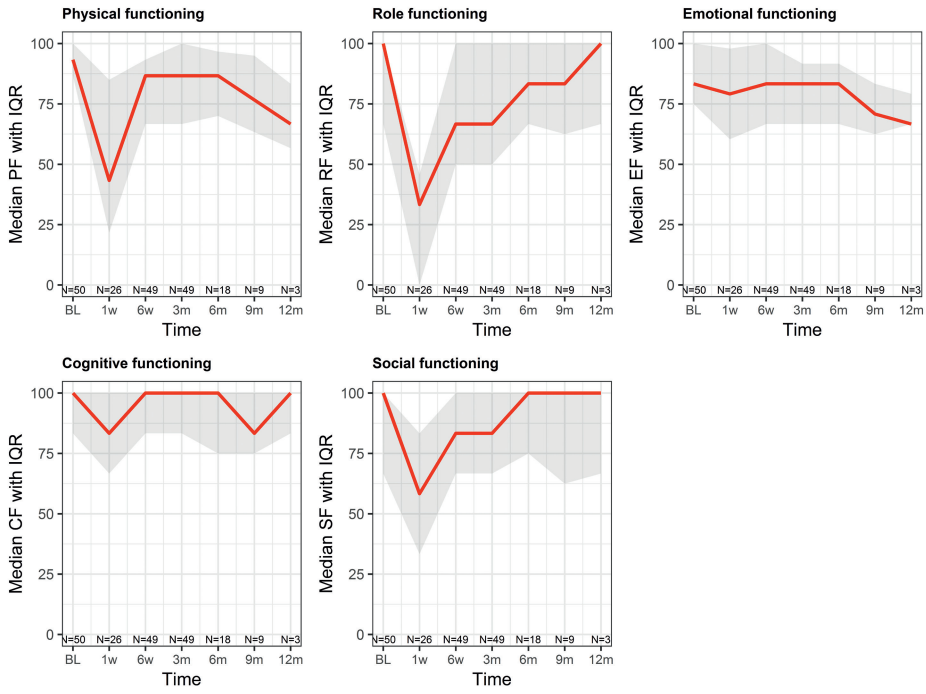

FIGURE 2. Median role functioning scores over time with interquartile ranges (shaded areas). BL = baseline, 1w = 1 week, 6w = 6 weeks, 3m = 3 months, 6m = 6 months, 9m = 9 months, 12m = 12 months. A high score represents good functioning.

DISCUSSION

The purpose of the current study was to evaluate the effect of ^{166}Ho-RE on QoL, which has never been studied before. The hypotheses were that there would be no significant change in QoL over time and that the post-embolization syndrome would have an impact on QoL. This study showed that the first hypothesis was correct: QoL was not significantly affected over time, although there was a lot of variation between and within patients. Regarding the second hypothesis; a decline in QoL and a rise of symptoms was seen at one week post-treatment, which is most likely due to the post-embolization syndrome, however, this was not statistically significantly different from the scores at baseline. In the linear mixed model analysis, it was shown that a higher WHO performance score significantly influenced PF, RF, SF, FA, DY, DI and LMCFati. This is not surprising, as patients with a higher WHO performance score are

known to be in a debilitating physical condition, which likely influences their QoL.

There were no other variables that had a significant influence on QoL.

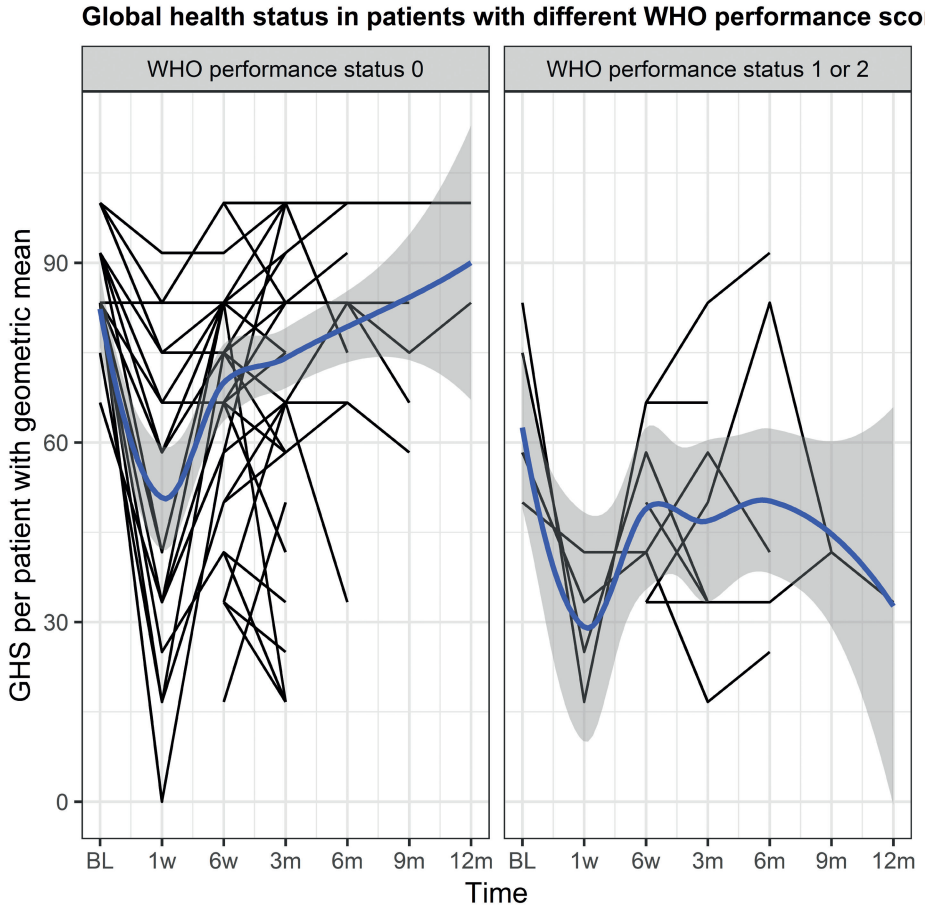

FIGURE 3. Global health status in patients with different WHO performance scores. The black lines depict the development of GHS per patient. The blue lines with shaded area represent the geometric mean with standard deviation. BL = baseline, 1w = 1 week, 6w = 6 weeks, 3m = 3 months, 6m = 6 months, 9m = 9 months, 12m = 12 months.

The GHS score was used as a general measure of QoL and is based on 2 questions. The other 49 questions (i.e. functioning and symptom scores) provide further insights why GHS changed. In this study, role functioning and

social functioning were the most affected functioning scales. Role functioning is based on the patient's ability to perform hobbies or other daily activities. Social functioning is measured to establish if one's family life and social activities are influenced. Factors other than the treatment itself may influence these scores. Social functioning may for instance be affected by the instructions for radiation safety: all RE patients are instructed to keep a safe distance to family and relatives for the first days after treatment. In addition, participation in a clinical study with intensive monitoring and follow-up visits poses a significant time, psychological and physical burden, which may be reflected in decreased role- and social functioning. For the symptom scores, there was a rise in fatigue, pain, appetite loss, eating and contact with friends. The latter is coherent with social functioning. The prominent rise in the pain and fatigue symptom scores is in accordance with the well-known side effects of RE: clinical side effects usually occur within the first 4 to 6 weeks after treatment and may consist of abdominal pain, nausea, vomiting, fatigue and slight fever (3).

In a subset of 26 patients, QoL assessment was added at 1 week post-treatment because it was thought this would better reflect the short-term adverse effects of the treatment. The steep decline in functioning scores and the rise of symptoms from baseline to 1 week is striking. This may be explained by the so-called post-embolization syndrome, which is known to occur after embolization therapies (3, 4, 37). Future interventional oncology studies are encouraged to evaluate QoL shortly after treatment (i.e. <2 weeks).

Due to a large number of differences between the available studies on QoL in patients treated with ^{90}Y-RE and the HEPAR studies, such as the use of different questionnaires, different timing of the QoL evaluations and concomitant treatment with chemotherapy, it is impossible to make a fair comparison. Only 3 studies studied QoL in patients treated with RE as a monotherapy, whereas the others studied RE in combination or in comparison with other therapies. Moreover, in the HEPAR studies, all patients received a whole-liver approach in a single session. This is a more aggressive treatment approach of RE and may have influenced QoL.

A higher number of ^{166}Ho- and ^{90}Y-resin microspheres (somewhere between 30-50 million) are typically injected for treatment in comparison with glass

microspheres (typically several million). ^{166}Ho- and ^{90}Y-resin microspheres will therefore have a larger embolic effect and likely also more post-embolic symptoms such as pain, fever and loss of appetite. The study of Cosimelli et al. is most comparable to the HEPAR I and II studies. Cosimelli et al. reported that QoL was not adversely affected in their cohort of patients with metastatic colorectal carcinoma. However, QoL was not tested shortly after treatment, which is an important difference (15).

The changes in QoL after RE were also investigated in a first-line setting. In the SIRFLOX, FOXFIRE and FOXFIRE-Global studies, the possible role for RE as a first-line treatment was investigated. QoL was assessed in the patient group receiving systemic therapy alone and in the patient group receiving RE as an addition to systemic therapy. QoL was slightly worse in the combination group at 2-3 months follow-up, but this was not deemed clinically meaningful (24).

There are several limitations to this study. First, the total number of patients was limited. Second, there was a large loss to follow-up since patients were excluded from the HEPAR II study after diagnosis of progressive disease. This may also have led to a biased representation of the QoL of our study population and it may explain why response category did not significantly influence QoL in the analyses. Third, the QLQ-LMC21 questionnaire, created for patients with colorectal liver metastases, was used to complement the more general QLQ-C30 questionnaire, although colorectal cancer was not the only tumor type in this study. One of the strengths of this study is its prospective nature and the high compliance rate regarding the QoL questionnaires. QoL was frequently assessed and especially the 1-week post treatment questionnaire offered valuable insight in the short-term effects on QoL and patients' transient symptoms. Another strength of this study is the use of a longitudinal approach for the data analysis. By using a mixed model with a random intercept per patient, the variation between patients and data clustering were taken into account.

More knowledge on the influence of ^{166}Ho-RE on QoL is important for several reasons. Above all, this information is needed to better inform patients on treatment-related adverse effects and may help them to make a well-informed choice between all the available palliative treatment options. In selected

populations, such as older patients or patients with multiple comorbidities, QoL is largely maintained. This can be a reason to prefer RE over other treatment modalities (28). Furthermore, since RE is becoming more important in the first- and second-line settings, the impact of this therapy on QoL is also becoming more significant.

CONCLUSION

In conclusion, QoL in salvage patients with liver metastases treated with ^{166}Ho-RE was not significantly affected over time, apart from a decline during the first week after treatment. Changes in QoL were most notable during the first week post-treatment, probably due to the post-embolization syndrome. A WHO performance score >0 at baseline significantly influenced QoL. Knowledge of the influence on quality of life of ^{166}Ho-RE is important for patients to make a deliberate choice between palliative treatment options.

LIST OF ABBREVIATIONS

^{90}Y	yttrium-90
^{99m}Tc-MAA	technetium ^{99m}Tc macro-aggregated albumin
^{166}Ho	holmium-166
AP	appetite loss
CF	cognitive functioning
CO	constipation
DI	diarrhoea
DY	dyspnoea
EF	emotional functioning
EORTC	European Organization for Research and Treatment of Cancer
FA	fatigue
FI	financial difficulties
GHS	global health status
HCC	hepatocellular carcinoma
LMCDM	dry mouth
LMCEp	emotional problems
LMCFati	fatigue

LMCFeelings	talking about feelings
LMCFr	contact with friends
LMCJ	jaundice
LMCPA	pain
LMCPN	peripheral neuropathy
LMCSM	sore mouth/tongue
LMCSx	sex life
LMCTA	taste
LMCWL	weight loss
LMNutri	eating
MRI	magnetic resonance imaging
NV	nausea and vomiting
PA	pain
PF	physical functioning
QoL	quality of life
RE	radioembolization
RECIST 1.1	Response Evaluation Criteria In Solid Tumours
RF	role functioning
SF	social functioning
SL	insomnia
SPECT	single photon emission computed tomography
WHO	world health organization

REFERENCES

1. Townsend AR, Chong LC, Karapetis C, Price TJ. Selective internal radiation therapy for liver metastases from colorectal cancer. Cancer treatment reviews. 2016;50:148-54. Epub 2016/10/01.

2. Smits ML, Elschot M, van den Bosch MA, van de Maat GH, van het Schip AD, Zonnenberg BA, et al. In vivo dosimetry based on SPECT and MR imaging of ^{166}Ho-microspheres for treatment of liver malignancies. J Nucl Med. 2013;54(12):2093-100. Epub 2013/10/19.

3. Braat AJ, Smits ML, Braat MN, van den Hoven AF, Prince JF, de Jong HW, et al. (9)(0)Y Hepatic Radioembolization: An Update on Current Practice and Recent Developments. J Nucl Med. 2015;56(7):1079-87. Epub 2015/05/09.

4. Riaz A, Awais R, Salem R. Side effects of yttrium-90 radioembolization. Front Oncol. 2014;4:198. Epub 2014/08/15.

5. Tominaga T, Nonaka T, Sumida Y, Hidaka S, Sawai T, Nagayasu T. The C-Reactive Protein to Albumin Ratio as a Predictor of Severe Side Effects of Adjuvant Chemotherapy in Stage III Colorectal Cancer Patients. PloS One. 2016;11(12):e0167967. Epub 2016/12/09.

6. Finlayson CS, Chen YT, Fu MR. The impact of patients' awareness of disease status on treatment preferences and quality of life among patients with metastatic cancer: a systematic review from 1997-2014. J Palliat Med. 2015;18(2):176-86. Epub 2014/09/27.

7. Laryionava K, Sklenarova H, Heussner P, Haun MW, Stiggelbout AM, Hartmann M, et al. Cancer patients' preferences for quantity or quality of life: German translation and validation of the quality and quantity questionnaire. Oncol Res Treat. 2014;37(9):472-8. Epub 2014/09/19.

8. Meropol NJ, Egleston BL, Buzaglo JS, Benson AB, 3rd, Cegala DJ, Diefenbach MA, et al. Cancer patient preferences for quality and length of life. Cancer. 2008;113(12):3459-66. Epub 2008/11/07.

9. Meropol NJ, Weinfurt KP, Burnett CB, Balshem A, Benson AB, 3rd, Castel L, et al. Perceptions of patients and physicians regarding phase I cancer clinical trials: implications for physician-patient communication. J Clin Oncol. 2003;21(13):2589-96. Epub 2003/06/28.

10. Thong MSY, Doege D, Koch-Gallenkamp L, Bertram H, Eberle A, Holleczek B, et al. Age at Diagnosis and Sex Are Associated With Long-term Deficits in Disease-Specific Health-Related Quality of Life of Survivors of Colon and Rectal Cancer: A Population-Based Study. Diseases of the colon and rectum. 2019. Epub 2019/10/01.

11. Heydarnejad MS, Hassanpour Dehkordi A, Solati Dehkordi K. Factors affecting quality of life in cancer patients undergoing chemotherapy. African Health Sciences. 2011;11(2):266-70.

12. Cheng KK, Yeung RM. Symptom distress in older adults during cancer therapy: impact on performance status and quality of life. J Geriatric Oncology. 2013;4(1):71-7. Epub 2013/09/28.

13. Prigerson HG, Bao Y, Shah MA, Paulk ME, LeBlanc TW, Schneider BJ, et al. Chemotherapy Use, Performance Status, and Quality of Life at the End of Life. JAMA Oncology. 2015;1(6):778-84. Epub 2015/07/24.

14. Tohme S, Sanin GD, Patel V, Bress K, Ahmed N, Krane A, et al. Health-Related Quality of Life as a Prognostic Factor in Patients After Resection of Hepatic Malignancies. J Surg Res. 2019;245:257-64. Epub 2019/08/20.

15. Cosimelli M, Golfieri R, Cagol PP, Carpanese L, Sciuto R, Maini CL, et al. Multi-centre phase II clinical trial of yttrium-90 resin microspheres alone in unresectable, chemotherapy refractory colorectal liver metastases. Br J Cancer. 2010;103(3):324-31. Epub 2010/07/16.

16. Kalinowski M, Dressler M, Konig A, El-Sheik M, Rinke A, Hoffken H, et al. Selective internal radiotherapy with Yttrium-90 microspheres for hepatic metastatic neuroendocrine tumors: a prospective single center study. Digestion. 2009;79(3):137-42. Epub 2009/03/25.

17. Salem R, Gilbertsen M, Butt Z, Memon K, Vouche M, Hickey R, et al. Increased quality of life among hepatocellular carcinoma patients treated with radioembolization, compared with chemoembolization. Clin Gastroenterol Hepatol. 2013;11(10):1358-65 e1. Epub 2013/05/07.

18. Steel J, Baum A, Carr B. Quality of life in patients diagnosed with primary hepatocellular carcinoma: hepatic arterial infusion of Cisplatin versus 90-Yttrium microspheres (Therasphere). Psycho-oncology. 2004;13(2):73-9. Epub 2004/02/12.

19. Kolligs FT, Bilbao JI, Jakobs T, Inarrairaegui M, Nagel JM, Rodriguez M, et al. Pilot randomized trial of selective internal radiation therapy vs. chemoembolization in unresectable hepatocellular carcinoma. Liver International. 2015;35(6):1715-21. Epub 2014/12/03.

20. Gray B, Van Hazel G, Hope M, Burton M, Moroz P, Anderson J, et al. Randomised trial of SIR-Spheres plus chemotherapy vs. chemotherapy alone for treating patients with liver metastases from primary large bowel cancer. Ann Oncol. 2001;12:1711-20.

21. Van Hazel G, Blackwell A, Anderson J, Price D, Moroz P, Bower G, et al. Randomised phase 2 trial of SIR-Spheres plus fluorouracil/leucovorin chemotherapy versus fluorouracil/leucovorin chemotherapy alone in advanced colorectal cancer. J Surg Oncol. 2004;88(2):78-85. Epub 2004/10/23.

22. Chow PKHP, D.Y.H.; Khin, M.W.; Singh, H.; Han, H.S.; Goh, A.S.W.; Choo, S.P.; Lai, H.K.; Lo, R.H.G.; Tay K.H.; Lim, T.G.; Gandhi, M.; Tan, S.B.; Soo, K.C. Multicenter Phase II Study of Sequential Radioembolization-Sorafenib Therapy for Inoperable Hepatocellular Carcinoma. PloS one. 2014;9(3).

23. Cramer B, Xing M, Kim HS. Prospective Longitudinal Quality of Life Assessment in Patients With Neuroendocrine Tumor Liver Metastases Treated With 90Y Radioembolization. Clin Nucl Med. 2016;41(12):e493-e7. Epub 2016/10/18.

24. Wasan HS, Gibbs P, Sharma NK, Taieb J, Heinemann V, Ricke J, et al. First-line selective internal radiotherapy plus chemotherapy versus chemotherapy alone in patients with liver metastases from colorectal cancer (FOXFIRE, SIRFLOX and FOXFIRE-Global): a combined analysis of three multicentre, randomised, phase 3 trials. Lancet Oncol. 2017.

25. Kirchner T, Marquardt S, Werncke T, Kirstein MM, Brunkhorst T, Wacker F, et al. Comparison of health-related quality of life after transarterial chemoembolization and transarterial radioembolization in patients with unresectable hepatocellular carcinoma. Abdom Radiol (NY). 2018. Epub 2018/10/13.

26. Gill J, Baiceanu A, Clark PJ, Langford A, Latiff J, Yang PM, et al. Insights into the hepatocellular carcinoma patient journey: results of the first global quality of life survey. Future Oncology. 2018;14(17):1701-10.

27. Xing M, Kokabi N, Camacho JC, Kim HS. Prospective longitudinal quality of life and survival outcomes in patients with advanced infiltrative hepatocellular carcinoma and portal vein thrombosis treated with Yttrium-90 radioembolization. BMC Cancer. 2018;18(1):75. Epub 2018/01/14.

28. Vilgrain V, Pereira H, Assenat E, Guiu B, Ilonca AD, Pageaux G-P, et al. Efficacy and safety of selective internal radiotherapy with yttrium-90 resin microspheres compared with sorafenb in locally advanced and inoperable hepatocellular carcinoma (SARAH): an open-label randomised controlled phase 3 trial. Lancet Oncol. 2019;18(12):1624-36.

29. Smits ML, Nijsen JF, van den Bosch MA, Lam MG, Vente MA, Huijbregts JE, et al. Holmium-166 radioembolization for the treatment of patients with liver metastases: design of the phase I HEPAR trial. J Exp Clin Cancer Res. 2010;29:70. Epub 2010/06/17.

30. Smits MLJ, Nijsen JFW, van den Bosch MAAJ, Lam MGEH, Vente MAD, Mali WPTM, et al. Holmium-166 radioembolisation in patients with unresectable, chemorefractory liver metastases (HEPAR trial): a phase 1, dose-escalation study. Lancet Oncol. 2012;13(10):1025-34.

31. Prince JF, van den Bosch M, Nijsen JFW, Smits MLJ, van den Hoven AF, Nikolakopoulos S, et al. Efficacy of radioembolization with holmium-166 microspheres in salvage patients with liver metastases: a phase 2 study. J Nucl Med. 2017. Epub 2017/09/17.

32. Blazeby JM, Fayers P, Conroy T, Sezer O, Ramage J, Rees M. Validation of the European Organization for Research and Treatment of Cancer QLQ-LMC21 questionnaire for assessment of patient-reported outcomes during treatment of colorectal liver metastases. Br J Surg. 2009;96(3):291-8. Epub 2009/02/19.

33. Fayers P, Bottomley A. Quality of life research within the EORTC - the EORTC QLQ-C30. Eur J Cancer. 2002;38:S125-S33.

34. Eisenhauer EA, Therasse P, Bogaerts J, Schwartz LH, Sargent D, Ford R, et al. New response evaluation criteria in solid tumours: revised RECIST guideline (version 1.1). Eur J Cancer. 2009;45(2):228-47. Epub 2008/12/23.

35. Dragset IG. Analysis of longitudinal data with missing values: Norwegian University of Science and Technology; 2009.

36. Colquhoun D. An investigation of the false discovery rate and the misinterpretation of p-values. Royal Society open science. 2014;1(3):140216. Epub 2015/06/13.

37. Mahnken AH. Current status of transarterial radioembolization. World J Radiol. 2016;8(5):449-59. Epub 2016/06/02.

SUPPLEMENTAL FIGURES

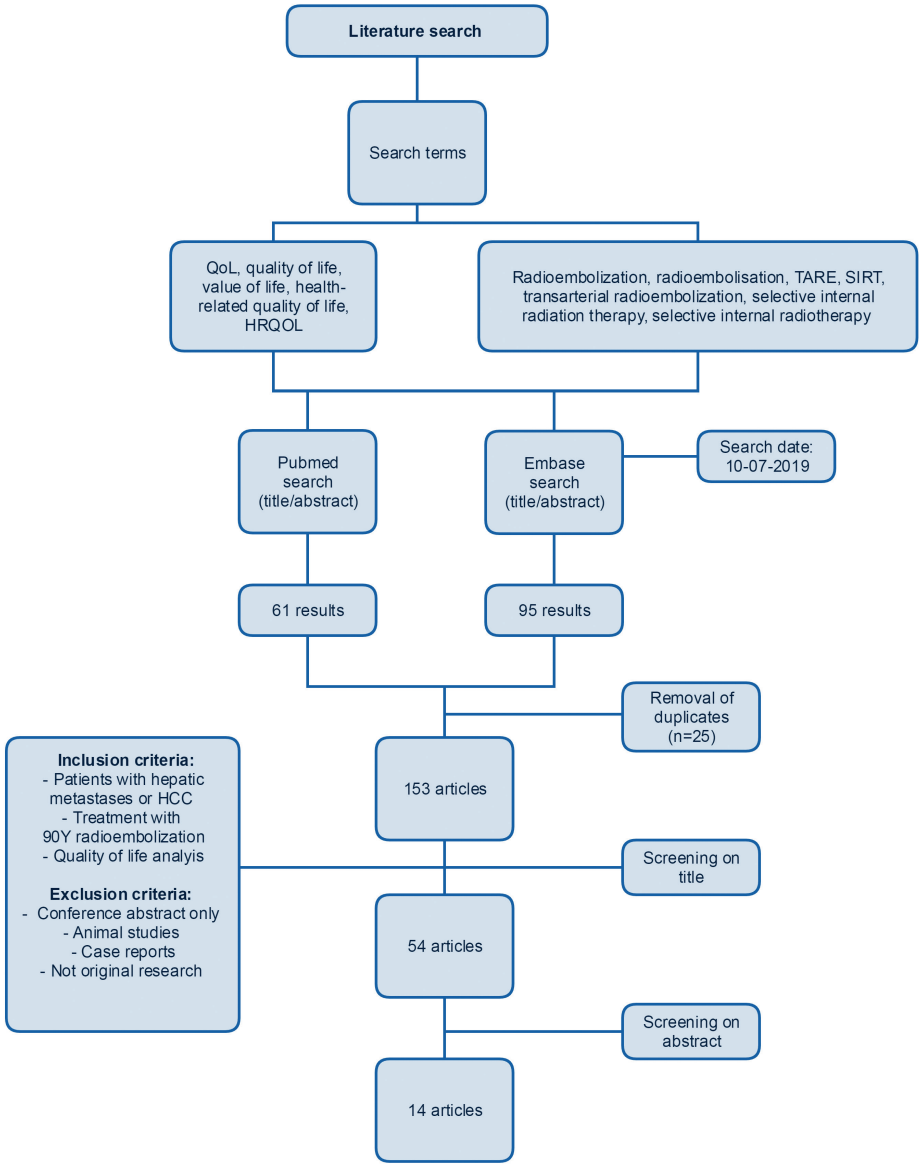

FIGURE S1. Search strategy for literature review of quality of life studies in patients treated with RE.

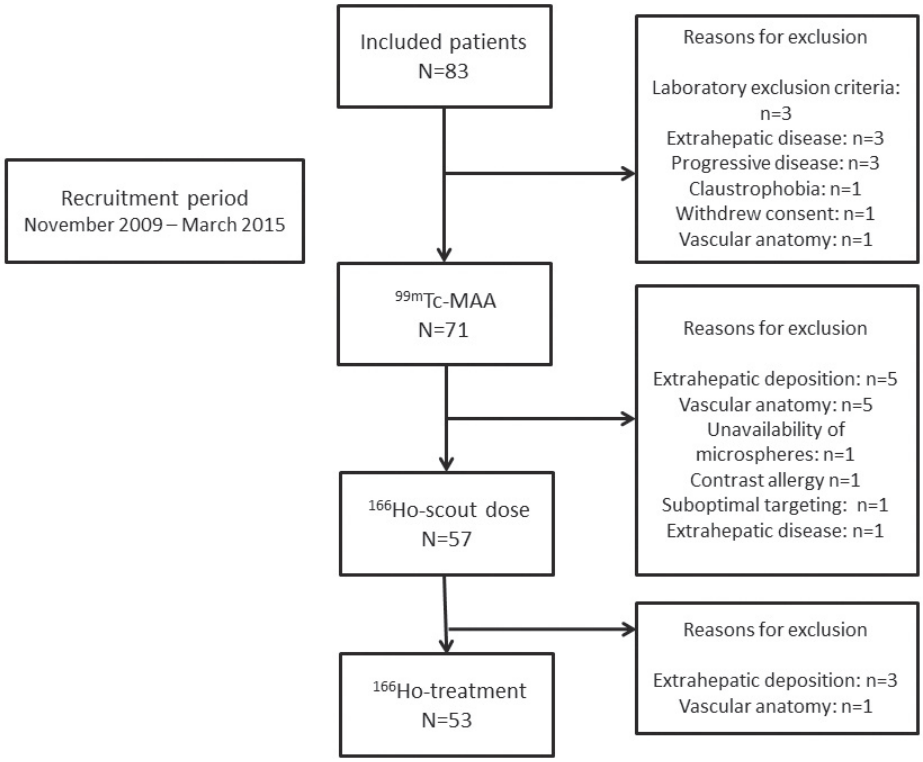

FIGURE S2. Flowchart of included patients in the HEPAR I and II studies.

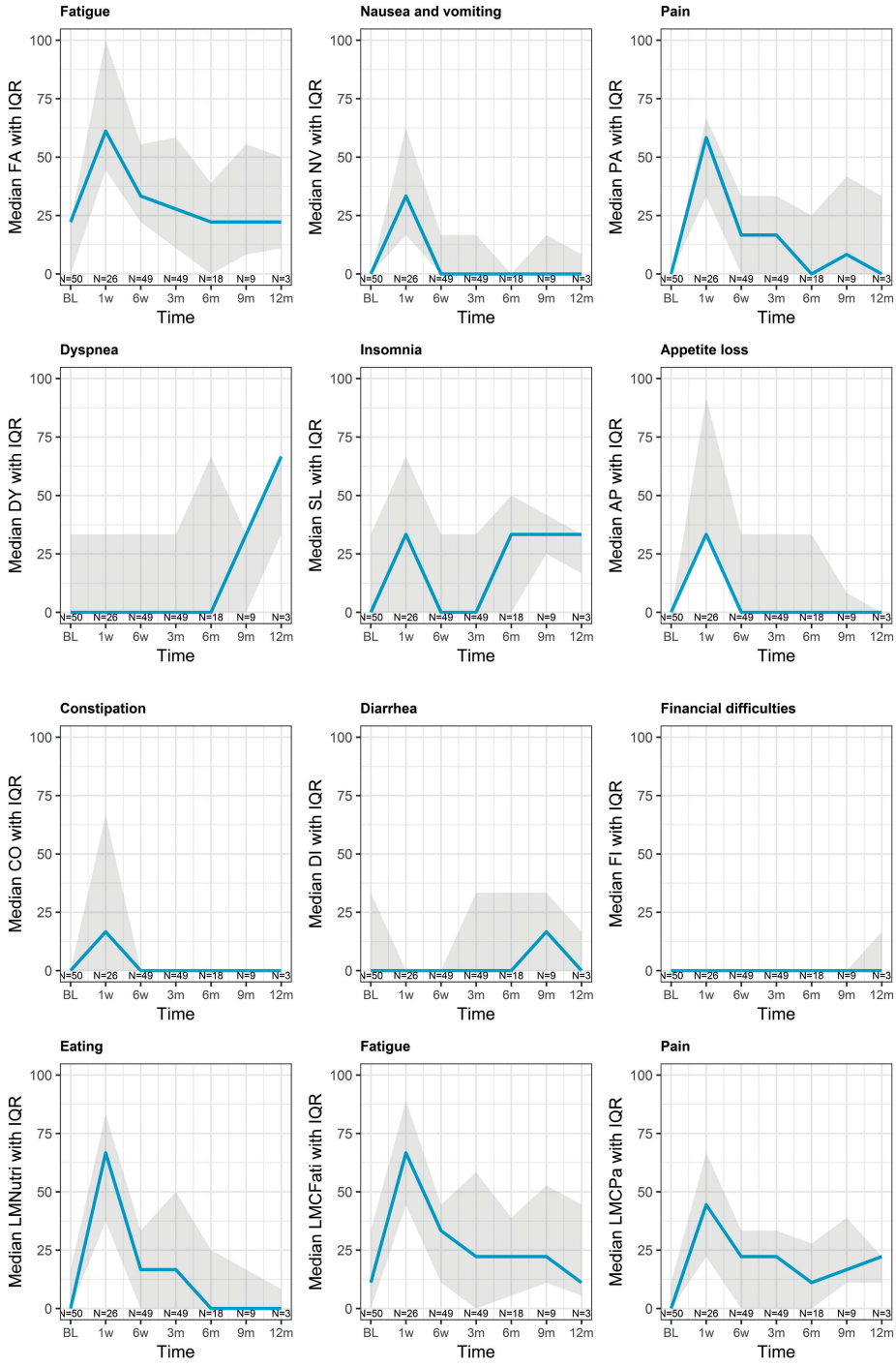
Fatigue
Median FA with IQR
Nausea and vomiting
Median NV with IQR
Pain
Median PA with IQR
Dyspnea
Median DY with IQR
Insomnia
Median SL with IQR
Appetite loss
Median AP with IQR
Constipation
Median CO with IQR
Diarrhea
Median DI with IQR
Financial difficulties
Median FI with IQR
Eating
Median LMNutri with IQR
Fatigue
Median LMCFati with IQR
Pain
Median LMCPa with IQR
0
25
50
75
100
N=50 N=26 N=49 N=49 N=18 N=9 N=3
BL 1w 6w 3m 6m 9m 12m
Time

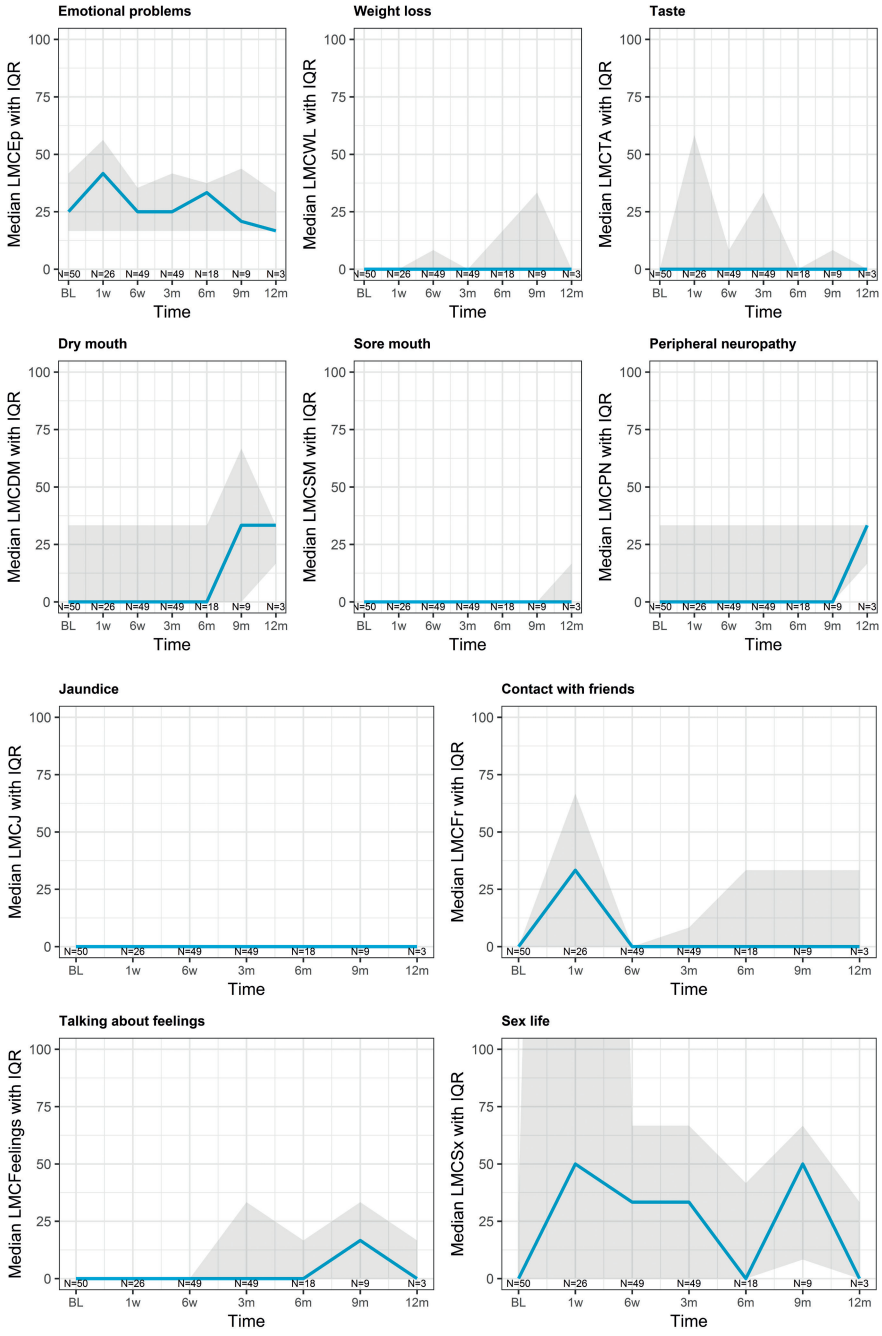

FIGURE S3A-D. Median symptom scores over time with interquartile ranges (shaded areas). BL = baseline, 1w = 1 week, 6w = 6 weeks, 3m = 3 months, 6m = 6 months, 9m = 9 months, 12m = 12 months. A high score represents a high level of symptomatology.

SUPPLEMENTAL TABLES

TABLE S1. Most important characteristics of the HEPAR I and HEPAR II patient population

Characteristic	HEPAR I (n=15)	HEPAR II (n=38)
Age (median, range)	55 (38-87)	66 (41-84)
Gender (n, %)		
Male	9 (60%)	22 (58%)
Female	6 (40%)	16 (42%)
WHO performance status (n, %)		
0	13 (87%)	32 (84%)
1	2 (13%)	5 (13%)
2	0 (0%)	1 (3%)
Primary malignancy (n, %)		
Colorectal	6 (40%)	23 (61%)
Breast	1 (7%)	4 (11%)
Cholangiocarcinoma	2 (13%)	4 (11%)
Neuroendocrine tumor	0 (0%)	2 (5%)
Uveal melanoma	6 (40%)	2 (5%)
Pancreas carcinoma	0 (0%)	1 (3%)
Gastric cancer	0 (0%)	1 (3%)
Thymoma	0 (0%)	1 (3%)
Extrahepatic disease at baseline (n,%)		
Yes	6 (40%)	10 (26%)
No	9 (60%)	28 (74%)

TABLE S2. Internal consistency of the multi-item scales at baseline, 6 weeks and 3 months

Scale	No. items	α* baseline	α* 6 weeks	α* 3 months
EORTC QLQ-C30				
Global health status/QoL	2	0.90	0.95	0.97
Physical functioning	5	0.88	0.88	0.89
Role functioning	2	0.87	0.95	0.95
Emotional functioning	4	0.86	0.85	0.88
Cognitive functioning	2	0.65	0.64	0.81
Social functioning	2	0.79	0.86	0.89
Fatigue	3	0.87	0.86	0.93
Nausea and vomiting	2	0.58	0.52	0.79
Pain	2	0.77	0.86	0.78
Dyspnea	1	N.A.	N.A.	N.A.
Insomnia	1	N.A.	N.A.	N.A.
Appetite	1	N.A.	N.A.	N.A.
Constipation	1	N.A.	N.A.	N.A.
Diarrhea	1	N.A.	N.A.	N.A.
Financial difficulties	1	N.A.	N.A.	N.A.
EORTC QLQ-LMC21				
Emotional problems	4	0.87	0.69	0.82
Nutritional problems	2	0.79	0.74	0.89
Fatigue	3	0.91	0.90	0.91
Pain	3	0.74	0.75	0.74
Problems with taste	1	N.A.	N.A.	N.A.
Dry mouth	1	N.A.	N.A.	N.A.
Sore mouth/tongue	1	N.A.	N.A.	N.A.
Peripheral neurophathy	1	N.A.	N.A.	N.A.
Jaundice	1	N.A.	N.A.	N.A.
Contact with friends	1	N.A.	N.A.	N.A.
Talking about feelings	1	N.A.	N.A.	N.A.
Sex life	1	N.A.	N.A.	N.A.

* Cronbach's alpha.
N.A.: not applicable since Cronbach's alpha can only be determined for scales with multiple items.

TABLE S3. Quality of life (median, IQR (25th and 75th percentile))

Scale	Baseline	1 week	6 weeks	3 months	6 months	9 months	12 months
	N=50	*N=26*	*N=49*	*N=49*	*N=18*	*N=9*	*N=3*
QLQ-C30							
GHS	83 (67-83)	41 (25-75)	66 (50-83)	66 (54-83)	83 (60-93)	75 (50-92)	83 (33--)
PF	93 (85-100)	43 (20-87)	87 (67-93)	87 (67-100)	87 (67-100)	77 (57-98)	67 (47--)
RF	100 (67-100)	33 (0-100)	67 (42-100)	67 (50-100)	83 (67-100)	83 (54-100)	100 (33--)
EF	83 (75-100)	79 (56-100)	83 (67-100)	83 (67-92)	83 (67-92)	71 (54-83)	67 (67--)
CF	100 (83-100)	83 (67-100)	100 (83-100)	100 (83-100)	100 (67-100)	83 (58-100)	100 (67--)
SF	100 (67-100)	58 (33-83)	83 (67-100)	83 (67-100)	100 (67-100)	100 (54-100)	100 (33--)
FA	22 (0-33)	61 (42-100)	33 (22-56)	22 (11-61)	22 (0-44)	22 (3-56)	22 (0--)
NV	0 (0-0)	33 (13-67)	0 (0-17)	0 (0-17)	0 (0-0)	0 (0-17)	8 (0--)
PA	0 (0-17)	58 (29-71)	17 (-33)	17 (0-33)	0 (0-33)	8 (0-58)	0 (0--)
DY	0 (0-33)	0 (0-33)	0 (0-33)	0 (0-33)	0 (0-67)	33 (0-33)	67 (0--)
SL	0 (0-33)	33 (0-67)	0 (0-33)	0 (0-33)	33 (0-67)	33 (8-58)	33 (0--)
AP	0 (0-0)	33 (33-100)	0 (0-33)	0 (0-33)	0 (0-33)	0 (0-25)	0 (0-0)
CO	0 (0-0)	17 (0-67)	0 (0-0)	0 (0-0)	0 (0-0)	0 (0-0)	0 (0-0)
DI	0 (0-33)	0 (0-0)	0 (0-0)	0 (0-33)	0 (0-33)	17 (0-33)	0 (0--)
FI	0 (0-0)	0 (0-0)	0 (0-0)	0 (0-0)	0 (0-0)	0 (0-0)	0 (0--)
QLQ-LMC21							
LMCNutri	0 (0-17)	67 (33-83)	17 (0-33)	17 (0-50)	0 (0-33)	0 (0-17)	0 (0--)
LMCFati	11 (0-33)	67 (42-92)	33 (11-44)	22 (0-61)	22 (0-44)	22 (11-69)	11 (0--)

TABLE S3. Quality of life (median, IQR (25th and 75th percentile)) (continued)

Scale	Baseline	1 week	6 weeks	3 months	6 months	9 months	12 months
	N=50	*N=26*	*N=49*	*N=49*	*N=18*	*N=9*	*N=3*
LMCPa	0 (0-14)	44 (22-67)	22 (0-33)	22 (0-33)	11 (0-33)	17 (11-50)	22 (0--)
LMCEp	25 (17-42)	42 (17-58)	25 (17-38)	25 (17-42)	33 (17-42)	21 (17-48)	17 (17--)
LMCWL	0 (0-0)	0 (0-0)	0 (0-17)	0 (0-0)	0 (0-33)	0 (0-33)	0 (0-0)
LMCTA	0 (0-0)	0 (0-67)	0 (0-17)	0 (0-33)	0 (0-0)	0 (0-25)	0 (0-0)
LMCDM	0 (0-33)	0 (0-42)	0 (0-33)	0 (0-33)	0 (0-33)	0 (0-67)	33 (0--)
LMCSM	0 (0-0)	0 (0-0)	0 (0-0)	0 (0-0)	0 (0-0)	0 (0-0)	0 (0--)
LMCPN	0 (0-33)	0 (0-33)	0 (0-33)	0 (0-33)	0 (0-33)	0 (0-33)	33 (0--)
LMCJ	0 (0-0)	0 (0-0)	0 (0-0)	0 (0-0)	0 (0-0)	0 (0-0)	0 (0--)
LMCFr	0 (0-0)	33 (0-67)	0 (0-0)	0 (0-16)	0 (0-33)	0 (0-33)	0 (0--)
LMCFeelings	0 (0-0)	0 (0-0)	0 (0-0)	0 (0-33)	0 (0-33)	17 (0-33)	0 (0--)
LMCSx	0 (0-33)	0 (0-67)	33 (0-33)	33 (0-67)	0 (0-58)	50 (0-67)	0 (0--)

Evaluation of the safety and feasibility of same day ^{166}Ho-radioembolization simulation and treatment of hepatic metastases

Caren van Roekel, Netanja I. Harlianto, Arthur J.A.T. Braat, Jip F. Prince, Andor F. van den Hoven, Rutger C.G. Bruijnen, Marnix G.E.H. Lam, Maarten L.J. Smits

Journal of Vascular and Interventional Radiology 2020

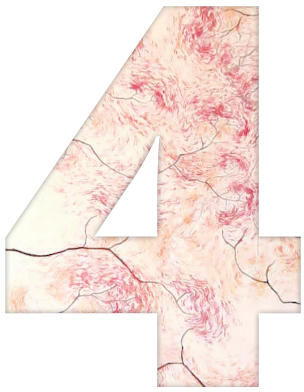

ABSTRACT

Purpose

To evaluate the safety and feasibility of one-day treatment, including the simulation procedure for assessment of intra- and extrahepatic distribution of the microspheres, with holmium-166 (^{166}Ho)-radioembolization.

Materials and methods

This was a secondary analysis of patients included in the four prospective studies (HEPAR I, II, PLuS and SIM studies) on ^{166}Ho-radioembolization. Technical success rate of the one-day treatment protocol was measured, which was defined as the number of patients who completed one-day treatment. Total in-room time, duration of the scout procedure, time to imaging and duration of the treatment procedure were recorded. Reasons for discontinuation or adjustment of treatment were identified. Adverse events (CTCAE v5.0) that occurred during the treatment day were recorded.

Results

105 of 120 scheduled patients completed one-day treatment with ^{166}Ho-radioembolization(success rate 88%). After the simulation procedure, treatment was cancelled in fifteen patients because of extrahepatic deposition (n=8), suboptimal tumor targeting (n=1), unanticipated vascular anatomy (n=5) and dissection (n=1). In another 14 patients, the treatment plan was adjusted. The median total procedure time (i.e. simulation, imaging and treatment) was 6:39 hours (range 3:58-9:17 hours). Back pain was a major same-day treatment related complaint (n=28).

Conclusion

^{166}Ho-radioembolization as a one-day treatment procedure is feasible in the majority of selected patients, although treatment was adjusted in 12% of patients and cancelled in 12% of patients. This approach may be beneficial for a select patient population, i.e. patients needing a radiation segmentectomy.

Keywords

Radioembolization, holmium-166, hepatic tumors

INTRODUCTION

Radioembolization is a minimally invasive treatment option for patients with primary or metastatic liver disease. Holmium-166 (^{166}Ho)-microspheres were developed as an alternative for yttrium-90 (^{90}Y)-microspheres because the same microspheres can be delivered both as a simulation dose (^{166}Ho-scout; 250 MBq) and as a treatment dose. This ^{166}Ho-scout has proven to be a more accurate predictor of lung shunt and intrahepatic distribution than the widely used technetium-99m macro aggregated albumin (^{99m}Tc-MAA), and its safety has been established (1-3).

Recently, interest in performing radioembolization as a one-day treatment procedure is growing, with several studies describing the feasibility and logistics of one-day treatment in ^{90}Y-radioembolization (4-6). A one-day procedure may be of clinical benefit for patients with rapidly progressive disease or symptomatic disease (e.g. in patients with neuro-endocrine tumors (NETs)), and it may be convenient for patients who need to travel long distances. Traditionally, treatment simulation is done 1-2 weeks before treatment, which provides the opportunity of personalized dosimetry.

The aim of the current study was to assess the safety, feasibility, and practicality of one-day treatment with ^{166}Ho-radioembolization.

MATERIALS AND METHODS

Patients

This was a secondary analysis of the patients from all the prospective studies on ^{166}Ho-radioembolization (i.e. the HEPAR I, HEPAR II, HEPAR PLuS and SIM studies), included between March 2012 and April 2019 (7-10). All patients in these studies were scheduled to undergo one-day ^{166}Ho-radioembolization. In total, 105 patients were treated. Three patients underwent whole-liver treatment in two stages and were included twice. Patient characteristics are summarized in Table 1. Before study inclusion, all patients provided written informed consent. The institution's Medical Ethics Committee approved all studies.

TABLE 1. Baseline characteristics of patients who underwent same-day simulation and treatment with ^{166}Ho-radioembolization

Characteristic	Value
N patients	120
Age (y) (median, range)	62 (37-87)
Sex	
Male	76 (63%)
Female	44 (37%)
Study	
HEPAR1	21
HEPAR2	46
HEPAR PLuS	29
SIM	24
Primary tumor	
Colorectalcarcinoma	62 (52%)
Neuroendocriene tumor	31 (26%)
Ocular melanoma	11 (9%)
Breast	6 (5%)
Cholangiocarcinoma	5 (4%)
Pancreatic cancer	2 (2%)
Gastric cancer	1 (1%)
Thymoma	1 (1%)
WHO performance status	
0	88 (73%)
1	29 (24%)
2	3 (3%)
Extrahepatic deposition	
No	99 (94%)
Yes	6 (6%)
Type of treatment	
Whole liver, single session	82
Whole liver, sequential	3
Right lobe only	16
Left lobe only	4
Activity ^{166}Ho scout in MBq (median, range)	264 (81-338)
Activity treatment in MBq (median, range)	6706 (1580-13,725)

The parameters post-treatment lung shunt fraction, extrahepatic deposition, type of treatment, activity scout and activity treatment are only given for the 105 patients who underwent treatment.

Study records were reviewed to assess clinical adverse events that occurred during the treatment day. Adverse events were scored according to the Common Terminology Criteria for Adverse Events (CTCAE) version 5.0 (11).

Technical success rate was defined as the number of patients scheduled to undergo one-day treatment with radioembolization who completed treatment. Findings that prevented continuation of treatment were identified.

In the HEPAR I and II studies, patients underwent a double work-up procedure with both administration of ^{99m}Tc-MAA and ^{166}Ho-scout to confirm the accuracy and safety of ^{166}Ho-scout (Figure 1). Findings encountered during or after the first simulation procedure using ^{99m}Tc-MAA were also regarded as prohibiting one-day treatment, because they were likely to have happened with ^{166}Ho-scout as well.

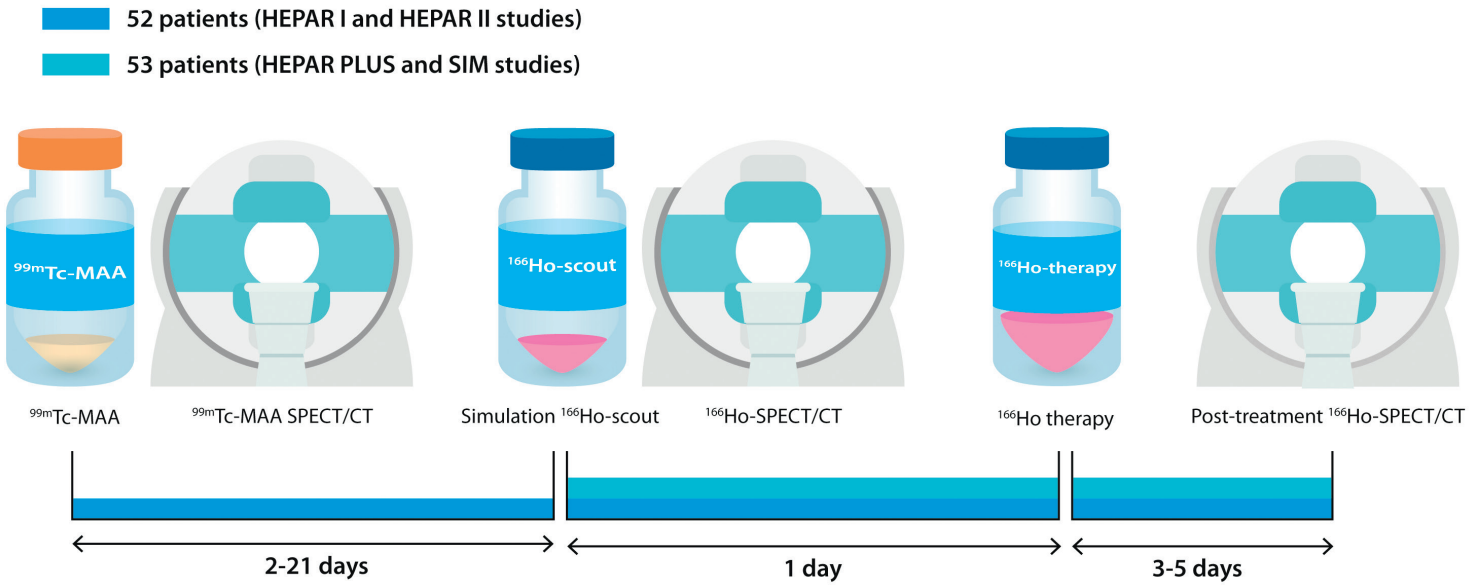

FIGURE 1. Timeline. Fifty-two patients of this study underwent two simulation procedures, one with administration of ^{99m}Tc-MAA and one with ^{166}Ho-scout, as per protocol of the HEPAR I and HEPAR II studies. Fifty-three patients underwent one simulation procedure with administration of ^{166}Ho-scout. After administration of ^{166}Ho-scout and the ^{166}Ho-treatment dose, ^{166}Ho-SPECT/CT images were made to assess the absorbed dose distribution.

Treatment work-up

Patients who were candidates for ^{166}Ho-radioembolization underwent triphasic contrast-enhanced abdominal CT at baseline.

^{166}Ho-scout activity was split according to the hepatic volume supplied by each injection position. Patients in the HEPAR I study received escalating doses of 20, 40, 60 and 80 Gy (depending on the dose cohort). All other patients received activity matching an average whole liver absorbed dose of 60 Gy, according to the following formula:

$$IA_{(MBq)} = liver\ weight\ (kg) * 3780\ \left(\frac{MBq}{kg}\right)$$

The scout activity was approximately 250 MBq.

On the ^{166}Ho-radioembolization treatment day, patients underwent a preparatory simulation angiography with ^{166}Ho-scout administration in the morning. No sedative medication was used during either angiography. In 72 patients, cone-beam CT was used to provide better visualization of the arterial supply and to assess hepatic perfusion. Standard microcatheters were used in all cases (Terumo, Progreat 2.7F), except for SIM study participants in whom both standard microcatheters and antireflux catheters were used (Surefire infusion system)(10). After administration of ^{166}Ho-scout, the catheters were removed while the vascular sheath remained in situ. The sheath was fixed to the skin with sterile adhesives and connected to a pressurized bag of saline for continuous flushing. Patients were transferred to the SPECT-scanner to undergo ^{166}Ho-SPECT/CT and were then transferred to the ward awaiting the treatment procedure. A nuclear medicine physician assessed the dose distribution and presence of extrahepatic activity. In case of relevant extrahepatic deposition (as determined in consensus between the nuclear medicine physician and the interventional radiologist), patients were excluded from treatment. Otherwise, they returned to the angio-suite in the afternoon to receive the treatment dose. Afterwards, patients had to lie supine for four hours to prevent groin bleeding. Patients received oral analgesics (paracetamol up to 4000 mg/24 h) post-treatment and were discharged within 24-48 hours after treatment. Overnight hospital stay was part of the study protocols because it allows for close monitoring of the patients.

RESULTS

Technical success rate

A total of 120 patients were scheduled to undergo treatment with ^{166}Ho-radioembolization. Sixty-seven patients were included in the HEPAR I and II studies and underwent both a preparatory simulation angiography with administration of ^{99m}Tc-MAA and ^{166}Ho-scout; the other 53 patients only received ^{166}Ho-scout. The median interval between the first simulation procedure using ^{99m}Tc-MAA, and the second simulation procedure using ^{166}Ho-scout was seven days (range 2-21 days). A total of 105 patients completed treatment on the same day (technical success rate 88%). An example case of a successful one-day treatment is shown in Figure 2.

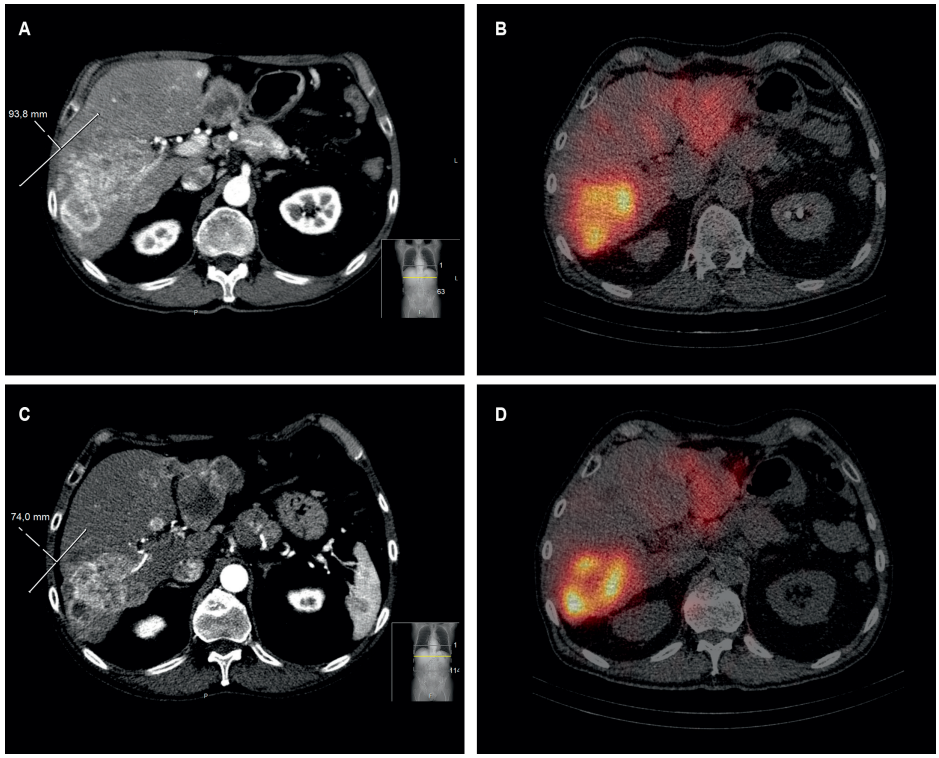

FIGURE 2. Example case. A 65-year-old male with neuroendocrine tumor metastases was treated with one-day ^{166}Ho-radioembolization. Figure a shows the baseline contrast-enhanced CT image with a large hypervascular metastasis in segment 6. Figure b shows the distribution of ^{166}Ho-scout on SPECT/CT. Figure c shows the contrast-enhanced CT image 3 months after treatment, with evident shrinkage (see annotation) of the metastasis in segment 6. Figure d shows the distribution of the ^{166}Ho-treatment dose on SPECT/CT.

Radioembolization was cancelled in 15 patients due to various reasons: extrahepatic deposition (n=8), suboptimal tumor targeting (n=1), unanticipated vascular anatomy (n=5) and dissection (n=1) (Figure 3). Unanticipated vascular anatomy led to more injection positions needed than anticipated because of arterial branches that were either not identified on the baseline contrast-enhanced CT or that could not be coil-embolized.

In 14 patients, the treatment plan was adjusted. Reasons for adjustment were extrahepatic deposition (n=4), suboptimal tumor targeting (n=9), and unanticipated vascular anatomy (n=1). In most cases, adjustment of the therapy plan meant a lobar treatment instead of a whole-liver approach and one of the two ordered vials was discarded. In one case with suboptimal tumor targeting, it was decided to only inject part of the ordered activity (which was done by splitting the activity in our radionuclide laboratory).

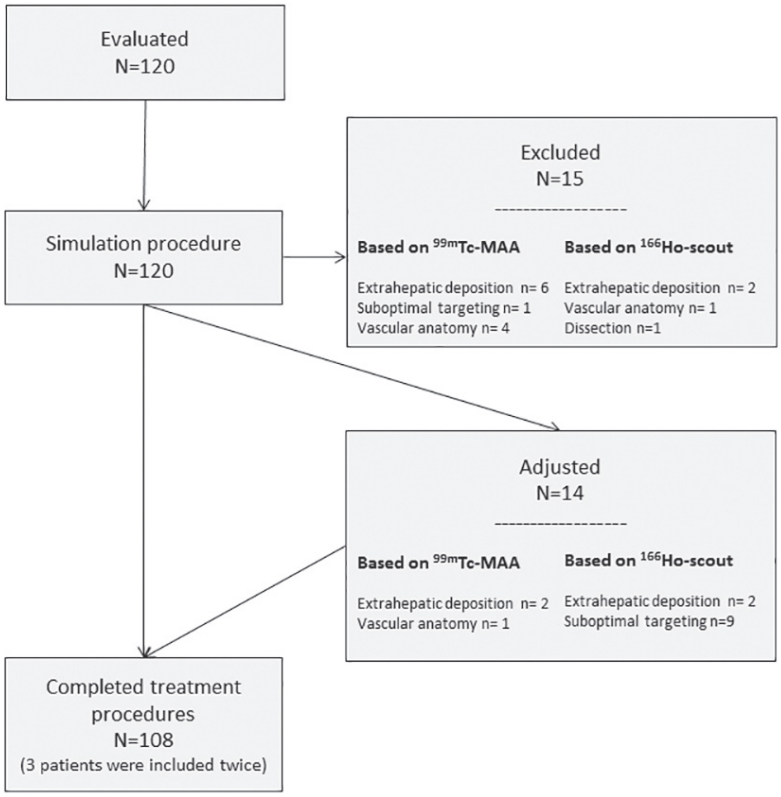

FIGURE 3. Flowchart of patients who were excluded from one-day ^{166}Ho-radioembolization and patients whose treatment plans were adjusted.

Treatment characteristics

Coil-embolization of non-target vessels was performed in 62 patients. The median duration of the simulation angiography with administration of ^{166}Ho-scout was 1:43 hours (range 0:31-4:40 hours). Patients had a median wait time of 31 minutes (range 0:10-2:45 hours) before imaging with ^{166}Ho-SPECT/CT was performed. After SPECT/CT imaging, median wait time was 2:28 hours (range 0:17-4:30 hours). The median duration of the treatment procedure was 1:11 hours (range 0:12-2:42 hours). The median total procedure time (i.e. simulation, imaging and treatment) was 6:39 hours (range 3:58-9:17 hours).

Extrahepatic deposition on SPECT/CT after treatment was seen in five patients (falciform ligament (n=3), the hepatoduodenal ligament (n=1) and a portocaval lymph node (n=1)), but did not have any clinical consequences during follow-up.

Safety

Overall, the one-day treatment procedure was well tolerated. After administration of ^{166}Ho-scout patients experienced back pain (19%), abdominal pain (5%), allergic contrast reaction (3%), nausea (1%), vomiting (1%), and dyspnea (1%). After administration of the therapeutic activity, patients experienced abdominal pain (51%), nausea (45%), vomiting (27%), back pain (27%), and chest pain (1%) (Table 2). Additional analgesics were administered in 30 patients during or after treatment (specifically for back pain in 17 patients). The indwelling arterial sheath, that remained in situ for a median duration of 6:39h, did not cause any adverse events. After removal, a minor bleeding occurred in three patients, which resolved with manual compression.

TABLE 2. CTCAE grading of reported adverse events during same-day treatment with ^{166}Ho-radioembolization

Adverse event	CTCAE grade I	CTCAE grade II	CTCAE grade III
Adverse events between simulation procedure and treatment procedure			
Back pain	N=13	N=6	N=1
Abdominal pain	N=4		N=1
Allergic reaction		N=3	
Nausea		N=1	
Vomiting		N=1	
Dyspnea	N=1		
Adverse events after treatment procedure on the treatment day			
Abdominal pain	N=14	N=26	N=12
Nausea	N=13	N=29	N=5
Vomiting	N=6	N=19	N=3
Back pain	N=14	N=11	N=3
Chest pain		N=1	

DISCUSSION

As shown in this study, same-day simulation and treatment in ^{166}Ho-radioembolization is feasible in most cases: 105 of 120 scheduled patients were treated. The treatment plan was adjusted in 14 patients based on the findings of the simulation angiography. The clinical adverse events that occurred during the treatment day were similar to the known side-effects of radioembolization, apart from additional back pain, which was likely caused by the long duration of lying in a supine position.

Although not part of this study, savings in time and costs can be potential advantages of a one-day treatment protocol (5). Especially patients who have to travel a long distance or have progressive disease can benefit from a timely treatment. In addition, leaving a vascular sheath in the groin between the two angiographies avoids repeated groin punctures.

However, a 12% cancellation rate and an additional 12% modification rate, as found in this study, may hamper cost-effectiveness. The ^{166}Ho-activity

was delivered in a predetermined number of vials and could not be changed after the simulation procedure. Unexpected findings in activity distribution and vascular anatomy led to exclusion from treatment or adjustment of the treatment plan.

Other disadvantages of a one-day treatment protocol include back pain. Fortunately, this pain resolved the next day in all cases and was probably caused by the long time that the patients had to lie supine, partly on uncomfortable angio- or SPECT-tables.

Gates et al. and Gabr et al. described the feasibility of single-session glass ^{90}Y-microspheres radioembolization. In their studies, a total of 78 patients were treated in one day. In all patients selected for this procedure, treatment was successful. The authors ordered multiple vials per patient without additional costs, allowing for some flexibility (5, 6).

Recently, Li et al. described a same-day treatment approach with resin ^{90}Y-microspheres radioembolization. Twenty-six patients were treated and all planned cases were technically successful. Based on pretreatment angiography, the planned resin ^{90}Y-microspheres treatment activity was changed in only one case. This was feasible because with resin ^{90}Y-microspheres, the patient-specific activity always needs to be drawn from a shipping vial containing approximately 3.0 GBq (4). In these three studies on one-day ^{90}Y-radioembolization, clinical adverse events during treatment day were not reported. Furthermore, most patients received either selective lobar treatment or superselective segmental treatment, lowering the chance of treatment adjustments (4, 5, 12). This is in contrast to our patient population who mostly received bilobar treatment from multiple injection sites.

A one-day treatment approach implies that only pretreatment dosimetric approaches, such as the body surface area (BSA) and MIRD method, are feasible (13). These predefined dosimetric approaches have many caveats and commonly lead to under- or overdosage (14-18). Compared with standard dosimetric approaches, a fully personalized treatment approach can lead to a better outcome, as was shown in a recent study in HCC patients (19).

Limitations of this study included the heterogeneous disease cohort. Furthermore, this study suffers from a selection bias due to the portion of patients treated in the HEPAR I and II studies who received an additional simulation angiography with administration of ^{99m}Tc-MAA. To overcome this issue findings on ^{99m}Tc-MAA were also taken into consideration. Another limitation and confounding factor was the learning curve. Over time, practical skills and knowledge increased, and certain practices that were used in patients in the HEPAR I study are now no longer common practice (e.g. routine coiling of the gastroduodenal artery and proper hepatic artery injections). The large percentage (12%) of patients who were excluded from treatment is expected to be much lower in current clinical practice. This learning curve also applies to the interpretation of the scintigraphic images after administration of ^{99m}Tc-MAA.

Given the findings of the current study, the same-day treatment method will no longer be standard for treating patients with ^{166}Ho-radioembolization at our center. Calculation and ordering of the prescribed activity limits the feasibility of same-day treatment. However, in those cases where exclusion or adjustment of treatment are unlikely (e.g. radiation segmentectomy) and prescribed activity can be pre-calculated, without the information from ^{166}Ho-scout, same-day treatment may still be an option.

In conclusion, ^{166}Ho-radioembolization as a one-day treatment procedure is feasible in the majority of selected patients, although treatment was adjusted in 12% of patients and cancelled in 12% of patients. This approach may be beneficial for a select patient population, however, personalized treatment planning based on ^{166}Ho-scout distribution does not allow for same-day procedures.

ACKNOWLEDGEMENTS

We thank Remmert de Roos and Gerard Krijger for preparing the microspheres. We thank Christiaan van Kesteren for his assistance in designing the figures.

REFERENCES

1. Elschot M, Nijsen JF, Lam MG, Smits ML, Prince JF, Viergever MA, et al. ((9)(9)m)Tc-MAA overestimates the absorbed dose to the lungs in radioembolization: a quantitative evaluation in patients treated with (1)(6)(6)Ho-microspheres. Eur J Nucl Med Mol Im. 2014;41(10):1965-75. Epub 2014/05/14.

2. Braat A, Prince JF, van Rooij R, Bruijnen RCG, van den Bosch M, Lam M. Safety analysis of holmium-166 microsphere scout dose imaging during radioembolisation work-up: A cohort study. Eur Radiol. 2018;28(3):920-8. Epub 2017/08/09.

3. Smits MLJ, Dassen MG, Prince JF, Braat A, Beijst C, Bruijnen RCG, et al. The superior predictive value of (^{166})Ho-scout compared with (99m)Tc-macroaggregated albumin prior to (^{166})Ho-microspheres radioembolization in patients with liver metastases. Eur J Nucl Med Mol Im. 2019. Epub 2019/08/11.

4. Li MD, Chu KF, DePietro A, Wu V, Wehrenberg-Klee E, Zurkiya O, et al. Same-Day Yttrium-90 Radioembolization: Feasibility with Resin Microspheres. J Vasc Interv Radiol. 2019;30(3):314-9. Epub 2019/03/02.

5. Gabr A, Kallini JR, Gates VL, Hickey R, Kulik L, Desai K, et al. Same-day (90)Y radioembolization: implementing a new treatment paradigm. Eur J Nucl Med Mol Im. 2016;43(13):2353-9. Epub 2016/11/05.

6. Gates VL, Marshall KG, Salzig K, Williams M, Lewandowski RJ, Salem R. Outpatient single-session yttrium-90 glass microsphere radioembolization. J Vasc Interv Radiol. 2014;25(2):266-70. Epub 2013/12/18.

7. Prince JF, van den Bosch M, Nijsen JFW, Smits MLJ, van den Hoven AF, Nikolakopoulos S, et al. Efficacy of Radioembolization with (^{166})Ho-Microspheres in Salvage Patients with Liver Metastases: A Phase 2 Study. J Nucl Med. 2018;59(4):582-8. Epub 2017/09/17.

8. Smits MLJ, Nijsen JFW, van den Bosch MAAJ, Lam MGEH, Vente MAD, Mali WPTM, et al. Holmium-166 radioembolisation in patients with unresectable, chemorefractory liver metastases (HEPAR trial): a phase 1, dose-escalation study. Lancet Oncol. 2012;13(10):1025-34.

9. Braat A, Kwekkeboom DJ, Kam BLR, Teunissen JJM, de Herder WW, Dreijerink KMA, et al. Additional hepatic (^{166})Ho-radioembolization in patients with neuroendocrine tumours treated with (177)Lu-DOTATATE; a single center, interventional, non-randomized, non-comparative, open label, phase II study (HEPAR PLUS trial). BMC Gastroenterol. 2018;18(1):84. Epub 2018/06/16.

10. Van den Bosch MA. Surefire Infusion System vs. Standard Microcatheter Use During Holmium-166 Radioembolization (SIM). clinicaltrials.gov; 2014 [cited 2019 December 24]; Available from: https://clinicaltrials.gov/ct2/show/NCT02208804?term=NCT02208804&draw=2&rank=1.

11. Kafrouni M, Allimant C, Fourcade M, Vauclin S, Delicque J, Ilonca AD, et al. Retrospective Voxel-Based Dosimetry for Assessing the Ability of the Body-Surface-Area Model to Predict Delivered Dose and Radioembolization Outcome. J Nucl Med. 2018;59(8):1289-95. Epub 2018/03/17.

12. Gates V, Salem R. Reply to "hepatic radioembolization as a true single-session treatment". J Vasc Interv Radiol. 2014;25(7):1144-6. Epub 2014/06/28.

13. Salem R, Thurston KG. Radioembolization with 90Yttrium microspheres: a state-of-the-art brachytherapy treatment for primary and secondary liver malignancies. Part 1: Technical and methodologic considerations. J Vasc Interv Radiol. 2006;17(8):1251-78. Epub 2006/08/23.

14. Chiesa C, Sjogreen Gleisner K, Flux G, Gear J, Walrand S, Bacher K, et al. The conflict between treatment optimization and registration of radiopharmaceuticals with fixed activity posology in oncological nuclear medicine therapy. Eur J Nucl Med Mol Im. 2017;44(11):1783-6. Epub 2017/05/26.

15. Tong AK, Kao YH, Too CW, Chin KF, Ng DC, Chow PK. Yttrium-90 hepatic radioembolization: clinical review and current techniques in interventional radiology and personalized dosimetry. Br J Radiol. 2016;89(1062):20150943. Epub 2016/03/05.

16. Braat AJAT, Kappadath SC, Bruijnen RCG, van den Hoven AF, Mahvash A, de Jong HWAM, et al. Adequate SIRT activity dose is as important as adequate chemotherapy dose. Lancet Oncol. 2017;18(11):e636.

17. Bastiaannet R, Kappadath SC, Kunnen B, Braat A, Lam M, de Jong H. The physics of radioembolization. EJNMMI Physics. 2018;5(1):22. Epub 2018/11/06.

18. Toskich BB, Liu DM. Y90 Radioembolization Dosimetry: Concepts for the Interventional Radiologist. Tech Vasc Interv Radiol. 2019;22(2):100-11. Epub 2019/05/14.

19. Garin E, Rolland Y, Pracht M, Le Sourd S, Laffont S, Mesbah H, et al. High impact of macroaggregated albumin-based tumour dose on response and overall survival in hepatocellular carcinoma patients treated with (90) Y-loaded glass microsphere radioembolization. Liver International. 2017;37(1):101-10. Epub 2016/08/16.

Mode of progression after radioembolization in patients with colorectal cancer liver metastases

Caren van Roekel, Jennifer M.J. Jongen, Maarten L.J. Smits, Sjoerd G. Elias, Miriam Koopman, Onno Kranenburg, Inne H.M. Borel Rinkes, Marnix G.E.H. Lam

EJNMMI Research 2020

ABSTRACT

Background

Radioembolization is an established treatment modality in colorectal cancer patients with liver-dominant disease in a salvage setting. Selection of patients who will benefit most is of vital importance. The aim of this study was to assess response (and mode of progression) at three months after radioembolization and the impact of baseline characteristics.

Methods

Three months after radioembolization with either yttrium-90 resin/glass or holmium-166, anatomic response, according to RECIST 1.1, was evaluated in 90 patients. Correlations between baseline characteristics and efficacy were evaluated. For more detailed analysis of progressive disease as a dismal clinical entity, distinction was made between intra- and extrahepatic progression, and between progression of existing metastases and new metastases.

Results

Forty-two patients (47%) had extrahepatic disease (up to five ≥1 cm lung nodules, and ≤2 cm lymph nodes) at baseline. No patients showed complete response, 5 (5.5%) patients had partial response, 16 (17.8%) stable disease and 69 (76.7%) progressive disease. Most progressive patients (67/69; 97%) had new metastases (intra-hepatic N=11, extrahepatic N=32; or both N=24). Significantly fewer patients had progressive disease in the group of patients presenting without extrahepatic metastases at baseline (63% versus 93%; p=0.0016). Median overall survival in patients with extrahepatic disease was 6.5 months, versus 10 months in patients without extrahepatic disease at baseline (hazard ratio 1.79, 95%CI 1.24-2.57.

Conclusions

Response at three-month follow-up and survival were heavily influenced by new metastases. Patients with extrahepatic disease at baseline had a worse outcome compared to patients without.

Keywords

Metastatic Colorectal Cancer, Radioembolization, Progression, RECIST, Extrahepatic Metastases

BACKGROUND

Approximately 45% of colorectal cancer patients develop metastases (1, 2). Without treatment, the median overall survival for colorectal cancer patients with hepatic metastases (mCRC) is only 4.5 months (3). The liver is the most common site of metastasis: up to 30% of mCRC patients develop hepatic metastases (4, 5). Radioembolization is a loco-regional treatment option for unresectable, systemic therapy-refractory patients with liver-only or liver-dominant disease (6, 7). Intra-arterial administration of radioactive microspheres is proven to be safe and effective (8). Microspheres (approximately 30 um) are loaded with the radioactive isotope yttrium-90 (^{90}Y) or holmium-166 (^{166}Ho) and injected through a microcatheter in the hepatic artery (9). For the treatment of metastatic colorectal cancer, ^{90}Y-resin microspheres (SIR-Spheres®, Sirtex) are FDA- and CE-approved. ^{90}Y -glass microspheres (TheraSphere®, BTG / Boston Scientific) and ^{166}Ho microspheres (QuiremSpheres®, Quirem) are CE-approved for this indication, not FDA-approved. The injected microspheres embolize the microvasculature surrounding the tumor and emit high-energy beta-radiation. The normal liver parenchyma is largely spared since healthy liver tissue is mainly supplied by the portal vein (10-12).

Although assessment of metabolic response has proven added benefit over anatomic response, not being hampered by i.e. the presence of intra-tumoral necrosis and cystic changes after treatment (13, 14), response of radioembolization in mCRC patients is still mostly evaluated by the Response Evaluation Criteria in Solid Tumors (RECIST) (15-17). When using these criteria, the results of most clinical studies in metastatic (liver) disease are modest, with many patients experiencing early progressive disease (18-21). Optimized treatment planning could improve response rates (22, 23), but selecting patients who will benefit most is another vital aspect. An important criterion in patient selection is the definition of liver-dominant disease. The extent of extrahepatic disease we are willing to accept is under constant debate at tumor board meetings in our center, but clear guidance is currently missing, due to the lack of data on this matter. Other prognostic factors that are known to influence response after treatment with radioembolization are (among others) KRAS status, primary tumor location, percentage tumor involvement and pre-

treatment CEA level (19, 24, 25). These factors could possibly be used in patient selection as well.

The aim of this study was to assess the impact of baseline characteristics on changes in intra- and extrahepatic mCRC disease from baseline to three months after radioembolization, across all currently available radioembolization treatment modalities.

METHODS

Patient selection and study design

A total of 129 chemorefractory, unresectable mCRC patients were treated with radioembolization at our institution between August 2009 and January 2017, predominantly as part of the HEPAR-2 (Holmium Embolization Particles for Arterial Radiotherapy II) (26), or RADAR trial (RADioembolization: Angiogenic factors and Response) (22). The studies were conducted in accordance with the institutions' Medical Ethical Committee and informed consent was obtained from the patients treated in the HEPAR-2 and RADAR studies before inclusion. For the other patients that were treated in routine clinical practice and also included in the current retrospective analysis, the need for informed consent was waived. Inclusion criteria for all patients regarding the presence of extrahepatic metastases or the primary tumor were similar: liver-dominant disease with a maximum of five lung nodules <1 cm and lymph nodes <2 cm. The presence of the primary tumor was not a contra-indication to treatment. Patients were included for response analysis in case CT and/or MRI scans were available at baseline and at (around) three-months follow-up; all patients were included for survival analysis. Patients were treated with ^{166}Ho-microspheres (n=24)(all as part of the HEPAR 2 study), glass ^{90}Y-microspheres (n=20), or resin ^{90}Y-microspheres (n=46). Imaging was performed three months after treatment (i.e. whole-liver or lobar treatment in one session). In case of sequential lobar treatment, imaging was performed three months after the last lobar treatment.

The electronic medical records were reviewed to obtain patient characteristics. The following established independent prognostic factors in patients with mCRC were compared: age, number of previous chemotherapy lines, type of microspheres, presence of extrahepatic disease at baseline, primary tumor in

situ, time since diagnosis of metastases, WHO performance status, KRAS wild type versus KRAS mutation, pre-treatment CEA level, primary tumor location (categorized as left sided (splenic flexure to rectum) or right sided (proximal to the splenic flexure)) and tumor load (percentage liver involvement, categorized as <25%, 25-50%, >50%) (21, 25, 27-33).

Radioembolization

The prescribed activity for the patients that were treated with glass ^{90}Y-microspheres was calculated according to the Medical Internal Radiation Dose (MIRD) method, with a desired absorbed dose of 80-120 Gy, according to the instructions for use (34-36). Visual and quantitative assessment of ^{99m}Tc-MAA distribution is weighted in this decision, also considering whole liver treatment in one session or sequentially. For the patients that were treated with resin ^{90}Y-microspheres, the body surface area (BSA) method was used. The injected activity for ^{166}Ho-microspheres was calculated based on the MIRD method with an aimed whole-liver absorbed dose of 60 Gy (37).

Response assessments

Two blinded readers independently performed measurements for tumor diameter on abdominal contrast-enhanced CT or MRI at baseline and three-months follow-up, using the same modality at both time points, according to RECIST version 1.1 (17). In case no consensus was reached, a third reader gave the final call. Finally, inter-observer variability between the two raters was assessed.

Response at three months was dichotomized as disease control (i.e. complete or partial response (CR or PR) and stable disease (SD)) or progressive disease (PD). For a more detailed assessment of mode of progressive disease a further subdivision was made in four categories: growth of intrahepatic metastases, growth of extrahepatic metastases, new intrahepatic metastases, and new extrahepatic metastases. All extrahepatic metastases were taken into account, regardless of their size.

Statistical analyses

Standard descriptive statistics were used to display patient demographics and summarize response measures. Cohen's kappa was used to determine agreement. Chi-Square was used to test for differences in whole body response

classification. Firth's logistic regression was used to explore associations between baseline characteristics and mode of progression. This type of analysis was chosen to correct for small-sample bias (38). The analysis for the association between extrahepatic disease at baseline and disease progression was adjusted for the following possible confounders: time from diagnosis of metastases to treatment, primary tumor in situ, KRAS mutation vs wild type, number of lines of previous systemic treatment (one versus two or more). The analysis for the association between type of microsphere used and disease progression was adjusted for the following possible confounders: age, time from diagnosis of metastases to treatment, primary tumor in situ, KRAS mutation vs wild type, number of lines of previous systemic treatment (one versus two or more) and presence of extrahepatic disease. Univariable survival analysis by the Kaplan-Meier method was used to estimate median overall survival (OS) in all treated patients. A Cox proportional hazards model with Firth's correction was used to test for differences in survival between patients with and without extrahepatic disease at baseline. All analyses were performed using R version 3.6.2 for Windows. We report effect estimates with associated 95%CIs and corresponding two-sided p-values.

RESULTS

Patient demographics

Of the total cohort of 129 treated patients in our institution, 39 patients (30%) did not have three-month follow-up imaging available because of the following reasons: follow-up imaging in other hospital (n=5), only follow-up imaging at one month post-treatment (n=21), only response evaluation using ^{18}F-FDG PET (with no accompanying contrast-enhanced CT) (n=5), clinical progression (n=5), no follow-up imaging available (n=2) and RFA artefacts (n=1). The remaining 90 patients had either CT (n=67, 74%) or MRI (n=23, 26%) images available at baseline and three-months follow-up. Median interval between baseline imaging and radioembolization was 18 days (range 1 – 46), between radioembolization and follow-up 91 days (range 62 – 165). Baseline- and treatment characteristics are summarized in Table 1. ^{166}Ho-microspheres, glass ^{90}Y-microspheres, and resin ^{90}Y-microspheres were used in 24 (27%), 20 (22%), and 46 patients (51%) respectively. None of the patients received systemic treatment before (<4 weeks), during or after (<3 months) radioembolization.

TABLE 1. Baseline and treatment characteristics

Characteristic	N (%) or median with range					
	^{90}Y-resin	*^{90}Y-glass*	*^{166}Ho*	*No extrahepatic disease*	*Extrahepatic disease at baseline*	*Total*
N	46 (51)	20 (22)	24 (27)	48 (53)	42 (47)	90 (100)
Age (years)	65 (35-84)	67 (45-78)	66 (40-84)	66 (34-84)	66 (40-84)	66 (35-84)
Gender						
Male	33 (72)	15 (75)	17 (63)	34 (71)	31 (74)	65 (72)
Female	13 (28)	5 (25)	7 (37)	14 (29)	11 (26)	25 (28)
WHO performance status						
0	24 (52)	15 (75)	19 (79)	29 (60)	29 (69)	58 (64)
1	19 (41)	5 (25)	5 (21)	18 (38)	11 (26)	29 (32)
2	3 (7)	0 (0)	0 (0)	1 (2)	2 (5)	3 (4)
Previous chemotherapy lines						
0	1 (2)	0 (0)	0 (0)	1 (2)	0 (0)	1 (1)
1	13 (28)	9 (45)	11 (46)	18 (38)	15 (36)	33 (37)
2	21 (46)	8 (40)	11 (46)	21 (44)	9 (21)	40 (44)
3	11 (24)	3 (15)	2 (8)	8 (17)	8 (19)	16 (18)
Bevacizumab	29 (63)	13 (65)	13 (54)	32 (67)	23 (55)	55 (61)
Capecitabine	42 (91)	18 (90)	20 (83)	41 (85)	39 (93)	80 (89)
Cetuximab	2 (4)	0 (0)	1 (4)	1 (2)	2 (5)	3 (4)
Cisplatin	1 (2)	0 (0)	0 (0)	1 (2)	0 (0)	1 (1)
Erlotinib	0 (0)	0 (0)	1 (4)	0 (0)	1 (2)	1 (1)

TABLE 1. Baseline and treatment characteristics (continued)

Characteristic	N (%) or median with range					
	^{90}Y-resin	*^{90}Y-glass*	*^{166}Ho*	*No extrahepatic disease*	*Extrahepatic disease at baseline*	*Total*
Irinotecan	26 (57)	9 (45)	10 (42)	23 (48)	22 (52)	45 (50)
Oxaliplatin	40 (87)	17 (85)	23 (96)	41 (85)	39 (93)	80 (89)
Paclitaxel	0 (0)	0 (0)	1 (4)	0 (0)	1 (1)	1 (1)
Panitumumab	8 (17)	4 (20)	3 (13)	9 (19)	6 (14)	15 (17)
5-FU	7 (15)	3 (15)	5 (21)	7 (15)	8 (19)	15 (17)
Previous locoregional treatment						
Yes	17 (37)	7 (35)	6 (25)	17 (35)	13 (31)	30 (33)
No	29 (63)	13 (65)	18 (75)	31 (65)	29 (69)	60 (67)
Metastasis pattern						
Synchronous	31 (67)	15 (75)	15 (63)	27 (56)	34 (81)	61 (68)
Metachronous	15 (33)	5 (25)	9 (37)	21 (44)	8 (19)	29 (32)
Time since diagnosis (months)	25 (3-97)	24 (11-110)	26 (6-92)	26 (3-110)	21 (5-92)	25 (3-110)
Time since diagnosis of metastatic disease (months)	17 (3-72)	23 (2-50)	18 (2-92)	17 (2-54)	21 (5-92)	19 (2-92)
KRAS status						
Wildtype	16 (35)	8 (40)	9 (37)	21 (44)	12 (29)	33 (37)
Mutation	11 (24)	3 (15)	6 (26)	7 (15)	13 (31)	20 (22)
Unknown	19 (41)	9 (45)	9 (37)	10 (21)	17 (40)	37 (41)
CEA level	72 (3-2700)	68 (3-640)	100 (2-6000)	61 (2-2700)	115 (3-6000)	88 (2-6000)

TABLE 1. Baseline and treatment characteristics (continued)

Characteristic	N (%) or median with range					
	^{90}Y-resin	*^{90}Y-glass*	*^{166}Ho*	*No extrahepatic disease*	*Extrahepatic disease at baseline*	*Total*
Unknown	12 (26)	4 (20)	1 (4)	7 (15)	10 (24)	17 (19)
Primary tumor in situ						
Yes	1 (2)	4 (20)	2 (8)	2 (4)	5 (12)	7 (8)
No	45 (98)	16 (80)	22 (92)	46 (96)	37 (88)	83 (92)
Extrahepatic disease (all metastases)						
None	27 (59)	9 (45)	10 (42)	48 (100)	0 (0)	48 (53)
Lymph node metastases	12 (26)	8 (40)	7 (29)	-	25 (60)	25 (28)
Lung metastases	8 (17)	2 (10)	7 (29)	-	17 (40)	17 (19)
Abdominal wall metastases	1 (2)	0 (0)	0 (0)	-	1 (2)	1 (1)
Spleen metastases	0 (0)	0 (0)	2 (8)	-	1 (2)	1 (1)
Adrenal gland metastases	0 (0)	2 (10)	0 (0)	-	2 (5)	2 (2)
Peritoneal metastases	1 (2)	0 (0)	2 (8)	-	3 (7)	3 (3)
Type of radioembolization						
Whole-liver	41 (89)	12 (60)	20 (83)	38 (79)	35 (83)	73 (81)
Lobar	5 (11)	8 (40)	4 (17)	10 (21)	7 (17)	17 (19)
Injected activity (MBq)	1526 (636-2320)	2037 (711-6277)	6565 (2213-11627)	1882 (636-11164)	1992 (680-11627)	Not applicable
Lungshunt (%)	5 (0.1-17)	2.3 (1-26)	4.6 (0.3-16)	4.5 (0.1-17)	3.4 (0.8-26)	4 (0.1-26)

Inter-observer variability

Discordant conclusions were drawn in five patients, for whom the third rater gave the final call. The level of agreement in RECIST categories was adequate with a Cohen's kappa of 0.895 (95% CI 0.805-0.985), p<0.001.

Response according to RECIST 1.1

At baseline, 42/90 (47%) patients had extrahepatic metastases, which increased to 67/90 (74%) patients at three-months follow-up (Figure 1).

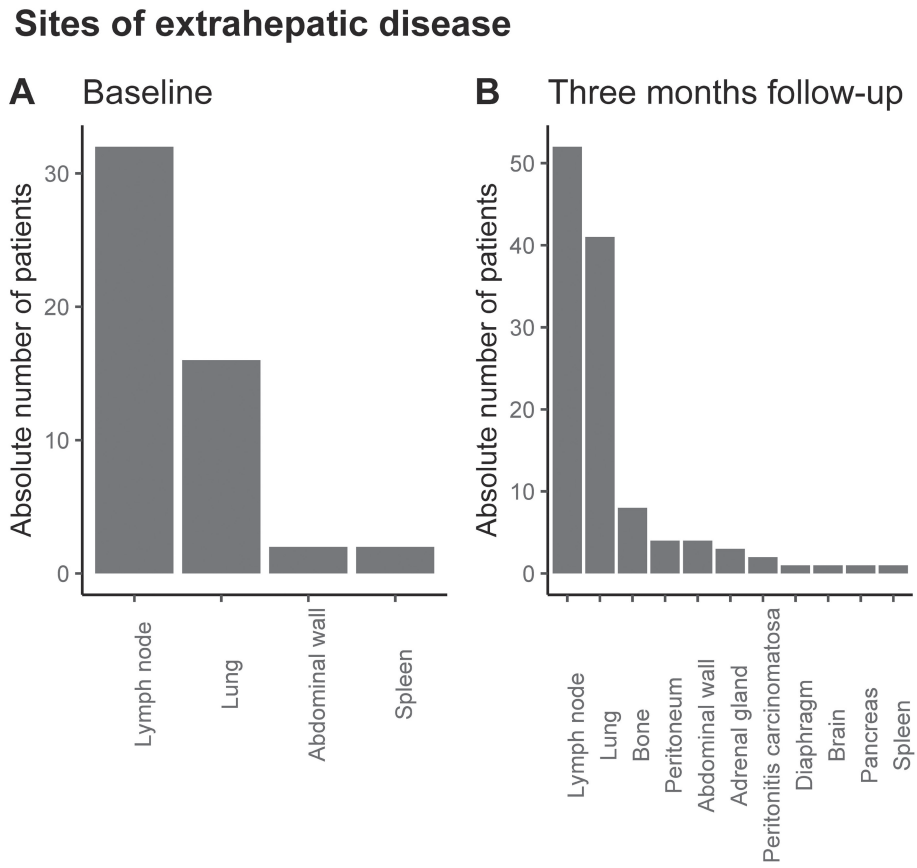

FIGURE 1. Site of extrahepatic metastases at baseline and at 3-months follow-up. (a) Type and number of affected organs in patients with extrahepatic metastases at baseline. Bars depict absolute number of patients. In total 50 affected organs in 42 patients. (b) As in (a), for three-months follow-up. In total 119 affected organs in 67 patients. Lymph nodes and lung are most affected at baseline and three-months follow-up.

Of the 90 patients, no patients showed CR, 5 (5.5%) patients had PR, 16 (17.8%) had SD and 69 (76.7%) had PD. According to RECIST, progressive disease can be based on growth of intrahepatic metastases, growth of extrahepatic metastases or new metastases (either intra- or extrahepatic). Growth of intrahepatic metastases was observed in 20 patients (29%), new intrahepatic metastases in 35 patients (51%), growth of extrahepatic metastases in 37 patients (54%), and 56 patients (81%) were diagnosed with new extrahepatic metastases. Most, 67/69 of the progressive patients (97%), had new (intra-hepatic N=11, extrahepatic N=32; or both N=24) metastases. Progression was most often seen on multiple levels (N=42, 61%) and was only based on growth of existing metastases in 5 patients (7%, intra-hepatic N=2, extrahepatic N=3) and on only new lesions in 23 patients (69%) (Figure 2a). In the subgroup of progressive patients with extrahepatic disease at baseline, new extrahepatic metastases were most common, in 28/42 (67%) patients (Figure 2b).

There was no significant difference in response between the three types of microspheres used: compared to ^{90}Y resin microspheres, the odds ratios for progressive disease with ^{90}Y glass and ^{166}Ho were 1.11 (95%CI 0.32-4.53) and 0.67 (95%CI 0.22-2.14), respectively (Table 2).

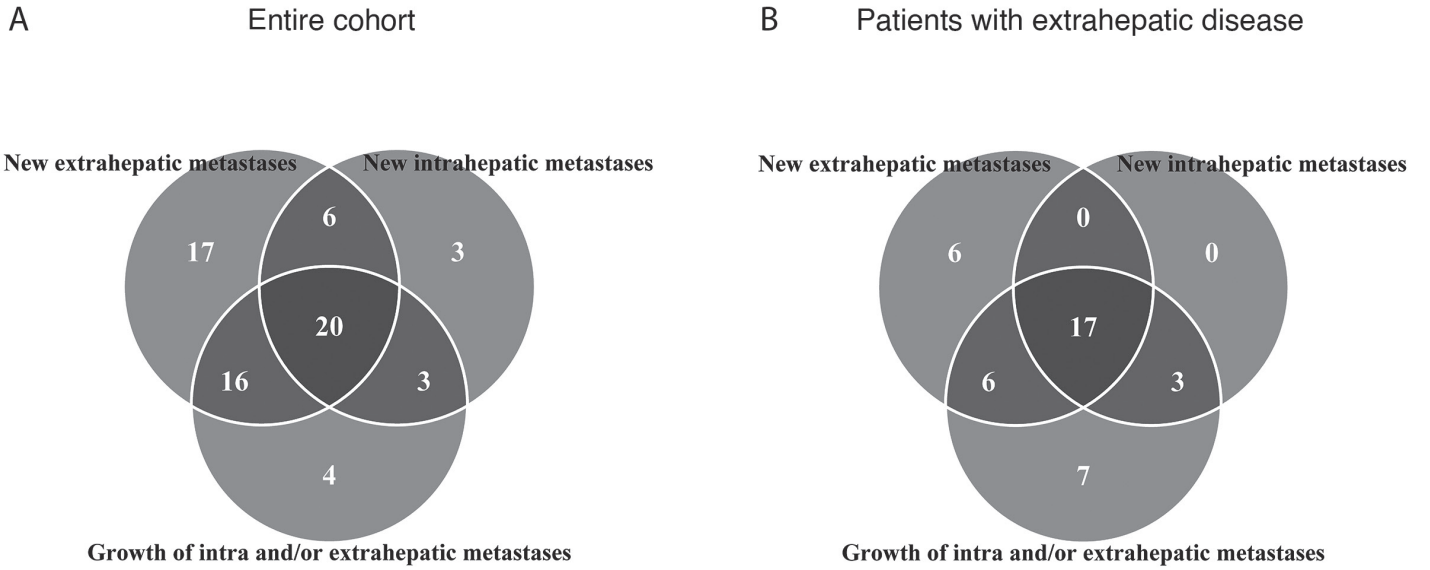

FIGURE 2. Mode of progression of the entire cohort (90 patients) (a) and specific for patients with extrahepatic disease at baseline (42 patients) (b). Numbers indicate the number of patients in the indicated (overlapping) group.

TABLE 2. Univariable Firth's logistic regression analysis for baseline characteristics and type of progression: OR (95%CI)

	PD	GIHM (n=20)	GEHM (n=37)	NIHM (n=35)	NEHM (n=57)	GM (n=45)	NM (n=63)
Age in years	1.02 (0.97;1.07)	0.99 (0.02;9.75)	1.01 (0.97;1.06)	1.02 (0.98, 1.06)	1.00 (0.96;1.05)	1.01 (0.97;1.06)	1.01 (0.97;1.05)
Chemotherapy*	0.88 (0.01;88.46)	0.74 (0.26;2.01)	0.87 (0.37;2.05)	0.37 (0.14;0.91)	0.63 (0.26;1.51)	0.57 (0.24;1.33)	0.48 (0.19;1.19)
Type of microspheres **–Glass	1.11 (0.32;4.53)	0.71 (0.18;2.41)	2.53 (0.87;7.56)	1.71 (0.59;4.99)	1.5 (0.50;4.89)	1.79 (0.62;5.35)	1.94 (0.59-7.65)
Type of microspheres - Holmium	0.67 (0.22;2.14)	0.57 (0.14;1.88)	1.75 (0.63;4.86)	0.85 (0.29;2.38)	0.90 (0.33;2.50)	1.19 (0.44;3.22)	0.81 (0.29-2.31)
Extrahepatic metastases at baseline	7.8 (2.37;35.53)	2.39 (0.89;6.84)	NA	1.83 (0.79;4.32)	3.06 (1.28;7.72)	NA	2.86 (1.14;7.66)
Primary tumor in situ	1.90 (0.30;37.11)	0.76 (0.08;3.96)	1.12 (0.24;4.88)	3.86 (0.87;22.5)	2.73 (0.54;27.1)	1.32 (0.30;6.21)	2.00 (0.39;19.9)
WHO status***	0.87 (0.32;2.46)	0.43 (0.10;1.43)	0.91 (0.35;2.33)	0.90 (0.33;2.33)	0.50 (0.19;1.31)	0.86 (0.34;2.19)	0.81 (0.30;2.27)
KRAS status§	3.38 (0.75;23.95)	1.88 (0.56;6.45)	2.75 (0.90;8.78)	4.78 (1.52;16.5)	3.92 (1.11;17.2)	2.85 (0.92;9.48)	2.67 (0.74;11.86)
Time since diagnosis of metastases§§	1.06 (1.01;1.11)	0.98 (0.94;1.01)	1.01 (0.99;1.04)	0.98 (0.95;1.01)	1.02 (0.99;1.05)	1.01 (0.98;1.03)	1.02 (0.99;1.07)
CEA level before treatment	1.00 (0.99-1.00)	1.00 (95%CI 0.99-1.00)	1.00 (95%CI 0.99-1.00)	1.00 (95%CI 0.99-1.00)	1.00 (0.99-1.00)	1.00 (0.99-1.01)	1.00 (0.99-1.01)
Primary tumor location	3.88 (1.00-25.75)	0.88 (0.26-2.63)	0.98 (0.35-2.63)	1.72 (0.65-4.59)	2.96 (0.98-11.11)	0.94 (0.36-2.49)	3.88 (1.00-25.76)
Tumor load† – 25%-50%	1.63 (0.50-6.35)	0.56 (0.14-1.79)	1.17 (0.42-3.16)	0.58 (0.20-1.59)	0.94 (0.34-2.72)	1.04 (0.39-2.74)	1.11 (0.36-3.90), 0.7
Tumor load - >50%	0.73 (0.20-3.10)	1.24 (0.30-4.49)	1.67 (0.47-5.76)	1.64 (0.48-5.76)	0.55 (0.16-1.95)	1.66 (0.49-6.12)	0.66 (0.18-2.77)

This table shows the associations (odds ratio and 95%CI) between baseline characteristics and modes of progression as described by RECIST at 3 months post-treatment.
* previous treatment with 1st versus 2nd line chemotherapy
** Yttrium-90 resin (reference) versus yttrium-90 glass and holmium-166
*** WHO performance status 0 versus 1, 2
§ KRAS mutation versus KRAS wild type
§§ Right-sided primary tumors versus left-sided primary tumors
† <25% liver involvement versus 25%-50% and >50% liver involvement
Abbreviations: GIHM = growth of intrahepatic metastases. GEHM = growth of extrahepatic metastases. NIHM = new intrahepatic metastases. NEHM = new extrahepatic metastases. GM = growth of metastases (GEHM + GIHM). NM = new metastases (NEHM + NIHM). NA = not applicable. RE = radioembolization. OR = odds ratio. PD = progressive disease. 95% CI = 95% confidence interval.

Correlations between baseline characteristics and response

The association between several baseline characteristics and response was assessed (Table 2). Presence of extrahepatic disease was the most significant risk factor for progressive disease, with an OR of 7.8 (95% CI 2.37-35.53) for patients with extrahepatic disease at baseline versus patients without extrahepatic disease at baseline (Figure 3). Extrahepatic metastases at baseline increased the risk of progressive disease for all modes of progression, mainly for new extrahepatic metastases (OR=3.06, 95% CI 1.28-7.72). Time since diagnosis of metastases was a significant risk factor for progressive disease as well, with an OR of 1.06 for every month increase in time (95%CI 1.01-1.11). Primary tumor location showed a strong trend, with an OR of 3.88 (95%CI 1.00-25.75) for patients with right-sided primary tumors versus patients with left-sided primary tumors. There was no significant difference between type of microspheres used.

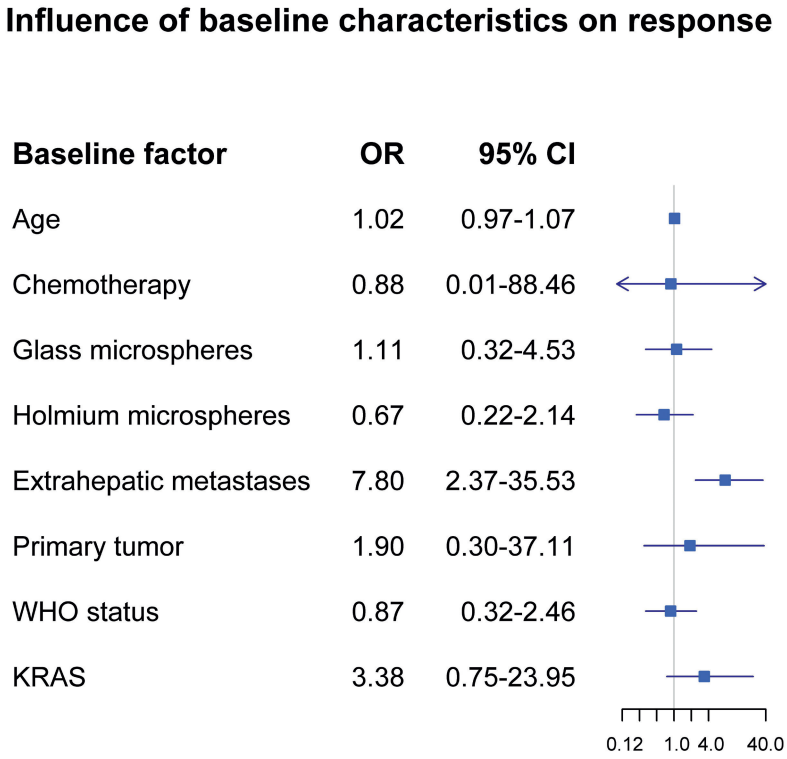

FIGURE 3. Forest plot of the influence of baseline characteristics on response (progression versus no progression according to RECIST 1.1), based on univariable analyses.

The difference in response evaluation was compared for patients with or without extrahepatic metastases at baseline. Of the group (n=42, 47%) presenting with extrahepatic metastases at baseline, 93% was diagnosed with PD at three-months follow-up. Significantly fewer patients (63%) were diagnosed with progressive disease in the group of patients (n=48, 53%) presenting without extrahepatic metastases at baseline (p=0.0017) (Table 3).

TABLE 3. RECIST 1.1 response classification at 3-months post-treatment

Total	No extrahepatic metastases at baseline		48(53%)
		Complete response	0 (0%)
		Partial response	5 (10%)
		Stable disease	13 (27%)
		Progressive disease	30 (63%)
	Extrahepatic metastases at baseline		42 (47%)
		Complete response	0 (0%)
		Partial response	0 (0%)
		Stable disease	3 (7%)
		Progressive disease	39 (93%)*
Yttrium-90 Resin	No extrahepatic metastases at baseline		28(61%)
		Complete response	0 (0%)
		Partial response	1 (4%)
		Stable disease	7 (25%)
		Progressive disease	20 (71%)
	Extrahepatic metastases at baseline		18 (39%)
		Complete response	0 (0%)
		Partial response	0 (0%)
		Stable disease	2 (11%)
		Progressive disease	16 (89%)
Yttrium-90 Glass	No extrahepatic metastases at baseline		9 (45%)
		Complete response	0 (0%)
		Partial response	2 (22%)
		Stable disease	2 (22%)
		Progressive disease	5 (56%)
	Extrahepatic metastases at baseline		11 (55%)
		Complete response	0 (0%)
		Partial response	0 (0%)

TABLE 3. RECIST 1.1 response classification at 3-months post-treatment (continued)

		Stable disease	0 (0%)
		Progressive disease	11 (100%)
Holmium-166	No extrahepatic metastases at baseline		11 (46%)
		Complete response	0 (0%)
		Partial response	2 (18%)
		Stable disease	4 (36%)
		Progressive disease	5 (46%)
	Extrahepatic metastases at baseline		13 (54%)
		Complete response	0 (0%)
		Partial response	0 (0%)
		Stable disease	1 (8%)
		Progressive disease	12 (92%) *

This table shows a comparison of RECIST 1.1 response classification at three-months post-treatment for patients with or without extrahepatic metastases at baseline. Numbers represent number of patients (% of total/subcategory). * marks significant difference between groups; $p<0.05$

Prognostic value of extrahepatic disease at baseline based on overall survival (OS)

Median OS for the 90 included patients was 10 months (95% CI 9-14 months). Presence of extrahepatic metastases at baseline showed a difference in median OS estimates with ten months (95% CI: 7-14) for patients with-, and 12 months (95% CI: 9-19) for patients without extrahepatic metastases at baseline (hazard ratio (HR) 1.68, 95%CI (1.09-2.59), p=0.019) (Figure 4).

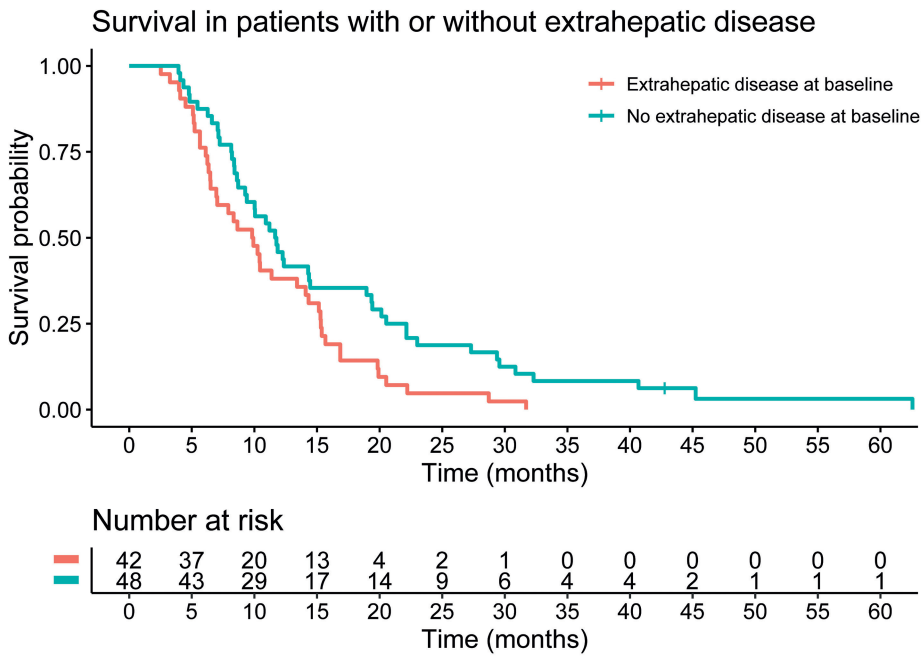

FIGURE 4. Kaplan-Meier survival curve stratified for extrahepatic metastases at baseline.

DISCUSSION

This study shows that a large proportion of end-stage mCRC patients have progressive disease after radioembolization due to the development of new metastases, and to a lesser extent on the growth of existing metastases. The presence of extrahepatic disease at baseline significantly increases the chance of early progressive disease at three months, especially the development of new metastases. Moreover, patients with extrahepatic metastases at baseline had a significantly worse overall survival.

At baseline, 48% of our study population was diagnosed with extrahepatic metastases. This is in line with other studies in which 35-77% of the included patients had extrahepatic metastases at baseline (18-20, 39-44). We found a difference in median OS with- and without the presence of extrahepatic metastases at baseline, respectively 7 versus 10 months (p=0.0018). Several

other studies with a comparable patient population also found that extrahepatic disease was a predictor of survival after radioembolization (24, 45-49). Other known prognostic factors are tumor load, baseline CEA level and location (left- versus right-sidedness) of the primary tumor (24, 49, 50). In our study, only location of the primary tumor showed a clear trend for significance, with the odds ratio for progressive disease being 3.88 (95%CI: 1.00-25.75) for patients with a right-sided primary tumor versus patients with a left-sided primary tumor.

Genetics and biomarkers are more and more recognized as prognostic factors. We investigated the possible role of CEA, since this was associated with poorer survival after radioembolization in multiple studies (19, 24, 51). However, just as in the study of Sofocleus et al., in our study no significant correlation between pre-treatment CEA level and disease progression was found (19). Patients with KRAS mutation generally have a worse prognosis after radioembolization than patients with KRAS wild type status (19, 24, 25, 52). In our study, although not significant, the odds ratios for all types of progressive disease showed a clear trend for a worse prognosis for patients with KRAS mutation versus patients with KRAS wild type (Table 2).

In The Netherlands, indications for radioembolization include liver-dominant, irresectable, systemic therapy-refractory disease. Patients with significant extrahepatic metastases are not considered eligible, but patients with stable, limited extrahepatic disease (defined by the Dutch National Healthcare Institute as a maximum of 5 lung nodules <1 cm and lymph nodes <2 cm) are eligible (53). This criterion was also used in the patients in this study. The SIRFLOX, FOXFIRE and FOXFIRE-Global (studying the added value of radioembolization to chemotherapy in first-line mCRC patients) used similar inclusion criteria with respect to extrahepatic disease (54). In these studies, no difference in OS or overall progression-free survival (PFS) was observed (55). One may argue that the large percentage of patients with extrahepatic disease in these studies (i.e. 36%) clouded the potential clinical benefit of radioembolization in a more stringent selected subset. In a subgroup of patients with right-sided primary tumors, the presence of extrahepatic metastases at baseline indeed proved to be a negative prognostic factor for OS, with a HR of 1.351 (95%CI 0.96-1.91)

(50). Importantly, these studies were performed in first line refractory disease. This limits comparison with our study in a more advanced-stage population.

Objective response (CR or PR) at three months after treatment was obtained in only 6% of our patients. This is in line with other studies in salvage mCRC patients, with reported response ranges of 6%-24% (24, 56, 57). Median OS in our study was ten months, which is also in line with other studies in a comparable patient population (22, 24, 58).

A reason for the modest treatment results in our study might be the dosimetric models that were used: the BSA and MIRD methods. These methods can lead to underdosing (59, 60). A personalized treatment approach, as was used in the DOSISPHERE study in HCC patients, could have led to a much higher response rate (61). The results of earlier studies on the dose-response relations in mCRC patients treated with ^{90}Y-resin or ^{166}Ho prove this point: a significant dose-response relationship was found in both studies (22, 62). Implementing the results of these studies in future patients, using an individualized treatment approach, likely will lead to a higher treatment accuracy.

In our study, response was evaluated using the anatomic criteria as defined by the RECIST guidelines. However, this can be hampered by the presence of necrosis, hemorrhage and cystic changes (63). Response assessment based on changes in functional metrics as determined on [^{18}F]-FDG PET/CT would be a better evaluation method, especially since several studies found that these are related with overall survival (13, 22, 64, 65). Unfortunately, not all patients in our study underwent baseline and post-treatment imaging by [^{18}F]-FDG PET/CT.

The added value of the present study to the existing knowledge on radioembolization in mCRC patients is the fact that the development of new metastases is the primary cause for progressive disease after treatment. Furthermore, the study shows that the development of new lesions, as well as progressive disease in general, is more common in patients with extrahepatic disease at baseline.

The current study also has several limitations. First of all, the sample size was small. Secondly, the retrospective setting was prone to selection bias. Since

radioembolization was used in a salvage setting, outcome was likely muddled by the effect of other, previous therapies (Table 1). However, since patients were selected for radioembolization based on their chemo-resistant tumors, the contribution of this variation in our patient population on the outcome of our study was considered minimal. Third, all patients were discussed in a multidisciplinary tumor board before treatment. Based on available imaging, the primary tumor was assessed for stability and the extrahepatic disease load was assessed for extent, however, not for stability. Also, although radioembolization is nowadays often performed in a lobar approach, a large fraction of patients that we studied received whole-liver treatment. Whole-liver treatment was in large part dictated by study protocols. Furthermore, three types of microspheres were used in our dataset. The differences with regard to the embolic nature of the treatment, the specific activity of the microspheres, the administered activities, and the absorbed doses may have influenced the incidence of early progressive disease, and potentially also the mode of progression, although our analyses did not show a significant difference between microsphere types. Last, KRAS status was unknown in 42% of the patients, making the number of patients for the subgroup analyses for KRAS rather small.

Proper selection of patients seems fundamental for the cost-effectiveness of radioembolization treatment. Future prospective studies in the salvage setting should therefore be conservative with regard to the acceptance of extrahepatic disease. Accurate baseline imaging, including FDG-PET, may aid patient selection (66). This will avoid futile treatments and unnecessary toxicity. However, the effect of radioembolization in patients with extrahepatic disease should be evaluated in prospective studies comparing radioembolization with best supportive care, before a firm statement can be made about the exclusion of patients with extrahepatic disease from treatment. Also, considering the development of new lesions as the major cause of progressive disease, a study in the third line, comparing TAS-102 or regorafenib with and without radioembolization would be interesting. The study of Hendlisz et al. showed that radioembolization combined with chemotherapy was safe and effective (58). Based on the results of this study, chemotherapy in addition to radioembolization was therefore recommended in the refractory setting.

Proper selection and individualized dosimetry-based treatment planning should ultimately lead to improved treatment accuracy in mCRC patients.

CONCLUSIONS

In conclusion, response at three-month follow-up and survival were heavily influenced by new intra- and extrahepatic metastases. Patients with extrahepatic disease at baseline had a worse outcome compared to patients without extrahepatic disease at baseline. Based on the results of this observational, retrospective study, extrahepatic disease may be considered a contraindication for treatment with radioembolization.

LIST OF ABBREVIATIONS

^{90}Y	yttrium-90
^{166}Ho	holmium-166
BSA	body surface area
CR	complete response
CRC	colorectal cancer
mCRC	colorectal cancer metastases
MIRD	medical internal adiation dose
OS	overall survival
HCC	hepatocellular carcinoma
HEPAR-2	Holmium Embolization Particles for Arterial Radiotherapy II
HR	hazard ratio
PD	progressive disease
PFS	progression-free survival
PR	partial response
RADAR	RADioembolization: Angiogenic factors and Response
RECIST	response evaluation criteria in solid tumors
SD	stable disease

REFERENCES

1. Norstein J, Silen W. Natural history of liver metastases from colorectal carcinoma. J Gastrointest Surg. 1997;1(5):398-407.

2. Ruers T, Bleichrodt RP. Treatment of liver metastases, an update on the possibilities and results. Eur J Cancer. 2002;38(7):1023-33.

3. Bengtsson G, Carlson G, Hafstrom L, Jonsson PE. Natural History of Patients With Untreated Liver Metastases From Colorectal Cancer. Am J Surg. 1981;141:586-9.

4. Manfredi S, Lepage C, Hatem C, Coatmeur O, Faivre J, Bouvier AM. Epidemiology and management of liver metastases from colorectal cancer. Ann Surg. 2006;244(2):254-9.

5. Engstrand J, Nilsson H, Stromberg C, Jonas E, Freedman J. Colorectal cancer liver metastases - a population-based study on incidence, management and survival. BMC Cancer. 2018;18(1):78.

6. Benson AB, Venook AP, Al-Hawary MM, Cederquist L, Chen YJ, Ciombor KK, et al. NCCN Guidelines Insights: Colon Cancer, Version 2.2018. J Natl Compr Canc Netw. 2018;16(4):359-69.

7. Van Cutsem E, Cervantes A, Adam R, Sobrero A, Van Krieken JH, Aderka D, et al. ESMO consensus guidelines for the management of patients with metastatic colorectal cancer. Ann Oncol. 2016;27(8):1386-422.

8. Murthy R, Habbu A, Salem R. Trans-arterial hepatic radioembolisation of yttrium-90 microspheres. Biomed Im Interv J. 2006;2(3):e43.

9. Smits ML, Prince JF, Rosenbaum CE, van den Hoven AF, Nijsen JF, Zonnenberg BA, et al. Intra-arterial radioembolization of breast cancer liver metastases: a structured review. Eur J Pharmacol. 2013;709(1-3):37-42.

10. Bierman HR, Byron RL, Jr., Kelley KH, Grady A. Studies on the blood supply of tumors in man. III. Vascular patterns of the liver by hepatic arteriography in vivo. J Natl Cancer Inst. 1951;12(1):107-31.

11. Breedis C, Young G. The blood supply of neoplasms in the liver. Am J Pathol. 1954;30(5):969-77.

12. Lien WM, Ackerman NB. The blood supply of experimental liver metastases. II. A microcirculatory study of the normal and tumor vessels of the liver with the use of perfused silicone rubber. Surgery. 1970;68(2):334-40.

13. Bastiaannet R, Lodge MA, de Jong H, Lam M. The Unique Role of Fluorodeoxyglucose-PET in Radioembolization. PET Clin. 2019;14(4):447-57.

14. Sager S, Akgun E, Uslu-Besli L, Asa S, Akovali B, Sahin O, et al. Comparison of PERCIST and RECIST criteria for evaluation of therapy response after yttrium-90 microsphere therapy in patients with hepatocellular carcinoma and those with metastatic colorectal carcinoma. Nucl Med Commun. 2019;40(5):461-8.

15. Buyse M, Thirion P, Carlson RW, Burzykowski T, Molenberghs G, Piedbois P. Relation between tumour response to first-line chemotherapy and survival in advanced colorectal cancer: a meta-analysis. Meta-Analysis Group in Cancer. Lancet (London, England). 2000;356(9227):373-8.

16. Therasse P, Arbuck SG, Eisenhauer EA, Wanders J, Kaplan RS, Rubinstein L, et al. New Guidelines to Evaluate the Response to Treatment in Solid Tumors. J Natl Cancer Inst. 2000;92(3):205-16.

17. Eisenhauer EA, Therasse P, Bogaerts J, Schwartz LH, Sargent D, Ford R, et al. New response evaluation criteria in solid tumours: revised RECIST guideline (version 1.1). Eur J Cancer. 2009;45(2):228-47.

18. Martin LK, Cucci A, Wei L, Rose J, Blazer M, Schmidt C, et al. Yttrium-90 radioembolization as salvage therapy for colorectal cancer with liver metastases. Clin Colorect Cancer. 2012;11(3):195-9.

19. Sofocleous CT, Violari EG, Sotirchos VS, Shady W, Gonen M, Pandit-Taskar N, et al. Radioembolization as a Salvage Therapy for Heavily Pretreated Patients With Colorectal Cancer Liver Metastases: Factors That Affect Outcomes. Clin Colorect Cancer. 2015;14(4):296-305.

20. Bester L, Meteling B, Pocock N, Pavlakis N, Chua TC, Saxena A, et al. Radioembolization versus standard care of hepatic metastases: comparative retrospective cohort study of survival outcomes and adverse events in salvage patients. J Vasc Interv Radiol. 2012;23(1):96-105.

21. Kennedy A, Cohn M, Coldwell DM, Drooz A, Ehrenwald E, Kaiser A, et al. Updated survival outcomes and analysis of long-term survivors from the MORE study on safety and efficacy of radioembolization in patients with unresectable colorectal cancer liver metastases. J Gastrointest Oncol. 2017;8(4):614-24.

22. Van den Hoven AF, Rosenbaum CE, Elias SG, de Jong HW, Koopman M, Verkooijen HM, et al. Insights into the Dose-Response Relationship of Radioembolization with Resin 90Y-Microspheres: A Prospective Cohort Study in Patients with Colorectal Cancer Liver Metastases. J Nucl Med. 2016;57(7):1014-9.

23. Salem R, Padia SA, Lam M, Bell J, Chiesa C, Fowers K, et al. Clinical and dosimetric considerations for Y90: recommendations from an international multidisciplinary working group. Eur J Nucl Med Mol Im. 2019;46(8):1695-704.

24. Kurilova I, Beets-Tan RGH, Flynn J, Gonen M, Ulaner G, Petre EN, et al. Factors Affecting Oncologic Outcomes of 90Y Radioembolization of Heavily Pre-Treated Patients With Colon Cancer Liver Metastases. Clinical Colorect Cancer. 2019;18(1):8-18.

25. Lahti SJ, Xing M, Zhang D, Lee JJ, Magnetta MJ, Kim HS. KRAS Status as an Independent Prognostic Factor for Survival after Yttrium-90 Radioembolization Therapy for Unresectable Colorectal Cancer Liver Metastases. J Vasc Interv Radiol. 2015;26(8):1102-11.

26. Prince JF, van den Bosch M, Nijsen JFW, Smits MLJ, van den Hoven AF, Nikolakopoulos S, et al. Efficacy of radioembolization with holmium-166 microspheres in salvage patients with liver metastases: a phase 2 study. J Nucl Med. 2017.

27. Kosmider S, Tan TH, Yip D, Dowling R, Lichtenstein M, Gibbs P. Radioembolization in combination with systemic chemotherapy as first-line therapy for liver metastases from colorectal cancer. J Vasc Interv Radiol. 2011;22(6):780-6.

28. Ahmadzadehfar H, Sabet A, Meyer C, Habibi E, Biersack HJ, Ezziddin S. The Importance of Tc-MAA SPECT/CT for Therapy Planning of Radioembolization in a Patient Treated With Bevacizumab. Clin Nucl Med. 2012;37:1129-30.

29. Lam MG, Banerjee S, Louie JD, Abdelmaksoud MH, Iagaru AH, Ennen RE, et al. Root cause analysis of gastroduodenal ulceration after yttrium-90 radioembolization. Cardiovasc Interv Radiol. 2013;36(6):1536-47.

30. Bhooshan N, Sharma NK, Badiyan S, Kaiser A, Moeslein FM, Kwok Y, et al. Pretreatment tumor volume as a prognostic factor in metastatic colorectal cancer treated with selective internal radiation to the liver using yttrium-90 resin microspheres. J Gastrointest Oncol. 2016;7(6):931-7.

31. Jakobs TF, Paprottka KJ, Raessler F, Strobl F, Lehner S, Ilhan H, et al. Robust evidence for long-term survival with (90) Y radioembolization in chemorefractory liver-predominant metastatic colorectal cancer. Eur Radiol. 2017;27(1):113-9.

32. Sato K, Lewandowski R, Mulcahy MF, Atassi B, Ryu RK, Gates VL, et al. Unresectable Chemorefractory Liver Metastases: Radioembolization with 90Y Microspheres—Safety, Efficacy, and Survival. Radiology. 2008;247(2):507-15.

33. Abbott AM, Kim R, Hoffe SE, Arslan B, Biebel B, Choi J, et al. Outcomes of Therasphere Radioembolization for Colorectal Metastases. Clin Colorect Cancer. 2015;14(3):146-53.

34. Salem R, Thurston KG. Radioembolization with 90Yttrium microspheres: a state-of-the-art brachytherapy treatment for primary and secondary liver malignancies. Part 1: Technical and methodologic considerations. J Vasc Interv Radiol. 2006;17(8):1251-78.

35. Salem R, Thurston KG. Radioembolization with 90yttrium microspheres: a state-of-the-art brachytherapy treatment for primary and secondary liver malignancies. Part 2: special topics. J Vasc Interv Radiol. 2006;17(9):1425-39.

36. Salem R, Thurston KG. Radioembolization with yttrium-90 microspheres: a state-of-the-art brachytherapy treatment for primary and secondary liver malignancies: part 3: comprehensive literature review and future direction. J Vasc Interv Radiol. 2006;17(10):1571-93.

37. Smits MLJ, Nijsen JFW, van den Bosch MAAJ, Lam MGEH, Vente MAD, Mali WPTM, et al. Holmium-166 radioembolisation in patients with unresectable, chemorefractory liver metastases (HEPAR trial): a phase 1, dose-escalation study. Lancet Oncol. 2012;13(10):1025-34.

38. Firth D. Bias reduction of maximum likelihood estimates. Biometrika. 1993;89(1):27-38.

39. Seidensticker R, Denecke T, Kraus P, Seidensticker M, Mohnike K, Fahlke J, et al. Matched-pair comparison of radioembolization plus best supportive care versus best supportive care alone for chemotherapy refractory liver-dominant colorectal metastases. Cardiovasc Interv Radiol. 2012;35(5):1066-73.

40. Kennedy AS, Ball DS, Cohen SJ, Cohn M, Coldwell DM, Drooz A, et al. Hepatic imaging response to radioembolization with yttrium-90-labeled resin microspheres for tumor progression during systemic chemotherapy in patients with colorectal liver metastases. J Gastrointest Oncol. 2015;6(6):594-604.

41. Lewandowski RJ, Memon K, Mulcahy MF, Hickey R, Marshall K, Williams M, et al. Twelve-year experience of radioembolization for colorectal hepatic metastases in 214 patients: survival by era and chemotherapy. Eur J Nucl Med Mol Im. 2014;41(10):1861-9.

42. Shady W, Petre EN, Gonen M, Erinjeri JP, Brown KT, Covey AM, et al. Percutaneous Radiofrequency Ablation of Colorectal Cancer Liver Metastases: Factors Affecting Outcomes--A 10-year Experience at a Single Center. Radiology. 2016;278(2):601-11.

43. Shady W, Sotirchos VS, Do RK, Pandit-Taskar N, Carrasquillo JA, Gonen M, et al. Surrogate Imaging Biomarkers of Response of Colorectal Liver Metastases After Salvage Radioembolization Using 90Y-Loaded Resin Microspheres. Am J Roentgenol. 2016;207(3):661-70.

44. Seidensticker R, Damm R, Enge J, Seidensticker M, Mohnike K, Pech M, et al. Local ablation or radioembolization of colorectal cancer metastases: comorbidities or older age do not affect overall survival. BMC Cancer. 2018;18(1):882.

45. Rosenbaum CE, van den Hoven AF, Braat MN, Koopman M, Lam MG, Zonnenberg BA, et al. Yttrium-90 radioembolization for colorectal cancer liver metastases: a prospective cohort study on circulating angiogenic factors and treatment response. EJNMMI Research. 2016;6(1):92.

46. Tohme S, Sukato D, Nace GW, Zajko A, Amesur N, Orons P, et al. Survival and tolerability of liver radioembolization: a comparison of elderly and younger patients with metastatic colorectal cancer. HPB. 2014;16(12):1110-6.

47. Soydal C, Kucuk NO, Balci D, Gecim E, Bilgic S, Elhan AH. Prognostic Importance of the Presence of Early Metabolic Response and Absence of Extrahepatic Metastasis After Selective Internal Radiation Therapy in Colorectal Cancer Liver Metastasis. Cancer Biother Radiopharm. 2016;31(9):342-6.

48. Paprottka KJ, Schoeppe F, Ingrisch M, Rubenthaler J, Sommer NN, De Toni E, et al. Pre-therapeutic factors for predicting survival after radioembolization: a single-center experience in 389 patients. Eur J Nucl Med Mol Im. 2017;44(7):1185-93.

49. Mulcahy MF, Lewandowski RJ, Ibrahim SM, Sato KT, Ryu RK, Atassi B, et al. Radioembolization of colorectal hepatic metastases using yttrium-90 microspheres. Cancer. 2009;115(9):1849-58.

50. Gibbs P, Heinemann V, Sharma NK, Taieb J, Ricke J, Peeters M, et al. Effect of Primary Tumor Side on Survival Outcomes in Untreated Patients With Metastatic Colorectal Cancer When Selective Internal Radiation Therapy Is Added to Chemotherapy: Combined Analysis of Two Randomized Controlled Studies. Clin Colorect Cancer. 2018;17(4):e617-e29.

51. Duffy MJ. Carcinoembryonic Antigen as a Marker for Colorectal Cancer: Is It Clinically Useful? Clinical Chemistry. 2001;47(4):624-30.

52. Ziv E, Bergen M, Yarmohammadi H, Boas FE, Petre EN, Sofocleous CT, et al. PI3K pathway mutations are associated with longer time to local progression after radioembolization of colorectal liver metastases. Oncotarget. 2017;8(14):23529-38.

53. Frankema-Mourer JS, Heymans J. Standpunt Yttrium-90 radioembolisatie bij colorectale levermetastasen. Zorginstituut Nederland. 2016.

54. Virdee PS, Moschandreas J, Gebski V, Love SB, Francis EA, Wasan HS, et al. Protocol for Combined Analysis of FOXFIRE, SIRFLOX, and FOXFIRE-Global Randomized Phase III Trials of Chemotherapy +/- Selective Internal Radiation Therapy as First-Line Treatment for Patients With Metastatic Colorectal Cancer. JMIR Research Protocols. 2017;6(3):e43.

55. Wasan HS, Gibbs P, Sharma NK, Taieb J, Heinemann V, Ricke J, et al. First-line selective internal radiotherapy plus chemotherapy versus chemotherapy alone in patients with liver metastases from colorectal cancer (FOXFIRE, SIRFLOX, and FOXFIRE-Global): a combined analysis of three multicentre, randomised, phase 3 trials. Lancet Oncol. 2017;18(9):1159-71.

56. Ulrich G, Dudeck O, Furth C, Ruf J, Grosser OS, Adolf D, et al. Predictive value of intratumoral 99mTc-macroaggregated albumin uptake in patients with colorectal liver metastases scheduled for radioembolization with 90Y-microspheres. J Nucl Med. 2013;54(4):516-22.

57. Jongen JMJ, Rosenbaum C, Braat M, van den Bosch M, Sze DY, Kranenburg O, et al. Anatomic versus Metabolic Tumor Response Assessment after Radioembolization Treatment. J Vasc Interv Radiol. 2018;29(2):244-53 e2.

58. Hendlisz A, Van den Eynde M, Peeters M, Maleux G, Lambert B, Vannoote J, et al. Phase III trial comparing protracted intravenous fluorouracil infusion alone or with yttrium-90 resin microspheres radioembolization for liver-limited metastatic colorectal cancer refractory to standard chemotherapy. J Clin Oncol. 2010;28(23):3687-94.

59. Braat AJAT, Kappadath SC, Bruijnen RC, Van den Hoven AF, Mahvash A, De Jong HW, et al. Adequate SIRT activity dose is as important as adequate chemotherapy dose. Lancet Oncol. 2017;18:e636.

60. Lam MG, Louie JD, Abdelmaksoud MH, Fisher GA, Cho-Phan CD, Sze DY. Limitations of body surface area-based activity calculation for radioembolization of hepatic metastases in colorectal cancer. J Vasc Interv Radiol. 2014;25(7):1085-93.

61. Garin E, Tzelikas L, Guiu B, Chalaye J, Edeline J, Baere TD, et al. Major impact of personalized dosimetry using 90Y loaded glass microspheres SIRT in HCC: Final overall survival analysis of a multicenter randomized phase II study (DOSISPHERE-01). J Clin Oncol. 2020;38(4_suppl):516-.

62. van Roekel C, Bastiaannet R, Smits MLJ, Bruijnen RC, Braat A, de Jong H, et al. Dose-effect relationships of holmium-166 radioembolization in colorectal cancer. J Nucl Med. 2020.

63. Zerizer I, Al-Nahhas A, Towey D, Tait P, Ariff B, Wasan H, et al. The role of early (1)(8)F-FDG PET/CT in prediction of progression-free survival after (9)(0) Y radioembolization: comparison with RECIST and tumour density criteria. Eur J Nucl Med Mol Im. 2012;39(9):1391-9.

64. Finessi M, Bellò M, Giunta FP, Veltri A, Deandreis D. Interventional locoregional treatment and metabolic response: advantages of using PET/CT in the evaluation of response to treatment. Q J Nuc Med Mol Imaging. 2018;62(2):165-84.

65. Shady W, Kishore S, Gavane S, Do RK, Osborne JR, Ulaner GA, et al. Metabolic tumor volume and total lesion glycolysis on FDG-PET/CT can predict overall survival after (90)Y radioembolization of colorectal liver metastases: A comparison with SUVmax, SUVpeak, and RECIST 1.0. Eur J Radiol. 2016;85(6):1224-31.

66. Rosenbaum CE, van den Bosch MA, Veldhuis WB, Huijbregts JE, Koopman M, Lam MG. Added value of FDG-PET imaging in the diagnostic workup for yttrium-90 radioembolisation in patients with colorectal cancer liver metastases. Eur J Radiol. 2013;23(4):931-7.

First evidence for a dose-response relationship in patients treated with ^{166}Ho-radioembolization: a prospective study

Remco Bastiaannet, Caren van Roekel, Maarten L.J. Smits, Sjoerd G. Elias, Wouter A.C. van Amsterdam, Dan Doan, Jip F. Prince, Rutger C.G. Bruijnen, Hugo W.A.M. de Jong, Marnix G.E.H. Lam

Journal of Nuclear Medicine 2020

ABSTRACT

Introduction

Holmium-166 (^{166}Ho)-microspheres have recently been approved for clinical use for hepatic radioembolization in the EU. The aim of this study was to investigate the absorbed dose-response relationship and its association with overall survival for ^{166}Ho-radioembolization in patients with liver metastases.

Methods

Patients who were treated in the HEPAR I and II studies and who underwent an FDG-PET/CT scan at baseline, a post-treatment ^{166}Ho-SPECT/CT scan and another FDG-PET/CT scan at three months follow-up, were included for analysis. The post-treatment ^{166}Ho-microspheres activity distributions were estimated with quantitative SPECT/CT reconstructions using a quantitative Monte Carlo-based reconstructor. Response of each individual tumor was based on the change in total lesion glycolysis (TLG) between baseline and follow-up and categorized in one of four categories, according to the PERCIST criteria, ranging from complete response to progressive disease. Patient level response was grouped according to the average change in TLG per patient. The absorbed dose-response relationship was assessed using a linear mixed-model to account for correlation of tumors within patients. Median overall survival was compared between patients with and without a metabolic liver response, using a log-rank test.

Results

In total 36 patients with a total of 98 tumors were included. The relation between tumor absorbed dose and both tumor level and patient level response was explored. At a tumor level, a significant difference in geometric mean absorbed dose was found between response categories complete response (232 Gy (95%-confidence interval (CI) 178-303 Gy); n=32) and stable disease (147 Gy (95% CI 113-191 Gy); n= 28), p=0.01. and between complete response and progressive disease (117 Gy (95% CI 87-159 Gy); n=21), p=0.0008). This constitutes a robust absorbed dose-response relationship. At a patient level, a significant difference was found between patients with complete or partial response (210 Gy (95% CI: 161-274 Gy); n=13) and patients with progressive disease (116 Gy (95% CI: 81-165 Gy); n=9), p=0.01. Patients were subsequently

grouped according to their average change in TLG. Patients with objective response (complete or partial response) exhibited a significantly higher overall survival than non-responding patients (stable or progressive disease) (median 19 months versus 7.5 months; Log-rank; p=0.01).

Conclusion

These results confirm a significant absorbed dose-response relationship in ^{166}Ho-radioembolization. Treatment response is associated with a higher overall survival.

Key words: Radioembolization; holmium; dose-response; dosimetry; dose personalization

INTRODUCTION

Radioembolization with yttrium-90 (^{90}Y) or holmium-166 (^{166}Ho) microspheres is increasingly used in the treatment of primary and secondary liver cancers (1). It is an intra-arterial therapeutic procedure in which radioactive microspheres are delivered to hepatic tumors via their nutrient arteries (2). The goal of radioembolization is to deliver a tumoricidal absorbed dose to tumors while sparing the healthy liver tissue. Although it has been shown in multiple studies that the likelihood for tumor response critically depends on tumor absorbed dose, the dosing methods that are predominantly used in clinical practice do not incorporate the patient-specific biodistribution (i.e. locally absorbed doses) (1,3).

Treatment with ^{166}Ho-radioembolization can be preceded by a scout dose consisting of a small batch (i.e. 250 MBq) of rheologically identical ^{166}Ho-microspheres. Official approval (CE-mark) was recently obtained in the EU (QuiremScout® and QuiremSpheres®; Quirem Medical B.V., Deventer, The Netherlands). It was demonstrated that this scout dose predicts the absorbed dose to the lungs more accurately than technetium-99m-macroaggregated albumin (^{99m}Tc-MAA) (4). And more recently, the scout dose was shown to have a superior predictive value for the intrahepatic therapy absorbed dose distribution (5). These findings support the use of a scout dose to better personalize dose planning (i.e. dosimetry) and patient selection. However, the relationship between tumor absorbed dose and response likelihood, needed for such a treatment personalization, has not yet been established.

The aim of this exploratory study was to analyze the relationship between tumor absorbed dose, treatment response and survival in patients treated with ^{166}Ho-radioembolization.

MATERIALS AND METHODS

Patient Selection

Candidates for this study were patients who were treated in the Holmium Embolization Particles for Arterial Radiotherapy I and II (HEPAR I and II; NCT01031784 (6) and NCT01612325 (7)) studies, which were conducted between 2009 and 2015. These studies were conducted in accordance with

the Declaration of Helsinki and were approved by the local research ethics committee. Before study entry, all patients provided written informed consent (6).

In HEPAR I and II, multimodality imaging with ^{18}F-fluorodeoxyglucose (FDG)-PET/CT and multiphasic liver CT were acquired during work-up. A preparatory angiography was performed several days before treatment in which extra-hepatic vessels were coil-embolized if necessary, and a scout dose of ^{99m}Tc-MAA (150 MBq, Technescan LyoMAA®; Mallinckrodt Medical B.V., Petten, The Netherlands) was administered to assess the safety and intra-hepatic distribution of subsequent administrations. On the day of treatment, ^{166}Ho-microspheres were administered as a second scout dose (i.e. 250 MBq) in the morning and as a treatment dose in the afternoon, with ^{166}Ho-SPECT/CT and MR acquisition after both injections. The total amount of administered activity was adjusted to the targeted liver volume, as measured on CT. In HEPAR II, the aimed absorbed dose was 60 Gy for the treated volume (MIRD mono-compartment method) (7). HEPAR I was a dose-escalation study, in which the aimed absorbed dose was varied between 20 and 80 Gy. Treatment was followed by a post-treatment ^{166}Ho-SPECT/CT and an FDG-PET/CT at three months follow-up. None of the included patients received concomitant anti-cancer therapies.

Included patients for the current study were those who underwent an FDG-PET/CT scan at our hospital at baseline and at three months follow-up, as well as a post-treatment ^{166}Ho-SPECT/CT as part of the HEPAR I or II studies.

Absorbed Dose-Response Evaluation

Absorbed dose-response evaluation was performed similarly to what was reported earlier by Van den Hoven et al. (8). The tumor outlines were automatically defined by setting a patient-relative threshold for activity concentration on the baseline FDG-PET/CT scan using the ROVER (ABX GmBH, Radeberg, Germany) software package (9). The threshold was based on the aortic blood pool activity and defined as 2x mean SUV corrected for lean body mass (SUL_{mean}) (10). Additionally, a volume restriction of 5 mL or more was used. SUL_{mean} and tumor volume were recorded. Total lesion glycolysis (TLG) was calculated by taking the product of SUL_{mean} and tumor volume. The liver was manually delineated on the accompanying low-dose CT, using ROVER.

The ^{166}Ho-microspheres activity distribution following treatment was estimated with quantitative SPECT/CT reconstructions using a quantitative fast Monte Carlo-based reconstructor (UMCS), which has been previously validated for ^{166}Ho (11).

The PET-based tumor and liver outlines were transferred to the corresponding ^{166}Ho-SPECT reconstructions, using a rigid registration of the CT scans of the PET and SPECT acquisitions (12). The liver contours served as a mask to focus the registration on the liver region only. The liver and tumor outlines were subsequently dilated with 1 cm, to minimize difference due to resolution, (respiratory) motion and local registration errors.

The tumor doses were estimated using the activity in these dilated masks and the mass of the original contour. The parenchymal dose was calculated in the same fashion, after subtracting the dilated tumor masks from the liver mask. The dose was assumed to be fully absorbed within each volume of origin (local deposition model) (13).

For the three-month follow-up scans, the tumors were automatically defined in ROVER, using the method described above. The change in TLG was used to determine the metabolic tumor response. The baseline and follow-up images were assessed side by side to ensure the same tumors were identified. Merged tumors on follow-up imaging were regarded as one tumor at baseline. In those cases, a weighted average of the absorbed dose was calculated, correcting for tumor volume.

Metabolic tumor response was grouped in categories according to the PERCIST criteria (10). Complete metabolic response (CR) was achieved if there was a 100% reduction in TLG, partial metabolic response (PR) when there was a decrease of at least 45%, progressive metabolic response (PD) was characterized by an increase of at least 75%, stable disease (STBD) was defined as an increase of less than 75% and a decrease of less than 45%. Furthermore, these categories were grouped according to objective response (CR + PR) and non-response (STBD + PD).

Statistical Analysis

The relation between tumor absorbed dose and response were assessed both at the level of individual tumors (local response) as well as at the patient level, in which case the patients were grouped according to PERCIST based

on the average change in TLG of all hepatic tumors. Patient-level analysis was performed both including and excluding tumors that formed after baseline (which were labeled as progressive disease). All other analyses ignored the formation of new lesions at follow-up, as they were not targeted by the treatment. Linear mixed-effect models were used to assess the relation between tumor absorbed dose and response and to account for correlation of tumors within patients. Dose was used as dependent variable and log-transformed to fulfill model assumptions. Nested models were compared using Akaike's Information Criterion. The dose-effect relationship was best explained using a random intercept per patient without random slopes. A geometric mean of the tumor absorbed dose per response category was estimated. On a patient level, response categories CR and PR were merged in the analysis due to otherwise too limited numbers per category. To test the hypothesis of an ordered relationship across response categories, a trend test was performed with response as a continuous variable in the model.

Overall survival was defined as the interval between treatment and death from any cause, with censoring of patients who were still alive at their last known follow-up date. The survival curve was estimated by the Kaplan-Meier method. A log-rank test was used to compare median overall survival between patients with and without a metabolic liver response. Baseline characteristics of these groups, consisting of primary tumor type, gender, age, previous treatments, WHO performance score, presence of extra hepatic disease, number of tumors and tumor load, were scrutinized for differences that could have biased the survival analysis. Analyses were performed using R statistical software, version 3.4.0. A two-sided p-value <0.05 was considered statistically significant.

RESULTS

Thirty-six patients with a total of 98 tumors were included in this study. Baseline characteristics are listed in Table 1. Eleven patients of the HEPAR I study were excluded because of absence of post-treatment ^{166}Ho-SPECT/CT (n=4) or due to unavailability of the corresponding low-dose CT with the ^{166}Ho-SPECT (n=7). Five patients of the HEPAR II study were excluded because of absence of post-treatment ^{166}Ho-SPECT/CT (n=2), absence of baseline FDG PET/CT (n=1), absence of follow-up FDG PET/CT (n=1) and no FDG-uptake in the tumor (n=1).

TABLE 1. Baseline characteristics (n=36 patients).

Characteristic	N or median (range)		
	All patients	**Responders**	**Non-responders**
Gender			
Male	17	6	11
Female	19	6	13
Age (y) at therapy	64 (40-84)	67.5 (44-84)	63 (40-74)
Primary tumor type			
Colorectal carcinoma	21	8	13
Breast carcinoma	4	1	3
Cholangiocarcinoma	4	0	4
Uveal melanoma	4	1	3
Neuro-endocrine neoplasm	1	1	0
Pancreas carcinoma	1	0	1
Thymoma	1	1	0
Liver volume (mL)	1,938 (1,155 – 3,842)		
Metabolic tumor volume (mL)	171 (5 -1,993)		
Administered activity (MBq)	6705 (3676 – 12,897)	7632 (3763 – 10,217)	6705 (3676 – 12,897)
Previous treatment			
Locoregional (liver)	8	3	5
Systemic	34	11	23
None	2	1	1
WHO status			
0	29	9	20
1	5	2	3
Unknown	2	1	1
Extrahepatic disease at baseline			
No	26	8	18
Yes	10	4	6

Three patients from the HEPAR I study were administered an activity corresponding to a uniform absorbed dose of 80 Gy to the target volume, all other patients were administered an activity that corresponded to 60 Gy. Median administered activity was 6705 MBq, with a range of 3676-12897 MBq. Thirty-five patients received whole liver treatment and one patient received lobar treatment.

Local Response

In total, 98 tumors were delineated. The median number of tumors per patient was 2 (range 1-9). Median tumor absorbed dose was 162.1 Gy (range 16.4 – 715.7 Gy). Median absorbed dose in the healthy liver tissue was 39.9 Gy (range 7.2 – 66.4 Gy).

Metabolic tumor response at three months follow-up was: CR in 32 tumors, PR in 17 tumors, STBD in 28 tumors and PD in 21 tumors. The local metabolic response versus absorbed dose is plotted graphically in Figure 1.

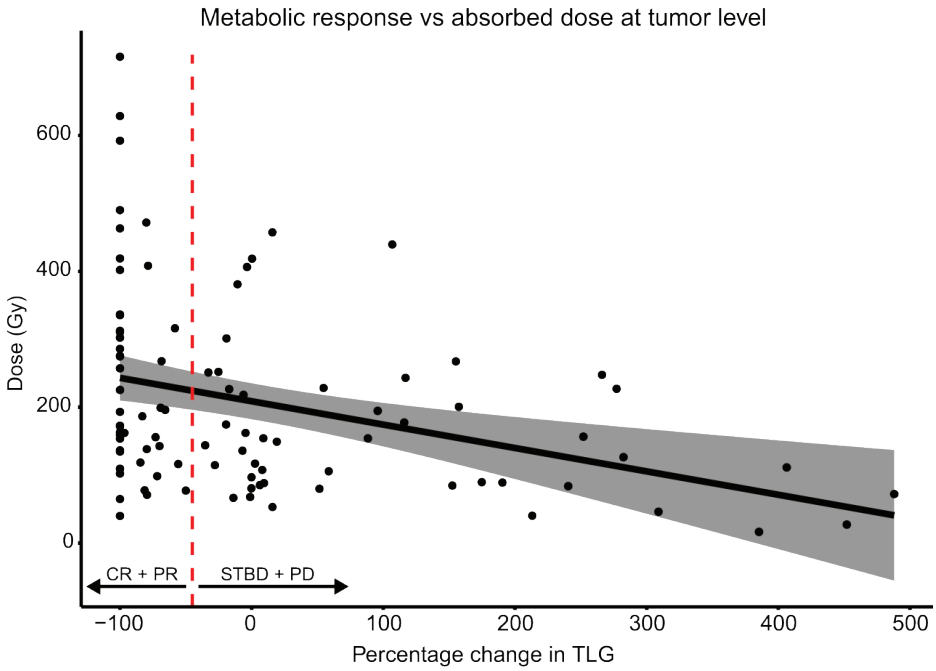

FIGURE 1. Graphical representation of the metabolic response (i.e. change in total lesion glycolysis (TLG)) versus absorbed dose of each individual tumor. A decrease in TLG is associated with a higher tumor absorbed dose. Vertical dashed line indicates the cut-off value for TLG change, below which a complete (CR) or partial (PR) response was observed, and above which response is defined as either stable (STBD) or progressive (PD) disease. Shaded area indicates 95% CI of the regression line.

Geometric mean tumor absorbed doses in the response categories at a tumor level were as follows: CR 232 Gy (95%-confidence interval (CI): 178-303 Gy), PR

168 Gy (95%CI 122-232 Gy), STBD 147 Gy (95% CI: 113-191 Gy) and PD 117 Gy (95% CI: 87-159 Gy). Significant differences between response categories CR and STBD (p=0.01) and CR and PD (p=0.0008) were found. The p-value for trend was 0.0005.

An example of a patient exhibiting CR in several tumors with a good preferential microsphere accumulation in and around the tumors is shown in Figure 2.

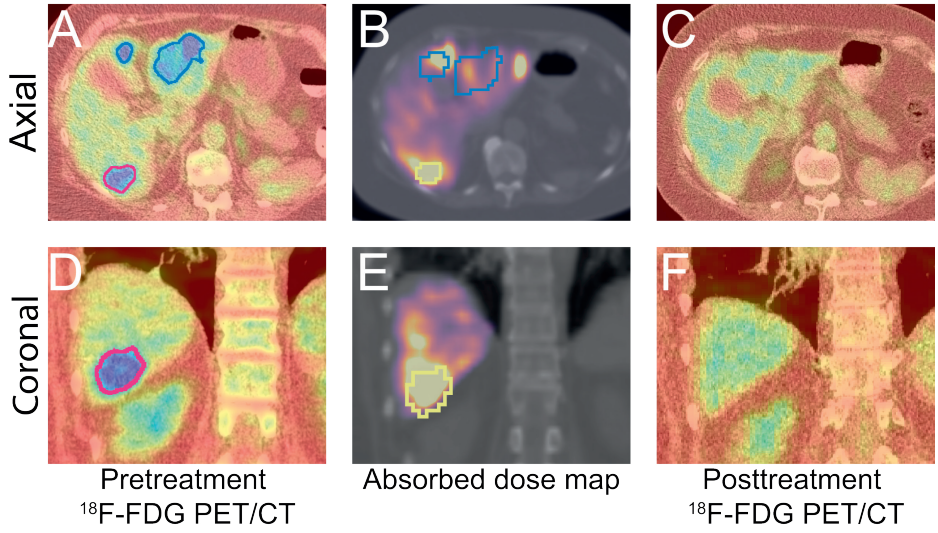

FIGURE 2. Exemplar case in which good spatial correspondence between pretreatment tumor metabolism (A and D) and absorbed dose (D_{avg} 120 Gy) (B and E) led to a complete response (C and F). Tumor outlines are transferred from the pretreatment FDG-PET/CT to the Absorbed dose maps through rigid registration of the appurtenant CTs of the SPECT/CT and FDG-PET/CTs. In many cases, this registration is imperfect, resulting in slight registration errors, such as evident in panel B.

Patient-Level Response

There were 2 patients with complete metabolic liver response, 11 patients with PR, 14 patients with STBD, and 9 patients with PD. Geometric mean tumor absorbed doses in the response categories at a patient-level were as follows: complete or partial response (CRPR) 210 Gy (95% CI: 161-274 Gy), STBD 152 Gy (95% CI: 117-198 Gy) and PD 116 Gy (95% CI: 81-165 Gy). The p-value for trend was 0.005.

There was a significant difference in tumor absorbed dose between patients that showed no response (PD or STBD) and patients from the CRPR group (p=0.008). Metabolic response at a whole liver level, considering the development of new tumors as well, was as follows: there were 2 patients with CR, 10 patients with PR, 7 patients with STBD and 17 patients with PD. There were 3 patients with new intrahepatic tumors, 2 patients with new extrahepatic tumors and 5 patients with both new extra- and intrahepatic tumors.

Survival

Median overall survival was 13.5 months (range 2-31 months; 95% confidence interval 10-16 months). Median survival was significantly longer in responders (CRPR patients) (19 months, range 8-31 months) compared with non-responders (7,5 months, range 2-27 months) (Log-rank; p=0.01) (Figure 1). Baseline characteristics of both groups were explored, but no clearly distinguishable differences were evident (Table 1).

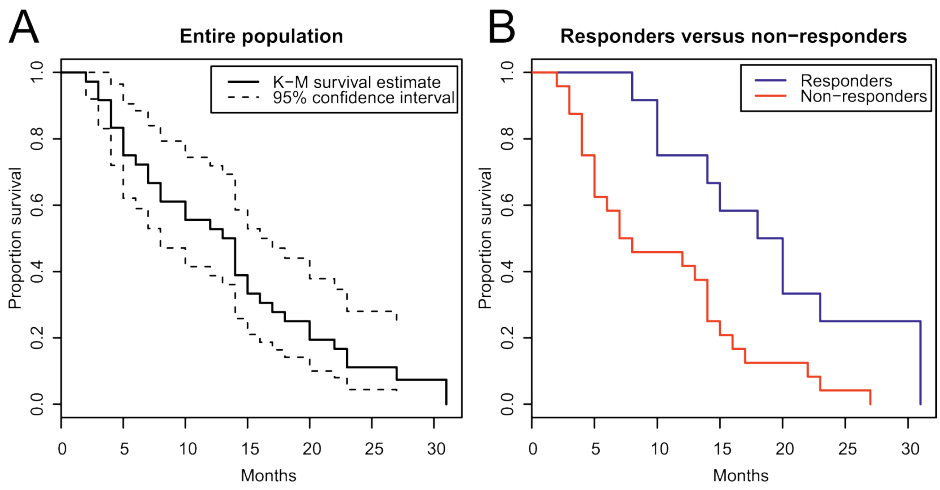

FIGURE 3. (A) Median overall survival for entire study population was 13.5 months (range 2-31; 95% confidence interval 10-16 months). (B) Median survival in responders was significantly longer (19 months, range 8-31 months) than in non-responders (7.5 months, range 2-27 months) (Log-rank; p=0.01).

DISCUSSION

This prospective exploratory study is the first to show clinical evidence of an absorbed dose-response relationship in patients treated with ^{166}Ho-radioembolization. Specifically, a high tumor absorbed dose was associated with individual tumor and per-patient response and the occurrence of patient-level objective response was associated with a significantly increased overall survival.

The efficacy of radioembolization with ^{166}Ho-microspheres for inducing anatomical response according to RECIST 1.1 has previously been demonstrated by Prince et al. (7). For this study, metabolic metrics were used to measure response. These metrics are more sensitive, often have an earlier onset and can be more predictive of overall survival (14). This was indeed reflected in the higher fraction of patients who were classified as responders at three months follow-up in the present study (12/36; 33%) versus in the study by Prince and colleagues (5/37; 14%). Furthermore, grouping according to metabolic response resulted in significant differences in overall survival between these groups. This metabolic response was associated with a higher tumor absorbed dose.

Van der Hoven, et al. conducted a study similar to this one, but with ^{90}Y resin microspheres in mCRC patients (8). Van der Hoven and colleagues conservatively estimated that a dose of 40-60 Gy would be needed to achieve a significant tumor response. Willowson et al. found ~50 Gy to be sufficient for a metabolic response (15) and Levillain and colleagues found that an average absorbed dose on all tumors higher than 39 Gy was a good predictor of both metabolic response as well as overall survival (16). Flamen et al. found a median of 46 Gy for the metabolic response group (17,18). All these studies used resin microspheres in mCRC patients. In the current study, the estimated dose needed for a local response was higher (geometric absorbed tumor dose was 232 Gy for CR and 168 Gy for PR). This likely reflects differences between the used microspheres and potentially also between the methods used for the actual dose estimation. Furthermore, a direct quantitative comparison with the present study is hampered by the heterogeneity in primary tumor types of included patient cohort. For a valid pair wise comparison, a more homogenous patient group is needed.

The semi-automatic method of thresholding the FDG scans to define tumor volumes, as used in the study, decreased the variance typically induced with manual delineation. By subsequently applying these masks to the corresponding ^{166}Ho dose maps using an automatic registration routine, the current method offered a non-subjective measure for both dose and response, maximizing reproducibility.

The current study was performed with a limited sample size of patients with hepatic metastases of different origins. Consequently, there was not enough statistical power to model the differences in FDG avidity, tumor biology and radio-sensitivity that might exist between the different tumor types. Furthermore, differences in patient positioning and breath-hold policy between PET and SPECT scans, combined with the relatively low resolution and contrast of the low-dose CT of the SPECT/CT increased the likelihood of (local) misregistrations. These effects increased the error in dose estimates of each response group, contributing to a larger spread in each response category, decreasing separability between response groups.

It has been argued that the different radioembolization devices (e.g. resin or glass) result in differences in micro-distribution and consequently the absorbed dose needed for tumor response and toxicity (3). ^{166}Ho-microspheres are positioned between resin and glass microspheres with respect to the number of injected particles and particle size (19). Based on these data, we expect the 'apparent' radio-sensitivity of ^{166}Ho-microspheres to lie in between as well. However, this will need to be confirmed in a future study in which only patients with the same tumor type are included.

The administered activity in the HEPAR I and II studies was based on the MIRD mono-compartment method. In this method, the activity calculation was based on the intended mean absorbed dose to the target liver mass. This method disregards the actual tumor load and the preferential uptake of the microspheres in the tumors, assuming a uniform microsphere distribution in the target volume. This can lead to a wide range in actual absorbed tumor doses. However, the treatment with ^{166}Ho-radioembolization is usually preceded by the administration of a smaller amount of the same microspheres. This scout dose has been shown, relative to ^{99m}Tc-MAA, to enable: i) a more accurate lung

shunt fraction estimation (4), ii) a safe and improved detection of extrahepatic depositions (20,21), and iii) a more accurate pretreatment prediction of the intrahepatic distribution (5). These predictive properties may be used for an improved patient selection and a more personalized activity prescription. This can be achieved by using the pretreatment biodistribution of the scout dose as input to a multi-compartment model (e.g. the partition model) (22). The prescribed treatment activity can then be maximized such that the absorbed dose in the parenchymal tissue remains below a certain toxicity threshold, whilst maximizing the tumor absorbed dose (23). Subsequent assessment of predicted tumor absorbed doses can guide patient selection by excluding patients for whom no tumor response is to be expected.

To that end, ^{166}Ho absorbed dose thresholds for specific tumor types need to be established. Future studies will need to focus on a single tumor type, increasing statistical power and enabling the identification of this tumoricidal dose threshold. Similarly, a larger study cohort is needed to establish safe absorbed dose thresholds for the parenchyma. The absorbed dose-response relationship demonstrated in this study shows the feasibility of such an effort and is the first step towards a more individualized treatment planning for ^{166}Ho-radioembolization.

CONCLUSION

In this study, an association of tumor absorbed dose with (local) response was found. Moreover, a patient-level metabolic response was associated with a significant increase in overall survival. Personalized dosimetry has the potential for improved outcome in radioembolization, as has been well-established for external beam radiotherapy.

REFERENCES

1. Reinders MTM, Mees E, Powerski MJ, Bruijnen RCG, Van den Bosch MAAJ, Lam MGEH et al. Radioembolisation in Europe: a survey amongst CIRSE members. Cardiovasc Intervent Radiol. 2018;41:1579-1589.

2. Townsend A, Chong LC, Karapetis C, Price TJ. Selective internal radiation therapy for liver metastases from colorectal cancer. Cochrane Database Syst Rev. 2016;50:148-154.

2. Bastiaannet R, Kappadath SC, Kunnen B, Braat AJAT, Lam MGEH, de Jong HWAM. The physics of radioembolization. EJNMMI Phys. 2018;5:22.

3. Elschot M, Nijsen JFW, Lam MGEH, Smits MLJ, Prince JF, Viergever MA et al. 99mTc-MAA overestimates the absorbed dose to the lungs in radioembolization: a quantitative evaluation in patients treated with ^{166}Ho-microspheres. Eur J Nucl Med Mol Im. 2014;41:1965-1975.

4. Smits MLJ, Dassen MG, Prince JF, Braat AJAT, Beijst C, Bruijnen RCG et al. The superior predictive value of ^{166}Ho-scout compared with 99mTc-macroaggregated albumin prior to ^{166}Ho-microspheres radioembolization in patients with liver metastases. Eur J Nucl Med Mol Imaging. 2020;47(4):798-806.

5. Smits MLJ, Nijsen JFW, van den Bosch MAAJ, Lam MGEH, Vente MAD, Mali WPTM, et al. Holmium-166 radioembolisation in patients with unresectable, chemorefractory liver metastases (HEPAR trial): a phase 1, dose-escalation study. Lancet Oncol. 2012;13(10):1025-34.

6. Prince JF, van den Bosch M, Nijsen JFW, Smits MLJ, van den Hoven AF, Nikolakopoulos S, et al. Efficacy of radioembolization with holmium-166 microspheres in salvage patients with liver metastases: a phase 2 study. J Nucl Med. 2017. Epub 2017/09/17.

7. van den Hoven AF, Rosenbaum CE, Elias SG, de Jong HW, Koopman M, Verkooijen HM, et al. Insights into the Dose-Response Relationship of Radioembolization with Resin 90Y-Microspheres: A Prospective Cohort Study in Patients with Colorectal Cancer Liver Metastases. J Nucl Med. 2016;57(7):1014-9. Epub 2016/02/26.

8. ABX advanced biochemical compounds GmbH. ROVER ROI Visualization, Evaluation and Image Registration. http://www.abx.de/rover/index.php/publishers-details.html. Accessed on August 26, 2019

9. O JH, Wahl RL. PERCIST in Perspective. Nucl Med Mol Imaging (2010). 2018;52:1-4

10. Elschot M, Smits MLJ, Nijsen JFW, Lam MGEH, Zonnenberg BA, Van den Bosch MAAJ et al. Quantitative Monte Carlo-based holmium-166 SPECT reconstruction. Med Phys. 2013;40(11):112502.

11. Klein S, Staring M, Murphy K, Viergever MA, Pluim J. Elastix: A Toolbox for Intensity-Based Medical Image Registration. IEEE Trans Med Imaging. 2010;29(1):196-205.

12. Mikell JK, Mahvash A, Siman W, Mourtada F, Kappadath SC. Comparing voxel-based absorbed dosimetry methods in tumors, liver, lung, and at the liver-lung interface for 90Y microsphere selective internal radiation therapy. EJNMMI Phys. 2015;2:16

13. Bastiaannet R, Lodge MA, de Jong H, Lam M. The unique role of fluorodeoxyglucose-PET in radioembolization. PET clinics. 2019;14(4):447-57. Epub 2019/09/02.

14. Willowson KP, Hayes AR, Chan DLH, Tapner M, Bernard EJ, Maher R, et al. Clinical and imaging-based prognostic factors in radioembolisation of liver metastases from colorectal cancer: a retrospective exploratory analysis. EJNMMI Research. 2017;7(1):46. Epub 2017/05/26.

15. Levillain H, Duran Derijckere I, Marin G, Guiot T, Vouche M, Reynaert N, et al. (90)Y-PET/CT-based dosimetry after selective internal radiation therapy predicts outcome in patients with liver metastases from colorectal cancer. EJNMMI Research. 2018;8(1):60. Epub 2018/07/15.

16. Flamen P, Vanderlinden B, Delatte P, Ghanem G, Ameye L, Van Den Eynde M, et al. Corrigendum: Multimodality imaging can predict the metabolic response of unresectable colorectal liver metastases to radioembolization therapy with Yttrium-90 labeled resin microspheres. Physics in medicine and biology. 2008;53(22):6591-603. Epub 2008/11/04.

17. Flamen P, Vanderlinden B, Delatte P, Ghanem G, Ameye L, Van Den Eynde M, et al. Multimodality imaging can predict the metabolic response of unresectable colorectal liver metastases to radioembolization therapy with Yttrium-90 labeled resin microspheres. Physics in medicine and biology. 2008;53(22):6591-603. Epub 2008/11/04.

18. Reinders MTM, Smits MLJ, van Roekel C, Braat AJAT. Holmium-166 Microsphere Radioembolization of Hepatic Malignancies. Semin Nucl Med. 2019;49(3):237-243.

19. Prince JF, van Rooij R, Bol GH, de Jong HWAM, van den Bosch MAAJ, Lam MGEH. Safety of a Scout Dose Preceding Hepatic Radioembolization with ^{166}Ho Microspheres. J Nucl Med. 2015;56(6):817-823.

20. Braat AJAT, Prince JF, Van Rooij R, Bruijnen RCG, Van den Bosch MAAJ, Lam MGEH. Safety analysis of holmium-166 microsphere scout dose imaging during radioembolisation work-up: a cohort study. Eur Radiol. 2018;28(3):920-928.

21. Ho S, Lau WY, Leung TWT, Chan M, Johnson PJ, Li AKC. Clinical evaluation of the partition model for estimating radiation doses from yttrium-90 microspheres in the treatment of hepatic cancer. Eur J Nucl Med. 1997;24(3):293-298.

22. Chiesa C, Sjogreen Gleisner K, Flux G, et al. The conflict between treatment optimization and registration of radiopharmaceuticals with fixed activity posology in oncological nuclear medicine therapy. Eur J Nucl Med Mol Imaging. 2017;44(11):1783-1786.

Dose-effect relationships of holmium-166 radioembolization in colorectal cancer

Caren van Roekel, Remco Bastiaannet, Maarten L.J. Smits, Rutger C. Bruijnen, Arthur J.A.T. Braat, Hugo W.A.M. de Jong, Sjoerd G. Elias, Marnix G.E.H. Lam

Journal of Nuclear Medicine 2020

ABSTRACT

Introduction

Radioembolization is a treatment option for colorectal cancer (CRC) patients with inoperable, chemorefractory hepatic metastases. Personalized treatment requires established dose thresholds. Hence, the aim of this study was to explore the relation between dose and effect (i.e. response and toxicity) in CRC patients treated with holmium-166 (^{166}Ho) radioembolization.

Materials and methods

CRC patients treated in the HEPAR II and SIM studies were analyzed. Absorbed doses were estimated using the activity distribution on post-treatment ^{166}Ho-SPECT/CT. Metabolic response was assessed using the change in total lesion glycolysis on ^{18}FDG-PET/CT between baseline and three-months follow-up. Toxicity between treatment and three months was evaluated according to the Common Terminology Criteria for Adverse Events (CTCAE) version 5, and its relation with parenchymal-absorbed dose was assessed using linear models. The relation between tumor-absorbed dose and patient- and tumor-level response was analyzed using linear mixed-models. Using a threshold of 100% sensitivity for response, the threshold for a minimal mean tumor-absorbed dose was determined and its impact on survival was assessed.

Results

Forty patients were included. The median parenchymal-absorbed dose was 37 Gy (range 12-55 Gy). New CTCAE grade ≥3 clinical and laboratory toxicity were present in eight and seven patients, respectively. For any clinical toxicity (highest grade per patient), the mean difference in parenchymal dose (Gy) per step increase in CTCAE grade category was 5.75 (95% confidence interval (CI) 1.18-10.32). On a patient level, metabolic response was: complete response (CR) n=1, partial response (PR) n=11, stable disease (StD) n=17 and progressive disease (PD) n=8. The mean tumor-absorbed dose was 84% higher in patients with CR/PR than in patients with PD (95%CI: 20-180%). Survival for patients with a mean tumor-absorbed dose >90 Gy was significantly better than for patients with a mean tumor-absorbed dose <90 Gy (hazard ratio=0.16, 95%CI 0.06-0.511).

Conclusion

A significant dose-response relationship in CRC patients treated with ^{166}Ho-radioembolization was established and a positive association between toxicity and parenchymal dose was found. For future patients, it is advocated to use ^{166}Ho-scout to select patients and personalize the administered activity targeting a mean tumor-absorbed dose of >90 Gy and a parenchymal dose <55 Gy.

Key words: radioembolization, holmium, dosimetry

INTRODUCTION

Colorectal cancer (CRC) is one of the most common types of cancer worldwide (1). The liver is the first site of hematogenous spread and 70-80% of patients with hepatic metastases are deemed unresectable because of tumor size, location, multifocality, or inadequate hepatic reserve (2). Hence, the majority of patients with metastatic CRC cannot be cured. Palliative treatment generally consists of several lines of systemic chemotherapy. If the available chemotherapeutic options fail, treatment with radioembolization should be considered for patients with liver-only or liver-dominant disease (3).

During radioembolization, radioactive microspheres are delivered intra-arterially to hepatic tumors. The rationale of this treatment is to administer a high local radiation dose to the tumors, while relatively sparing the healthy liver parenchyma by using the predominant arterial blood flow to tumors. Currently, three types of microspheres are available: yttrium-90 (^{90}Y) resin (SIRspheres®, Sirtex), ^{90}Y glass (TheraSphere®, BTG/Boston Scientific) and holmium-166 (^{166}Ho) microspheres (Quiremspheres®, Quirem Medical).

One advantage of ^{166}Ho-radioembolization is that treatment can be preceded by a scout dose of the same microspheres, using only limited activity (250 MBq). This ^{166}Ho-scout has proven to be a more accurate predictor of the distribution of the treatment dose (4). Another advantage is that ^{166}Ho-microspheres can be visualized by both MRI and SPECT/CT (5). The safety and efficacy of ^{166}Ho-radioembolization was determined in the HEPAR and SIM studies (6-9). In these studies, activity calculation was based on a whole-liver absorbed dose of 60 Gy. To allow for personalized, or optimized treatment, reference levels for efficacy and toxicity are needed (10). Hence, the aims of this study were to determine the relationship between dose and toxicity and to determine the relation between dose and metabolic response, in CRC patients who were treated with ^{166}Ho-radioembolization.

MATERIALS AND METHODS

Patients

This was a retrospective analysis of CRC patients who were treated with ^{166}Ho-radioembolization in the HEPAR II (NCT01612325 (6)) and the SIM (NCT02208804 (8)). Before study inclusion, all patients provided written informed consent. The institution's Medical Ethics Committee approved both studies. The CRC patients of the HEPAR II study were already part of a preliminary mixed tumor-type cohort analysis and were also included in this CRC-only analysis (11).

Treatment Procedures

During work-up, laboratory and clinical examinations were performed and patients underwent multiphasic liver CT and ^{18}FDG-PET/CT at a median of 16 days before treatment (range 6-42). Pre-treatment activity calculation was performed using a method similar to the medical internal radiation dosimetry (MIRD) method (12). The injected activity (IA) to reach an average absorbed dose of 60 Gy in the target volume was calculated as (7):

$$IA_{(MBq)} = target\ volume\ weight\ (kg) * 3780\ \left(\frac{MBq}{kg}\right)$$

The IA was not adjusted for lung shunt fraction, in line with the instructions for use for Quiremspheres. Since the abundance of gamma photons invokes detector dead-time, patients underwent a quantitative ^{166}Ho-SPECT/CT to assess the therapeutic dose distribution three to five days after treatment. The threshold used for tumor delineation was defined per patient, based on twice the mean aortic blood pool SUV corrected for lean body mass. Using this patient-relative threshold and the volume restriction of 5 mL, tumors were automatically defined. This way, only regions with metabolic activity, significantly exceeding the background activity of the liver, were defined. The threshold used to delineate tumors at follow-up was defined again on the 3-month ^{18}FDG PET/CT.

A rigid registration (using Elastix software (13)) of the CT scans of the PET and SPECT acquisitions was used to transfer the PET-based tumor- and liver contours to the corresponding ^{166}Ho-SPECT reconstructions. The previously manually contoured livers acted as a mask to focus registration on this region

exclusively. All registration results were checked visually (RB). Minor manual adjustments were allowed, but only based on CT and never on nuclear imaging. A 1 cm dilation of the tumor and liver contours was used, to account for breathing movement, errors in registration and resolution differences. The counts in the dilated contours were used for activity calculation, but the volume of the non-dilated VOIs was used for absorbed dose calculation. The quantitative Monte Carlo-based SPECT reconstruction used in this study yields voxels that contain absolute activity (in units of MBq). The absorbed dose (Gy) in each voxel was subsequently calculated using the local deposition model, which posits that -at the resolution of SPECT- all dose is deposited within the voxel of origin. The average doses in parenchymal tissue and tumors was calculated using the transferred delineations, as described previously (Figure 1).

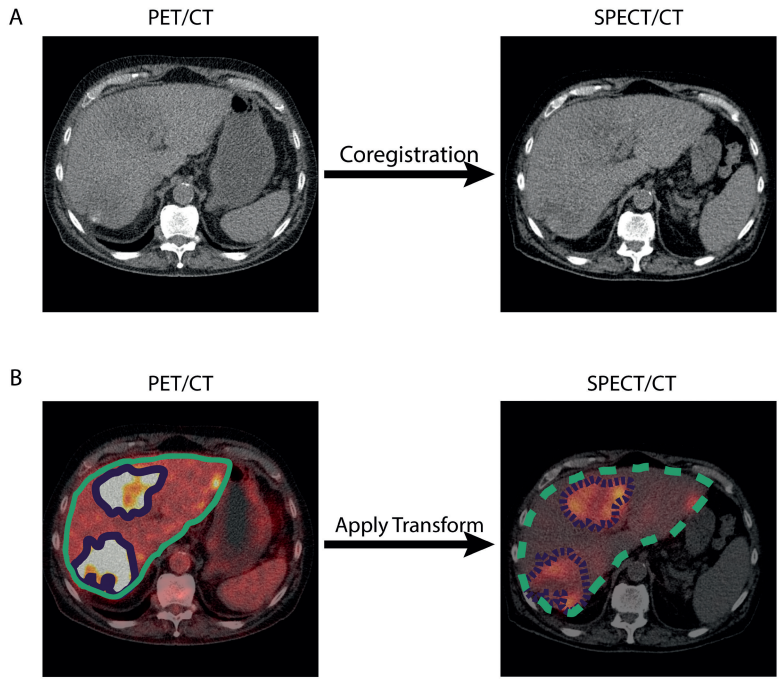

FIGURE 1. Example of tumor delineation and absorbed-dose estimation. Using the liver contour, the low-dose CT of the PET was matched to the low-dose CT of the SPECT (A). The tumors were automatically defined using a threshold. Liver- and tumor contours were transferred from the PET/CT to the SPECT/CT and absorbed doses were calculated (B).

In case of fused lesions at follow-up, a volume-weighted average of the absorbed dose of the different components at baseline was calculated. Also, a weighted average, correcting for tumor volume, was calculated to obtain the mean tumor-absorbed dose per patient. The parenchymal-absorbed dose was determined using the activity in the entire (dilated) liver contour, with the activity in the (dilated) tumor regions subtracted.

Toxicity Evaluation

The emergence of clinical toxicity between treatment and three months post-treatment was recorded, with exception of clinical adverse events during the first week after treatment, to allow for distinction between adverse events due to embolization and adverse events due to radiation. Laboratory toxicity between treatment and three months post-treatment was evaluated using the following parameters: albumin, alkaline phosphatase (AP), alanine aminotransferase (ALAT), aspartate aminotransferase (ASAT), bilirubin and gamma-glutamyltransferase (GGT). Common terminology criteria for adverse events (CTCAE) version 5.0 was used for grading (14). Since version 5.0 allows for higher values of laboratory parameters when these were already abnormal at baseline, relative change in laboratory values between baseline and three months follow-up was calculated as well. Furthermore, presence of ascites and encephalopathy (as part of radioembolization-induced liver disease (REILD)) was determined at three-months follow-up.

Efficacy Evaluation

Metabolic response to treatment was evaluated on ^{18}FDG PET/CT at three-month follow-up.

Tumors were automatically defined based on standardized uptake value (SUV) and lesion total lesion glycolysis (TLG) was obtained. To avoid misidentification, baseline and follow-up images were evaluated in parallel. Metabolic response of hepatic lesions was defined based on the change in TLG between baseline and follow-up, according to the PERCIST criteria (15). Hepatic tumor response was also assessed according to the Response evaluation criteria in solid tumours (RECIST) version 1.1 (16).

Statistical Analyses

Patient demographics and treatment characteristics were summarized using descriptive analyses. The strength of association between CTCAE toxicity grade and parenchymal-absorbed dose was assessed using linear regression models with CTCAE grade in categories as the dependent continuous variable and parenchymal absorbed dose as the independent continuous variable. For clinical significance, CTCAE grading of any clinical and laboratory toxicity was also dichotomized in the following categories: grade 0/I/II versus grade III/IV/V and analyzed using logistic regression with Firth's correction for small sample bias (17). The association between relative change in laboratory parameters (represented as Δ laboratory parameter) and healthy liver tissue dose was analyzed using simple linear regression models with percentage change as the dependent continuous variable and parenchymal absorbed dose as the independent continuous variable, after log-transformation of the dependent variable to fulfill model assumptions. All toxicity analyses were also adjusted for response to therapy (binary coded as response/non-response), previous treatment (defined as number of prior systemic treatment lines, categorical variable) and tumor load (defined as percentage involvement of the liver by tumors, continuous variable) as possible confounders, which were identified by making directed acyclic graphs.

The relationship between tumor-absorbed dose and response was analyzed using a linear mixed-effects regression model with tumor-absorbed dose as the dependent variable. This type of analysis was chosen to account for correlation of tumors within patients. To fulfill model assumptions, dose was log-transformed. Nested models were compared using Akaike's Information Criterion (AIC). The dose-effect relationship was best explained using a random intercept per patient without random slopes. A geometric mean of the tumor-absorbed dose per patient per response category was estimated because the anti-log of the arithmetic mean of log-transformed values is the geometric mean. A trend test was also done with response as a continuous variable in the model, to test the presence of an ordered relationship across response categories. By including them as co-variables, analyses were adjusted for the following possible confounders: previous treatment (coded as factor with the following categories: yes/no previous treatment with anti-VEGF medication) and tumor load (continuous). An ROC analysis, according for clustered data,

was done to determine the discriminatory power of tumor dose in response estimation (18). The 95% confidence interval of the area under the curve shows the boundaries of the likely discriminative ability of tumor dose for response in this cohort. Using a threshold of 100% sensitivity for response (CR/PR), the threshold for a minimal mean tumor-absorbed dose was determined and used in the survival analyses. The same threshold of 100% sensitivity for response was used to determine the threshold for a minimal tumor-absorbed dose (lesion-level).

The agreement between response according to PERCIST and according to RECIST was analyzed using Cohen's kappa, with disagreements weighted according to their squared distance from perfect agreement.

Overall survival was defined as the interval between treatment and death from any cause. Cox regression models were made using Firth's correction for small sample bias (17). Analyses were adjusted for the following possible confounders: tumor load, parenchymal dose and the presence of extrahepatic disease at baseline. Inspection of Schoenfeld residuals showed that the proportionality of the hazard assumption was not violated. Analyses were performed using R statistical software, version 3.6.2 for Windows. The following R libraries were used: readxl version 1.3.1, dplyr version 0.8.3, data.table version 1.12.8, lme4 version 1.1-21, nlme version 3.1-143, ggplot2 version 3.2.1, gdata version 2.18.0, gmodels version 2.18.1, ggpubr version 0.2.4, Hmisc version 4.3-0, lmerTest version 3.1.0, foreign version 0.8-72, ggfortify version 0.4.8, logistf version 1.23, grid version 3.6.2, car version 3.0-5, pROC version 1.15.3, ggeffects version 0.14.0, splines version 3.6.2, sjmisc version 2.8.3, rel version 1.4.1 and rcompanion version 2.3.21. We report effect estimates with associated 95%CIs and corresponding two-sided p-values.

RESULTS

Forty patients were included, with a total of 133 hepatic lesions. Three patients did not have follow-up imaging for tumor-response assessment and were only included in the survival- and toxicity analyses. Patient- and treatment characteristics are summarized in Table 1.

TABLE 1. Baseline patient and treatment characteristics

Characteristic	N (%) or median + range
Gender	
Male	25 (62.5)
Female	15 (37.5)
Age (y)	64 (37-84)
WHO performance score	
0	28 (70)
1	11 (27.5)
2	1 (2.5)
Previous therapy*	
Locoregional (liver)	
EBRT	2 (5)
Metastasectomy	5 (12.5)
Radiofrequency ablation	3 (7.5)
Lines of prior systemic treatment	
1	8 (20)
2	20 (50)
3	7 (17.5)
4	5 (12.5)
Extrahepatic disease before treatment	
Lymph node	10 (25)
Lung	10 (25)
No	23 (57.5)
Liver volume (mL)	1987 (1272-3167)
Metabolic tumor volume (mL)	320 (26-1446)
Fractional tumorload	0.15 (0.01-0.49)
Radioembolization treatment	
Whole-liver	39 (97.5)
Lobar (right lobe only)	1 (2.5)
Administered activity (MBq)	6387 (3822-12386)

*No patient received synchronous systemic treatment.

Toxicity

The median parenchymal-absorbed dose was 37 Gy (range 12-55 Gy). Toxicity incidence during three months post-treatment and CTCAE grades are summarized in Table 2. New grade ≥3 clinical toxicity was present in eight patients (20%) and new grade ≥3 laboratory toxicity was present in seven patients (17.5%). There was one patient (2.5%) who developed REILD, evidenced by hyperbilirubinemia, hypoalbuminemia and ascites, without evidence of progression or biliary obstruction. The mean parenchymal-absorbed dose of this patient was 34 Gy.

The results of the linear clinical toxicity regression analyses suggested a positive association between higher parenchymal dose and increase in CTCAE grade clinical toxicity (Table S1). The mean difference in parenchymal dose for patients with CTCAE grade 0/1/2 any clinical toxicity versus CTCAE grade 3/4/5 was 11.6 Gy (95%CI 3.4-19.7, p=0.0070). The odds ratio for CTCAE grade 3/4/5 any clinical toxicity versus CTCAE grade 0/1/2 per 10 Gy increase in parenchymal dose was 7.62 (95%CI 1.95-249.03, p=0.0063) (Table S2).

For laboratory toxicity, the results of the linear regression analyses for both the CTCAE grades and the relative change in laboratory parameters showed that a higher parenchymal-absorbed dose is related with an increase in laboratory toxicity (Table S3a-b and Figures 2a-f).

TABLE 2. CTCAE grading of new clinical toxicity per patient during three months after treatment

Toxicity	CTCAE grade I	CTCAE grade II	CTCAE grade III	CTCAE grade IV	CTCAE grade V
Abdominal pain	16	10	4		
Nausea	15	9	2		
Fatigue	21	10	2		
Anorexia	10	5			
Dyspnea	4	1			
Fever	7	1	1		
Ascites	1		2		
Flu like symptoms	2	1			
Malaise	4	1			
Hepatic failure			1		1*
Weight loss	2				
Chest pain	1	2			
Vomiting	9	5			
Dyspepsia	1	1			
Metal taste	3				
Contrast allergy	1	2			
Hematoma	1				
Diarrhea	1				
Constipation	4				
Upper GI tract bleeding			1		
Limb edema	2				
Dizziness	1				
Chills	2				
Any clinical toxicity	13	19	7		1
Lowered albumin	9	4			
Elevated ALAT	24	1	1		
Elevated AP	4	14	2		
Elevated ASAT	28	2			
Elevated bilirubin	2	1		2	
Elevated GGT	5	15	5		
Any laboratory toxicity	7	23	5	2	

CTCAE scores of new toxicity (highest CTCAE grades per clinical symptom or laboratory value are represented). *Radioembolization-induced liver disease.

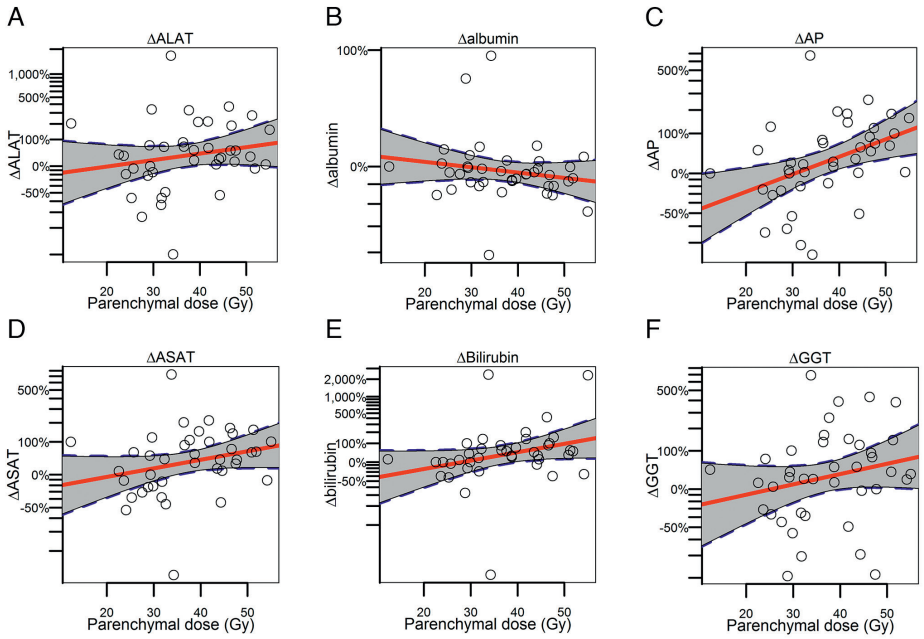

FIGURE 2A-F. Association between change in laboratory parameters and parenchymal absorbed dose. The red lines are the regression lines, with the 95%CIs indicated as the surrounding grey areas.

Efficacy

Solely based on the metabolic response of measurable hepatic metastases at baseline, there was one patient with CR, PR was reached in 11 patients, 17 patients had StD and PD was found in eight patients at three-months follow-up. On a lesion level, CR occurred in 23 lesions, PR in 20 lesions, StD in 49 lesions and 23 lesions were progressive. A significant dose-response relation was found on patient- and tumor-level. The mean tumor-absorbed dose was 77% higher in patients with CR/PR than in patients with PD (95%CI: 18-164%, p=0.011) and the mean absorbed dose was 95% higher in lesions with CR than in lesions with PD (34-188%, p=0.00065) (Table 3). Mean absorbed doses per response category are visualized in Figure 3.

TABLE 3. Percentage change in mean absorbed dose (Gy) per response category (95%CI)

	Progressive disease	**Stable disease**	**Partial response**	**Complete response***	
Patient-level	n=8	n=17	n=11	n=1	
Unadjusted	*reference*	53.8 (5.6 - 24.2)	74.6 (18.6 - 57.6)	-	P_{trend}=*0.012*
Adjusted†	*reference*	62.0(10.4 - 136.0)	77.3 (18.3 - 163.6)	-	P_{trend}=*0.019*
Patient-level‡	n=23	n=6	n=7	n=1	
Unadjusted	*reference*	29.8 (-15.1 - 98.6)	44.4 (1.4 - 106.0)	-	P_{trend}=*0.041*
Adjusted†	*reference*	18.7 (-24.3 - 85.4)	38.1 (-5.8 - 101.9)	-	P_{trend}=*0.12*
Tumor-level	n=23	n=49	n=20	n=23	
Unadjusted	*reference*	31.1 (-3.2 - 78.8)	71.5 (17.1 - 150.4)	95.2 (34.7 - 183.6)	P_{trend}=*0.00030*
Adjusted	*reference*	35.2 (0.2 - 87.5)	72.2 (16.6 - 151.3)	94.8 (33.9 - 188.4)	P_{trend}=*0.00068*

Interpretation at tumor level: the average dose is 95.23% higher in CR than PD (95%CI 4.69-183.62%). *as there was only one patient with complete metabolic response, the categories complete response and partial response were taken together at a patient level. † The analyses were adjusted for previous treatment and tumorload or tumor volume (tumor-level analyses). ‡including the development of new lesions, in which case patients were categorized as having progressive disease.

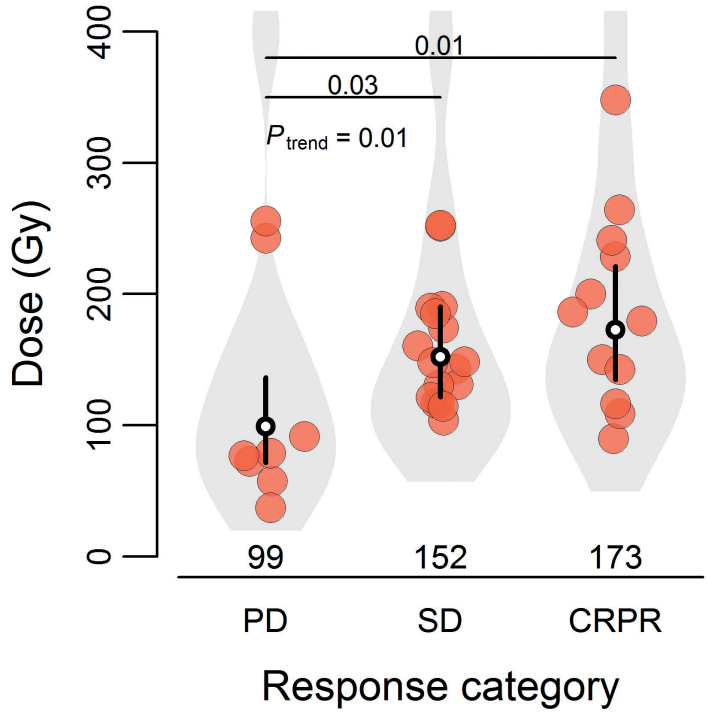

FIGURE 3. Relationship between mean tumor-absorbed dose per patient and metabolic response to treatment at three-months follow-up. The bullets show the mean tumor-absorbed dose per patient. Black vertical lines are the 95%CIs of the mean doses per response category, with the white dot in the middle indicating the mean tumor-absorbed dose per response category. This figure is based on the unadjusted linear mixed-effects regression model as described in Table 3.

Based on ROC analysis, the ability of tumor-absorbed dose to discriminate between patients with and without metabolic response was 0.671 (95%CI: 0.54-0.80) and the ability of mean tumor-absorbed dose per patient to differentiate between responders and non-responders was 0.698 (95%CI: 0.45-0.95) (Figure 4a,b). At a mean tumor-absorbed dose threshold with 100% sensitivity (95%CI: 48-100%) for CR/PR at a patient level (90 Gy), specificity was 38% (95%CI: 21-56%). At a tumor-level, without accounting for clustered data, sensitivity was 100% using a tumor-absorbed dose threshold of 80 Gy (95%CI: 74-100%) and specificity was 41% (95%CI: 31-51%). Agreement between PERCIST and RECIST was minimal, with κ=0.345 (95%CI 0.14-0.55). Anatomic response was lower than metabolic response in 15 cases (40.5%) and higher in seven cases (18.9%).

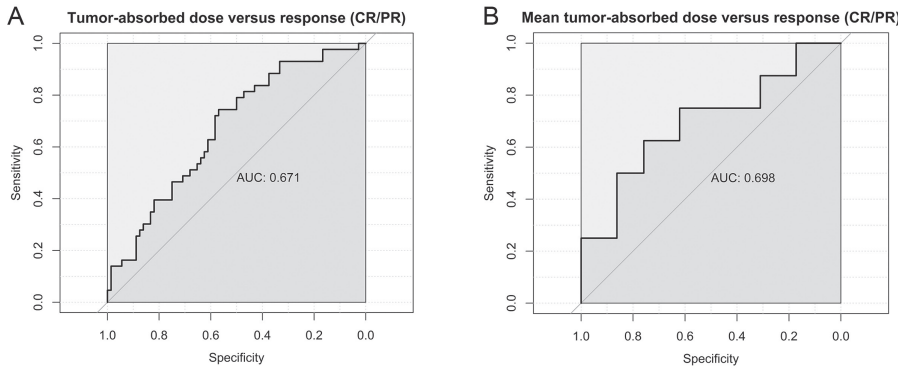

FIGURE 4A,B*. ROC-curve showing the discriminative value of tumor-absorbed dose for response (a) and ROC-curve showing the ability of mean tumor-absorbed dose per patient to discriminate between patients with CR/PR versus StD/PD (b). *The AUCs are based on a clustered data analysis, however, the ROC-curves are not.

Survival

Median overall survival was 10.7 months (95% CI: 7.2 – 13.4). Survival was significantly different in patients without a metabolic response (including the development of new intra- or extrahepatic lesions) versus patients with a metabolic response (HR=2.34, 95% CI 1.09 - 5.69, p=0.029). After adjusting for tumor load, extrahepatic disease at baseline and parenchymal dose, the HR for non-responders was 2.54 (95% CI: 1.13 - 6.52, p=0.023). Median overall survival in responders was 14.8 months (95% CI 14.2 - ∞, n=8) versus 8.6 months (95% CI 6.4 – 13.4 months, n=29) in non-responders (Figure 5a-b). Furthermore, there was a significant difference in overall survival between patients with a mean tumor-absorbed dose >90 Gy versus a mean tumor-absorbed dose <90 Gy (HR=0.16, 95%CI 0.06-0.511), p=0.0031), Figure 6.

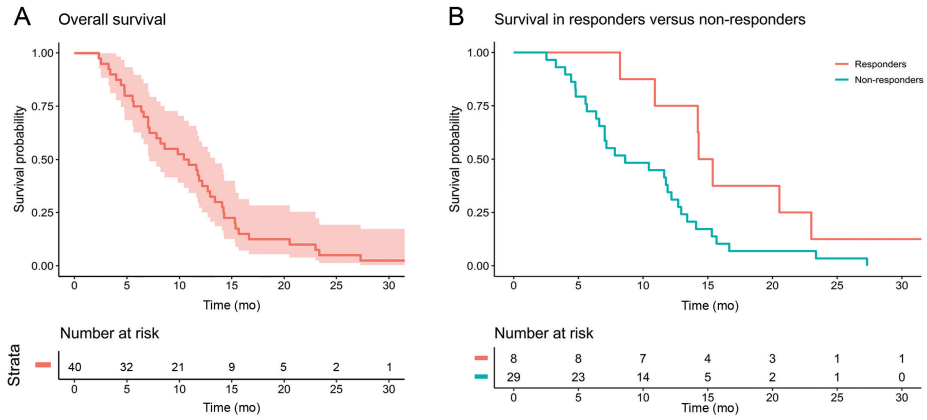

FIGURES 5A,B. Overall survival curve (a). Survival curves for patients with and without a metabolic response (including the development of new lesions) at three months (b).

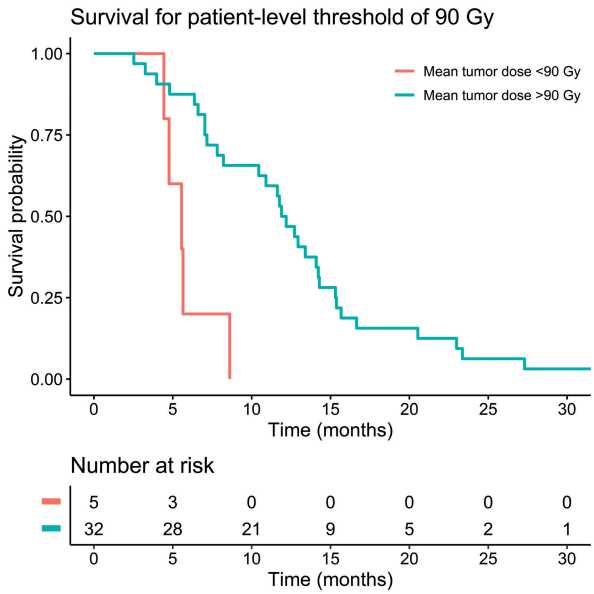

FIGURE 6. Survival curves for patients with a higher (>90 Gy) or lower (<90 Gy) mean tumor-absorbed dose.

DISCUSSION

Building on the establishment of a dose-response relationship in patients treated with ^{166}Ho-radioembolization by Bastiaannet et al. (11), this study explored the dose-response relationship in a homogenous population of patients with CRC only. Furthermore, dose-toxicity relationships were studied. Our results suggest a positive association between a higher parenchymal-absorbed dose and increase in CTCAE grade toxicity, both for clinical and laboratory toxicity. Furthermore, our data unveils, both at a lesion- and at a patient-level, a significant dose-response relationship. Also, a mean tumor-absorbed dose >90 Gy – the minimal mean tumor-absorbed dose in the group of patients with CR/PR - was associated with a significantly longer survival.

In this study, treatment with radioembolization was well tolerated. The most frequent clinical adverse events were CTCAE grade 1-2 abdominal pain, nausea and fatigue. These adverse events are well-known side effects of treatment with radioembolization (19). One patient of our study died of hepatic failure. This safety profile is compliant with the results of the MORE study, which showed that treatment with ^{90}Y-resin radioembolization is safe in a patient population highly comparable to ours, namely CRC patients who received several lines of prior chemotherapy (20). A study on the safety of ^{90}Y-glass radioembolization in CRC patients showed similar results, with the most frequent side effects being fatigue, abdominal pain and nausea (21). The incidence of grade ≥3 laboratory toxicity is also comparable between the three types of microspheres (20, 21).

Regarding efficacy, the metabolic response rate (CR/PR) at a tumor level was 36%, comparable to previous dose-response data on resin microspheres in a similar patient cohort, treated in the same hospital (22). In other studies, higher tumor-response rates up to 75% were found, with dose thresholds of 46 and 60 Gy (23, 24). However, it is difficult to compare these studies with our study, as those patients were less heavily pretreated or received concomitant systemic therapy (23, 24). Also, their thresholds cannot be compared to our data, as there are major differences between microsphere types in specific activity, size, number of particles and half-life. There was only minimal agreement in response between the PERCIST and the RECIST assessments. In 15 patients of our study, RECIST underestimated response according to PERCIST. This finding is

in accordance with other studies comparing these response assessments after radioembolization (25, 26). Metabolic response assessment is not hampered by the presence of necrosis, cystic changes and hemorrhage, as can be the case with size evaluation on transaxial images (27). Moreover, several studies found that changes in functional metrics, such as TLG, were related with overall survival and were more accurate predictors than anatomic changes (22, 27, 28).

Although the majority of our patients underwent ≥2 prior lines of systemic treatment, the response rate seems suboptimal. Before treatment, patients with CRC are currently selected based on clinical criteria, such as WHO performance status and progressive disease after several lines of chemotherapy (29). In case patients are deemed eligible for treatment with radioembolization, a second selection criterion should be the activity distribution based on either ^{99m}Tc-MAA or ^{166}Ho-scout. Based on the results of this study, we would argue that patients should only be selected for treatment if there is a favorable activity distribution with a sufficient mean tumor-absorbed dose >90 Gy and a parenchymal-absorbed dose of <55 Gy. Although a causal relationship cannot be claimed solely based on these observational data, the findings of this study suggest that below a mean tumor-absorbed dose of 90 Gy, metabolic response seems unlikely. However, since the discriminatory power of absorbed dose for response is limited, this number should be used with caution.

The need for personalized dosimetry is widely accepted, with several studies showing a dose-response relationship in CRC patients treated with ^{90}Y-resin radioembolization (22-24, 28). There also is growing evidence for the possibility of improving treatment outcomes by using personalized treatment planning in radioembolization (10, 11). However, thus far, the DOSISPHERE study was the only study implementing personalized radioembolization planning in a prospective clinical study, investigating the tumor-absorbed dose and response rate in HCC patients using a standard versus a personalized dosimetric approach with ^{90}Y glass microspheres. Preliminary results showed that both the response rates and tumor-absorbed doses were significantly higher in the personalized dosimetry arm (30).

Strengths of this study are the homogenous patient population, the standardized methods for tumor delineation, the use of a mixed-effects regression model accounting for clustered data, and the analyses of both safety and efficacy. This study also has several limitations. First, it is a single-center retrospective evaluation and there is a level of subjectivity in identifying the response of existing lesions, possibly leading to inter-operator variations in estimated doses. Second, the sample size was limited and due to the low incidence of toxicity, there was not enough data to draw a strong conclusion on the maximum tolerable parenchymal dose. Furthermore, the discriminatory value of absorbed dose for response estimation is limited and a causal dose-response relationship cannot be claimed based on these observational data. Hence, the reference values obtained should be interpreted with uttermost caution and only be used as a direction. The rigid co-registrations used in this study are likely affected by differences in patient positioning, differences in breath-hold policy and the relatively low resolution of the low-dose CT of the SPECT/CT. The resulting (local) errors are likely to propagate as underestimated tumor doses and (slightly) overestimated parenchymal doses, which contributes to the error in each response category, decreasing statistical power.

In future studies on radioembolization in CRC patients, personalized dosimetry should be used. By using dosimetry-based optimized treatment planning, treatment doses can be tailored to the individual patient to acquire a maximum response while minimizing the chance of toxicity. As the incidence of toxicity was low, it is difficult to establish an absolute threshold for a maximum parenchymal dose. At the same time, it is likely that the parenchymal-absorbed dose threshold is different for each individual patient, dependent on many clinical characteristics. We therefore advise a pragmatic and clinically feasible approach, with activity calculation in order to obtain a sufficient tumor-absorbed dose and a parenchymal-absorbed dose of up to 55 Gy, dependent on individual patient characteristics. With a median parenchymal-absorbed dose of 37 Gy and a maximum of 55 Gy, this was proven to be a safe approach, with only one case of REILD. Furthermore, those patients for whom no meaningful mean tumor-absorbed dose (>90 Gy) can be reached at an acceptable parenchymal-absorbed dose threshold should be excluded from radioembolization treatment. On a tumor-level, based on our results, treatment strategy should be adjusted to guarantee a tumor-absorbed dose of at least

80 Gy for every tumor. Partition-modeling and multiple injection positions can be used to reach that objective. In other words, planning should be primarily based on applying a safe parenchymal-absorbed dose threshold, and selection of patients on a sufficient tumor-absorbed dose.

CONCLUSION

In CRC patients treated with ^{166}Ho-radioembolization, a positive association between tumor-absorbed dose and metabolic response was established. Survival for patients with a mean tumor-absorbed dose >90 Gy was significantly better than for patients with a mean tumor-absorbed dose <90 Gy. There also was a positive association between parenchymal-absorbed dose and both laboratory and clinical toxicity. A treatment approach with selection of patients based on the activity distribution of the ^{166}Ho-scout and personalized treatment activity calculation is advocated.

REFERENCES

1. Bray F, Ferlay J, Soerjomataram I, Siegel RL, Torre LA, Jemal A. Global cancer statistics 2018: GLOBOCAN estimates of incidence and mortality worldwide for 36 cancers in 185 countries. CA Cancer J Clin. 2018;68(6):394-424. Epub 2018/09/13.

2. Donadon M, Ribero D, Morris-Stiff G, Abdalla EK, Vauthey JN. New paradigm in the management of liver-only metastases from colorectal cancer. Gastrointest Cancer Res. 2007;1(1):20-7.

3. Network NCC. NCCN Guidelines Version 1.2018 Colon Cancer. 2018 [cited 2019 September 12]; Available from: https://oncolife.com.ua/doc/nccn/Colon_Cancer.pdf.

4. Smits MLJ, Dassen MG, Prince JF, Braat A, Beijst C, Bruijnen RCG, et al. The superior predictive value of (^{166})Ho-scout compared with (99m)Tc-macroaggregated albumin prior to (^{166})Ho-microspheres radioembolization in patients with liver metastases. Eur J Nucl Med Mol Im. 2020;47(4):798-806. Epub 2019/08/11.

5. Reinders MTM, Smits MLJ, van Roekel C, Braat A. Holmium-166 Microsphere Radioembolization of Hepatic Malignancies. Sem Nucl Med. 2019;49(3):237-43. Epub 2019/04/08.

6. Prince JF, van den Bosch M, Nijsen JFW, Smits MLJ, van den Hoven AF, Nikolakopoulos S, et al. Efficacy of radioembolization with (^{166})Ho-microspheres in salvage patients with liver metastases: a phase 2 study. J Nucl Med. 2018;59(4):582-8. Epub 2017/09/17.

7. Smits MLJ, Nijsen JFW, van den Bosch MAAJ, Lam MGEH, Vente MAD, Mali WPTM, et al. Holmium-166 radioembolisation in patients with unresectable, chemorefractory liver metastases (HEPAR trial): a phase 1, dose-escalation study. Lancet Oncol. 2012;13(10):1025-34.

8. van den Hoven AF, Prince JF, Bruijnen RC, Verkooijen HM, Krijger GC, Lam MG, et al. Surefire infusion system versus standard microcatheter use during holmium-166 radioembolization: study protocol for a randomized controlled trial. Trials. 2016;17(1):520. Epub 2016/10/27.

9. Braat AJAT, Bruijnen RCG, van Rooij R, Braat MNGJA, Wessels FJ, van Leeuwaarde RS, et al. Additional holmium-166 radioembolisation after lutetium-177-dotatate in patients with neuroendocrine tumour liver metastases (HEPAR PLuS): a single-centre, single-arm, open-label, phase 2 study. Lancet Oncol. 2020;21(4):561-70.

10. Kafrouni M, Allimant C, Fourcade M, Vauclin S, Delicque J, Ilonca AD, et al. Retrospective voxel-based dosimetry for assessing the ability of the body-surface-area model to predict delivered dose and radioembolization outcome. J Nucl Med. 2018;59(8):1289-95. Epub 2018/03/17.

11. Bastiaannet R, van Roekel C, Smits MLJ, Elias SG, van Amsterdam WAC, Doan DT, et al. First evidence for a dose-response relationship in patients treated with (^{166})Ho-radioembolization: a prospective study. J Nucl Med. 2019;61(4):608-12. Epub 2019/10/12.

12. Salem R, Thurston KG. Radioembolization with 90Yttrium microspheres: a state-of-the-art brachytherapy treatment for primary and secondary liver malignancies. Part 1: Technical and methodologic considerations. J Vasc Interv Radiol. 2006;17(8):1251-78. Epub 2006/08/23.

13. Klein S, Staring M, Murphy K, Viergever MA. Elastix: a toolbox for intensity-based medical image registration. IEEE Trans Med Imaging. 2010;29:196-205.

14. Cancer IN. Common terminology criteria for adverse events (CTCAE) v5.0. Cancer Therapy Evaluation Program; 2018.

15. O JH, Lodge MA, Wahl RL. Practical PERCIST: a simplified guide to PET response criteria in solid tumors 1.0. Radiology. 2016;280(2):576-84.

16. Eisenhauer EA, Therasse P, Bogaerts J, Schwartz LH, Sargent D, Ford R, et al. New response evaluation criteria in solid tumours: revised RECIST guideline (version 1.1). Eur J Cancer. 2009;45(2):228-47. Epub 2008/12/23.

17. Heinze G, Dunkler D. Avoiding infinite estimates of time-dependent effects in small-sample survival studies. Stat Med. 2008;30(27):6455-69.

18. Obuchowski NA. Nonparametric analysis of clustered ROC curve data. Biometrics. 1997;53(2):567-78.

19. Riaz A, Awais R, Salem R. Side effects of yttrium-90 radioembolization. Front Oncol. 2014;4:198. Epub 2014/08/15.

20. Kennedy AS, Ball D, Cohen SJ, Cohn M, Coldwell DM, Drooz A, et al. Multicenter evaluation of the safety and efficacy of radioembolization in patients with unresectable colorectal liver metastases selected as candidates for (90)Y resin microspheres. J Gastrointest Oncol. 2015;6(2):134-42. Epub 2015/04/02.

21. Hickey R, Lewandowski RJ, Prudhomme T, Ehrenwald E, Baigorri B, Critchfield J, et al. 90Y Radioembolization of colorectal hepatic metastases using glass microspheres: safety and survival outcomes from a 531-patient multicenter study. J Nucl Med. 2016;57(5):665-71. Epub 2015/12/05.

22. van den Hoven AF, Rosenbaum CE, Elias SG, de Jong HW, Koopman M, Verkooijen HM, et al. Insights into the Dose-Response Relationship of Radioembolization with Resin 90Y-Microspheres: A Prospective Cohort Study in Patients with Colorectal Cancer Liver Metastases. J Nucl Med. 2016;57(7):1014-9. Epub 2016/02/26.

23. Flamen P, Vanderlinden B, Delatte P, Ghanem G, Ameye L, Van Den Eynde M, et al. Multimodality imaging can predict the metabolic response of unresectable colorectal liver metastases to radioembolization therapy with Yttrium-90 labeled resin microspheres. Phys Med Biol. 2008;53(22):6591-603. Epub 2008/11/04.

24. Levillain H, Duran Derijckere I, Marin G, Guiot T, Vouche M, Reynaert N, et al. (90)Y-PET/CT-based dosimetry after selective internal radiation therapy predicts outcome in patients with liver metastases from colorectal cancer. EJNMMI research. 2018;8(1):60. Epub 2018/07/15.

25. Jongen JMJ, Rosenbaum C, Braat M, van den Bosch M, Sze DY, Kranenburg O, et al. Anatomic versus metabolic tumor response assessment after radioembolization treatment. J Vasc Interv Radiol. 2018;29(2):244-53 e2. Epub 2017/12/19.

26. Sager S, Akgun E, Uslu-Besli L, Asa S, Akovali B, Sahin O, et al. Comparison of PERCIST and RECIST criteria for evaluation of therapy response after yttrium-90 microsphere therapy in patients with hepatocellular carcinoma and those with metastatic colorectal carcinoma. Nucl Med Comm. 2019;40(5):461-8. Epub 2019/03/22.

27. Bastiaannet R, Lodge MA, de Jong H, Lam M. The unique role of fluorodeoxyglucose-PET in radioembolization. PET Clinics. 2019;14(4):447-57. Epub 2019/09/02.

28. Willowson KP, Hayes AR, Chan DLH, Tapner M, Bernard EJ, Maher R, et al. Clinical and imaging-based prognostic factors in radioembolisation of liver metastases from colorectal cancer: a retrospective exploratory analysis. EJNMMI Research. 2017;7(1):46. Epub 2017/05/26.

29. Dendy MS, Ludwig JM, Kim HS. Predictors and prognosticators for survival with Yttrium-90 radioembolization therapy for unresectable colorectal cancer liver metastasis. Oncotarget. 2017;8(23):37912-22.

30. Garin E. A multicentric and randomized study demonstrating the impact of MAA based dosimetry on tumor response in SIRT for HCC. 2019 [cited 2019 December 12]; Available from: https://www.eventscribe.com/2019/GEST/fsPopup.asp?Mode=presInfo&PresentationID=521844.

SUPPLEMENTAL TABLES

TABLE S1. Relation between parenchymal dose (Gy) and clinical toxicity based on linear regression analyses with parenchymal dose as the dependent variable

Independent variable	Number of patients with toxicity	CTCAE grade 0 -V	
		Mean change in parenchymal dose (Gy) per step increase in CTCAE grade category (95% CI); p-value	
		Unadjusted	Adjusted (for tumor dose, previous treatment and response)
Any variable, highest grade	40	3.43 (-0.23 – 7.10); 0.065	6.56 (1.96 – 11.16); 0.0067
Abdominal pain	30	0.26 (-3.24 – 3.77); 0.88	0.99 (-3.06 – 5.04); 0.62
Nausea	26	3.09 (-0.46 – 6.65); 0.086	2.62 (-0.99 – 6.22); 0.15
Vomiting	14	1.70 (-2.87 – 6.26); 0.46	2.33 (-2.27 – 6.93); 0.31
Fatigue	33	3.78 (-0.25 – 7.81); 0.065	3.66 (-0.60 – 7.91); 0.090
Fever	9	3.61 (-1.32 – 8.55); 0.15	4.85 (-2.44 – 12.13); 0.18
Anorexia	15	1.13 (-3.46 – 5.71); 0.62	0.47 (-4.42 – 5.37); 0.85
Ascites	3	2.92 (-1.86 – 7.70); 0.22	6.86 (0.53 – 13.19); 0.035

The mean change indicates the average increase or decrease in parenchymal dose per step increase in CTCAE grade toxicity. For example, for any clinical toxicity: a unit increase in toxicity results in an increase in average parenchymal dose of 3.4 Gy (unadjusted analysis).

TABLE S2. Relation between parenchymal dose (Gy) and cumulative toxicity over three months, based on logistic regression analyses using Firth's correction with parenchymal dose (per 10 Gy) as the independent variable

Dependent variable	CTCAE grade 0-II vs III-V	
	Odds ratio for toxicity parameter per 10 Gy increase in parenchymal dose (95% CI); p-value	
	Unadjusted model	Adjusted model (for tumor dose, previous treatment and response)
Any variable laboratory toxicity, highest grade (n=33 vs n=7)	1.05 (0.46 – 2.48); 0.91	1.08 (0.39 – 3.12); 0.88
Any variable clinical toxicity, highest grade (n=32 vs n=8)	3.61 (1.37 – 13.10); 0.022	9.68 (2.18 – 124.20); 0.019

The odds ratio represents the odds for a CTCAE grade III-V toxicity for every 10 Gy increase in parenchymal absorbed dose.

TABLE S3A. Relation between parenchymal dose (Gy) and cumulative laboratory toxicity over three months, based on linear regression analyses with parenchymal dose as the dependent variable

Independent variable	Number of patients with toxicity	CTCAE grade 0-V	
		Mean change (95% CI); p-value	
		Unadjusted	Adjusted for tumor dose, previous treatment and response
Any variable, highest grade	37	2.51 (-1.05 – 6.07); 0.16	3.47 (-0.82 – 7.75); 0.11
GGT	25	2.06 (-0.87 – 4.98); 0.16	2.07 (-1.19 – 5.33); 0.20
AP	20	3.64 (0.65 – 6.63); 0.018	3.34 (-0.09 – 6.78); 0.057
Albumin	13	2.75 (-2.07 – 7.56); 0.26	3.20 (-2.26 – 8.66); 0.24
Bilirubin	5	1.98 (-1.71 – 5.66); 0.29	4.98 (0.02 – 9.93); 0.049
ALAT	26	0.48 (-4.44 – 5.41); 0.84	0.84 (-5.58 – 7.27); 0.79
ASAT	30	3.30 (-2.22 – 8.81); 0.23	4.49 (-1.98 – 10.96); 0.17

The mean change indicates the average increase or decrease in parenchymal dose per unit increase in CTCAE grade toxicity. For example, for GGT: a unit increase in toxicity results in an increase in average parenchymal dose of 2.06 Gy (unadjusted analysis).

TABLE S3B. Relation between parenchymal dose (Gy) and change in laboratory parameters over three months, based on linear regression analyses with parenchymal dose (per 10 Gy) as the independent variable

Dependent variable	Mean percent change (95% CI); p-value	
	Unadjusted	Adjusted for tumor dose, previous treatment and response
ΔGGT	19.6% (-9.1 – 57.3); 0.17	34.1.2% (0.5 – 79.7), 0.043
ΔAP	34.5% (8.5 – 66.7); 0.0063	33.3% (6.5 – 66.6), 0.011
ΔAlbumin	-4.1% (-9.7 – 1.8); 0.28	-3.1% (-9.1 – 1.8), 0.71
ΔASAT	18.9% (-4.9 – 48.5); 0.11	14.5% (-9.1 – 44.1), 0.21
ΔALAT	17.3% (-12.7 – 57.7); 0.25	13.3% (-16.5 – 53.6), 0.37
ΔBilirubin	35.1% (-4.5 – 90.7); 0.077	46.6% (3.4 – 107.7), 0.029

The mean change indicates the increase or decrease in average toxicity per 10 Gy increase in parenchymal dose. For example, for GGT: for every 10 Gy increase in parenchymal dose, there is a 19.6% increase in GGT (unadjusted analysis).

The efficacy of coil-embolization to obtain intrahepatic redistribution in radioembolization: qualitative and quantitative analyses

Ahmed A. Alsultan, Caren van Roekel, Maarten W. Barentsz, Arthur J.A.T. Braat, Pieter Jan van Doormaal, Marnix. G.E.H. Lam, Maarten L.J. Smits

Cardiovascular and Interventional Radiology 2020

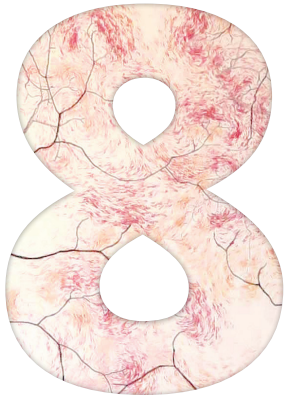

ABSTRACT

Purpose

To evaluate the efficacy of coil-embolization to obtain intrahepatic redistribution in patients undergoing radioembolization.

Materials and methods

All patients treated with radioembolization at our institute were retrospectively analyzed, and all cases in which a tumor-feeding vessel was coil-embolized were selected. Two nuclear medicine physicians visually assessed the effect of redistribution. Furthermore, the redistribution of microspheres was measured by quantifying the activity distributed to the coil-embolized (dependent) segment relative to the other (non-dependent) segments, and to the tumor(s) in that segment. Quantitative analysis was performed on post-treatment ^{90}Y-PET and ^{166}Ho-SPECT using Simplicit^{90}Y (Mirada Medical Ltd, Oxford, UK) software.

Results

Out of 37 cases, 32 were suitable for quantitative analysis and 37 for qualitative analysis. In the qualitative analysis, redistribution was deemed successful in 69% of cases. The quantitative analysis showed that the median ratio of the activity to the dependent embolized segments and the non-dependent segments was 0.88 (range 0.26 – 2.05), and 0.80 (range 0.19 – 1.62) for tumors in dependent segments compared with tumors in non-dependent segments. Using a cutoff ratio of 0.7 (30% lower activity concentration in comparison with the rest of the liver), 57% of cases were successful.

Conclusion

Coil-embolization of hepatic arteries to induce redistribution of microspheres has a limited success rate. Redistribution tends to be overrated in visual assessment.

INTRODUCTION

Radioembolization is increasingly used for the treatment of primary and secondary liver tumors. The treatment consists of an intra-arterial injection of microspheres loaded with yttrium-90 (^{90}Y) or holmium-166 (^{166}Ho). The microspheres are commonly injected in a lobar or segmental fashion (1). Injection can be challenged by the presence of early bifurcations, replaced or accessory hepatic arteries, and 'parasitized' arteries (i.e. non-hepatic arteries contributing to the vascular supply of the liver tumors), or by the proximity to non-target vessels. Therefore, multiple injection positions may be required.

Each injection position requires a change of the vial, microcatheter, and tubing, and the injected activity needs to be adjusted to the target volume. Consequently, radioembolization procedures requiring multiple injection positions are more prone to catheter-related complications and dosing errors. Multiple injection positions are also costly due to the higher material costs and prolonged procedure time.

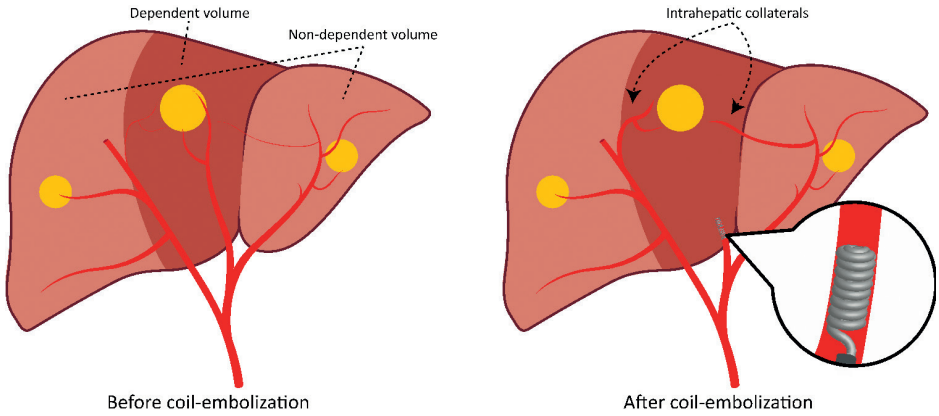

FIGURE 1. The principle of redistribution. A typical situation with a middle hepatic artery (or segment IV artery) that would require three separate injections in case of whole-liver treatment (right hepatic artery, middle hepatic artery, and left hepatic artery). Coil-embolization of the middle hepatic artery can be performed to reduce the number of injection positions and rely on redistribution of microspheres through intrahepatic collaterals.

To overcome these problems, techniques are used to reduce the number of injection positions. One of these techniques is embolizing one of the tumor-feeding arteries, leading to redistribution of blood flow through collateral pathways from adjacent hepatic arteries (Figure 1+2) (2,3). Various publications have reported on the success of redistribution in radioembolization(4–8). However, mixed results were reported in our practice.

The aim of this study was to evaluate and quantify the effect of coil-embolization of tumor-feeding vessels on the redistribution of blood flow and to study patient and treatment factors that affect redistribution.

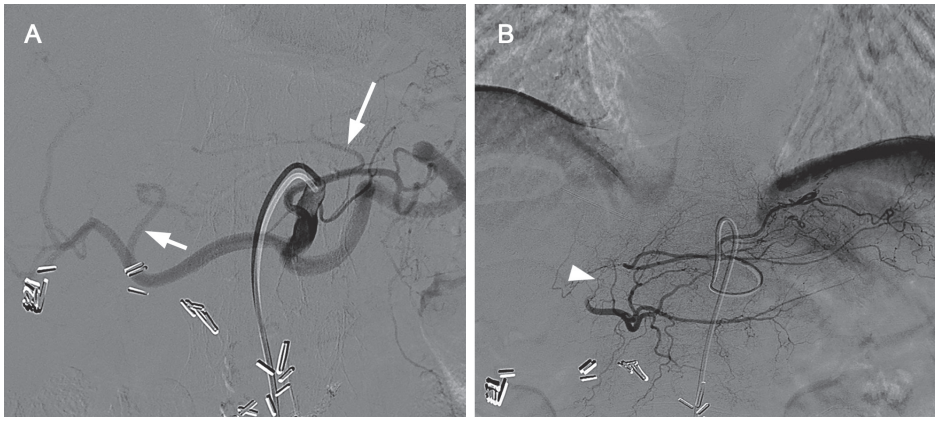

FIGURE 2. Intrahepatic collateral pathways on DSA. A. Celiac trunk overview shows the native left hepatic artery (short arrow) and accessory left hepatic artery arising from the left gastric artery (long arrow). B. Selective angiography from the accessory left hepatic artery shows filling of the native left hepatic artery, demonstrating a patent connection (arrowhead) even without coil-embolization.

METHODS

Patient selection and data collection

All patients scheduled to undergo radioembolization at our institute for primary or metastatic hepatic cancer between June 2011 and October 2017 were evaluated for inclusion. Radioembolization treatments were performed with both glass (Therasphere®, Biocompatibles UK Ltd.) and resin ^{90}Y microspheres (SIR-Spheres®, Sirtex medical Ltd.), as well as ^{166}Ho microspheres

(QuiremSpheres®, Quirem Medical B.V.). Patients were included if they had undergone embolization of at least one tumor-feeding arterial branch. Patients were excluded when post-treatment imaging was not available.

Both angiography images and cone-beam CT images, acquired during the work-up procedure of the included patients, were reviewed to identify the coil-embolized artery and the liver volume that was vascularized by it (i.e. dependent liver volume). Baseline characteristics were obtained, including type of primary tumor, gender, age, injection sites, and interval between coil-embolization and radioembolization.

Our institute's medical ethics committee waived the need for informed consent for this retrospective study.

Qualitative analysis

Distribution was analyzed qualitatively by visual assessment performed by two nuclear medicine physicians with >5 years of experience with radioembolization. Data on gender, age, embolized artery, dependent embolized segment, intended target volume, and relevant information regarding patients' medical history (e.g. history of hepatic surgery, radio frequency ablation) was provided. Relevant digital subtraction angiography images and cone-beam CT images were also available. All other data was blinded. The redistribution was visually rated in a nominal scale: 1) no redistribution, 2) dubious redistribution, and 3) successful redistribution. Rating was performed independently, and any disagreement was resolved by consensus.

Quantitative analysis

The distribution of microspheres was also analyzed quantitatively by measuring the average activity concentration in the dependent segments (i.e. segments that rely on a coil-embolized artery for blood supply), using post-treatment imaging. These activity concentrations were compared to the activity concentrations measured in non-dependent segments (i.e. all liver segments that did not rely on the coil-embolized artery). The activity concentration in dependent tumors was also compared to the activity concentration in non-dependent tumors.

Quantitative analysis was performed using Simplict^{90}Y (Mirada Medical Ltd, Oxford, United Kingdom) software. Activity calculations were performed using volumes drawn on contrast-enhanced CT (CECT) images that were registered to low-dose CT images of nuclear imaging datasets. In this process, only rigid transformations were used.

Volumes of interest (VOI) were delineated using the axial reconstruction of a portal venous phase CECT. VOIs of the perfused volume of all injection locations, all measurable tumors (defined as having a diameter ≥ 20mm), and the dependent segment were drawn. The dependent segment VOIs were preferably drawn using cone-beam CT imaging, otherwise segmentation was performed based on the Couinaud classification of segmental hepatic anatomy. The non-dependent segment VOI was created by subtracting the dependent segment from the whole liver VOI. The activity concentrations were calculated using the net administered activity (i.e. corrected for residual activity). Activity concentrations in patients treated with holmium were also calculated using Simplicit^{90}Y software. As part of this study, activity measurements obtained in Simplicit^{90}Y were compared with measurements made using in-house developed dosimetry software in order to validate the use of Simplicit^{90}Y for ^{166}Ho-microspheres.(9) The differences were found to be negligible.

Patients in whom not all above mentioned VOIs could be delineated were excluded from this analysis, as well as cases where accurate registration of CECT to post-treatment imaging was impossible.

Sequential lobar therapy cases

Patients receiving sequential lobar therapy underwent post-treatment imaging twice (i.e. once for every radioembolization procedure) but were counted as one case. In the visual analysis, both post-treatment scans (i.e. the left and right hemi-liver scans) were assessed separately and the results were subsequently merged, counting the highest score. In the quantitative analysis, the activity concentrations of all VOIs were calculated on both scans and the results were averaged.

Time interval

To investigate the effects of the time interval between coil-embolization and administration of the microspheres on redistribution, the patients were dichotomized using a threshold of 24 hours. This threshold was chosen as almost half of the patients included in this analysis received treatment within the same day of coil-embolization. Segment activity ratios and tumor activity ratios were then compared. Patients receiving sequential lobar treatment were excluded from this subgroup analysis.

Statistical analysis

Descriptive statistics were used as proportions and medians with ranges. Ratios of activity concentrations were calculated between dependent and non-dependent segments (the segment ratio) and dependent and non-dependent tumors (the tumor ratio). Since there is no definition of successful redistribution, the success rates for a 10%, 20% and 30% difference in activity concentration between the dependent and non-dependent volumes were calculated, corresponding to dose ratios of 0.9, 0.8, and 0.7, respectively. Ratios in the time interval analysis were compared with an independent samples t-test. Inter-rater reliability was evaluated by means of a weighted Cohen's kappa. All statistical analyses were performed with IBM SPSS Statistics for Windows, version 22 (IBM Corp., Armonk, N.Y., USA).

RESULTS

Within the studied timeframe, a total of 517 radioembolization procedures were performed at our institute, of which 37 patients were selected for this study (Figure 3). In most cases (n=36) microcoils were used as embolization agent, and in one case cyanoacryl glue (Histoacryl®, B. Braun Surgical S.A.) was used. The baseline characteristics are shown in Table 1. Cone-beam CT images were available in 27 of 37 cases. In 10 cases, cone-beam CT series were acquired after selective injection of contrast-agent in the artery that was to be coiled and were helpful in delineating the dependent volume.

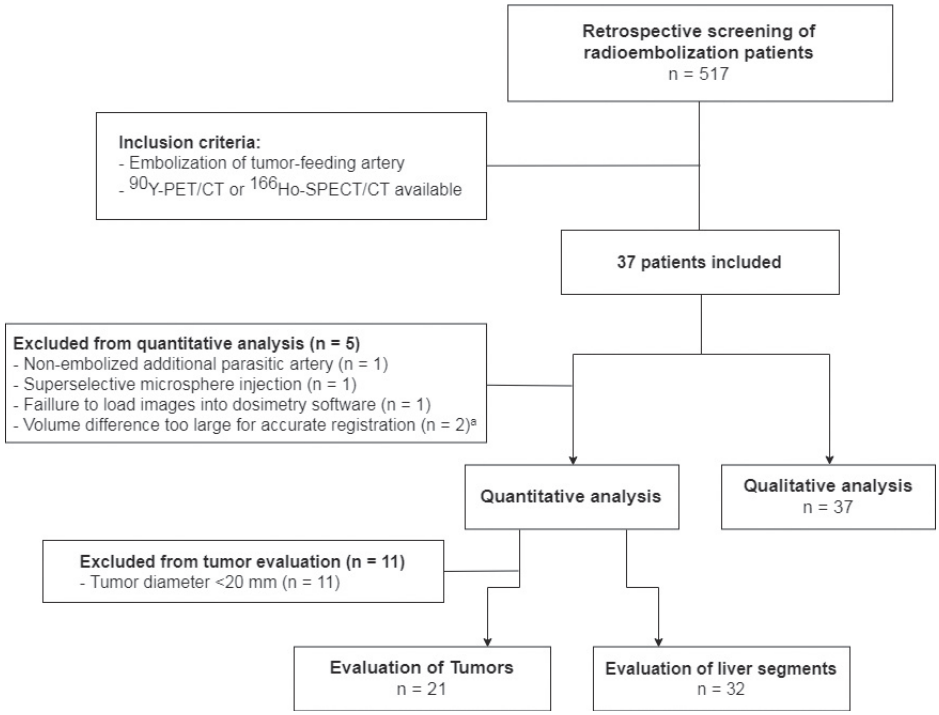

FIGURE 3. Flow chart of study patients. [a] significant hypertrophy of the contralateral lobe occurred in patients that were treated sequentially, making rigid registration with pre-treatment CT imaging impossible.

TABLE 1. Baseline characteristics

Baseline/Treatment characteristics	Value
Mean age in years ± SD	61 ± 9
Gender	
Male	20 (54%)
Female	17 (46%)
Primary Neoplasm	
Colorectal carcinoma	17 (46%)
Neuroendocrine tumor	11 (30%)
Cholangiocarcinoma	3 (8%)
Breast carcinoma	2 (5%)
Hepatocellular carcinoma	1 (3%)
Other	3 (8%)

TABLE 1. Baseline characteristics (continued)

Baseline/Treatment characteristics	Value
Embolized artery	
MHA/Segment IV artery	23 (62%)
aLHA	9 (24%)
rLHA	1 (3%)
Parasitized artery[a]	4 (11%)
Embolization method	
Microcoil	36 (97%)
Cyanoacryl glue	1 (3%)
Segments involved per case	
IV	25 (68%)
II	4 (11%)
II and III	2 (5%)
II, III and IV	2 (5%)
I	1 (3%)
I and VIII	1 (3%)
II and IV	1 (3%)
VII	1 (3%)
Type of microsphere	
Yttrium-90	21 (57%)
Resin	14 (38%)
Glass	7 (19%)
Holmium-166	16 (43%)
Treatment	
Whole liver	23 (62%)
Sequential lobar[b]	5 (14%)
Right lobe only[c]	6 (16%)
Left lobe only[d]	3 (8%)

Age displayed in mean with standard deviation.
[a] Right inferior phrenic artery (n = 3), Right internal mammary artery (n = 1).
[b] Median interval between sequential treatments was 53.5 days.
[c] After right hemi-hepatectomy (n = 1).
[d] After left hemi-hepatectomy (n = 1).
MHA = Middle hepatic artery, aLHA = accessory left hepatic artery, rLHA = replaced left hepatic artery.

Qualitative analysis

Redistribution was rated as successful in 26/37 (70%) cases, dubious in 5/37 (14%) cases, and no redistribution was found in 6/37 (16%) cases. Inter-rater agreement was considered high (κ = 0.82).

Quantitative analyses

Five patients were excluded from the quantitative analyses. One patient had an additional parasitized artery that could not be coil-embolized, one had a superselective injection of microspheres, in which the healthy liver VOI could not be determined, one had corrupted post-treatment imaging files, and two were treated sequentially and had a large volume increase in one liver lobe making accurate image registration impossible. The median ratio of the dependent to non-dependent segment activity concentration was 0.88 (range 0.26 – 2.05). This means that the activity concentration in the coiled segments amounted to 88% of the activity concentration to the rest of the treated volume. For tumors the median ratio was 0.80 (range 0.19 – 1.62). Success-rates for redistribution based on activity concentration (using cut-off ratios of 0.9, 0.8, and 0.7) were 29%, 43% and 57%, respectively (Table 2 and figure 4a).

Influencing factors

Redistribution of segment IV arteries showed the highest rate of successful redistribution to the tumors (31%, 46% and 69%, using cut-off ratios of 0.9, 0.8, and 0.7 respectively) and parasitized arteries the lowest (0%, 33% and 33%). There was no notable difference in success rates between the microspheres used (^{90}Y glass, ^{90}Y resin, or ^{166}Ho microspheres). Comparison between the two largest tumor categories, colorectal carcinoma (CRC) and neuroendocrine tumor (NET), showed markedly lower success rates in NET patients (27%, 55%, 72% vs 0%, 0%, 0%).

In parasitized arteries, 0/4 were deemed successful on the visual assessment, 1/4 (25%) was dubious and 3/4 (75%) were unsuccessful. In the quantitative analysis the success-rate was 0%, 33%, 33%, using cut-off ratios of 0.9, 0.8, and 0.7 respectively.

TABLE 2. Quantitative analysis

	Activity ratios		Success rate of redistribution					
			Tumor			Segment		
	Tumor	**Segment**	**0.9 cutoff**	**0.8 cutoff**	**0.7 cutoff**	**0.9 cutoff**	**0.8 cutoff**	**0.7 cutoff**
All patients	0.80 (0.19-1.62)	0.88 (0.26-2.05)	6/21 (29%)	9/21 (43%)	12/21 (57%)	15/32 (47%)	20/32 (63%)	22/32 (69%)
Embolized artery								
MHA/Segment IV artery	0.80 (0.19-1.62)	0.89 (0.42-2.05)	4/13 (31%)	6/13 (46%)	9/13 (69%)	10/20 (50%)	13/20 (65%)	14/20 (70%)
aLHA/rLHA	0.50 (0.32-1.41)	0.82 (0.37-1.42)	2/5 (40%)	2/5 (40%)	2/5 (40%)	4/8 (50%)	4/8 (50%)	5/8 (64%)
Parasitized artery	0.49 (0.33-0.84)	0.85 (0.26- 0.93)	0/3	1/3 (33%)	1/3 (33%)	1/4 (25%)	3/4 (75%)	3/4 (75%)
Primary neoplasm								
CRC	0.83 (0.40-1.41)	0.97 (0.26-1.47)	3/11 (27%)	6/11 (55%)	8/11 (72%)	7/14 (50%)	10/14 (71%)	11/14 (79%)
NET	0.49 (0.18-0.80)	0.72 (0.53-1.45)	0/5	0/5	0/5	3/9 (33%)	4/9 (44%)	5/9 (56%)

Medians of the activity ratios are displayed with the range between parentheses. The number of successful redistributions was calculated using cutoff values based on activity concentration decreases of 10, 20 and 30%.
MHA = middle hepatic artery, aLHA = accessory left hepatic artery, rLHA = replaced left hepatic artery, CRC = Colorectal carcinoma, NET = Neuroendocrine tumor.

Time Interval

A total of 28 patients were included in the time interval subgroup analysis. Fourteen of which had coil-embolization performed on the same day as the treatment procedure, while the comparison group had a median time interval of 10 days (2-32 days). Mean activity ratios in patients treated on the same day were higher than those in the comparison group. Respectively, 0.94 vs 0.80 in segment ratios and 0.72 vs 0.69 in tumor ratios, however the differences were not statistically significant (figure 4b).

DISCUSSION

This study aimed to evaluate the use of coil-embolization for inducing redistribution of hepatic blood flow in radioembolization, by qualitatively and quantitatively analyzing the post-treatment distribution of microspheres. Visual assessment of post-treatment imaging found that 70% of redistribution cases had a similar distribution of microspheres in the dependent and non-dependent segments. However, quantitative assessment demonstrated notably lower absorbed doses in both dependent tumors and segments, 71% of dependent tumors had an activity concentration that was ≥ 10% lower than their non-dependent counterparts.

Several studies have previously reported on the redistribution method(4–8). Three studies visually assessed blood flow redistribution. Lauenstein *et al.* and Spreafico *et al.* examined the appearance of collaterals on DSA after coil-embolization, as well as the visual presence of ^{99m}Tc-MAA or ^{90}Y-microspheres in the dependent segments (5,7). Redistribution of flow was found in 89% (24/27) and in 100% (n=17) of cases, respectively. Bilbao *et al.* assessed and scored the accumulation of ^{99m}Tc-MAA in the dependent tumors (8). ^{99m}Tc-MAA activity was visually present in 95% (23/24) of the dependent tumors. In 66% (16/24) of patients the distribution of ^{99m}Tc-MAA in dependent tumors was considered similar to the non-dependent segments, which was in concordance with the findings of our visual assessment.

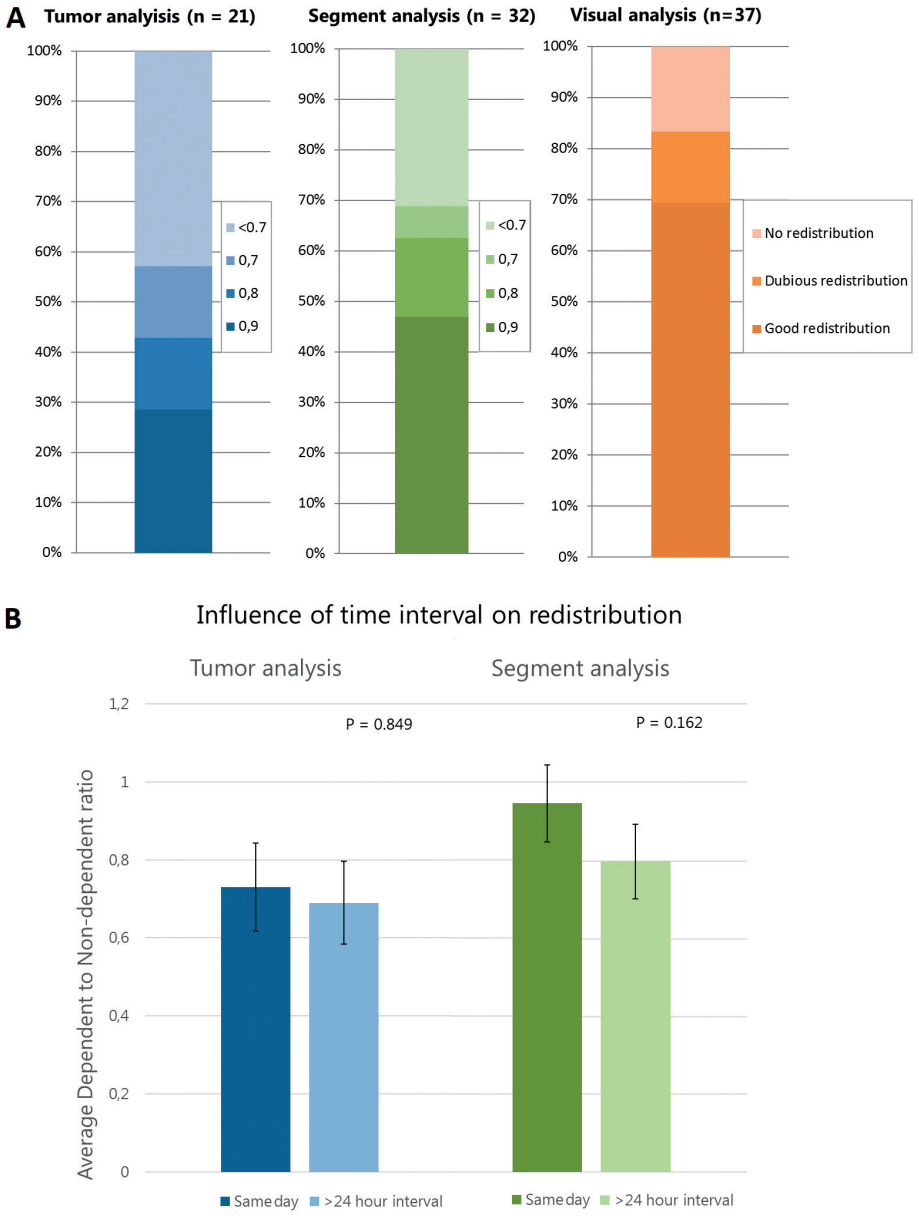

FIGURE 4. A. Visual representation of the proportion of successful redistribution cases in both the quantitative and the visual analysis. In the quantitative analysis, success rate was determined based on cut-off values representing activity concentration differences of 10%, 20%, and 30%. B. Bar chart of the averages in tumor and segment activity-ratios for patients treated on the same day after coil-embolization versus patients treated after a >24 hour interval.

Other studies evaluated the efficacy of redistribution by assessment of the treatment response, and found favorable response rates in the dependent tumors (4,6–8). Spreafico *et al.* found an overall response rate of 100% (3 CR, 8 PR, and 6 SD, according to mRECIST) in dependent tumors at three months after treatment (7). Abdelmaksoud *et al.* compared tumor response in dependent tumors to their non-dependent counterparts and found inferior response in only one case out of twenty two (4.5%) (6). While it does support the efficacy of radioembolization treatment in tumors with redistributed blood flow, the endpoint of tumor response does not provide insight into the differences in activity distribution.

Subgroup analysis showed that middle hepatic artery / segment IV artery redistribution was most successful, which may be attributable to the central location in the liver and the potential intrahepatic collaterals that can reroute blood flow from both the right and the left hepatic artery (Figure 5). Success rates for obtaining redistribution were lowest when parasitized arteries were embolized (Figure 6). This is possibly explained by the fact that these arteries were newly recruited by the tumorous process and did not (yet) have adequate collateral connections with the adjacent hepatic arteries. Furthermore, the distance between parasitized arteries and hepatic arteries may be an exacerbating factor, as parasitized arteries often vascularize peripheral parts of the liver.

In our comparison between primary tumor types we found substantially better redistribution rates in CRC compared to NET metastases. This difference was most pronounced in the tumor analysis, in which all NET patients had an absorbed dose difference of ≥ 30%. This was expected to some extent, as hypervascular tumors are more likely to recruit parasitized arteries. However, this could not account for the entire difference, as only one NET case involved a parasitized artery. Perhaps also the hypervascular nature of the tumors make these tumors more prone for under-dosing after redistribution. Other primary tumor types could not be compared due to the small sample size.

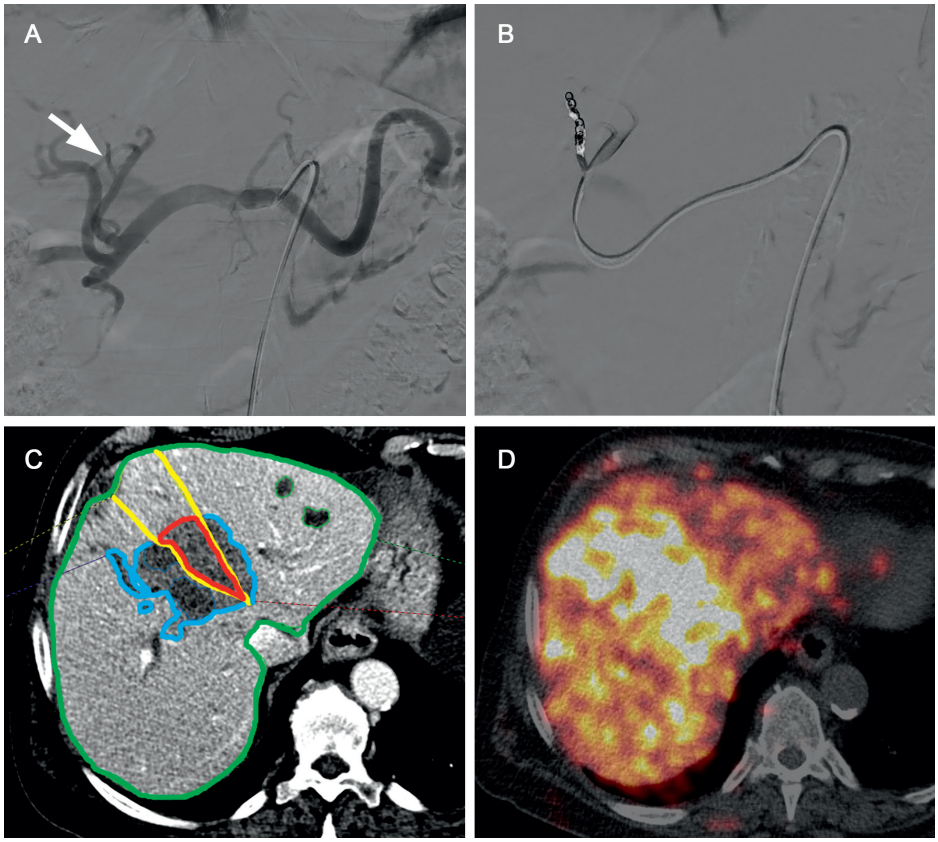

FIGURE 5. Example of successful redistribution in a patient with cholangiocarcinoma. A. DSA showing the liver vasculature including the left hepatic artery origin of the segment-IV branch (white arrow). B. Coil-embolization of the segment IV branch. C Volumes of interest drawn using Simplicit^{90}Y™ software, the dependent segment (IV) was drawn based on Couinaud's classification of segmental anatomy. D. ^{90}Y-PET/CT after treatment demonstrates a high concentration of microspheres throughout the liver, especially in segment IV.

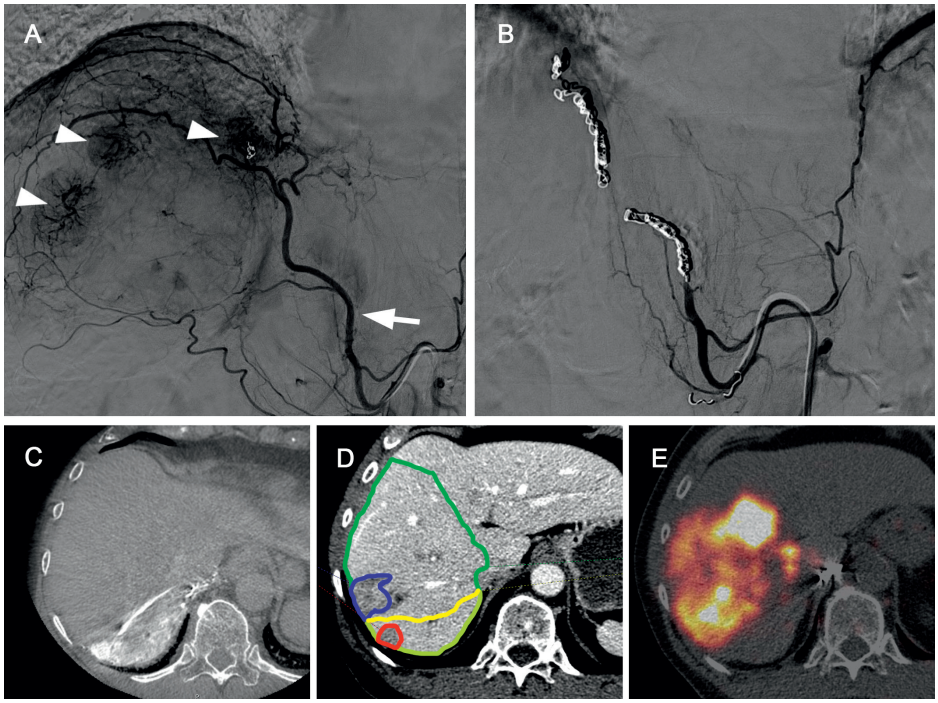

FIGURE 6. Example of poor redistribution. A. DSA showing parasitized blood supply to several liver tumors (arrow heads) from the right inferior phrenic artery (arrow). B. Coil-embolization of the phrenic artery. C. Cone-beam CT of the right phrenic artery shows enhancement of tumors in segment VII (prior to coil-embolization). D. Volumes of interest drawn in Simplicit^{90}Y software, the liver volume supplied by the phrenic artery segment was delineated using Cone-beam CT data. E. ^{90}Y-PET/CT after injection of ^{90}Y-microspheres in the right hepatic artery shows no redistribution to segment VII.

In some of the cases, coil-embolization and the injection of microspheres took place on the same day. All other patients had a time interval between coil-embolization and treatment of up to four weeks. In contrast to what we expected, a longer interval between coil-embolization and treatment did not result in a higher success rate. In fact, patients who were embolized and treated on the same day had higher activity ratios, although not statistically significant. It is important to note that all 'same day patients' received treatment with ^{166}Ho microspheres. However, this higher success rate was not found when comparing ^{166}Ho to ^{90}Y microspheres.

What this study adds to the existing literature is the quantitative analysis to evaluate the actual microsphere distribution post-treatment, and the use of ^{90}Y-PET/CT instead of ^{90}Y-Bremsstrahlung-SPECT as it offers better spatial resolution and contrast for optimized quantification of ^{90}Y-activity (11,12).

The study had several limitations that were mainly related to the quantitative analyses. Registration errors occurred when fusing the CECT and the post-treatment images, especially in patients with multiple small bilobar tumors. Furthermore, errors were introduced due to manual segmentation, heterogeneity due to the use of multiple microsphere types, and the use of two different post-treatment imaging modalities (i.e. ^{90}Y-PET/CT and ^{166}Ho-SPECT/CT). Lastly, the study was limited by its retrospective nature as well as small sample size.

Based on the results of this study we recommend using the redistribution technique only when deemed absolutely necessary. The best results are achieved in coil-embolization of the segment IV artery. Coil-embolization of parasitized arteries showed the least favorable redistribution of microspheres, caution is therefore advised in the treatment of hypervascular tumors.

In conclusion, visual evaluation of post-treatment imaging tends to overestimate the effect of redistribution. Quantitative analysis demonstrated significantly lower absorbed doses in redistributed dependent parts of the liver.

REFERENCES

1. Reinders MTM, Mees E, Powerski MJ, Bruijnen RCG, van den Bosch MAAJ, Lam MGEH, et al. Radioembolisation in Europe: A Survey Amongst CIRSE Members. Cardiovasc Intervent Radiol 2018; 41(10):1579–89.

2. Chuang VP, Wallace S. Hepatic arterial redistribution for intraarterial infusion of hepatic neoplasms. Radiology 1980; 135(2):295–9.

3. Civalleri D, Scopinaro G, Simoni G, Claudiani F, Repetto M, Decian F, et al. Starch microsphere-induced arterial flow redistribution after occlusion of replaced hepatic arteries in patients with liver metastases. Cancer. 1986; 58(9): 2151–5.

4. Karunanithy N, Gordon F, Hodolic M, Al-Nahhas A, Wasan HS, Habib N, et al. Embolization of hepatic arterial branches to simplify hepatic blood flow before yttrium 90 Radioembolization: A useful technique in the presence of challenging anatomy. Cardiovasc Intervent Radiol. 2011; 34(2):287–94.

5. Lauenstein TC, Heusner TA, Hamami M, Ertle J, Schlaak JF, Gerken G, et al. Radioembolization of hepatic tumors: Flow redistribution after the occlusion of intrahepatic arteries. Rofo. 2011; 183(11):1058–64.

6. Abdelmaksoud MHK, Louie JD, Kothary N, Hwang GL, Kuo WT, Hofmann L V., et al. Consolidation of hepatic arterial inflow by embolization of variant hepatic arteries in preparation for yttrium-90 radioembolization. J Vasc Interv Radiol. 2011; 22(10):1364–71.

7. Spreafico C, Morosi C, Maccauro M, Romito R, Lanocita R, Civelli EM, et al. Intrahepatic Flow Redistribution in Patients Treated with Radioembolization. Cardiovasc Intervent Radiol. 2015; 38(2):322–8.

8. Bilbao JI, Garrastachu P, Herraiz MJ, Rodríguez M, Iñarrairaegui M, Rodríguez J, et al. Safety and efficacy assessment of flow redistribution by occlusion of intrahepatic vessels prior to radioembolization in the treatment of liver tumors. Cardiovasc Intervent Radiol. 2010; 33(3):523–31.

9. Bol GH, Kotte ANTJ, Lagendijk JJW. Volumetool: an image evaluation, registration, and delineation system for radiotherapy. Phys Medica 2003.

10. Ikeda O, Tamura Y, Nakasone Y, Shiraishi S, Kawanaka K, Tomiguchi S, et al. Evaluation of intrahepatic perfusion on fusion imaging using a combined CT/SPECT system: Influence of anatomic variations on hemodynamic modification before installation of implantable port systems for hepatic arterial infusion chemotherapy. Cardiovasc Intervent Radiol. 2007; 30(3):383–91.

11. Fabbri C, Bartolomei M, Mattone V, Casi M, De Lauro F, Bartolini N, et al. ^{90} Y-PET/CT Imaging Quantification for Dosimetry in Peptide Receptor Radionuclide Therapy: Analysis and Corrections of the Impairing Factors. Cancer Biother Radiopharm. 2015; 30(5):200–10.

12. Piasecki P, Brzozowski K, Zięcina P, Podgajny Z, Budzyńska A, Korniluk J, et al. The use of ^{90}Y-PET imaging in evaluation of ^{90}Y-microspheres distribution in the liver: Initial results. Nucl Med Rev. 2015; 18(2):92–6.

Use of an anti-reflux catheter to improve tumor targeting for holmium-166 radioembolization – a prospective, within-patient randomized study

Caren van Roekel, Andor van den Hoven, Remco Bastiaannet, Rutger Bruijnen, Arthur Braat, Bart de Keizer, Marnix Lam, Maarten Smits

European Journal of Nuclear Medicine and Molecular Imaging 2020

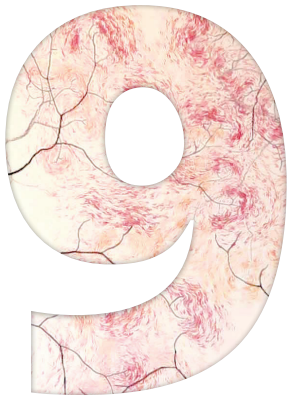

ABSTRACT

Purpose The objective of this study was to investigate whether the use of an anti-reflux catheter improves tumor targeting for colorectal cancer patients with unresectable, chemorefractory liver metastases (mCRC) treated with holmium-166 (^{166}Ho)-radioembolization.

Materials and Methods In this prospective, within-patient randomized study, left and right hepatic perfusion territories were randomized between infusion with a Surefire® anti-reflux catheter or a standard microcatheter. The primary outcome was the difference in tumor to non-tumor (T/N) activity distribution. Secondary outcomes included the difference in infusion efficiency, absorbed doses, predictive value of ^{166}Ho-scout, dose-response relation, and survival.

Results Twenty-one patients were treated in this study (the intended number of patients was 25). The median T/N activity concentration ratio with the use of the anti-reflux catheter was 3.2 (range 0.9-8.7) versus 3.6 (range 0.8-13.3) with a standard microcatheter. There was no difference in infusion efficiency (0.04% vs. 0.03% residual activity for the standard microcatheter and anti-reflux catheter, respectively) (95%CI -0.05 – 0.03). No influence of the anti-reflux catheter on the dose-response rate was found. Median overall survival was 7.8 months (95%CI 6-13).

Conclusion Using a Surefire® anti-reflux catheter did not result in a higher T/N activity concentration ratio in mCRC patients treated with ^{166}Ho-radioembolization, nor did it result in improved secondary outcomes measures.

Trial registration: clinicaltrials.gov identifier NCT02208804, registered August 5th 2014.

Keywords: radioembolization, holmium-166, colorectal cancer, anti-reflux catheter, Surefire

INTRODUCTION

Radioembolization is an established treatment option for colorectal cancer patients with liver-dominant, chemorefractory, unresectable metastases (mCRC) (1, 2).

Unfortunately, mCRC patients generally have relatively hypovascular, disseminated liver metastases, often leading to a suboptimal activity distribution (3, 4). It has been hypothesized that the use of an anti-reflux catheter may improve treatment outcomes in two ways. First, (partial) obstruction of the vascular lumen induces a decreased downstream pressure, possibly leading to a better tumor targeting (5-10). Also, the anti-reflux catheter causes a turbulent flow allowing particles to cross the laminar blood flow, leading to a more homogenous distribution (5). In a small pilot study of nine patients with various tumor types, the use of an anti-reflux catheter led to a significant decrease in hepatic non-target embolization and a significant increase in activity deposition in the tumors (11).

Holmium-166 (^{166}Ho)-microspheres (QuiremSpheres®, Quirem Medical, The Netherlands) were developed as an alternative to yttrium-90 (^{90}Y)-microspheres. Instead of using ^{99m}Tc-MAA as a predictor of activity distribution, ^{166}Ho-scout (QuiremScout®, Quirem Medical, The Netherlands), a small batch of identical ^{166}Ho-microspheres, can be used. This ^{166}Ho-scout has proven to be a more accurate predictor of the distribution of the treatment dose (12). ^{166}Ho can be visualized in-vivo by SPECT and MRI to assess activity distribution (13). Precise quantification of ^{166}Ho is possible using Monte Carlo simulation that simultaneously compensates for scatter, attenuation and collimator-detector response (14).

The aim of this study was to investigate whether the use of an anti-reflux catheter increases tumor targeting in comparison with a standard microcatheter in mCRC patients treated with ^{166}Ho-radioembolization (15).

MATERIALS AND METHODS

Patients

The SIM study ('Surefire Infusion system® versus standard Microcatheter use during holmium-166 radioembolization') was a single-center, within-

patient, randomized controlled study (Clinicaltrials.gov: NCT02208804) (see also the Consort reporting checklist in the supplemental files). Patients with unresectable, chemorefractory, liver-dominant mCRC were eligible for this study if they had: a pathologically confirmed diagnosis of CRC, hepatic metastases (≥1 cm and measurable on CT) in both the right and left hepatic arterial perfusion territory, a suitable arterial anatomy (not too tortuous vessels, with a large enough diameter to be accessible with the anti-reflux catheter), progressive disease after at least second-line systemic treatment, adequate liver-, renal- and bone marrow function, and a life expectancy of >3 months (see study protocol (15)). All patients provided written informed consent for participation in this study. The institutional review board provided ethical approval and the study was undertaken in accordance with the Declaration of Helsinki. An independent monitor verified all data.

Procedures

Before treatment, patients underwent ^{18}F-FDG PET/CT and a dual-phase contrast-enhanced CT. The hepatic arterial anatomy was assessed on the contrast-enhanced CT images and the perfusion territories of the left and right hepatic arteries (or their variants in case of aberrant vascular anatomy) were estimated. Metabolic hepatic tumor burden was assessed on the PET/CT images using ROVER software (ABX, Germany). Pre-treatment activity calculation was done using the standard formula for ^{166}Ho-microspheres to reach an absorbed dose of 60 Gy in the target volume (in this study the whole liver) (16) :

$$IA_{(MBq)} = liver\ weight\ (kg) * 3780\ \left(\frac{MBq}{kg}\right)$$

In which IA is the injected activity and 3780 is the constant specific for ^{166}Ho. The prescribed activity was split according to the perfusion volume of the left and right hepatic arteries as estimated on pre-treatment contrast-enhanced CT. Before treatment, patients' perfusion territories were randomized by the investigator between injection with a standard microcatheter and an anti-reflux catheter, using a computer-generated stratified block randomization with difference in tumor burden (above or below 10%) as a stratification factor. The result of randomization was applied for both the ^{166}Ho-scout and the therapeutic activity (Figure 1).

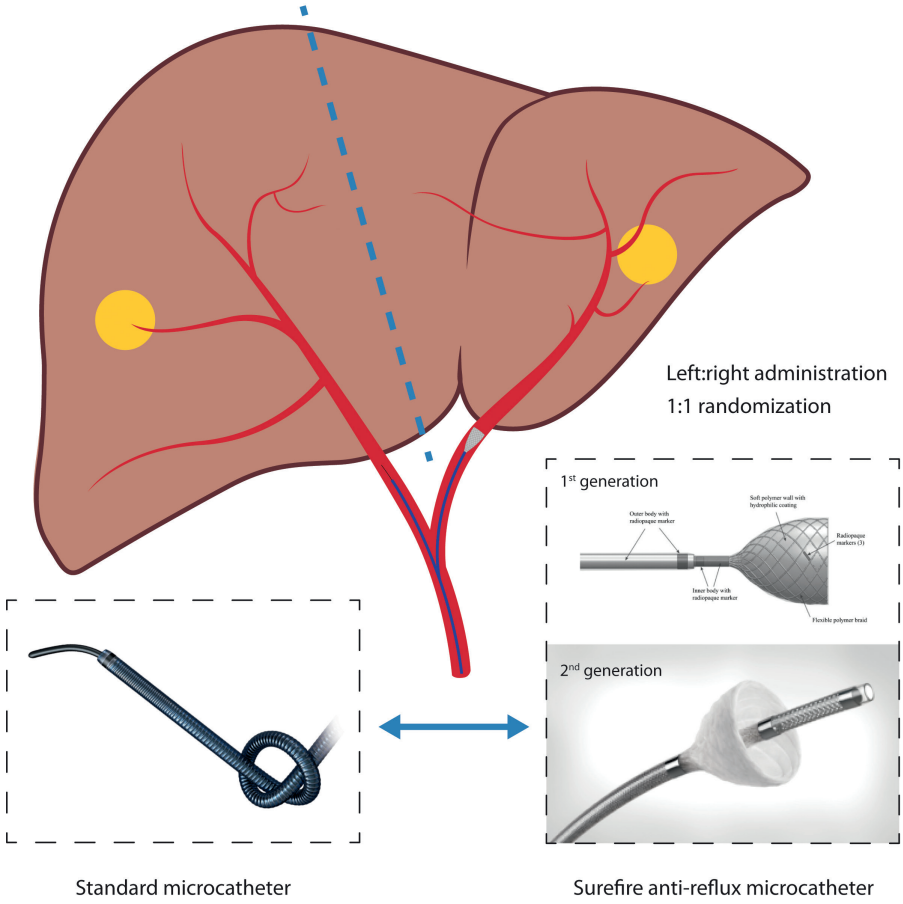

FIGURE 1. Schematic representation of within-patient randomized treatment with a standard microcatheter in the right hepatic artery and an anti-reflux catheter in the left hepatic artery. First-generation anti-reflux systems were used until August 2017 and were then replaced by the second-generation anti-reflux systems.

On the day of treatment, randomization was disclosed to the interventional radiologist. Two types of anti-reflux catheters were used during the study period. The first version of the Surefire® anti-reflux catheter (TriSalus Life Sciences, Westminster, CO, USA) was initially used, but this catheter became unavailable during the course of the study. Since January 2018, the updated Surefire® Precision infusion system was used. The standard microcatheter was a Progreat 2.4F or 2.7F microcatheter (Terumo Europe NV, Leuven, Belgium).

The price of the anti-reflux catheter was €1500 excluding VAT and the prices of the standard microcatheters were €275-€295 excluding VAT. Patients received ^{166}Ho-scout in the morning, followed by ^{166}Ho-SPECT/CT imaging. In the absence of relevant extrahepatic deposition, patients received the therapeutic activity in the afternoon as part of a one-day protocol. Three to five days later, another ^{166}Ho-SPECT/CT was acquired to assess the therapeutic absorbed dose distribution. SPECT-imaging cannot be performed directly after administration, since the abundance of gamma photons invokes detector dead-time: the recorded photon produces a pulse of a certain duration during which no second pulse can be detected (17). The distribution on the post-treatment ^{166}Ho-SPECT/CT was the basis for the primary endpoint.

SPECT/CT imaging after ^{166}Ho-scout and after ^{166}Ho-treatment was performed on a Symbia T16 system (Siemens Health Care) with a medium-energy collimator. Images were acquired on a 128x128 matrix 120 angles over a 360° non-circular orbit (30 sec/projection) with an energy window of 81 keV. Afterwards, a low-dose CT scan was fused with the SPECT images. The reconstruction of the data was done using the Utrecht Monte Carlo System software (18).

After treatment, toxicity was assessed during a telephone consultation at two weeks after treatment and by physical and laboratory examination at one and three months after treatment. Adverse events were graded according to the Common Terminology Criteria for Adverse Events (CTCAE) version 5.0. The maximum severity of each adverse event was reported. Response to treatment was assessed on PET/CT and contrast-enhanced CT three months after treatment, blinded for catheter allocation. Response analyses were based on metabolic response to treatment, based on a change in total lesion glycolysis between baseline and three months post-treatment, according to the PERCIST guidelines (19). The primary outcome of this study was the difference in tumor to non-tumor (T/N) activity concentration ratio between the right and left liver lobes, randomized between administration with an anti-reflux and a standard microcatheter. Secondary outcomes included the difference in infusion efficiency (the percentage of activity administered), absorbed doses, the predictive value of the ^{166}Ho-scout, the dose-response relation and survival. For the analyses, the contours of the tumors and the parenchyma were used, that were identified on the baseline [^{18}F]-FDG PET/CT. The left/right

lobe delineation was done on the accompanying low-dose CTs of the baseline [^{18}F]-FDG PET/CT using the cone-beam CT images on the side as a reference. The tumor contours were obtained using a threshold-based approach, based on the PERCIST guidelines. The resulting volumes of interest were transferred from the [^{18}F]-FDG PET/CT to the ^{166}Ho-SPECT/CT using a rigid coregistration of the accompanying low-dose CTs, as described before (20) (Figure 2).

Statistical analyses

The sample size calculation, based on a difference of 0.4 in mean tumor to non-tumor (T/N) activity ratio between the catheters, showed that at least 23 patients needed to be treated (15). The intent was to treat 25 patients (15). The differences in mean post-treatment T/N activity ratio and mean tumor- and healthy liver-absorbed dose on SPECT/CT between administration with an anti-reflux catheter and a standard microcatheter were assessed using a paired t-test. The infusion efficiency was calculated as percentage residual activity and compared using a McNemar's test for paired data. The predictive value of the ^{166}Ho-scout was assessed using Bland-Altman analysis. The relation between tumor-absorbed dose and response was best explained using a linear mixed-effects regression model, using a random intercept per patient, to account for correlation of tumors within patients. The influence of the anti-reflux catheter on tumor response was analyzed with logistic regression. Analyses were primarily performed according to the intention-to-treat (ITT) principle. Per-protocol analyses were also performed. A subgroup analysis was performed in patients in whom the anti-reflux catheter was deployed in the right hepatic artery, under the hypothesis that its effect on hemodynamics and dose distribution would be most notable in wide vessels. Furthermore, a subgroup analysis was performed in liver lobes treated with the anti-reflux catheter only, to evaluate the influence of spasm (as evident during angiography) on T/N activity concentration ratio. Overall survival was defined as the interval between treatment and death from any cause. Cox regression models were made using Firth's correction for small sample bias (21). Analyses were performed using R statistical software for Windows, version 3.6.2. We report effect estimates with associated 95% confidence intervals and corresponding two-sided p-values.

Stepwise process of absorbed-dose estimation

1. Left-right delineation

Low-dose CT from baseline PET/CT

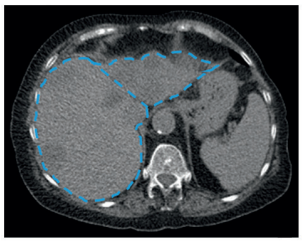

Cone-beam CT (if available)

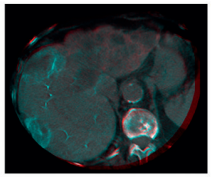

or

Baseline contrast-enhanced CT

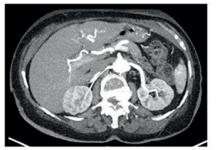

2. Tumor delineation

Baseline PET/CT

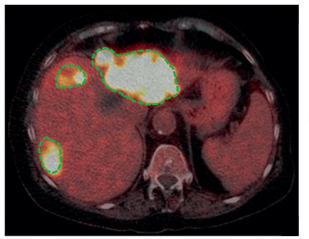

Using automatic thresholding

3. Tranformation from PET/CT to SPECT/CT

Low-dose CT from baseline PET/CT

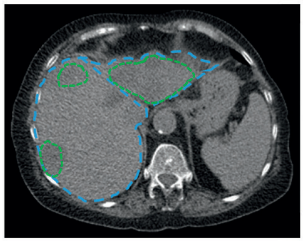

Low-dose CT from post-therapy SPECT/CT

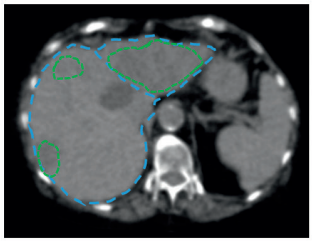

Using rigid coregistration

4. Dosimetry

Low-dose CT from post-therapy SPECT/CT

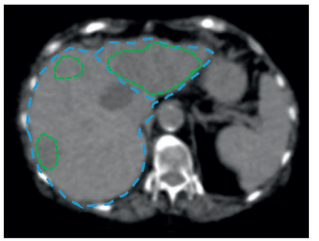

Post-therapy SPECT/CT

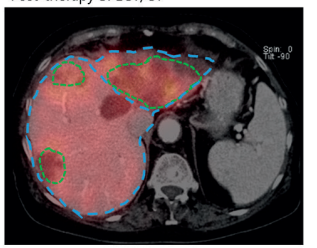

Determination of:
- Left- and right tumor dose
- Left- and right parenchymal dose

FIGURE 2. Stepwise process of absorbed-dose estimation after treatment. First, left- and right perfusion territories were manually delineated on the low-dose CT from the baseline [^{18}F]-FDG PET/CT, based on the cone-beam CTs (if available) or the baseline contrast-enhanced CTs. Afterwards, tumors were automatically defined on the baseline [^{18}F]-FDG PET/CT using a threshold-based approach. Then, the low-dose CTs of the baseline [^{18}F]-FDG PET/CT and the post-treatment ^{166}Ho-SPECT/CT were coregistered. Using a rigid transformation, the volumes of interest of the tumors and the healthy liver tissue (the left and right perfusion territories) were transferred to the ^{166}Ho-SPECT/CT and absorbed doses were obtained.

RESULTS

This study was discontinued prematurely because of slow recruitment and a high drop-out rate. In total, 28 patients were included in this study between June 2014 and April 2019. Two patients were diagnosed with rapid progressive disease and no longer meeting the inclusion criteria and excluded before administration of ^{166}Ho-scout and/or ^{166}Ho-radioembolization. In five patients (18%) an anti-reflux catheter could not be used because of unsuitable vascularity, meaning that because of vessel size, tortuosity or the occurrence of vasospasm, an adequate injection position with the anti-reflux catheter could not be obtained. Twenty-one patients received ^{166}Ho-radioembolization using the anti-reflux catheter(Table 1, Figure 3). Median time from pre-treatment imaging using [^{18}F]-FDG PET/CT to treatment was 14 days (range 6-42 days) and median time from pre-treatment imaging to post-treatment ^{166}Ho-SPECT/CT was 17 days (range 9-46 days). Administration characteristics are listed in Table 2. In two of these patients, catheter allocation was switched during treatment because of vessel size and tortuosity. In one patient, due to a vial deficiency, only a small part (15% in one lobe) of the activity was injected in the liver. Furthermore, follow-up imaging was not (fully) available in two patients and a post-therapy ^{166}Ho-SPECT/CT was not acquired in one patient (Figure 1). Sixteen patients were treated with the first version of the Surefire® anti-reflux catheter and five patients were treated with the updated second version: the Surefire Precision infusion system®. In six of 21 treated patients (29%), vasospasm occurred during the use of the anti-reflux catheter, both with the initial version (5/16 patients) and with the newer Surefire Precision system® (1/5 patients). Nitroglycerin was administered in 18/21 Surefire® injections during vasospasm or as prophylaxis to prevent vasospasm. Adverse device effects are listed in Table 3.

TABLE 1. Patient and treatment characteristics

Characteristic	**n or median + range**	
	All included patients(n=28)	*Treated population (n=21)*
Gender		
Male	17	13
Female	11	8
Age (y)	60 (37-83)	63 (45-83)
WHO performance score		
0	18	16
1	9	5
2	1	0
Primary tumor location		
Left	21	14
Right	7	7
Previous therapy		
Locoregional (liver)	3	3
Metastasectomy	3	3
Systemic	28	21
5-FU	9	6
Bevacizumab	24	18
Capecitabine	24	19
Cetuximab	2	2
Folinic acid	9	6
Irinotecan	19	14
Oxaliplatin	26	19
Panitumumab	9	7
Regorafenib	1	1
TAS-102	3	1
Trifluridine+tipiracil	1	0
Extrahepatic disease before treatment		
Lymph node	12	9
Lung	9	7
Ovaries	1	0
Peritoneum	1	0
No	11	9

TABLE 1. Patient and treatment characteristics (continued)

Characteristic	**n or median + range**	
	All included patients(n=28)	*Treated population (n=21)*
Liver volume (mL)	1968 (1560-3134)	1923 (1428-2952)
Metabolic tumor volume (mL)	271 (88-769)	311 (70-769)
Tumor load (%)	15 (5-35)	16 (5-26)
Total prescribed activity (MBq)	7607 (4850-12782)	7862 (4325-12782)
Total residual activity (MBq)	346 (98-4107)	495 (98-4107)
Administered therapeutic activity (MBq)	7119 (3142-12386)	7099 (3142-12386)
Administered ^{166}Ho scout activity (MBq)	246 (163-156)	238 (163-356)

TABLE 2. Administration characteristics of 21 treated patients

Characteristic	**n or median + range**			
	Standard microcatheter	*Anti-reflux catheter*	*Anti-reflux catheter – Surefire Infusion System (1st generation)*	*Anti-reflux catheter – Surefire Precision Infusion System (2nd generation)*
Perfusion territory volume (mL)	711 (157-1901)	1104 (462-1685)	938 (462-1685)	711 (704-1271)
Tumor volume	101 (14-417)	175 (43-379)	175 (43-379)	178 (86-256)
Tumor burden (%)	15 (2-46)	16 (6-72)	17 (6-72)	13 (8-20)
Anatomy				
Standard	13	16	12	4
Replaced main perfusion territory artery	6	4	3	1
Early branching pattern	2	1	1	0
Coil-embolization*	1	0	0	0
Total administered activity (MBq)	2206 (671-5867)	3525 (680-5995)	4443 (1777-5525)	4075 (680-5995)

*Coil-embolization of a main perfusion territory artery

TABLE 3. Adverse device effects in 21 included patients

	Standard microcatheter	Anti-reflux catheter	Anti-reflux catheter – Surefire Infusion System (1st generation)	Anti-reflux catheter – Surefire Precision Infusion System (2nd generation)
Spasm	1/21	5/21	5/16	1/5
Stasis	3/21	3/21		
Unstable injection position	0/21	3/21	3/16	0/5
Inability to reach desired injection position	0/21	5/21 (LHA n=4)	5/16	0/5
Inadvertent vessel occlusion	0/21	1/21	0/16	1/5

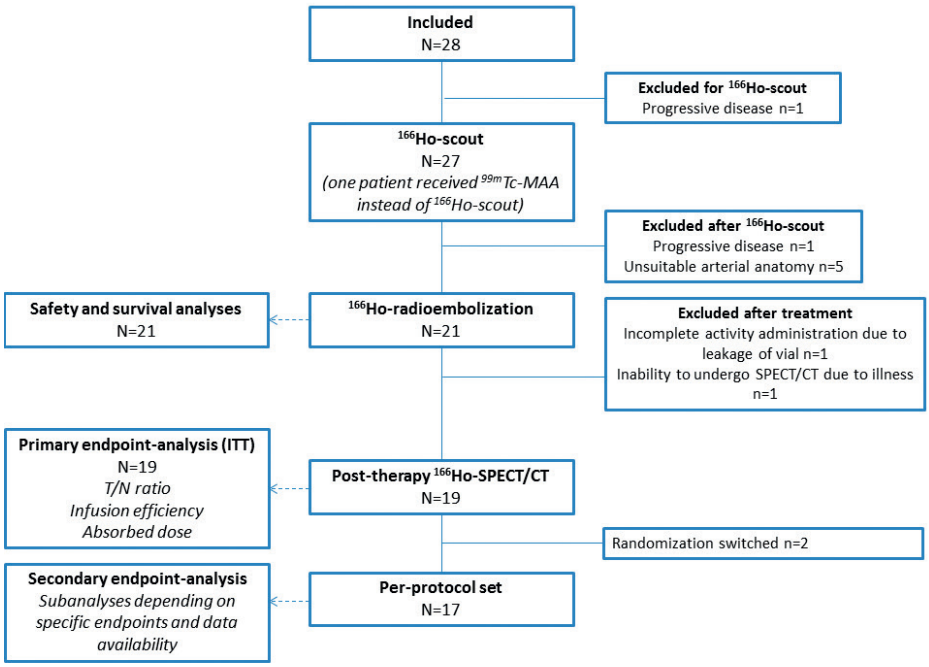

FIGURE 3. Flowchart of study procedures in included patients.

Treatment

The ITT analyses were performed on 19/21 evaluable patients, including the two patients in whom catheter allocation was switched (i.e. the volume that was intended to be treated with the anti-reflux catheter was counted as volume treated with the anti-reflux catheter and vice versa). In one patient, ^{166}Ho-scout was not available due to a production failure and treatment simulation was performed using ^{99m}Tc-MAA, but this patient was still evaluable for the primary endpoint. The patient with incomplete activity administration due to vial leakage (in one lobe, only 15% of calculated activity was administered) and the patient without a post-therapy ^{166}Ho-SPECT/CT were excluded from these analyses. The median T/N activity concentration ratio with the use of the anti-reflux catheter was 3.2 (range 0.9-8.7) versus 3.6 with a standard microcatheter (range 0.8-13.3) (difference in median -0.4, 95%CI -1.22 – 1.29, p=0.92) (Figure 4a). The median T/N activity concentration ratio with the anti-reflux catheter in the presence of spasm was 3.5 (range 2.4-4.7) versus 3.7 (range 0.9-8.7) without the occurrence of spasm (p=0.31, 95%CI -3.95 – 1.55). Both the median tumor-absorbed dose and the parenchymal-absorbed dose were (not-significantly) higher with the use of the anti-reflux catheter (difference in median tumor-absorbed dose +25 Gy, 95%CI -27 – 62, p=0.54 and difference in median parenchymal-absorbed dose +8 Gy, 95%CI -0.2 – 15.2, p=0.06) (Figure 4b,c). There was no difference in infusion efficiency between the use of the anti-reflux catheter (median residual activity 0.03%, range 0.001-0.37) and the standard microcatheter (median residual activity 0.04%, range 0.006-0.17) (difference in median -0.01%, 95%CI -0.05 – 0.03, p=0.93) (Figure 4d).

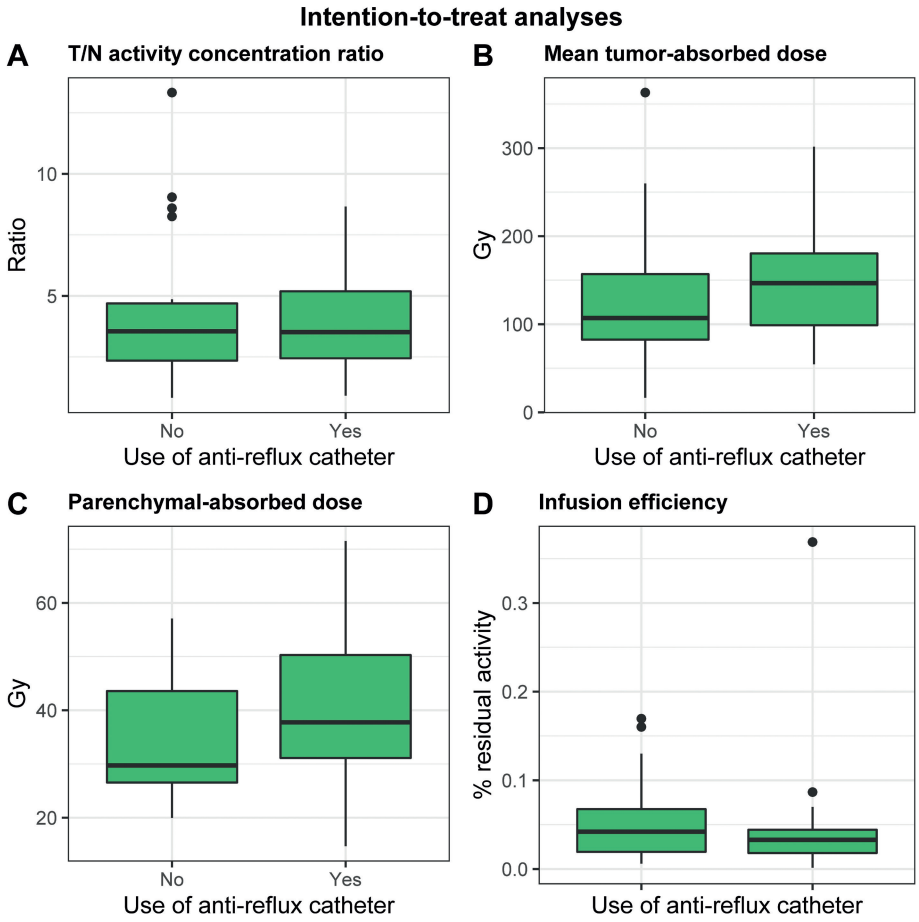

FIGURE 4A-D. Intention-to-treat analyses of effect of anti-reflux catheter on T/N activity concentration ratio (a), mean tumor-absorbed dose (b), mean parenchymal-absorbed dose (c) and infusion efficiency (d).

The per-protocol analyses were performed in 17 patients. Median T/N activity concentration ratio with the antireflux catheter was 3.2 (range 0.9-8.7); with the standard microcatheter 3.6 (range 0.8-13.3) (p=0.82, 95%CI -1.19 - 1.24). Median tumor-absorbed dose was 129 Gy (range 55-302) with the anti-reflux catheter versus 107 Gy (range 17-363) with the standard microcatheter (p=0.61, 95%CI -33 - 49). Median parenchymal-absorbed dose was 38 Gy (range 15-67) with the anti-reflux catheter and 30 Gy (range 20-57) with the standard microcatheter (p=0.13, 95%CI -3-14). Infusion efficiency with the anti-reflux catheter was

0.03 (range 0.0012-0.37) versus 0.04 (range 0.006-0.17) with the standard microcatheter (p=0.53, 95%CI -0.06-0.17) (Figure S1a-d).

At a tumor-level, a significant dose-response relationship was established. The mean tumor-absorbed dose in tumors with complete metabolic response was on average 138% higher than in progressive tumors (222 Gy vs. 103Gy, respectively; 95%CI 8-243%). The mean tumor-absorbed dose was 3.8% higher with the use of the anti-reflux catheter than with the standard microcatheter (170 Gy vs. 145 Gy, respectively; 95%CI -37-71%, p=0.89). The odds ratio for metabolic response (complete or partial response) with the use of the anti-reflux catheter was 0.75 (95%CI 0.25-2.25). Tumor- and patient-level metabolic response is summarized in Table S1 and Figure 5.

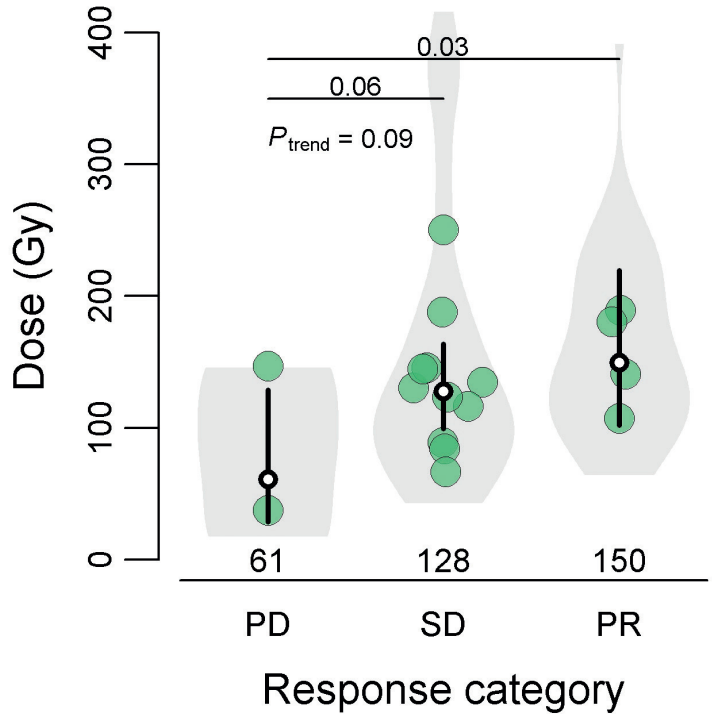

FIGURE 5. Relationship between mean tumor-absorbed dose per patient and metabolic response to treatment at three-months follow-up. The bullets show the mean tumor-absorbed dose per patient. Black vertical lines are the 95%CIs of the mean doses per response category, with the white dot in the middle indicating the mean tumor-absorbed dose per response category. This figure is based on the linear mixed-effects regression model as described in Table S1.

Exploratory sub-analysis of impact of anti-reflux catheter in right hepatic artery only

The anti-reflux catheter was deployed in the right hepatic artery in twelve patients (per protocol analysis). The median T/N activity concentration ratio with the anti-reflux catheter was 4.0 (range 0.9-8.7) versus 3.8 with the standard microcatheter (range 0.8-9.0) (difference in median +0.2, 95%CI -1.11 – 2.32, p=0.42).

Safety

Grade ≥3 laboratory toxicity was present in three patients (14%), and four patients (19%) experienced grade ≥3 clinical toxicity. Two deaths occurred within three months after treatment: one patient died of disease progression (5%), the other of radioembolization-induced liver disease (5%) (Table S2. Median overall survival was 7.8 months (95%CI 6.4-12.9).

Agreement between ^{166}Ho-scout and ^{166}Ho-therapy

The agreement between the dose distribution on ^{166}Ho-scout and ^{166}Ho-therapy was calculated for 17 patients. Four patients were excluded from the analysis, for the following reasons: treatment simulation by ^{99m}Tc-MAA (n=1; ^{166}Ho-scout was not available due to a production failure and treatment simulation was performed using ^{99m}Tc-MAA), no post-treatment ^{166}Ho-SPECT/CT performed (n=1), stasis during treatment (defined as retrograde flow into adjacent arteries) (n=1), and ^{166}Ho-scout activity for the left hepatic territory abusively administered in the right hepatic artery (n=1). Using the anti-reflux catheter led to a substantially worse agreement for estimating the tumor-absorbed dose with ^{166}Ho-scout (95% limits of agreement -58 Gy and +49 Gy) than when using the standard microcatheter (95% limits of agreement -27 Gy and +29 Gy) (Figure S2a,b). The agreement for estimating the parenchymal dose was similar between both catheter types (95% limits of agreement -3 Gy and +2 Gy for the anti-reflux catheter and -3 Gy and +3 Gy for the standard microcatheter) (Figure S2c,d).

DISCUSSION

Colorectal cancer liver metastases are challenging to treat with radioembolization. These tumors are often diffusely metastasized throughout

the liver, and are hypovascular compared to other tumor types (3, 4). As a consequence, tumor targeting is often poor and response rates after radioembolization in mCRC patients are modest (22, 23). The hypothesis was tested that the use of an anti-reflux catheter improves tumor targeting during radioembolization. However, in this within-patient RCT, the use of the anti-reflux catheter did not lead to significant differences in T/N activity concentration ratio, tumor- and parenchymal-absorbed dose or infusion efficiency.

To our knowledge, this is the first prospective study in humans investigating the supposed improved tumor targeting when using the Surefire® anti-reflux catheter for radioembolization. In the first study investigating this anti-reflux catheter, renal artery embolization with tantalum beads in a porcine model was performed with a standard microcatheter (n=3) versus an anti-reflux catheter (n=3). Embolization efficiency was 99.9%±1 with the anti-reflux catheter, versus 72%±13 with a standard microcatheter (9). Early studies found that infusion efficiency with the anti-reflux catheter was significantly improved due to a decrease in blood pressure in the downstream vascular territory (7, 8). Mean blood pressure with the tip closed was 79 mm Hg versus 58 mm Hg with the tip expanded (7). Besides a higher infusion efficiency, the use of anti-reflux catheters was found to lead to a higher tumor-absorbed dose in a mixed tumor-type cohort of nine patients who received pre-treatment infusion with ^{99m}Tc-MAA twice, using both the anti-reflux catheter and a standard microcatheter. Relative increase in tumor deposition ranged from 33%-90% (11). Most studies were performed with the first version of the Surefire® anti-reflux catheter. A new version, the Surefire Precision Infusion System®, was introduced in January 2018 and is expected to have similar effects, although it has a different deployment mechanism: the anti-reflux umbrella is no longer situated at the tip of the catheter but is positioned slightly more proximal. Also, the catheter-shaft of the later version is less rigid. In contrast to the studies described before, we did not find significant differences between the anti-reflux catheter and the standard microcatheter. Possible reasons for this are the differences in patient population (only mCRC versus mixed tumor-type cohorts / even porcine models), embolic device (^{166}Ho versus ^{90}Y, ^{99m}Tc-MAA, tantalum beads or chemoembolization particles) and treatment approach (lobar versus segmental). In addition, the manufacturer of the anti-reflux was in no way involved in this investigator-initiated study.

We met several challenges while conducting this innovatively-designed trial. Ultimately, this study was stopped prematurely due to slow accrual and a high drop-out rate. During weekly tumor boards, possible candidates were screened for eligibility. Based on contrast-enhanced CT, many patients were already deemed unsuitable because of their vascular anatomy (mostly because of arteries that were deemed too small or too tortuous for the relatively rigid anti-reflux catheter). Nevertheless, despite careful pre-selection and studying of anatomy before treatment, five included patients (18%) were still excluded during angiography because the desired injection position could not be obtained with the anti-reflux catheter. Positioning was challenging as the catheter sometimes moved forward with the deployment of the anti-reflux system, rendering it difficult to reach a stable injection position. Furthermore, with the use of the anti-reflux catheter, vasospasm occurred very frequently (in 24% of cases), which required the administration of intra-arterial nitroglycerin in most cases. The effect of nitroglycerin on the T/N ratio is unknown. Vasospasms occurred probably because of the relatively rigid catheter shaft and due to contact between the deployed anti-reflux system and the vessel wall. These technical difficulties were most pronounced with the first version of the anti-reflux catheter, as the shaft of the second generation catheter was more flexible and the anti-reflux system could be more easily deployed while maintaining a stable injection position.

Strengths of this study were the within-patient randomized study design and the homogenous patient population. The main limitation of this study was the small number of patients, which may have caused potential differences in primary or secondary outcomes to remain undetected. However, in our study, no effect (even a small negative effect) of the anti-reflux catheter on the primary and secondary outcomes was found. Based on our results, it is unlikely that with enough power, a large positive effect of the anti-reflux catheter will be seen. Also, the frequent occurrence of technical adverse events with the anti-reflux catheter likely contributed to the lack of a positive influence on treatment outcomes. The occurrence of vasospasm, for example, probably had an influence on activity distribution. Another limitation is the time between pre-treatment imaging with [^{18}F]-FDG PET/CT and post-treatment ^{166}Ho-SPECT/CT. Although much effort was done to limit time between baseline imaging and treatment, an increase of tumor and/or hepatic volume may have occurred,

leading to imperfections in segmentation. Furthermore, in this study, the perfusion volumes of the left and right hepatic arteries were estimated on pretreatment CT. The more accurate method of using perprocedural C-arm CT with contrast injection via a microcatheter in the left and right hepatic arteries was logistically not possible since patients underwent the work-up angiography on the same day as the treatment angiography and ^{166}Ho-microspheres need to be ordered 7 days in advance.

This study had a within-subjects design, which has several advantages. First, patients serve as their own control, limiting possible confounding by extraneous patient variables (24) and requiring less subjects to detect meaningful effects. However, a within-patient design is only applicable, when the treatment of one body part (in our case functional liver half) is unlikely to affect the other body part for the outcome under study. While designing this study, we judged that the technical nature of the relationship between catheter design and particle distribution was suitable for this study design, because we assumed that this interplay is limited to local fluid-dynamics and that systemic carry-across effects are unlikely (25). If, however, systemic effects (e.g. the activation of vasogenic factors during the occurrence of near-stasis) do play a role, they may have negated potential differences in preferential tumor targeting between the anti-reflux and standard microcatheter. In our patient population, some tumors were located close to the so-called watershed areas and may actually have received blood supply from both perfusion territories (although this was not observed on cone-beam CT). Another disadvantage of our design was that although patient-level characteristics are accounted for, there are still within-patient characteristics that may cause random error. The anti-reflux catheter was, for example, much easier deployed in the right hepatic artery, as this often was a much larger, less tortuous vessel. The new version of the anti-reflux catheter was (due to randomization, not deliberately) only used in right hepatic arteries, which may explain the difference in occurrence of vasospasm between the two anti-reflux catheter versions. In our experience, the standard microcatheter used in this study had a much more flexible shaft and was therefore superior in tracking the guidewire and navigating the liver vasculature, when compared to both versions of the anti-reflux catheter. Also, although accounted for in the randomization, the tumor burden was not always equal between perfusion territories.

The agreement between the ^{166}Ho-scout and ^{166}Ho-therapy dose distribution in our study was high and in line with a previous study (26). These results support the use of ^{166}Ho-scout for treatment planning. Surprisingly, the agreement with the anti-reflux catheter at a tumor level, was worse compared with a standard microcatheter. The mechanical pressure of the anti-reflux catheter on the vascular wall may have caused a larger variation in flow between the administration of ^{166}Ho-scout and ^{166}Ho-therapy.

CONCLUSION

In this study, no differences in post-treatment T/N activity concentration ratio, tumor- and parenchymal-absorbed dose and infusion efficiency were found between the use of an anti-reflux catheter and a standard microcatheter in mCRC patients treated with ^{166}Ho-radioembolization.

REFERENCES

1. Van Cutsem E, Cervantes A, Adam R, Sobrero A, Van Krieken JH, Aderka D, et al. ESMO consensus guidelines for the management of patients with metastatic colorectal cancer. Ann Oncol. 2016;27(8):1386-422.
2. Siegel RL, Miller KD, Jemal A. Cancer statistics, 2019. CA. 2019;69(1):7-34.
3. Tirumani SH, Kim KW, Nishino M, Howards SA, Krajewski KM, Jagannathan JP, et al. Update on the Role of Imaging in Management of Metastatic Colorectal Cancer. Radiographics. 2014;34:1908-28.
4. Boas FE, Bodei L, Sofocleous CT. Radioembolization of Colorectal Liver Metastases: Indications, Technique, and Outcomes. J Nucl Med. 2017;58(Suppl 2):104S-11S.
5. van den Hoven AF, Lam MG, Jernigan S, van den Bosch MA, Buckner GD. Innovation in catheter design for intra-arterial liver cancer treatments results in favorable particle-fluid dynamics. J Exp Clin Cancer Res. 2015;34:74.
6. van den Hoven AF, Prince JF, Samim M, Arepally A, Zonnenberg BA, Lam MG, et al. Posttreatment PET-CT-confirmed intrahepatic radioembolization performed without coil embolization, by using the antireflux Surefire Infusion System. Cardiovasc Interv Radiol. 2014;37(2):523-8.
7. Rose SC, Kikolski SG, Chomas JE. Downstream hepatic arterial blood pressure changes caused by deployment of the surefire antireflux expandable tip. Cardiovasc Interv Radiol. 2013;36(5):1262-9.
8. Rose SC, Narsinh KH, Newton IG. Quantification of Blood Pressure Changes in the Vascular Compartment When Using an Anti-Reflux Catheter during Chemoembolization versus Radioembolization: A Retrospective Case Series. J Vasc Interv Radiol. 2017;28(1):103-10.
9. Arepally A, Chomas J, Kraitchman D, Hong K. Quantification and reduction of reflux during embolotherapy using an antireflux catheter and tantalum microspheres: ex vivo analysis. J Vasc Interv Radiol. 2013;24(4):575-80.
10. Rose SC, Narsinh KH, Isaacson AJ, Fischman AM, Golzarian J. The Beauty and Bane of Pressure-Directed Embolotherapy: Hemodynamic Principles and Preliminary Clinical Evidence. Am J Roentgenol. 2019;212(3):686-95.
11. Pasciak AS, McElmurray JH, Bourgeois AC, Heidel RE, Bradley YC. The impact of an antireflux catheter on target volume particulate distribution in liver-directed embolotherapy: a pilot study. J Vasc Interv Radiol. 2015;26(5):660-9.
12. Smits MLJ, Dassen MG, Prince JF, Braat A, Beijst C, Bruijnen RCG, et al. The superior predictive value of (^{166})Ho-scout compared with (99m)Tc-macroaggregated albumin prior to (^{166})Ho-microspheres radioembolization in patients with liver metastases. Eur J Nucl Med Mol Im. 2020;47(4):798-806.
13. Smits ML, Elschot M, van den Bosch MA, van de Maat GH, van het Schip AD, Zonnenberg BA, et al. In vivo dosimetry based on SPECT and MR imaging of ^{166}Ho-microspheres for treatment of liver malignancies. J Nucl Med. 2013;54(12):2093-100.

14. Elschot M, Nijsen JF, Dam AJ, de Jong HW. Quantitative evaluation of scintillation camera imaging characteristics of isotopes used in liver radioembolization. PloS One. 2011;6(11):e26174.

15. van den Hoven AF, Prince JF, Bruijnen RC, Verkooijen HM, Krijger GC, Lam MG, et al. Surefire infusion system versus standard microcatheter use during holmium-166 radioembolization: study protocol for a randomized controlled trial. Trials. 2016;17(1):520.

16. Medical Q. Instructions for use Quiremspheres: Quirem Medical; 2020 [Available from: https://www.quirem.com/ifu/.

17. Elschot M, Nijsen JF, Dam AJ, De Jong HW. Quantitative evaluation of scintillation camera imaging characteristics of isotopes used in liver radioembolization. PloS One. 2011.

18. Elschot M, Smits ML, Nijsen JF, Lam MG, Zonnenberg BA, van den Bosch MA, et al. Quantitative Monte Carlo-based holmium-166 SPECT reconstruction. Medical Physics. 2013;40(11):112502.

19. Hyun O J, Lodge MA, Wahl RL. Practical PERCIST: A simplified guide to PET response criteria in solid tumors 1.0. Radiology. 2016;280(2):576-84.

20. Bastiaannet R, van Roekel C, Smits MLJ, Elias SG, van Amsterdam WAC, Doan D, et al. First Evidence for a Dose-Response Relationship in Patients Treated with (^{166})Ho Radioembolization: A Prospective Study. J Nucl Med. 2020;61(4):608-12.

21. Heinze G, Dunkler D. Avoiding infinite estimates of time-dependent effects in small-sample survival studies. Stat Med. 2008;30(27):6455-69.

22. van den Hoven AF, Rosenbaum CE, Elias SG, de Jong HW, Koopman M, Verkooijen HM, et al. Insights into the Dose-Response Relationship of Radioembolization with Resin 90Y-Microspheres: A Prospective Cohort Study in Patients with Colorectal Cancer Liver Metastases. J Nucl Med. 2016;57(7):1014-9.

23. Sofocleous CT, Violari EG, Sotirchos VS, Shady W, Gonen M, Pandit-Taskar N, et al. Radioembolization as a Salvage Therapy for Heavily Pretreated Patients With Colorectal Cancer Liver Metastases: Factors That Affect Outcomes. Clin Colorect Cancer. 2015;14(4):296-305.

24. Shaughnessy JJ, Zechmeister EB, Zechmeister JS. Research methods in psychology. 5 ed: McGraw-Hill; 2000.

25. Lesaffre E, Philstrom B, Needleman I, Worthington H. The design and analysis of split-mouth studies: what statisticians and clinicians should know. Stat Med. 2009;28(28):3470-82.

26. Smits MLJ, Dassen MG, Prince JF, Braat A, Beijst C, Bruijnen RCG, et al. The superior predictive value of (^{166})Ho-scout compared with (99m)Tc-macroaggregated albumin prior to (^{166})Ho-microspheres radioembolization in patients with liver metastases. Eur J Nucl Med Mol Im. 2020;47(4):798-806. Epub 2019/08/11.

SUPPLEMENTAL TABLES AND FIGURES

TABLE S1. Percentage change in mean absorbed dose (Gy) per response category (95%CI)

	Progressive disease	Stable disease	Partial response	Complete response	
Patient-level	n=2	n=11	n=4	n=0	
Mean dose (Gy)	*61 (29;129)*	*128 (100;164)*	*150 (102;219)*	-	
Unadjusted	*reference*	110 0.1;344)	146 (-14;433)	-	P_{trend}=*0.094*
Tumor-level	n=14	n=25	n=8	n=5	
Mean dose (Gy)	*103 (72;146)*	*121 (94;156)*	*163 (109;243)*	*222 (118;418)*	
Unadjusted	*reference*	18 (-19;173)	58 (-4;161)	116 (8;330)	P_{trend}=*0.023*
Adjusted[§]	*reference*	21 (-16;80)	68 (-1;178)	136 (18;372)	P_{trend}=*0.015*

The dose-response relation was analyzed in seventeen patients that were treated and had availability of both the post-treatment ^{166}Ho-SPECT/CT and the three-month follow-up [^{18}F]-FDG PET/CT. Interpretation at tumor level: the average dose is 138% higher in CR than PD (95%CI 8;423) (unadjusted analysis).
[§]Analysis at a tumor-level was adjusted for catheter type (yes/no anti-reflux catheter)

TABLE S2. CTCAE grading of new toxicity per patient during three months from baseline*

Toxicity	Grade 1	Grade 2	Grade 3	Grade 4	Grade 5
	Laboratory toxicity				
Hypoalbuminemia	**2**	**1**			
Elevated ALT	**9**	**1**	**1**		
Elevated alkaline phosphatase	**2**	**7**	**1**		
Elevated AST	**12**	**2**			
Elevated bilirubin	**1**			**1**	
Elevated γ-glutamyltransferase	**2**	**8**	**3**		
Any laboratory toxicity	**10**	**9**	**3**	**1**	
	Clinical toxicity				
Abdominal pain	**6**	**9**	**3**		
Nausea	**14**	**4**			
Fatigue	**10**	**8**	**1**		
Anorexia	**4**	**1**			
Dyspnea	**1**				
Fever	**4**	**1**	**1**		
Chest pain	**1**		**1**		
Vomiting	**5**	**2**			

TABLE S2. CTCAE grading of new toxicity per patient during three months from baseline* (continued)

Toxicity	Grade 1	Grade 2	Grade 3	Grade 4	Grade 5
Back pain	3	1			
Bloating	1	1			
Joint pain	4				
Nocturnal transpiration	1				
Diarrhea	1				
Constipation	2				
Cough		1			
Hypotensia		1			
Chills	2				
Ascites	1		2		
Malaise	3	1			
Hepatic failure					1**
Weight loss	5				
Any clinical toxicity	6	12	4		1

CTCAE scores of new laboratory and toxicity during three months after treatment (highest CTCAE grades per laboratory value are represented). *Represented for the 21 patients who underwent treatment. **Radioembolization-induced liver disease.

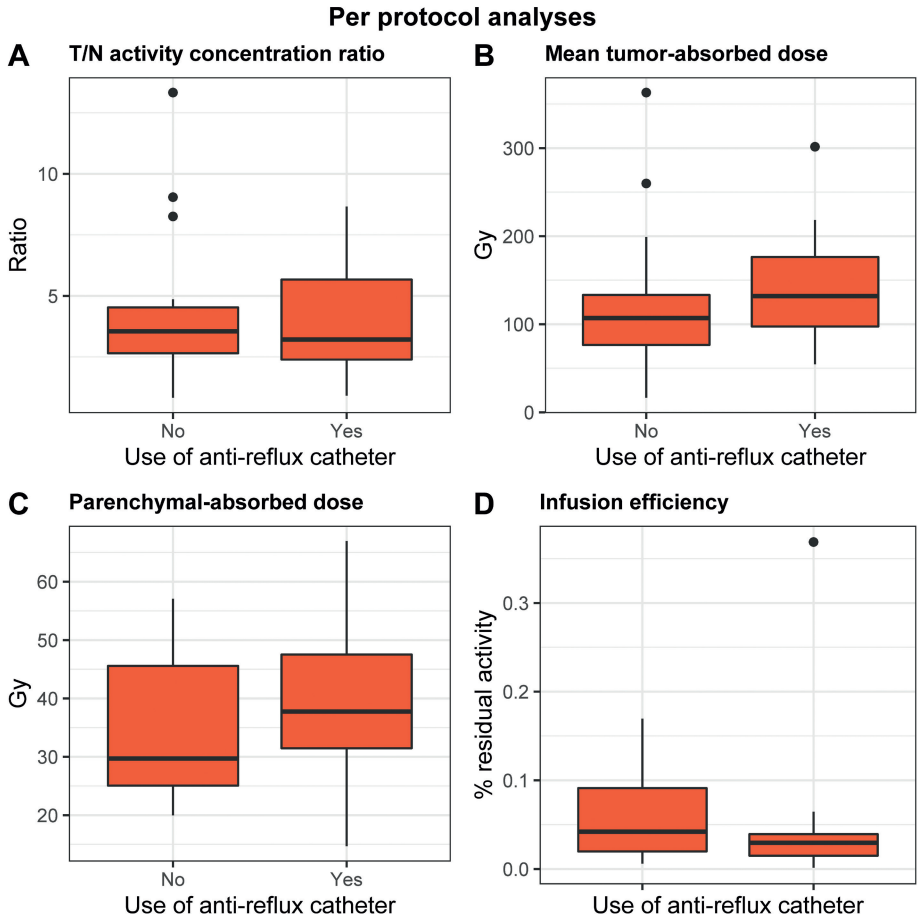

FIGURE S1A-D. Per protocol analysis of effect of anti-reflux catheter on T/N activity concentration ratio (a), mean tumor-absorbed dose (b), mean parenchymal-absorbed dose (c) and infusion efficiency (d).

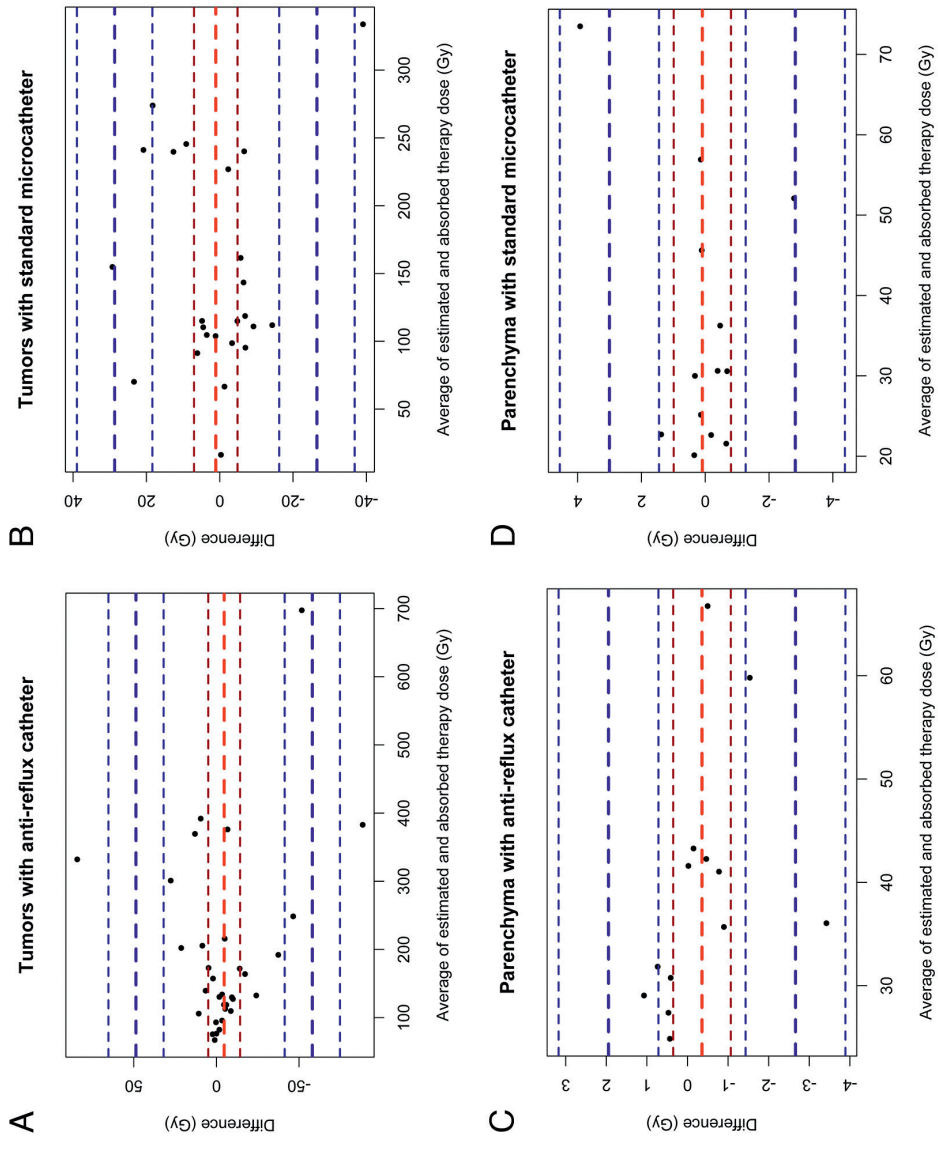
A
Tumors with anti-reflux catheter
Difference (Gy)
50
0
-50
100
200
300
400
500
600
700
Average of estimated and absorbed therapy dose (Gy)
B
Tumors with standard microcatheter
Difference (Gy)
40
20
0
-20
-40
50
100
150
200
250
300
Average of estimated and absorbed therapy dose (Gy)
C
Parenchyma with anti-reflux catheter
Difference (Gy)
3
2
1
0
-1
-2
-3
-4
30
40
50
60
Average of estimated and absorbed therapy dose (Gy)
D
Parenchyma with standard microcatheter
Difference (Gy)
4
2
0
-2
-4
20
30
40
50
60
70
Average of estimated and absorbed therapy dose (Gy)

FIGURE S2A-D. Bland-Altman plot for the agreement between estimated absorbed doses based on ^{166}Ho-scout and the actual absorbed doses with ^{166}Ho-therapy. Tumor-absorbed doses with the anti-reflux catheter and the standard microcatheter are visualized in A,B. Figures C and D show the estimated parenchymal-absorbed doses for the two catheter types.

Discussion

What are the treatment options for patients with colorectal cancer liver metastases and when comes radioembolization into play?

Without treatment, the median overall survival for patients with colorectal liver metastases upon diagnosis is only 4.5 months (1). As a disease-free status offers the best chance on long-term survival, theoretically, the most logical order of treatment options would be surgery, followed by local-regional therapies such as radiofrequency ablation (RFA). In the case of disease confined to the liver, but not amenable to surgery or ablation strategies, radioembolization, as another local-regional strategy, could theoretically be treatment of choice, giving local control and/or a bridge to surgery with limited impact on quality of life. If local-regional treatment options fail, systemic treatment would be indicated. However, this 'local-followed-by-systemic' approach is not (yet) according to the guidelines and current clinical practice, as radioembolization is only indicated in unresectable, systemic therapy-refractory patients (2, 3). An explanation of the reason why radioembolization is not given prior to systemic treatment will be given below, after a summary on the treatment options for colorectal liver metastases.

The treatment of choice for patients with liver-limited disease remains surgical resection. Surgical resection offers the best chance on long-term survival or even cure, with five-year survival rates of up to 60% (4, 5). Surgery is indicated when a radical excision (R0 resection) is possible, with a future liver remnant of ≥20% (3). Unfortunately, up to 80% of patients with hepatic metastases is deemed unresectable because of multifocality, tumor size or inadequate hepatic reserve (6). Furthermore, patient factors such as age and comorbidities may preclude surgery. However, patients may become amenable for surgery after neoadjuvant chemotherapy. Ten to twenty percent of patients with initially unresectable, liver-isolated disease fall into this category after treatment with neoadjuvant chemotherapy (7). After surgery of hepatic metastases, disease recurrence occurs in up to 45% of patients, and over 50% occurs in the liver (8). Repeated hepatic surgery is possible in some patients and if so, it was found to be associated with improved survival (9). Otherwise, patients will be treated with systemic therapy and have a five-year survival of less than 10% (10).

Besides surgery, other therapeutic options for colorectal cancer liver metastases are ablation (e.g. radiofrequency ablation, microwave ablation, cryoablation, irreversible electroporation), either solely or in combination with resection. There is growing evidence on these techniques, with studies showing similar overall survival rates with these ablative strategies compared with resection (11, 12). Ablative strategies can also be combined with systemic therapy: in the CLOCC trial, patients with unresectable colorectal cancer liver metastases were assigned to systemic treatment alone or systemic treatment plus local treatment by radiofrequency ablation with or without resection. Overall survival was significantly longer in the patients that received combination treatment: median 45.6 months versus 40.5 months in the systemic therapy-alone group (hazard ratio 0.58, 95%CI 0.38-0.88). Progression-free survival was significantly prolonged by almost 7 months in the combined treatment arm (hazard ratio 0.57, 95%CI 0.38-0.85) (13). These findings show that in carefully selected patients, ablative strategies can be a substitute for resection.

In the ongoing COLLISION trial, CRC patients with at least one resectable and ablatable hepatic metastasis (up to 3 cm) are randomized between ablation (either radiofrequency ablation or microwave ablation) and resection (14). If ablation proves to be non-inferior compared to resection, this study will change management for many patients. As ablation is associated with less post-procedure morbidity and mortality and a shorter hospital stay, this will have an impact on both patients and clinical costs.

For patients with truly unresectable disease, chemotherapy is indicated. Median overall survival for patients treated with chemotherapy is improving, with median survival rates of more than 20 months (15, 16). Most survival gain is caused by improvements in first-line therapies (17). Currently, there are at least nine different types of systemic treatment options for metastatic colorectal cancer (18):

- Fluoropyrimidines (including fluorouracil, leucovorin and capecitabine) (by conversion to fluorodeoxyuridine monophosphate, the enzyme thymidylate synthase is inhibited. This leads to inhibition of RNA synthesis and DNA strand breaks, inhibiting cell growth (19))

- Irinotecan (a camptothecin analog that stabilizes the topisomerase I complex, resulting in single-strand DNA breaks and ultimately cell death (20))
- Oxaliplatin (an alkylating agent, which binds to DNA, inhibiting DNA replication and transcription, resulting in cell death)
- Cetuximab and panitumumab (monoclonal antibodies, directed against the epidermal growth factor receptor)
- Bevacizumab (monoclonal antibody, directed against the vascular endothelial growth factor receptor (VEGF))
- Aflibercept (a recombinant fusion protein that prevents intra- and extravascular receptor binding of VEGF-A, VEGF-B and placenta growth factor)
- Regorafenib (an inhibitor of angiogenic tyrosine kinases)
- Trifluridine-tipiracil (TAS-102) (this consists of the nucleoside analog trifuridine that causes DNA strand breaks, inhibiting proliferation of tumor cells, and of tipiracil that prevents breakdown of trifuridine, enabling its function)
- Nivolumab, pembrolizumab (immune checkpoint inhibitors targeting the programmed death receptor PD-1)

There are inconsistencies in the literature as to whether patients should be treated with sequential single agents or with initial combination chemotherapy. The use of sequential single agents could reduce overall toxicity. Two randomized trials, the FOCUS and CAIRO trials, found a similar median overall survival for sequential versus initial combination therapy. However, progression-free survival was better with combination therapy (median progression-free survival 6 versus 8 months) (21, 22). According to the Dutch guidelines, for patients in a good clinical condition, first-line treatment consists of a fluoropyrimidine combined with bevacizumab, or fluoropyrimidine only. Patients in a poor clinical condition are to receive a combination of a fluoropyrimidine with oxaliplatin or irinotecan. Further treatment lines may consist of a combination of irinotecan, oxaliplatin, a monoclonal antibody, with or without bevacizumab (23). For patients who are chemotherapy-refractory after all common treatment options, a longer overall survival (median 1.8 months) may be obtained after treatment with TAS-102 (24).

The choice of chemotherapy regimens is dependent on many factors, such as RAS/BRAF mutation status, clinical performance status, presence of comorbidities and location of the primary tumor. RAS mutant status is associated with a higher risk of extrahepatic disease, poor response to cetuximab, panitumumab, irinotecan and oxaliplatin and patients with this mutation are less likely to have resectable hepatic metastases (25-27). BRAF mutant status is associated with higher stage disease, higher incidence of extrahepatic metastases and a worse survival after surgery (28). The location of the primary tumor can be divided into right (caecum, ascending colon, hepatic flexure and transverse colon) and left (splenic flexure, descending colon, sigmoid and rectum). In general, patients with right-sided primary tumors have a worse prognosis (29).

The most common adverse events include hypersensitivity reactions, cardiac ischemia, thrombosis, hand-foot skin reaction, diarrhea, nausea, vomiting, sensory neuropathy and hematological adverse events such as anemia and neutropenia (21). The use of chemotherapy can also induce liver injury: the so-called chemotherapy-associated liver injury syndrome, with three stages: steatosis, steatohepatitis and sinusoidal obstruction syndrome. Liver injury is mostly associated with the use of oxaliplatin and irinotecan (30, 31). Colorectal cancer mainly occurs in elderly people; the median age at diagnosis is 68 years for men, and 72 years for women (32). Due to age-related function decline and medical comorbidities, patients of older age may experience more adverse events of systemic therapy (33).

According to the European Society for Medical Oncology, radioembolization is indicated for 'patients with liver-limited disease failing the available chemotherapeutic options'. In these patients, 'radioembolization with yttrium-90 (^{90}Y) microspheres should be considered' (2). The guidelines from the National Comprehensive Cancer Network adhere to the same indication: radioembolization is indicated in the salvage setting for patients with liver-dominant metastases (34). In The Netherlands, treatment with radioembolization (with either ^{90}Y or holmium-166 (^{166}Ho) microspheres is reimbursed for patients with unresectable liver metastases with chemo-refractory disease or with unacceptable toxicity after systemic treatment (3).

Theoretically, the combination of systemic treatment and a local therapy may be beneficial. The possible benefit of radioembolization as an addition to systemic therapy in the first line was investigated in the SIRFLOX, FOXFIRE and FOXFIRE-Global studies. Patients with unresectable disease who did not receive prior systemic therapy were randomized to FOLFOX (5-Fluorouracil combined with oxaliplatin) alone or FOLFOX plus radioembolization. In total, 1103 patients were included. Overall progression-free survival (11.0 versus 10.3 months) and overall survival (22.6 versus 23.3 months) were not significantly different between the combination group versus the FOLFOX alone group. There was a statistically significant difference in cumulative incidence of first progression in the liver (22% in the FOLFOX plus radioembolization group versus 39% in the FOLFOX alone group) (35). Based on the results of these studies, treatment with radioembolization in a first-line setting cannot be recommended. However, the results of these trials should be interpreted with caution, as there were flaws in the study design with regard to the dosimetry used and patient selection. The body surface area (BSA) method (see below) was used for activity calculation. This method often leads to under- or overdosing (36). In the FOLFOX study, underdosing was most often the case, since activity was reduced based on tumor involvement and lung shunt fraction (35). Furthermore, a large percentage of included patients had extrahepatic disease at baseline, which is a known dismal prognostic factor, also for treatment with radioembolization (37, 38). Radioembolization in the first-line setting may still be of value, for example in frail, elderly patients. In this patient population, first-line systemic treatment generally consists of capecitabine with bevacizumab. However, the risk of adverse events is higher in elderly patients. In a comparative study on patients treated with capecitabine, the incidence of grade 3 or 4 adverse events was higher in patients ≥80 years compared with the overall population (60% versus 40%) (39). The addition of bevacizumab to capecitabine is associated with a longer progression-free survival (9 months versus 5 months for monotherapy), but also with more side effects, especially hemorrhage (25% versus 7%) and venous thromboembolic events (12% versus 5%), as shown in the AVEX trial in chemotherapy-naïve, elderly patients (40). Radioembolization is as efficient in younger patients as it is in the elderly and the side effects are usually mild (41, 42). Therefore, it would be interesting to study radioembolization as a substitute for systemic treatment in the first line in a select group of patients.

In the second line, there may also be a place for radioembolization, possibly combined with a radiosensitizer such as irinotecan. There are a few studies reporting on overall survival in patients treated with radioembolization in the second line, with median overall survival ranging from 12.0-14.7 months (43-45). The combination of treatment with irinotecan and radioembolization was analyzed in 25 patients. A favorable response rate of 48% was found, while the incidence of toxicity was comparable to treatment with irinotecan alone (46). Another study compared the combination of various systemic treatment options with radioembolization versus radioembolization alone and found an improved response rate (45% versus 27%) as well, with acceptable toxicity (47). These results support the possibility of radioembolization as a second-line treatment. In the EPOCH trial, the safety and efficacy of second-line chemotherapy alone versus radioembolization combined with second-line chemotherapy in mCRC patients are investigated. Patient enrollment has finished, but the results are still awaited (48). These results are expected to be of great importance in the role of radioembolization in the second line, especially since this study accounts for prognostic patient-factors such as tumor load, KRAS status and prior first-line chemotherapy. The study will also shed a light on the tolerability of radioembolization combined with second-line chemotherapy, which will likely have important consequences for clinical decision making.

In the third line, patients are often treated with TAS-102. However, an early study showed only a marginal benefit of treatment with TAS102 versus placebo, with a median survival gain of only 1.8 months (median overall survival 7.1 months versus 5.3 months) (49). A more recent study compared the use of TAS102 combined with bevacizumab versus TAS102 alone in the third line. The addition of bevacizumab increased median overall survival by 2.7 months (median overall survival 9.4 months versus 6.7 months) (50). So even with the addition of bevacizumab, overall survival after treatment with TAS102 is limited. Moreover, the incidence of grade 3 or higher adverse events was high: 69% with combined therapy and 30% with monotherapy (49, 50). These data raise questions on the benefit/harm ratio of this treatment. As stated before, toxicity after radioembolization is usually mild and median overall survival rates after two lines of chemotherapy are comparable (44, 45, 51). Therefore, there may be a role for radioembolization in the third line.

Currently, radioembolization is indicated in the salvage setting. Studies on radioembolization in this stage of disease found median overall survival rates ranging from 5.7-12.8 months, with a median overall survival of 10 months (44, 52, 53). As median overall survival in chemotherapy-refractory, unresectable patients was reported to be around 6 months, radioembolization seems to offer a meaningful survival benefit (53). The most common toxicity after radioembolization is the so-called post-embolization syndrome, which consists of nausea, fatigue, abdominal pain and fever and occurs within 4-6 weeks after treatment, but is usually mild (51, 54). The most severe, possibly lethal complication is radioembolization-induced liver disease (REILD). REILD occurs in <5% of patients and is characterized by hyperbilirubinemia, ascites, hypoalbuminemia and liver failure (55). Other complications may result from extrahepatic activity deposition, such as radiation cholecystitis or radiation pneumonitis. In the MORE study, the safety and overall survival associated with ^{90}Y-radioembolization (resin microspheres) was assessed in colorectal cancer patients with liver-dominant, unresectable metastases who were chemorefractory or not suitable for systemic therapy (56). A total of 606 patients were included. The most common CTCAE grade 3 or higher adverse events were abdominal pain (6.1%), fatigue (5.5%), hyperbilirubinemia (5.4%) and there were five patients (0.8%) with hepatic failure. Overall survival was 10 months (95%CI 9.2-11.8 months). Prognostic factors for survival included performance status, a large tumor burden, liver function, presence of anemia at baseline, lung shunt fraction and number of previous chemotherapy lines (45, 56). This study showed that even after disease progression after several lines of systemic therapy, ^{90}Y-radioembolization can offer a survival benefit (compared to patients treated with systemic therapy or best supportive care in similar settings), with limited side effects.

Outside the palliative setting, radioembolization is more and more used as a bridge to surgery. In patients with unilobar hepatic metastases, hemihepatectomy can be performed. However, in many cases, the function of the future liver remnant is not good enough to allow for surgery. Currently, portal vein embolization is often performed to induce hypertrophy of the future liver remnant. However, radioembolization of one liver lobe can also induce sufficient hypertrophy of the untreated lobe, albeit not as fast as portal vein embolization (PVE). An advantage of using radioembolization is that it not

only induces hypertrophy, but that it also offers tumor control, in contrast with PVE. Also, it provides a test-of-time: because of the prolonged interval between radioembolization and surgery, subclinical, previously undetected metastases may become detectable (57). Moreover, radioembolization can be used to improve the secondary resectability rate: in a substudy on patients of the SIRFLOX trial, the resectability rates after treatment with chemotherapy versus treatment with chemotherapy combined with radioembolization were assessed. Thirty-eight percent of patients who were treated in the combination arm became resectable, which was significantly more than the 29% in the chemotherapy-only group (58).

What patients are good candidates for treatment with radioembolization?

Currently, radioembolization is reimbursed in The Netherlands for patients with unresectable, liver-dominant, chemotherapy-refractory disease. They have to be in relatively good clinical condition (performance status 0-2) with a life expectancy of at least three months and adequate hepatic function (albumin >30g/L and bilirubin ≤1.5*upper limit of normal). Liver-dominant disease is defined as a maximum of 5 lung nodules <1 cm and lymph nodes <2 cm (3).

The question is whether one should accept extrahepatic metastases at all? Several studies indicate that the presence of extrahepatic disease at baseline is a poor prognostic factor (35, 37, 38, 59). Our own study confirms this finding: patients with extrahepatic metastases had a significantly worse median overall survival (6.5 months versus 10 months in patients without extrahepatic disease at baseline). Also, treatment response was worse: 93% was diagnosed with progressive disease at three months after treatment, versus 63% of patients without extrahepatic disease at baseline. Although this was a retrospective, observational study, its results and the results of other studies indicate that it may be better to exclude patients with extrahepatic disease from treatment with radioembolization. However, although the benefit of radioembolization seems minimal in patients with extrahepatic disease, to verify its true potential, it should be compared with best supportive care only (e.g. in a randomized clinical trial).

Other important factors in the selection process of patients are age, location of the primary tumor, mutation status and liver function. Age is no contra-indication for treatment with radioembolization. A sub-analysis in patients <70 and ≥70 years treated in the MORE study showed no difference in overall survival (9.7 months versus 9.3 months) or incidence of grade ≥3 adverse events (18.8% versus 16.9%) (41). Most co-morbidities, except for renal insufficiency, do not affect outcome after radioembolization (42).

On the other hand, the location of the primary tumor may play a role in the selection process. In general, patients with right-sided primary tumors have a worse prognosis than patients with a left-sided primary tumor. This was reported for systemic treatment, but also for local treatment of hepatic metastases: patients with a right-sided primary tumor had a significantly decreased survival (hazard ratio 1.60, 95%CI 1.30-1.98) and recurrence free-survival (hazard ratio 1.35, 95%CI 1.04-1.77) compared to patients with left-sided primary tumors (60). This could potentially make patients with right-sided primary tumors less favorable candidates for treatment with radioembolization, as they will likely benefit less than patients with left-sided primaries (61). However, before using this as an exclusion criterion, a randomized study in patients with right-sided primary tumors should be performed, comparing best supportive care with radioembolization. Furthermore, the impact of radioembolization in patients with a right-sided primary tumor may be different in the first-line setting. A post-hoc analysis of the SIRFLOX, FOXFIRE and FOXFIRE-Global studies showed that the addition of radioembolization to systemic therapy in the first-line led to a significant survival benefit of almost 5 months (hazard ratio 0.64, 95%CI 0.46-0.89) in patients with right-sided primaries. In patients with a left-sided primary tumor, no significant difference in survival was found (62). The first-line treatment generally has the most impact on prognosis. In patients with a right-sided primary tumor, who have a poor prognosis after standard treatment, an early aggressive approach may be warranted. This could potentially include the addition of radioembolization in the first line (63).

Mutation status matters too: patients with KRAS wild type have a longer median overall survival compared with patients with KRAS mutation (9.5 months versus 4.8 months) and also a longer progression-free survival (166 days versus 91 days) after treatment with radioembolization (64, 65).

Which imaging work-up procedures need to be performed before treatment with radioembolization?

Before treatment with radioembolization, the first step in the selection process of a patient is imaging with ^{18}FDG-PET/CT. This is performed to assess the extent of a patient's disease, especially to rule out the presence of significant extrahepatic disease. It was shown that ^{18}FDG-PET/CT showed significantly more extrahepatic disease than conventional CT, often leading to a change of management in patients who are candidates for radioembolization (66).

Secondly, patients' anatomy should be carefully evaluated on contrast-enhanced CT, using an early arterial phase. Van den Hoven et al. described that there are as many as sixteen different hepatic arterial segmental vascularization patterns (67). A timely assessment of the hepatic vascularity allows for personalized treatment planning with the definition of the number of injection positions, target volumes and activity calculation (67, 68).

Depending on the primary tumor (in case of hepatocellular carcinoma (HCC), MRI is the imaging modality of choice), the contrast-enhanced CT or –MRI can be used for segmentation of the tumors and the healthy liver tissue. The (target) volumes obtained are used for activity calculation.

To ensure patients' safety, which is especially important in patients with HCC, who often have a cirrhotic liver, the distribution of the liver function can be determined using hepatobiliary scintigraphy. Currently, hepatobiliary scintigraphy is mostly used to assess the future liver remnant in patients scheduled for hepatic surgery. However, it can also be used in the work-up for radioembolization. Treatment may be adapted based on liver function distribution, e.g. choosing sequential lobar treatment instead of a whole-liver approach (57).

Why is treatment with radioembolization preceded by a scout dose?

Before treatment with radioembolization, a preparatory angiography with administration of a scout dose of either ^{99m}Tc-MAA or ^{166}Ho-scout is performed. This is done for several reasons: to map the arterial anatomy, to assess the necessity of coil-embolization of arterial branches, to determine the optimal

catheter position and to assess the activity distribution. The latter is necessary to rule out extrahepatic deposition, determine the lung shunt fraction and determine treatment volumes for ordering activity.

Usually, the preparatory angiography and scout dose administration precede treatment by 1-2 weeks. However, the question was raised if this can be done in a single day. Possible advantages include time- and cost savings: it saves time for patients, which is especially favorable in patients with rapidly progressive disease or in patients with highly symptomatic disease, for example in patients with hepatic metastases from an insulinoma. A one-day treatment approach can save costs for both patients and hospitals: patients don't have to travel twice (which is especially convenient for patients who have to travel a long distance) and hospitals have less admission costs. Studies in the three available types of microspheres showed that radioembolization as a single-day procedure is feasible and safe (69-71). In our study on one-day treatment, a disadvantage of this approach was the increased incidence of back pain. As patients have to lie down for many hours (in our study, a median of more than 10 hours), back pain easily occurs. The most important disadvantage however, is that a single-day procedure implies that only predefined dosimetric approaches, such as the body surface area (BSA) and MIRD method, can be used, because activity needs to be pre-ordered and can therefore not be adjusted based on scout dose distribution (72). With the increasing use of personalized treatment strategies, based on the results of the preparatory angiography and scout dose distribution, a one-day treatment strategy may not be preferred to allow for careful treatment planning.

Which types of microspheres are available for radioembolization?

Currently, three different types of radioactive microspheres are commercially available: ^{90}Y resin (SIR-Spheres®, SIRTeX Medical Ltd., Australia), ^{90}Y glass (TheraSphere®, Boston Scientific, US) and holmium-166 (^{166}Ho) microspheres (Quiremspheres®, Quirem Medical, The Netherlands).

The characteristics of these three types of microspheres are listed in Table 1.

TABLE 1.

Characteristic	^{90}Y resin	^{90}Y glass	^{166}Ho
Half-life (h)	64.1	64.1	26.8
Type of radiation	β	β	β, γ
Decay product	Zirconium-90	Zirconium-90	Erbium-166
Diameter (μm)	32.5±2.5	25±10	30±15
Density (g/mL)	1.6	3.3	1.4
Activity/microsphere (Bq)	40-70	2400-2700	300-330
Number per dose	50,000,000	4,000,000	33,000,000

The most apparent differences between the three types of microspheres are the type of radiation they emit and their specific activity. ^{166}Ho emits γ-radiation, which allows it to be visualized by SPECT/CT. It is also paramagnetic, so it can be visualized by MRI as well. On the contrary, imaging of ^{90}Y is possible by using either bremsstrahlung-SPECT/CT (73, 74) or PET/CT (75).

The differences in specific activity are large: the amount of energy released per microsphere is smallest for ^{90}Y resin and greatest for ^{90}Y glass, with ^{166}Ho having a specific activity somewhere in between. This has many consequences: first, the difference in specific activity is translated into the number of particles injected, leading to a much larger embolic effect (and risk of stasis) for ^{90}Y resin and ^{166}Ho than for ^{90}Y glass. Also, the tolerability of the liver is different for the three types of microspheres, leading to a difference in safety thresholds. A higher number of microspheres leads to a higher number of targeted liver clusters (i.e. healthy liver parenchyma) and a more homogeneous distribution in the liver (76). With ^{90}Y glass microspheres, there generally is a more heterogeneous distribution of the microspheres, leading to a higher tolerability. This explains why the thresholds for safety are different for the three types of microspheres. Likewise, a more homogeneous distribution, as obtained with ^{90}Y resin and ^{166}Ho, most likely also requires lower tumor-absorbed doses to be effective. This is indeed reflected in the thresholds found in the literature, further described below. However, one should take into account that this also depends on the tumor type. Hepatocellular carcinomas are generally hypervascular, and will receive a high tumor-absorbed dose even with a small number of ^{90}Y glass microspheres, whereas colorectal carcinoma metastases are generally hypovascular, possibly

resulting in more homogeneous distribution of the microspheres in the tumors and healthy liver tissue, regardless of the number of microspheres infused.

With ^{90}Y glass microspheres, it is possible to increase or decrease the number of microspheres per dose, by varying the specific activity: the twelve-day shelf-life post-calibration allows for a wide range. At 16 days post-calibration, the activity per microsphere is only 70 Bq, whereas at four days post-calibration, the activity per sphere is 1532 Bq (76). In a preclinical study, the risk of complications to the healthy liver tissue was low up to eight days post-calibration (76).

There are no guidelines on when to use which type of microsphere. For so-called radiation segmentectomy (i.e. a high radiation dose to one or two segments), the risk of stasis should be kept in mind, which is higher with a high number of microspheres injected in a limited target volume. Therefore, ^{90}Y glass microspheres are the type of choice, which was proven to be safe and effective for this purpose (77). Since conclusive comparative data is lacking, no other recommendations can be provided.

Which treatment planning methods are currently used?

For resin microspheres, the so-called body surface area (BSA) method is mostly used. This method adjusts the prescribed activity for the patient's BSA and the fractional tumor burden. The formula for the injected activity (IA) is:

$$IA_{(GBq)} = (BSA - 0{,}2) + \frac{tumor\ volume}{(tumor\ volume + liver\ volume)}$$ (54, 78).

The prescribed activity is reduced in case of lung shunting (79). The BSA method assumes a correlation between BSA and liver weight. However, this is not necessarily true and may result in an undertreatment of small patients with large livers, and an overtreatment of large patients with small livers. Another limitation of this method is that it does not take the degree of tumor uptake into account (54, 78).

For glass microspheres, the Medical Internal Radiation Dose (MIRD) method was developed (72). The prescribed activity is determined by calculating the activity required to achieve a desired average absorbed dose in the perfused or target volume (i.e. between 80-150 Gy). The MIRD method assumes a homogenous

intrahepatic microsphere distribution throughout the treated portion of the liver, and an assumed yield of 50 Gy per GBq ^{90}Y per kilogram of liver tissue. This method also does not take into account the degree of tumor uptake, nor does it account for fractional or total tumor burden. The formula for the IA is:

$$IA_{(GBq)} = \frac{\left(Desired\ average\ absorbed\ dose\ (Gy) * M_{Target}(kg)\right)}{50\left(\frac{J}{GBq}\right)}$$

where M_{Target} is the mass of the target volume.

For ^{166}Ho, a method comparable to the MIRD method for ^{90}Y is currently used. Based on findings of the HEPAR I trial, a maximum tolerable absorbed dose for the whole liver was set at 60 Gy (80). The absorbed dose in Gy delivered by 1 GBq in 1 kg tissue is 15.87 Gy for ^{166}Ho, under the assumption of homogenous distribution in the target volume and absorption of all energy within that volume. The formula for the IA is:

$$IA_{(GBq)} = \frac{\left(Desired\ average\ absorbed\ dose\ (Gy) * M_{Target}(kg)\right)}{16\left(\frac{J}{GBq}\right)}$$

Another method that can be used for personalized dosimetry is the partition model. In general, the tumor and healthy liver tissue are delineated on anatomical imaging modalities. The anticipated activity in these delineated compartments is calculated on pre-treatment ^{99m}Tc-MAA SPECT/CT (or ^{166}Ho-SPECT/CT). The tumor to non-tumor (T/N) ratio based on ^{99m}Tc-MAA or ^{166}Ho-scout is calculated as:

$$\frac{T}{N} = \frac{\frac{Activity_{tumor}(GBq)}{Mass_{tumor}(kg)}}{\frac{Activity_{liver}(Gbq)}{Mass_{liver}(kg)}}$$

The formula for the injected activity (IA) is:

$$IA(GBq) = \frac{Dose\ (Gy) * \left(\left[\frac{T}{N} * Mass_{tumor}(kg)\right] + Mass_{healthy\ liver\ tissue}(kg)\right)}{49.67 * (1 - lung\ shunt\ fraction)}$$

In this formula Dose (in Gy) is defined as the planned dose in healthy liver tissue and mass (in kg) is the delineated volume (in ml) multiplied by the conversion factor for soft tissue (1.06 g/cm^3). The ^{90}Y conversion factor of 49.67 is based on previous work by Ho et al., stating that 1 µCurie in 1 gram soft tissue results in an absorbed dose of 183.78 cGy. In other words, 1 GBq of ^{90}Y in 1 kg soft tissue results in 49.67 Gy absorbed dose(81). For ^{166}Ho, the conversion factor in the formula for injected activity is 15.87 (82).

The lung shunt fraction (LSF) is defined as (78, 83):

$$LSF = \frac{\sqrt{lungs_{anterior} * lungs_{posterior}}}{\sqrt{lungs_{anterior} * lungs_{posterior}}) + \sqrt{liver_{anterior} * liver_{posterior}}}$$

The main benefit of the partition method over single compartment models is the separation between tumor and non-tumor tissue in the calculation of their respective absorbed dose. The previously described formula allows the physician to describe a certain absorbed dose to the healthy tissue (Dose (Gy)). Subsequently, as an indication of expected mean tumor-absorbed dose, the physician can multiply the described healthy tissue dose with the T/N ratio. Thus, based on the maximum acceptable healthy liver tissue dose, a physician can assess whether or not an efficacy threshold (minimal tumor-absorbed dose) will be reached.

Limitations of the partition model is its assumption of a homogenous distribution of microspheres within the compartments, it is more time-consuming than single compartment models and tumor and healthy liver tissue delineation can be quite challenging on anatomical imaging, especially in patients with ill-defined tumors (54, 79). The partition method does correct for the difference in tumor and non-tumor absorbed dose.

Most methods use a (variant of a) 'one size fits all' approach. Unfortunately, this has led to failure of studies, for example the large SIRFLOX, FOXFIRE and FOXFIRE-Global studies. In these studies, the BSA method was used for activity calculation, but as stated before, this method does not differentiate between tumor and the healthy liver tissue activity distribution and often leads to under- or overdosing (84). As the treatment activity was reduced in case of lung shunting or on the basis of the tumor burden, under-dosing is likely what

happened in these studies. The low incidence of serious radioembolization-related adverse effects (hepatic failure, portal vein thrombosis, radiation hepatitis; occurring in only four patients (0.8%)) contributes to this assumption (35).

A different treatment planning approach was chosen in the DOSISPHERE study. In this study, 56 patients with hepatocellular carcinoma were randomly assigned to treatment with radioembolization using standard dosimetry or to treatment with radioembolization using personalized dosimetry with the goal to deliver at least 205 Gy to the tumor. For safety reasons, in the personalized dosimetry group, the maximum tolerable dose on the healthy liver tissue was set at 120 Gy in case of lobar treatment. With segmental treatment, the parenchymal-absorbed dose could be higher than 120 Gy, provided that there was a hepatic reserve >30%. Thus, some flexibility in activity prescription was possible, allowing for high enough tumor-absorbed doses. Dosimetry was based on the distribution of ^{99m}Tc-MAA and response was evaluated after three months. In the standard dosimetry arm, the response rate was 36%, versus 71% in the personalized dosimetry arm. A significant dose-response relationship was established and mean tumor-absorbed doses were significantly higher in the personalized dosimetry group (324 Gy versus 221 Gy) (85). Although this study was done in patients with hepatocellular carcinoma, it is a very important study for mCRC patients as well, as it is the first study to show that a personalized treatment planning leads to higher response rates.

Although several studies showed a dose-response relation in mCRC patients treated with radioembolization (86-88), a prospective study to validate the thresholds was not performed yet. For ^{90}Y-resin, the tumor-absorbed dose thresholds needed for response vary from 40-60 Gy (86-90) (Table 1). For ^{90}Y-glass, dose-response studies in mCRC patients are still awaited but in HCC patients, the tumor-absorbed dose needed for response is set around 200 Gy (85), although higher thresholds (up to 500 Gy) were reported in earlier studies (91). The safety and efficacy thresholds are different mainly because of differences in specific activity.

In mCRC patients treated with ^{166}Ho-radioembolization, an evident dose-response relationship was found, both at a patient- and at a tumor-level. An

attempt was made to find thresholds for both safety and efficacy. A patient-based threshold for efficacy was established at 90 Gy. However, not only the tumor-absorbed dose is important for personalized dosimetry: to avoid treatment-related complications, the parenchymal-absorbed dose should be taken into account as well. In our study, the incidence of toxicity was low, rendering it difficult to draw a strong conclusion on the maximum tolerable parenchymal-absorbed dose. There was only one patient with radioembolization-induced liver disease who had received 34 Gy to the parenchyma, while patients with much higher parenchymal-absorbed doses did not have much toxicity. Hence, it was concluded that a parenchymal-absorbed dose up to 55 Gy (the highest observed parenchymal-absorbed dose in our cohort) has an acceptable safety profile, depending on individual patient characteristics. For future mCRC patients who are planned for treatment with ^{166}Ho-radioembolization, it is advised to use a flexible parenchymal-absorbed dose threshold, with a maximum of 55 Gy. Depending an the physicians preference, one can either opt for maximizing tumor-absorbed dose (>90 Gy mean tumor-absorbed dose) by maximizing the parenchymal-absorbed dose up to the safety threshold (=55 Gy) or limiting healthy tissue irradiation (<55 Gy) while maintaining the minimal efficacy threshold for tumor tissue (≥90 Gy). In case the minimal efficacy threshold for tumor tissue is not reached (<90 Gy), while maximizing the healthy tissue absorbed dose (=55 Gy), that particular patient should not be eligible for a radioembolization treatment. In future studies, this personalized treatment approach should be used.

How can radioembolization be further improved and why is this needed?

Patients with CRC generally have relatively hypovascular hepatic metastases and a suboptimal activity distribution (51, 92). Response rates after radioembolization are modest: in our dose-response study in mCRC patients treated with ^{166}Ho-radioembolization, response rate was only 30%. In patients treated with ^{90}Y-radioembolization, comparable results are obtained, with a response rate of 37% (87). These numbers illustrate the need for treatment optimization. As mentioned earlier in this discussion, patient selection and personalized dosimetry are the most important factors to improve radioembolization, but there are other factors that can influence treatment outcome.

It was hypothesized that the use of an anti-reflux catheter could lead to higher response rates by improving the T/N ratio. An improved T/N ratio means that the ratio between absorbed-dose in the tumors versus the parenchyma is favorable, with a high tumor-absorbed dose and a low parenchymal-absorbed dose. The manufacturer of the Surefire® (TriSalus Life Sciences, Westminster, CO, USA) anti-reflux catheter claims that this catheter can effectuate an improved T/N ratio by inducing a more homogeneous distribution of the microspheres. Due to the expandable tip, the laminar flow columns are disrupted and a turbulent particle flow pattern is induced (93). Also, due to the expandable tip, a decrease in blood pressure in the downstream vascular territory can be observed, which would lead to a higher infusion efficiency with higher tumor deposition compared with surrounding healthy liver tissue (94, 95).

In a retrospective study of 88 hepatocellular carcinoma patients, the use of a standard end-hole catheter versus an anti-reflux catheter in transarterial chemoembolization was investigated. Explant analysis showed a higher T/N ratio with the use of an anti-reflux catheter (89% versus 55% intra-tumoral microsphere deposition) and a higher percentage tumor necrosis in the anti-reflux catheter group (89.0% versus 56.1%) (96). In our study, the SIM study, we did not find a significant difference in tumor to non-tumor activity concentration ratio. Moreover, these innovative catheters were not easy to use, since they often induced vasospasm. Hence, we cannot recommend the use of this type of anti-reflux catheters to increase T/N ratios. It may be different however, for balloon-catheters such as the Occlusafe® (Terumo). This type of catheter fully occludes the vascular lumen, possibly leading to a reversal of flow towards the tumors in the peripheral vasculature due to the downstream hypotension.

Besides anti-reflux catheters, T/N ratios may also be improved pharmacologically, for instance by using angiotensin II. Tumor vessels are not well developed, with an immature smooth muscle compartment of the vessel wall and immature neurovascular innervation. Therefore, they do not respond to the infusion of a vasoconstrictive agent, whereas the vasculature of the healthy liver tissue does. This leads to an increase in preferential blood flow to the tumors, increasing the T/N ratio (97).

How should response to treatment be evaluated?

First of all, there is a difference in response evaluation between medical products (i.e. pharmaceuticals) and medical devices. In patients with liver-dominant disease with a few enlarged lymph nodes, chemotherapy will have an effect on both the liver and on the lymph nodes. On the contrary, a medical device such as radioactive microspheres, is implanted in an organ and only has a local effect. In the case of radioembolization, this effect is on the liver lesions only. In the case of response evaluation on a whole-body level, patients who have complete response in the liver but growth of extrahepatic metastases may still be categorized as having progressive disease (98). In such cases, it may seem that treatment with radioembolization is ineffective, while it actually worked very well.

Secondly, the efficacy of treatment can be measured in many ways: not only as local response, but also as progression-free survival (PFS) or overall survival (OS). In the case of patients with colorectal cancer metastases who are treated in the first line, PFS is a better endpoint than OS since patients often receive multiple subsequent lines of treatment. OS can still be used, but in that case, the efficacy of the combination of treatments that patients receive should be evaluated.

There are several measures for response evaluation as a surrogate endpoint. The two most commonly used response metrics in the field of radioembolization are the Response Evaluation Criteria In Solid Tumors (RECIST) version 1.1 (98), and the Positron Emission Tomography Response Criteria In Solid Tumors (PERCIST) (99). RECIST is based on anatomical response, whereas PERCIST is based on metabolic response. In both metrics, response is categorized in complete response (CR), partial response (PR), stable disease (SD) or progressive disease (PD). A drawback of both methods, however, is that the definition of stable disease allows for a minor shrinkage or a minor growth of tumors, which may oversimplify the process (100). Another drawback of these methods is that target lesions (one per organ for PERCIST, a maximum of two per organ for RECIST 1.1) need to be defined. This is not always easy, because patients can have disseminated disease with confluent tumors. In the case of PET, if there is only one connecting voxel between two lesions, they may appear as one confluent lesion, rendering separate evaluation difficult. Furthermore, target

lesions may be fused at follow-up evaluation. Both anatomical and metabolic response-rates have been related to OS. Yet, agreement between both methods is often lacking, with metabolic response generally overestimating anatomic response (101), as was also seen in our dose-response study. For radioembolization, metabolic response is believed to be the best assessment method, as this is not hampered by the presence of necrosis, cystic changes and hemorrhage, which can be the case with size evaluation (102).

An alternative, more individualized approach to response evaluation is depth of response (DpR). This indicates the maximum tumor shrinkage observed in a patient, compared with baseline. The extent of tumor response is quantified and it is a continuous measure that can also become negative (in case of tumor growth). It can be based on tumor volume or size (100). In retrospective and prospective studies on systemic therapy for mCRC patients, DpR was significantly associated with post-progression survival (PPS) and OS (100, 103, 104). In theory, DpR could also be used for response evaluation after radioembolization. However, the largest reduction in tumor size or volume is generally observed after first-line treatment. Therefore, its use may be optimal when radioembolization is performed in a first-line setting.

Although response to treatment obviously is of paramount importance, so is the development of quality of life. As patients receiving radioembolization are generally in a palliative stage, quality of life is extremely important. Treatment selection should be based on expected gain in survival AND adverse event profile. In our review on studies reporting quality of life after treatment with radioembolization, most included studies reported no significant change in quality of life (105). Our own study results are compliant with this finding: although there was a decline in quality of life after one week, overall, quality of life was not significantly affected over time (105). Based on these findings in palliative patients, the impact of radioembolization on quality of life is limited. The impact of radioembolization in addition to chemotherapy was investigated in the first line setting as well. In the SIRFLOX, FOXFIRE and FOXFIRE-Global studies, quality of life was assessed at baseline, three months, six months, 12 months and 24 months. In the patient group that was treated with both radioembolization and chemotherapy, quality of life was significantly lower compared with the chemotherapy group at three months post-treatment. After

three months, there were no significant differences. Between baseline and three months post-treatment, patients in the combination group experienced more symptoms of fatigue and appetite loss, but fewer symptoms of sore mouth/tongue and diarrhea. Therefore, the worse quality of life scores were not deemed clinically relevant (106).

In conclusion, radioembolization for the treatment of colorectal liver metastases is safe, with limited side effects, usually of short duration, and it is effective, with improved overall survival rates shown in multiple studies. However, its true potential can only be shown in properly selected patients, using a personalized treatment approach. In the future, robust selection criteria and personalized activity planning should be implemented.

REFERENCES

1. Bengtsson G, Carlsson G, Hafstrom L, Jonsson PE. Natural history of patients with untreated liver metastases from colorectal cancer. Am J Surg. 1981;141:586-9.

2. Van Cutsem E, Cervantes A, Adam R, Sobrero A, Van Krieken JH, Aderka D, et al. ESMO consensus guidelines for the management of patients with metastatic colorectal cancer. Ann Oncol. 2016;27(8):1386-422. Epub 2016/07/07.

3. Nederland Z. Yttrium-90/holmium-166 radioembolisatie bij niet-resectabele colorectale levermetatasen in de salvage setting. 2018.

4. House MG, Ito H, Gonen M, Fong Y, Allen PJ, DeMatteo RP, et al. Survival after hepatic resection for metastatic colorectal cancer: trends in outcomes for 1,600 patients during two decades at a single institution. J Am Coll Surg. 2010;210(5):744-52, 52-5. Epub 2010/04/28.

5. Leal JN, Bressan AK, Vachharajani N, Gonen M, Kingham TP, D'Angelica MI, et al. Time-to-Surgery and Survival Outcomes in Resectable Colorectal Liver Metastases: A Multi-Institutional Evaluation. J Am Coll Surg. 2016;222(5):766-79. Epub 2016/04/27.

6. Donadon M, Ribero D, Morris-Stiff G, Abdalla EK, Vauthey JN. New paradigm in the management of liver-only metastases from colorectal cancer. Gastrointest Cancer Res. 2007;1(1):20-7.

7. Adam R, Delvart V, Pascal G, Valeanu A, Castaing D, Azoulay D, et al. Rescue surgery for unresectable colorectal liver metastases downstaged by chemotherapy: a model to predict long-term survival. Ann Surg. 2004;240(4):644-57; discussion 57-8. Epub 2004/09/24.

8. Vigano L, Capussotti L, Lapointe R, Barroso E, Hubert C, Giuliante F, et al. Early recurrence after liver resection for colorectal metastases: risk factors, prognosis, and treatment. A LiverMetSurvey-based study of 6,025 patients. Ann Surg Oncology. 2014;21(4):1276-86. Epub 2013/12/19.

9. Wurster EF, Tenckhoff S, Probst P, Jensen K, Dolger E, Knebel P, et al. A systematic review and meta-analysis of the utility of repeated versus single hepatic resection for colorectal cancer liver metastases. HPB. 2017;19(6):491-7. Epub 2017/03/30.

10. Sanoff HK, Sargent DJ, Campbell ME, Morton RF, Fuchs CS, Ramanathan RK, et al. Five-year data and prognostic factor analysis of oxaliplatin and irinotecan combinations for advanced colorectal cancer: N9741. J Clin Oncol. 2008;26(35):5721-7. Epub 2008/11/13.

11. Gillams AR, Lees WR. Five-year survival in 309 patients with colorectal liver metastases treated with radiofrequency ablation. Eur Radiol. 2009;19(5):1206-13. Epub 2009/01/13.

12. Shibata T, Niinobu T, Ogata N, Takami M. Microwave coagulation therapy for multiple hepatic metastases from colorectal carcinoma. Cancer. 2000;89(2):276-84.

13. Ruers T, Van Coevorden F, Punt CJ, Pierie JE, Borel-Rinkes I, Ledermann JA, et al. Local Treatment of Unresectable Colorectal Liver Metastases: Results of a Randomized Phase II Trial. J Natl Cancer Inst. 2017;109(9). Epub 2017/04/05.

14. Puijk RS, Ruarus AH, Vroomen L, van Tilborg A, Scheffer HJ, Nielsen K, et al. Colorectal liver metastases: surgery versus thermal ablation (COLLISION) - a phase III single-blind prospective randomized controlled trial. BMC Cancer. 2018;18(1):821. Epub 2018/08/17.

15. Renouf DJ, Lim HJ, Speers C, Villa D, Gill S, Blanke CD, et al. Survival for metastatic colorectal cancer in the bevacizumab era: a population-based analysis. Clin Colorect Cancer. 2011;10(2):97-101. Epub 2011/08/24.

16. Heinemann V, von Weikersthal LF, Decker T, Kiani A, Vehling-Kaiser U, Al-Batran S-E, et al. FOLFIRI plus cetuximab versus FOLFIRI plus bevacizumab as first-line treatment for patients with metastatic colorectal cancer (FIRE-3): a randomised, open-label, phase 3 trial. Lancet Oncol. 2014;15(10):1065-75.

17. Jawed I, Wilkerson J, Prasad V, Duffy AG, Fojo T. Colorectal Cancer Survival Gains and Novel Treatment Regimens: A Systematic Review and Analysis. JAMA Oncology. 2015;1(6):787-95. Epub 2015/07/17.

18. J.W. C, Grothey A. Systemic chemotherapy for nonoperable metastatic colorectal cancer: Treatment recommendations. 2020 [cited 2020 March 9]; Available from: https://www.uptodate.com/contents/systemic-chemotherapy-for-nonoperable-metastatic-colorectal-cancer-treatment-recommendations?search=colorectal%20cancer%20systemic%20treatment&source=search_result&selectedTitle=1~150&usage_type=default&display_rank=1.

19. Lamont EB, Schilsky RL. The oral fluoropyrimidines in cancer chemotherapy. Clinl Cancer Res. 1999;5:2289-96.

20. Fujita K, Kubota Y, Ishida H, Sasaki Y. Irinotecan, a key chemotherapeutic drug for metastatic colorectal cancer. World J Gastroenterol. 2015;21(43):12234-48. Epub 2015/11/26.

21. Koopman M, Antonini NF, Douma J, Wals J, Honkoop AH, Erdkamp FLG, et al. Sequential versus combination chemotherapy with capecitabine, irinotecan, and oxaliplatin in advanced colorectal cancer (CAIRO): a phase III randomised controlled trial. Lancet. 2007;370(9582):135-42.

22. Seymour MT, Maughan TS, Ledermann JA, Topham C, James R, Gwyther SJ, et al. Different strategies of sequential and combination chemotherapy for patients with poor prognosis advanced colorectal cancer (MRC FOCUS): a randomised controlled trial. Lancet. 2007;370(9582):143-52.

23. IKNL. Colorectaalcarcinoom. Landelijke richtlijn, Versie: 3.0. 2014.

24. BOM N-c. TAS-102 voor het gemetastaseerd colorectaalcarcinoom. Medische Oncologie. 2016;19(8):55-7.

25. Brudvik KW, Kopetz SE, Li L, Conrad C, Aloia TA, Vauthey JN. Meta-analysis of KRAS mutations and survival after resection of colorectal liver metastases. Br J Surg. 2015;102(10):1175-83. Epub 2015/07/25.

26. Vauthey JN, Zimmitti G, Kopetz SE, Shindoh J, Chen SS, Andreou A, et al. RAS mutation status predicts survival and patterns of recurrence in patients undergoing hepatectomy for colorectal liver metastases. Ann Surg. 2013;258(4):619-26; discussion 26-7. Epub 2013/09/11.

27. Zimmitti G, Shindoh J, Mise Y, Kopetz S, Loyer EM, Andreou A, et al. RAS mutations predict radiologic and pathologic response in patients treated with chemotherapy before resection of colorectal liver metastases. Ann Surg Oncol. 2015;22(3):834-42. Epub 2014/09/18.

28. Yaeger R, Cercek A, Chou JF, Sylvester BE, Kemeny NE, Hechtman JF, et al. BRAF mutation predicts for poor outcomes after metastasectomy in patients with metastatic colorectal cancer. Cancer. 2014;120(15):2316-24. Epub 2014/04/17.

29. Wang Z, Wang X, Zhang Z, Chen M, Lu L, Zhu W, et al. Association between Primary Tumor Location and Prognostic Survival in Synchronous Colorectal Liver Metastases after Surgical Treatment: A Retrospective Analysis of SEER Data. J Cancer. 2019;10(7):1593-600. Epub 2019/06/18.

30. Kooby DA, Fong Y, Suriawinata A, Gonen M, Allen PJ, Klimstra DS, et al. Impact of steatosis on perioperative outcome following hepatic resection. J Gastrointest Surg. 2003;7(8).

31. Rubbia-Brandt L, Audard V, Sartoretti P, Roth AD, Brezault C, Le Charpentier M, et al. Severe hepatic sinusoidal obstruction associated with oxaliplatin-based chemotherapy in patients with metastatic colorectal cancer. Ann Oncol. 2004;15(3):460-6. Epub 2004/03/05.

32. Society AC. Colorectal Cancer Facts and Figures 2017-2019. Atlanta; 2019 [cited 2020 March 12]; Available from: https://www.cancer.org/content/dam/cancer-org/research/cancer-facts-and-statistics/colorectal-cancer-facts-and-figures/colorectal-cancer-facts-and-figures-2017-2019.pdf.

33. Lichtman SM, Hesketh PJ, Schmader KE. Systemic chemotherapy for cancer in older adults. UptoDate; 2019 [cited 2020 March 12]; Available from: https://www.uptodate.com/contents/systemic-chemotherapy-for-cancer-in-older-adults?search=chemotherapy%20side%20effects%20colorectal%20cancer&source=search_result&selectedTitle=2~150&usage_type=default&display_rank=2#H2.

34. Network NCC. Clinical practice guidelines in oncology: colon cancer. National Comprehensive Cancer Network; 2016 [cited 2020 March 12]; Available from: https://www.nccn.org/professionals/physician_gls/PDF/colon.pdf.

35. Wasan HS, Gibbs P, Sharma NK, Taieb J, Heinemann V, Ricke J, et al. First-line selective internal radiotherapy plus chemotherapy versus chemotherapy alone in patients with liver metastases from colorectal cancer (FOXFIRE, SIRFLOX, and FOXFIRE-Global): a combined analysis of three multicentre, randomised, phase 3 trials. Lancet Oncol. 2017.

36. Lam MG, Louie JD, Abdelmaksoud MH, Fisher GA, Cho-Phan CD, Sze DY. Limitations of body surface area-based activity calculation for radioembolization of hepatic metastases in colorectal cancer. J Vasc Interv Radiol. 2014;25(7):1085-93. Epub 2014/01/25.

37. Tohme S, Sukato D, Nace GW, Zajko A, Amesur N, Orons P, et al. Survival and tolerability of liver radioembolization: a comparison of elderly and younger patients with metastatic colorectal cancer. HPB. 2014;16(12):1110-6. Epub 2014/08/16.

38. Soydal C, Kucuk NO, Balci D, Gecim E, Bilgic S, Elhan AH. Prognostic Importance of the Presence of Early Metabolic Response and Absence of Extrahepatic Metastasis After Selective Internal Radiation Therapy in Colorectal Cancer Liver Metastasis. Cancer Biother Radiopharm. 2016;31(9):342-6. Epub 2016/11/11.

39. Cassidy J, Twelves C, Van Cutsem E, Hoff P, Bajetta E, Boyer M, et al. First-line oral capecitabine therapy in metastatic colorectal cancer: a favorable safety profile compared with intravenous 5-fluorouracil/leucovorin. Ann Oncol. 2002;13(4):566-75. Epub 2002/06/12.

40. Cunningham D, Lang I, Marcuello E, Lorusso V, Ocvirk J, Shin DB, et al. Bevacizumab plus capecitabine versus capecitabine alone in elderly patients with previously untreated metastatic colorectal cancer (AVEX): an open-label, randomised phase 3 trial. Lancet Oncol. 2013;14(11):1077-85.

41. Kennedy AS, Ball DS, Cohen SJ, Cohn M, Coldwell D, Drooz A, et al. Safety and Efficacy of Radioembolization in Elderly (>/= 70 Years) and Younger Patients With Unresectable Liver-Dominant Colorectal Cancer. Clin Colorect Cancer. 2016;15(2):141-51 e6. Epub 2015/11/07.

42. Seidensticker R, Damm R, Enge J, Seidensticker M, Mohnike K, Pech M, et al. Local ablation or radioembolization of colorectal cancer metastases: comorbidities or older age do not affect overall survival. BMC Cancer. 2018;18(1):882. Epub 2018/09/12.

43. Hickey R, Lewandowski RJ, Prudhomme T, Ehrenwald E, Baigorri B, Critchfield J, et al. 90Y Radioembolization of Colorectal Hepatic Metastases Using Glass Microspheres: Safety and Survival Outcomes from a 531-Patient Multicenter Study. J Nucl Med. 2016;57(5):665-71. Epub 2015/12/05.

44. Saxena A, Meteling B, Kapoor J, Golani S, Morris DL, Bester L. Is yttrium-90 radioembolization a viable treatment option for unresectable, chemorefractory colorectal cancer liver metastases? A large single-center experience of 302 patients. Ann Surg Oncol. 2015;22(3):794-802. Epub 2014/10/18.

45. Kennedy A, Cohn M, Coldwell DM, Drooz A, Ehrenwald E, Kaiser A, et al. Updated survival outcomes and analysis of long-term survivors from the MORE study on safety and efficacy of radioembolization in patients with unresectable colorectal cancer liver metastases. J Gastrointest Oncol. 2017;8(4):614-24. Epub 2017/09/12.

46. van Hazel GA, Pavlakis N, Goldstein D, Olver IN, Tapner MJ, Price D, et al. Treatment of fluorouracil-refractory patients with liver metastases from colorectal cancer by using yttrium-90 resin microspheres plus concomitant systemic irinotecan chemotherapy. J Clin Oncol. 2009;27(25):4089-95. Epub 2009/08/05.

47. Chua TC, Bester L, Saxena A, Morris DL. Radioembolization and systemic chemotherapy improves response and survival for unresectable colorectal liver metastases. J Cancer Res Clin Oncol. 2011;137(5):865-73. Epub 2010/09/23.

48. Chauhan N, Mulcahy MF, Salem R, Benson Iii AB, Boucher E, Bukovcan J, et al. TheraSphere Yttrium-90 Glass Microspheres Combined With Chemotherapy Versus Chemotherapy Alone in Second-Line Treatment of Patients With Metastatic Colorectal Carcinoma of the Liver: Protocol for the EPOCH Phase 3 Randomized Clinical Trial. JMIR Res Protoc. 2019;8(1):e11545. Epub 2019/01/22.

49. Sabet A, Meyer C, Aouf A, Ghamari S, Pieper CC, Mayer K, et al. Early post-treatment FDG PET predicts survival after 90Y microsphere radioembolization in liver-dominant metastatic colorectal cancer. Eur J Nucl Med Mol Im. 2015;42(3):370-6. Epub 2014/10/30.

50. Pfeiffer P, Yilmaz M, Möller S, Zitnjak D, Krogh M, Petersen LN, et al. TAS-102 with or without bevacizumab in patients with chemorefractory metastatic colorectal cancer: an investigator-initiated, open-label, randomised, phase 2 trial. Lancet Oncol. 2020;21(3):412-20.

51. Boas FE, Bodei L, Sofocleous CT. Radioembolization of Colorectal Liver Metastases: Indications, Technique, and Outcomes. J Nucl Med. 2017;58(Suppl 2):104S-11S. Epub 2017/09/03.

52. Turk G, Eldem G, Kilickap S, Bozkurt FM, Salanci BV, Cil BE, et al. Outcomes of Radioembolization in Patients with Chemorefractory Colorectal Cancer Liver Metastasis: a Single-Center Experience. J Gastrointest Cancer. 2019;50(2):236-43. Epub 2018/01/23.

53. Wang DS, Louie JD, Sze DY. Evidence-Based Integration of Yttrium-90 Radioembolization in the Contemporary Management of Hepatic Metastases from Colorectal Cancer. Techniques in vascular and interventional radiology. 2019;22(2):74-80. Epub 2019/05/14.

54. Braat AJ, Smits ML, Braat MN, van den Hoven AF, Prince JF, de Jong HW, et al. (9)(0)Y Hepatic Radioembolization: An Update on Current Practice and Recent Developments. J Nucl Med. 2015;56(7):1079-87. Epub 2015/05/09.

55. Braat MN, van Erpecum KJ, Zonnenberg BA, van den Bosch MA, Lam MG. Radioembolization-induced liver disease: a systematic review. Eur J Gastroenterol Hepatol. 2017;29(2):144-52. Epub 2016/12/08.

56. Kennedy AS, Ball D, Cohen SJ, Cohn M, Coldwell DM, Drooz A, et al. Multicenter evaluation of the safety and efficacy of radioembolization in patients with unresectable colorectal liver metastases selected as candidates for (90)Y resin microspheres. J Gastrointest oncol. 2015;6(2):134-42. Epub 2015/04/02.

57. van Roekel C, Reinders MTM, van der Velden S, Lam M, Braat M. Hepatobiliary Imaging in Liver-directed Treatments. Semin Nucl Med. 2019;49(3):227-36. Epub 2019/04/08.

58. Garlipp B, Gibbs P, Van Hazel GA, Jeyarajah R, Martin RCG, Bruns CJ, et al. Secondary technical resectability of colorectal cancer liver metastases after chemotherapy with or without selective internal radiotherapy in the randomized SIRFLOX trial. Br J Surg. 2019;106(13):1837-46. Epub 2019/08/20.

59. Paprottka KJ, Schoeppe F, Ingrisch M, Rubenthaler J, Sommer NN, De Toni E, et al. Pre-therapeutic factors for predicting survival after radioembolization: a single-center experience in 389 patients. Eur J Nucl Med Mol Im. 2017;44(7):1185-93. Epub 2017/02/16.

60. Buisman FE, Galjart B, Buettner S, Groot Koerkamp B, Grunhagen DJ, Verhoef C. Primary tumor location and the prognosis of patients after local treatment of colorectal liver metastases: a systematic review and meta-analysis. HPB. 2020;22(3):351-7. Epub 2019/11/02.

61. Singh K, Savin J, Savin M, Wong C. Abstract No. 544 Radioembolization for metastatic colon cancer: survival differences between right- and left-sided primary sites. J Vasc Interv Radiol. 2018;29(4):S228.

62. Gibbs P, Heinemann V, Sharma NK, Taieb J, Ricke J, Peeters M, et al. Effect of Primary Tumor Side on Survival Outcomes in Untreated Patients With Metastatic Colorectal Cancer When Selective Internal Radiation Therapy Is Added to Chemotherapy: Combined Analysis of Two Randomized Controlled Studies. Clin Colorect Cancer. 2018;17(4):e617-e29. Epub 2018/07/24.

63. Garlipp B, Gibbs P, Van Hazel GA, Jeyarajah R, Martin RCG, Bruns CJ, et al. Secondary technical resectability of colorectal cancer liver metastases after chemotherapy with or without selective internal radiotherapy in the randomized SIRFLOX trial. British J Surg. 2019. Epub 2019/08/20.

64. Lahti SJ, Xing M, Zhang D, Lee JJ, Magnetta MJ, Kim HS. KRAS Status as an Independent Prognostic Factor for Survival after Yttrium-90 Radioembolization Therapy for Unresectable Colorectal Cancer Liver Metastases. J Vasc Interv Radiol. 2015;26(8):1102-11. Epub 2015/07/27.

65. Magnetta MJ, Ghodadra A, Lahti SJ, Xing M, Zhang D, Kim HS. Connecting cancer biology and clinical outcomes to imaging in KRAS mutant and wild-type colorectal cancer liver tumors following selective internal radiation therapy with yttrium-90. Abdom Radiol (NY). 2017;42(2):451-9. Epub 2016/09/08.

66. Rosenbaum CE, van den Bosch MA, Veldhuis WB, Huijbregts JE, Koopman M, Lam MG. Added value of FDG-PET imaging in the diagnostic workup for yttrium-90 radioembolisation in patients with colorectal cancer liver metastases. Eur Radiol. 2013;23(4):931-7. Epub 2012/11/01.

67. van den Hoven AF, van Leeuwen MS, Lam MG, van den Bosch MA. Hepatic arterial configuration in relation to the segmental anatomy of the liver; observations on MDCT and DSA relevant to radioembolization treatment. Cardiovasc Interv Radiol. 2015;38(1):100-11. Epub 2014/03/08.

68. van den Hoven AF, Smits ML, de Keizer B, van Leeuwen MS, van den Bosch MA, Lam MG. Identifying aberrant hepatic arteries prior to intra-arterial radioembolization. Cardiovasc Interv Radiol. 2014;37(6):1482-93. Epub 2014/01/29.

69. Gabr A, Kallini JR, Gates VL, Hickey R, Kulik L, Desai K, et al. Same-day (90) Y radioembolization: implementing a new treatment paradigm. Eur J Nucl Med Mol Im. 2016;43(13):2353-9. Epub 2016/11/05.

70. Gates VL, Marshall KG, Salzig K, Williams M, Lewandowski RJ, Salem R. Outpatient single-session yttrium-90 glass microsphere radioembolization. J Vasc Interv Radiol. 2014;25(2):266-70. Epub 2013/12/18.

71. Li MD, Chu KF, DePietro A, Wu V, Wehrenberg-Klee E, Zurkiya O, et al. Same-Day Yttrium-90 Radioembolization: Feasibility with Resin Microspheres. J Vasc Interv Radiol. 2019;30(3):314-9. Epub 2019/03/02.

72. Salem R, Thurston KG. Radioembolization with 90Yttrium microspheres: a state-of-the-art brachytherapy treatment for primary and secondary liver malignancies. Part 1: Technical and methodologic considerations. J Vasc Interv Radiol. 2006;17(8):1251-78. Epub 2006/08/23.

73. Ahmadzadehfar H, Muckle M, Sabet A, Wilhelm K, Kuhl C, Biermann K, et al. The significance of bremsstrahlung SPECT/CT after yttrium-90 radioembolization treatment in the prediction of extrahepatic side effects. Eur J Nucl Med Mol Im. 2011. Epub 2011/10/07.

74. Wang XD, Yang RJ, Cao XC, Tan J, Li B. Dose delivery estimated by bremsstrahlung imaging and partition model correlated with response following intra-arterial radioembolization with 32P-glass microspheres for the treatment of hepatocellular carcinoma. J Gastrointest Surg. 2010;14(5):858-66. Epub 2010/03/13.

75. Gates VL, Esmail AA, Marshall K, Spies S, Salem R. Internal pair production of 90Y permits hepatic localization of microspheres using routine PET: proof of concept. J Nucl Med. 2011;52(1):72-6. Epub 2010/12/15.

76. Pasciak AS, Abiola G, Liddell RP, Crookston N, Besharati S, Donahue D, et al. The number of microspheres in Y90 radioembolization directly affects normal tissue radiation exposure. Eur J Nucl Med Mol Im. 2020;47(4):816-27. Epub 2019/11/20.

77. Riaz A, Gates VL, Atassi B, Lewandowski RJ, Mulcahy MF, Ryu RK, et al. Radiation segmentectomy: a novel approach to increase safety and efficacy of radioembolization. Int J Radiat Oncol Biol Phys. 2011;79(1):163-71. Epub 2010/04/28.

78. Giammarile F, Bodei L, Chiesa C, Flux G, Forrer F, Kraeber-Bodere F, et al. EANM procedure guideline for the treatment of liver cancer and liver metastases with intra-arterial radioactive compounds. Eur J Nucl Med Mol Im. 2011;38(7):1393-406. Epub 2011/04/16.

79. Smits ML, Elschot M, Sze DY, Kao YH, Nijsen JF, Iagaru AH, et al. Radioembolization dosimetry: the road ahead. Cardiovasc Interv Radiol. 2015;38(2):261-9. Epub 2014/12/30.

80. Smits MLJ, Nijsen JFW, van den Bosch MAAJ, Lam MGEH, Vente MAD, Mali WPTM, et al. Holmium-166 radioembolisation in patients with unresectable, chemorefractory liver metastases (HEPAR trial): a phase 1, dose-escalation study. Lancet Oncol. 2012;13(10):1025-34.

81. Ho S, Lau WY, Leung TWT, Chan M, Ngar YK, Johnson PC, et al. Partition model for estimating radiation doses from yttrium-90 microspheres in treating hepatic tumours Eur J Nucl Med. 1996;23:947-52.

82. Elschot M, Smits ML, Nijsen JF, Lam MG, Zonnenberg BA, van den Bosch MA, et al. Quantitative Monte Carlo-based holmium-166 SPECT reconstruction. Medical physics. 2013;40(11):112502. Epub 2013/12/11.

83. Garin E, Rolland Y, Laffont S, Edeline J. Clinical impact of (99m)Tc-MAA SPECT/CT-based dosimetry in the radioembolization of liver malignancies with (90)Y-loaded microspheres. Eur J Nucl Med Mol Im. 2016;43(3):559-75. Epub 2015/09/05.

84. Braat AJAT, Kappadath SC, Bruijnen RCG, Van den Hoven AF, Mahvash A, De Jong HWAM, et al. Adequate SIRT activity dose is as important as adequate chemotherapy dose. Lancet Oncol. 2017;18:e636.

85. Garin E. A multicentric and randomized study demonstrating the impact of MAA based dosimetry on tumor response in SIRT for HCC. 2019 [cited 2019 December 12]; Available from: https://www.eventscribe.com/2019/GEST/fsPopup.asp?Mode=presInfo&PresentationID=521844.

86. Flamen P, Vanderlinden B, Delatte P, Ghanem G, Ameye L, Van Den Eynde M, et al. Multimodality imaging can predict the metabolic response of unresectable colorectal liver metastases to radioembolization therapy with Yttrium-90 labeled resin microspheres. Phys Med Biol. 2008;53(22):6591-603. Epub 2008/11/04.

87. van den Hoven AF, Rosenbaum CE, Elias SG, de Jong HW, Koopman M, Verkooijen HM, et al. Insights into the Dose-Response Relationship of Radioembolization with Resin 90Y-Microspheres: A Prospective Cohort Study in Patients with Colorectal Cancer Liver Metastases. J Nucl Med. 2016;57(7):1014-9. Epub 2016/02/26.

88. Levillain H, Duran Derijckere I, Marin G, Guiot T, Vouche M, Reynaert N, et al. (90)Y-PET/CT-based dosimetry after selective internal radiation therapy predicts outcome in patients with liver metastases from colorectal cancer. EJNMMI research. 2018;8(1):60. Epub 2018/07/15.

89. Willowson KP, Hayes AR, Chan DLH, Tapner M, Bernard EJ, Maher R, et al. Clinical and imaging-based prognostic factors in radioembolisation of liver metastases from colorectal cancer: a retrospective exploratory analysis. EJNMMI research. 2017;7(1):46. Epub 2017/05/26.

90. Abbott EM, Falzone N, Lee BQ, Kartsonaki C, Winter H, Greenhalgh TA, et al. The Impact of Radiobiologically-Informed Dose Prescription on the Clinical Benefit of Yttrium-90 SIRT in Colorectal Cancer Patients. J Nucl Med. 2020. Epub 2020/05/03.

91. Cremonesi M, Chiesa C, Strigari L, Ferrari M, Botta F, Guerriero F, et al. Radioembolization of hepatic lesions from a radiobiology and dosimetric perspective. Front Oncol. 2014;4:210. Epub 2014/09/06.

92. Tirumani SH, Kim KW, Nishino M, Howard SA, Krajewski KM, Jagannathan JP, et al. Update on the role of imaging in management of metastatic colorectal cancer. RadioGraphics. 2014;34:1908-28.

93. van den Hoven AF, Lam MG, Jernigan S, van den Bosch MA, Buckner GD. Innovation in catheter design for intra-arterial liver cancer treatments results in favorable particle-fluid dynamics. J Exp Clin Cancer Res. 2015;34:74. Epub 2015/08/02.

94. Rose SC, Narsinh KH, Newton IG. Quantification of Blood Pressure Changes in the Vascular Compartment When Using an Anti-Reflux Catheter during Chemoembolization versus Radioembolization: A Retrospective Case Series. J Vasc Interv Radiol. 2017;28(1):103-10. Epub 2016/11/15.

95. Pasciak AS, McElmurray JH, Bourgeois AC, Heidel RE, Bradley YC. The impact of an antireflux catheter on target volume particulate distribution in liver-directed embolotherapy: a pilot study. J Vasc Interv Radiol. 2015;26(5):660-9. Epub 2015/03/25.

96. Titano JJ, Fischman AM, Cherian A, Tully M, Stein LL, Jacobs L, et al. End-hole Versus Microvalve Infusion Catheters in Patients Undergoing Drug-Eluting Microspheres-TACE for Solitary Hepatocellular Carcinoma Tumors: A Retrospective Analysis. Cardiovasc Interv Radiol. 2019;42(4):560-8. Epub 2019/01/13.

97. van den Hoven AF, Smits ML, Rosenbaum CE, Verkooijen HM, van den Bosch MA, Lam MG. The effect of intra-arterial angiotensin II on the hepatic tumor to non-tumor blood flow ratio for radioembolization: a systematic review. PloS One. 2014;9(1):e86394. Epub 2014/01/28.

98. Eisenhauer EA, Therasse P, Bogaerts J, Schwartz LH, Sargent D, Ford R, et al. New response evaluation criteria in solid tumours: revised RECIST guideline (version 1.1). Eur J Cancer. 2009;45(2):228-47. Epub 2008/12/23.

99. Hyun O, J. , Lodge MA, Wahl RL. Practical PERCIST: A simplified guide to PET response criteria in solid tumors. RadioGraphics. 2016;280(2):576-84.

100. Heinemann V, Stintzing S, Modest DP, Giessen-Jung C, Michl M, Mansmann UR. Early tumour shrinkage (ETS) and depth of response (DpR) in the treatment of patients with metastatic colorectal cancer (mCRC). Eur J Cancer. 2015;51(14):1927-36. Epub 2015/07/21.

101. Sager S, Akgun E, Uslu-Besli L, Asa S, Akovali B, Sahin O, et al. Comparison of PERCIST and RECIST criteria for evaluation of therapy response after yttrium-90 microsphere therapy in patients with hepatocellular carcinoma and those with metastatic colorectal carcinoma. Nucl Med Commun. 2019;40(5):461-8. Epub 2019/03/22.

102. Bastiaannet R, Lodge MA, de Jong H, Lam M. The Unique Role of Fluorodeoxyglucose-PET in Radioembolization. PET Clin. 2019;14(4):447-57. Epub 2019/09/02.

103. Tsuji A, Sunakawa Y, Ichikawa W, Nakamura M, Kochi M, Denda T, et al. Early Tumor Shrinkage and Depth of Response as Predictors of Favorable Treatment Outcomes in Patients with Metastatic Colorectal Cancer Treated with FOLFOX Plus Cetuximab (JACCRO CC-05). Target Oncol. 2016;11(6):799-806. Epub 2016/06/17.

104. Sunakawa Y, Tsuji A, Denda T, Segawa Y, Negoro Y, Shimada K, et al. CEA Response and Depth of Response (DpR) to Predict Clinical Outcomes of First-Line Cetuximab Treatment for Metastatic Colorectal Cancer. Target Oncol. 2017;12(6):787-94. Epub 2017/10/25.

105. van Roekel C, Smits MLJ, Prince JF, Bruijnen RCG, van den Bosch M, Lam M. Quality of life in patients with liver tumors treated with holmium-166 radioembolization. Clin Exp Metastasis. 2020;37(1):95-105. Epub 2019/11/17.

106. Wolstenholme J, Fusco F, Gray AM, Moschandreas J, Virdee PS, Love S, et al. Quality of life in the FOXFIRE, SIRFLOX and FOXFIRE-global randomised trials of selective internal radiotherapy for metastatic colorectal cancer. Int J Cancer. 2019. Epub 2019/12/17.

Summary

This thesis describes the application of holmium-166 (^{166}Ho) radioembolization for patients with hepatic metastases of colorectal carcinoma (mCRC patients). The chapters describe different treatment-related aspects that can be used for individualized treatment. Chapter 3 describes the quality of life, which is especially important in elderly people in a salvage setting. Chapter 4 describes the benefits and drawbacks of a one-day treatment strategy, that could be beneficial for selected patients. Chapter 5 describes the types of response and the influence of several baseline characteristics on response. This could be used for patient selection. Chapters 6 and 7 describe the dose-response relation, which is of vital importance in individualized treatment planning and activity calculation. Chapters 8 and 9, finally, describe the effect of procedure-related interventions: the use of coil-embolization and the use of an anti-reflux catheter.

FIGURE 1. Work-up procedure for radioembolization in the angiography suite.

In chapter 2, the basic aspects of radioembolization are covered: the indications, the different types of microspheres that can be used, the methods for activity calculation, the work-up procedure, the common adverse events and response after treatment.

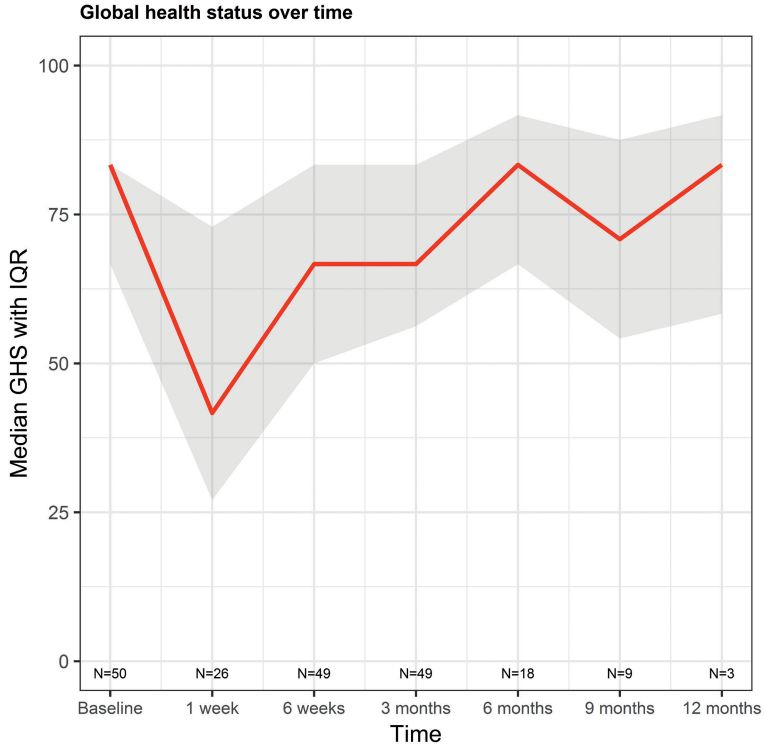

FIGURE 2. Quality of life in patients treated with ^{166}Ho-radioembolization. GHS – Global Health Status (a score of 100 indicates excellent quality of life)

Chapter 3 describes the quality of life in 50 patients treated with ^{166}Ho-radioembolization. Two questionnaires, the EORTC QLQ-C30 and the QLQ-LMC21 were used to evaluate quality of life at baseline, 1 week, 6 weeks and at 6, 9 and 12 months after treatment. The questionnaires comprised of many different aspects, such as symptoms (e.g. pain, nausea, fatigue) and functioning scales (e.g. physical functioning, social functioning). The global health status was a general indicator of the quality of life. Quality of life was not significantly affected over time. However, in almost all scales, a decline in quality of life and a rise of symptomatology was seen at one week after treatment. This is most likely due to the post-embolization syndrome, which occurs shortly after treatment and is self-limiting (which explains the normalization after one month).

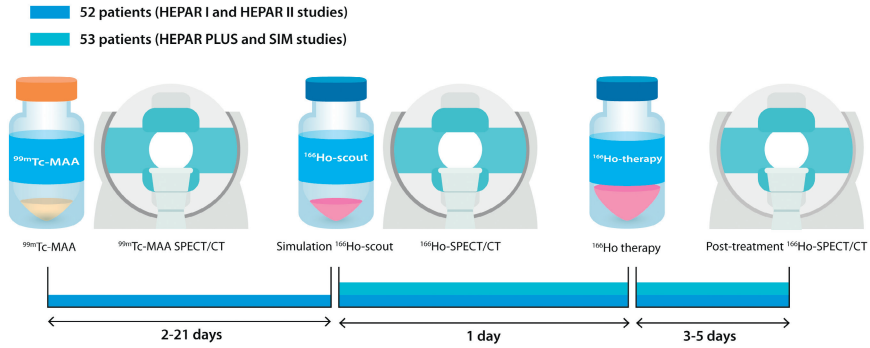

FIGURE 3. Timeline. Fifty-two patients of this study underwent two simulation procedures, one with administration of ^{99m}Tc-MAA and one with ^{166}Ho-scout, as per protocol of the HEPAR I and HEPAR II studies. Fifty-three patients underwent one simulation procedure with administration of ^{166}Ho-scout. After administration of ^{166}Ho-scout and the ^{166}Ho-treatment dose, ^{166}Ho-SPECT/CT images were made to assess the absorbed dose distribution.

In chapter 4, the safety and feasibility of a one-day treatment protocol for ^{166}Ho-radioembolization was evaluated. It was shown that a large percentage of patients (12%) was excluded from treatment based on findings of the simulation procedures. In another 12% of patients, treatment had to be adjusted. The main reasons for this were extrahepatic deposition of activity, vascular anatomy and suboptimal targeting (the activity distribution within the liver: in the tumors versus the healthy liver parenchyma). Another drawback of this one-day procedure was that many patients (27%) complained of back pain, which was likely due to the long duration of laying supine, inherent to the one-day protocol. Based on these results, a one-day treatment approach should only be considered in a select patient population.

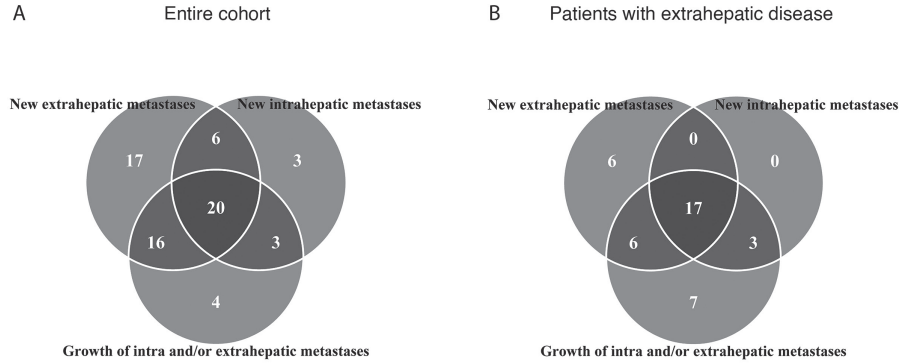

FIGURE 4. Mode of progression of the entire cohort (90 patients) (a) and specific for patients with extrahepatic disease at baseline (42 patients) (b).

In chapter 5, the mode of progression at three months after treatment with ^{166}Ho or ^{90}Y-radioembolization was assessed according to RECIST 1.1. A distinction was made between progression based on growth of existing intra- or extrahepatic metastases and the development of new intra- or extrahepatic metastases. In 90 included patients, 69 (77%) had progressive disease, of which 97% had new metastases. Patients with extrahepatic disease at baseline had a worse prognosis than patients without extrahepatic disease; with an odds ratio of 7.8 for progressive disease and a median 3.5 months shorter overall survival.

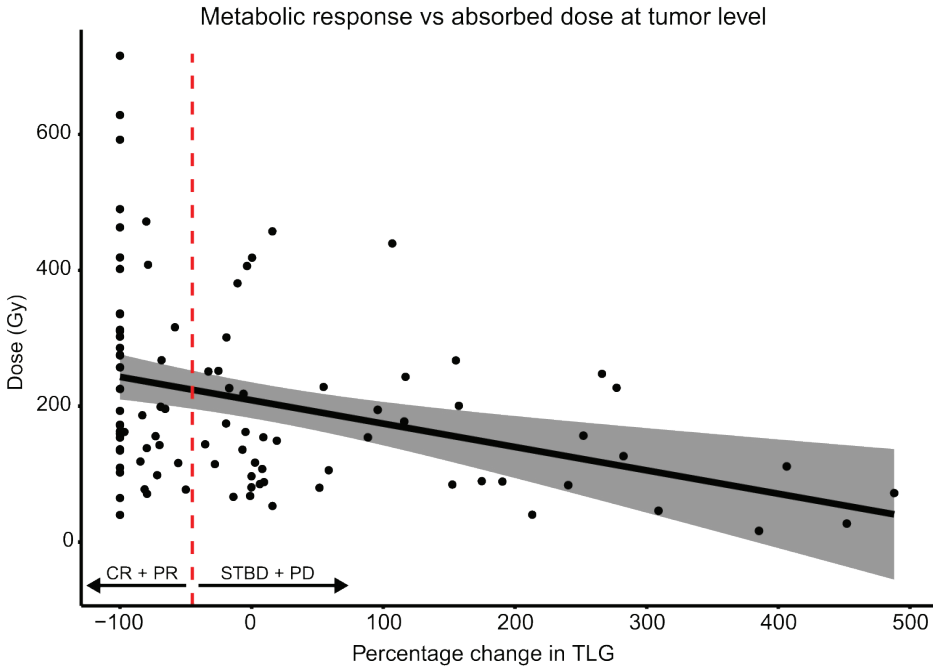

FIGURE 5. Graphical representation of the metabolic response versus absorbed dose of each individual tumor. A decrease in TLG is associated with a higher dose. The vertical dashed line indicates the cut-off value for TLG change, below which metabolic response is defined is complete response or partial response and above which response is defined as either stable disease or progressive disease. Shaded area indicates 95% CI of the regression line.

Chapter 6 is the first of two dose-response studies in ^{166}Ho-radioembolization. In a cohort of patients with various primary tumors, the relation between dose and response was assessed. In 36 patients, metabolic response (based on changes in total lesion glycolysis (TLG) on baseline and follow-up [^{18}F]-FDG PET/CT) was determined and categorized into complete response (CR), partial response (PR), stable disease (STBD) or progressive disease (PD). The absorbed doses in the tumors were determined on the post-treatment ^{166}Ho-SPECT/CT. In the analyses, it was taken into account that the majority of patients had multiple lesions. Analyses were done at both patient- and tumor-level. At both levels, a significant dose-response relationship was established. Also, patients with response (CR or PR) had a significantly longer overall survival than patients without response (median 19 months versus 7.5 months).

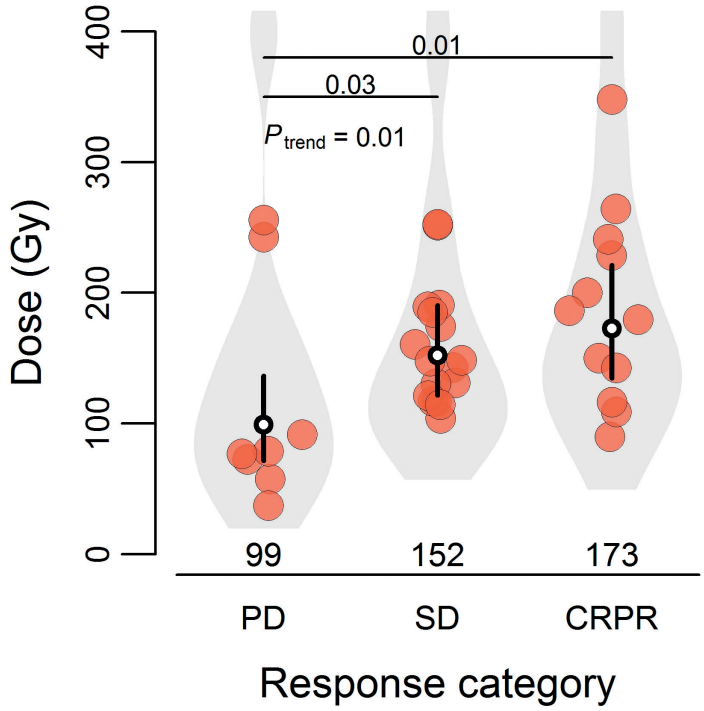

FIGURE 6. Relationship between mean tumor-absorbed dose per patient and metabolic response to treatment at three-months follow-up. The bullets show the mean tumor-absorbed dose per patient. Black vertical lines are the 95%CIs of the mean doses per response category (complete- or partial response CRPR, stable disease SD, progressive disease PD), with the white dot in the middle indicating the mean tumor-absorbed dose per response category.

In chapter 7, the dose-response relation in ^{166}Ho-radioembolization was further analyzed in a homogeneous cohort of 40 mCRC patients. Also, the dose-toxicity relation was explored using the parenchymal-absorbed dose and clinical and laboratory toxicity based on the CTCAE grading system. Again, a significant dose-response relationship was established at both patient- and tumor-level. Using a threshold of 100% sensitivity (meaning that below this dose, no patient had response), a mean tumor-absorbed dose of 90 Gy was identified. This could be used for future treatment planning. Also, a dose-toxicity relation was found: patients with a higher parenchymal-absorbed dose had more toxicity (Figure 7).

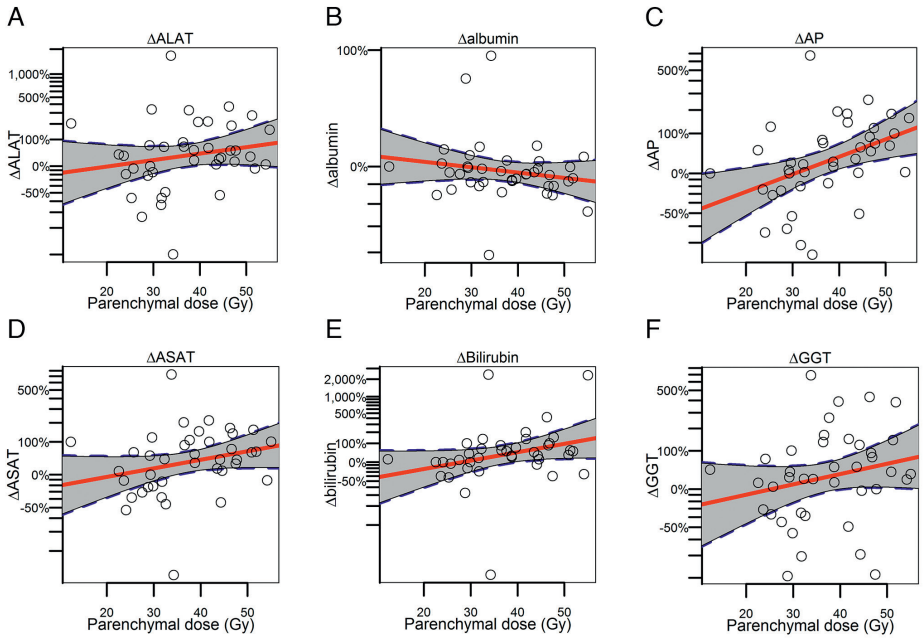

FIGURE 7. Association between change in laboratory parameters and parenchymal absorbed dose. The red lines are the regression lines, with the 95%CIs indicated as the surrounding grey areas.

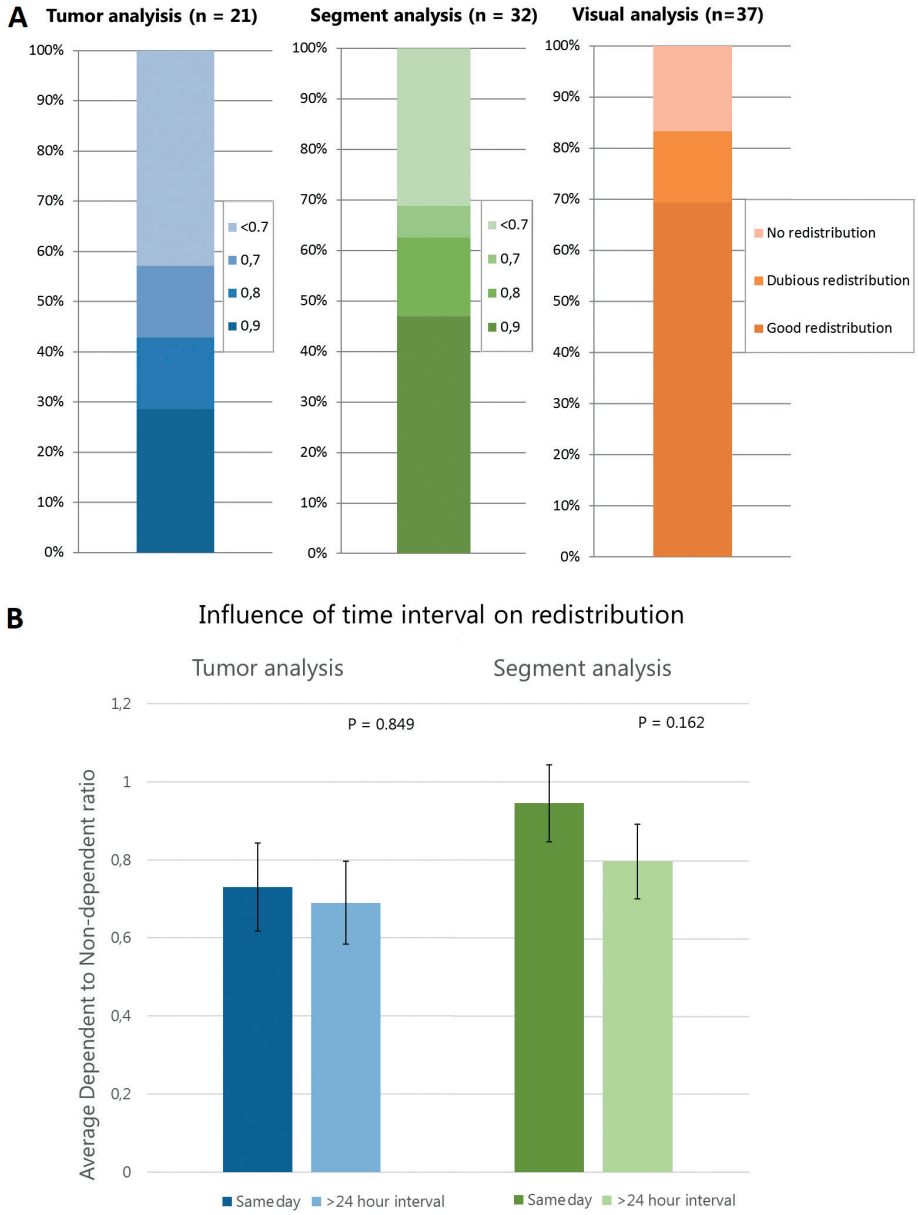

FIGURE 8. Visual representation of the proportion of successful redistribution cases in both the quantitative and the visual analysis. A. In the quantitative analysis, success rate was determined based on cutoff values representing activity concentration differences of 10%, 20%, and 30%. B. Bar chart of the averages in tumor and segment activity ratios for patients treated on the same day after coil embolization versus patients treated after a >24-h interval.

In chapter 8, the effect of coil-embolization of tumor-feeding arteries to obtain intrahepatic redistribution was assessed in 37 patients. This was done both qualitatively and quantitatively, using a visual scale and using the ratio of the activity distribution in the coil-embolized segments/tumors versus the other segments/tumors. In the qualitative analysis, redistribution was deemed successful in 69% of cases. The median activity concentration ratio was 0.88 (range 0.26-2.05) for segments and 0.80 (range 0.19-162) for tumors. Different cutoff values (see figure 8A) were used to determine the percentage of successful cases. For example, using a cutoff value of 0.8 (20% lower activity concentration in the coil-embolized segments than in the other segments), the success rate was 43%. Based on these results, it is recommended to use the redistribution technique only when deemed absolutely necessary.

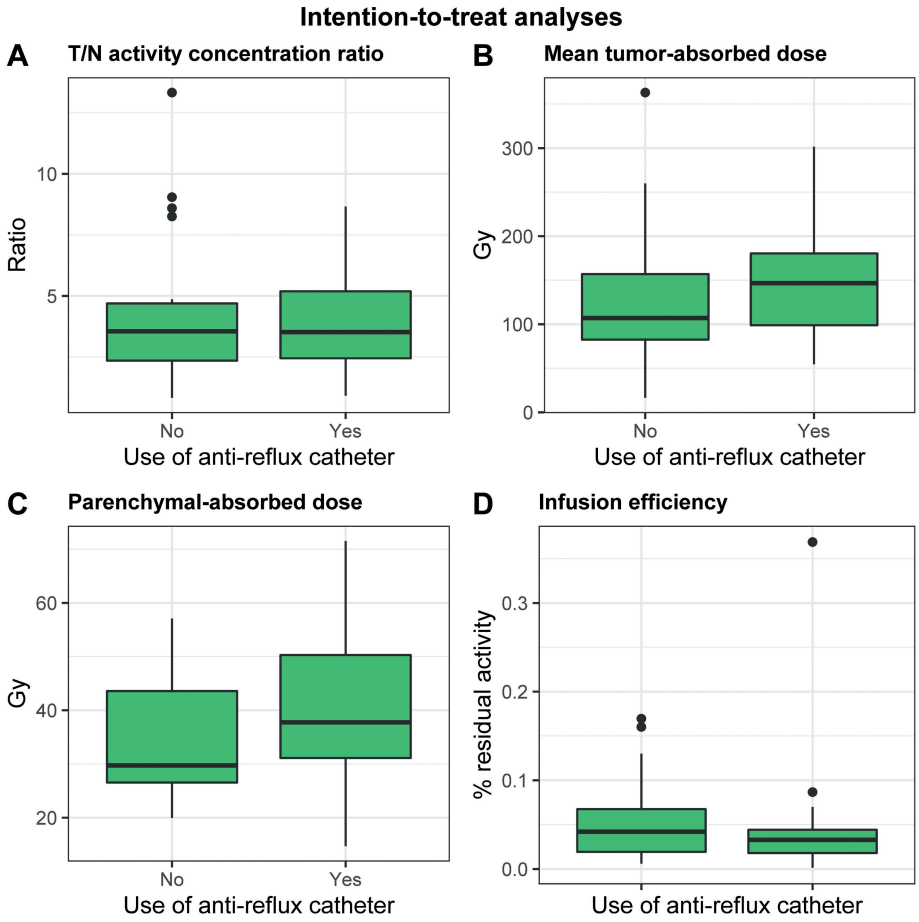

FIGURE 9. Intention-to-treat analyses of effect of anti-reflux catheter on T/N activity concentration ratio (a), mean tumor-absorbed dose (b), mean parenchymal-absorbed dose (c) and infusion efficiency (d).

Chapter 9 describes the results of the SIM study, in which the effect of an anti-reflux catheter on tumor- to non-tumor activity concentration ratio, tumor-absorbed dose, parenchymal-absorbed dose and infusion efficiency was investigated. Twenty-one mCRC patients were treated in this study. The use of the Surefire anti-reflux catheter did not lead to improved tumor targeting (median tumor to non-tumor activity concentration ratio 3.2 versus 3.6 with a standard microcatheter), nor did it lead to improved infusion efficiency (0.04% vs. 0.03% residual activity for the standard microcatheter and anti-

reflux catheter, respectively). Therefore, we do not recommend the use of the Surefire anti-reflux catheter to improve tumor targeting in patients with colorectal metastases.

Nederlandse samenvatting

Dit proefschrift beschrijft de behandeling van patiënten met hepatogeen gemetastaseerd colorectaalcarcinoom met holmium-166 (^{166}Ho) radioembolisatie. De hoofdstukken behandelen verschillende aspecten van deze therapie, die gebruikt kunnen worden voor een gepersonaliseerd behandelplan. Hoofdstuk 3 beschrijft de kwaliteit van leven; dit is met name belangrijk bij oudere patiënten in een palliatief stadium. Hoofdstuk 4 behandelt de voor- en nadelen van behandeling met radioembolisatie op 1 dag. Hoofdstuk 5 gaat over de verschillende soorten respons na radioembolisatie die op kunnen treden en over welke factoren hierop van invloed zijn. Hoofdstukken 6 en 7 beschrijven de relatie tussen dosis en respons: dit is met name belangrijk bij het opstellen van een behandelplan, waarbij de benodigde hoeveelheid radioactiviteit berekend wordt. Hoofdstukken 8 en 9 gaan over twee behandelprocedure-gerelateerde aspecten: het gebruik van coil-embolisatie en het gebruik van een anti-reflux katheter.

FIGUUR 1. Voorbereidingsprocedure in de angiokamer voorafgaand aan behandeling met radioembolisatie.

Hoofdstuk 2 is een uitgebreide samenvatting van de belangrijkste aspecten van radioembolisatie: de indicaties voor behandeling, de verschillende typen microsferen die gebruikt kunnen worden, de methoden om de radioactiviteit te berekenen, de voorbereidingsprocedure, de meest voorkomende bijwerkingen van de behandeling en de respons na behandeling.

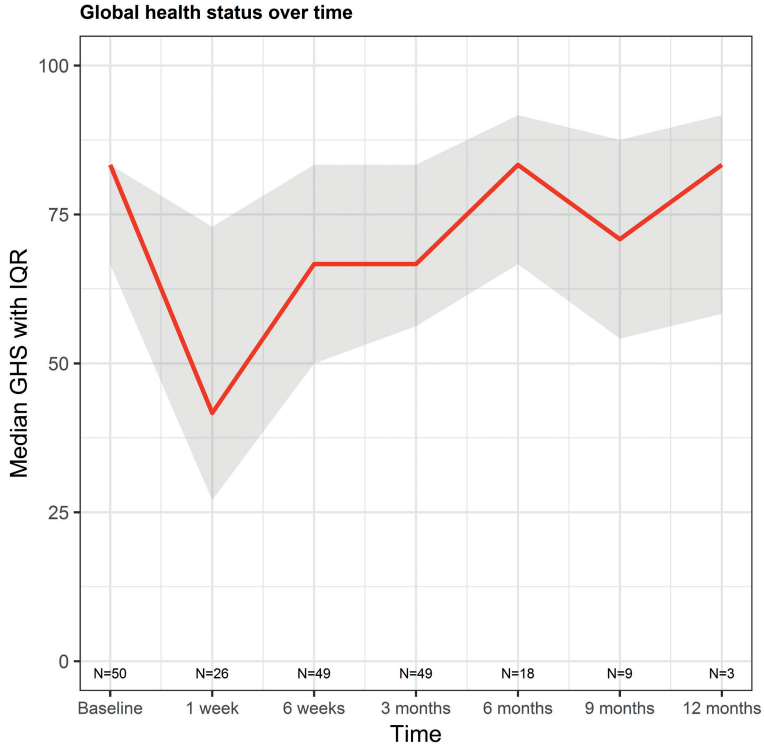

FIGUUR 2. Kwaliteit van leven van patiënten die behandeld zijn met ^{166}Ho-radioembolisatie. GHS – Global Health Status; globale indicatie van de gezondheid (een score van 100 betekent een uitstekende kwaliteit van leven).

Hoofdstuk 3 beschrijft de kwaliteit van leven van 50 patiënten die behandeld zijn met ^{166}Ho-radioembolisatie. De kwaliteit van leven werd geëvalueerd middels twee vragenlijsten: de EORTC QLQ-C30 en de QLQ-LMC21. Deze werden afgenomen bij baseline en vervolgens 1 week, 6 weken, 3, 6, 9 en 12 maanden na behandeling. De vragenlijsten bestaan uit verschillende aspecten, zoals symptomen (bijvoorbeeld pijn, misselijkheid, moeheid) en functioneren (bijvoorbeeld fysiek en sociaal functioneren). De global health status (GHS) was een globale indicatie van de gezondheid en daarmee de kwaliteit van leven. Uit de evaluatie van de vragenlijsten bleek dat de kwaliteit van leven van deze 50 patiënten niet significant veranderde na behandeling met radioembolisatie. Echter, 1 week na behandeling werd een toename in symptomen en een afname van de kwaliteit van leven gezien, wat daarna weer normaliseerde. Dit berust waarschijnlijk op het post-embolisatiesyndroom, dat kort na behandeling ontstaat en vanzelf weer overgaat.

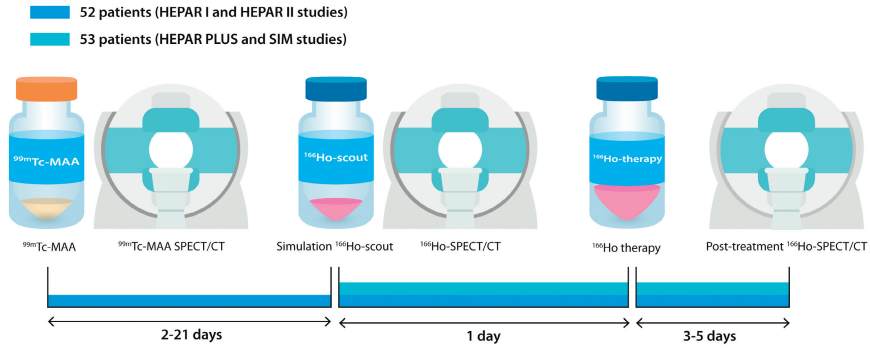

FIGUUR 3. Tijdlijn. Tweeënvijftig patiënten van deze studie ondergingen twee voorbereidingsprocedures; bij de een werd ^{99m}Tc-MAA toegediend en bij de ander ^{166}Ho-scout, volgens het protocol van de HEPAR I en II studies. Drieënvijftig patiënten ondergingen alleen een voorbereidingsprocedure met toediening van ^{166}Ho-scout. Na toediening van ^{166}Ho-scout en de therapeutische dosis ^{166}Ho, werd beeldvorming gedaan middels ^{166}Ho-SPECT/CT om de verdeling van de activiteit te onderzoeken.

In hoofdstuk 4 worden de veiligheid en haalbaarheid van een eendaags behandelprotocol voor ^{166}Ho-radioembolisatie onderzocht. Twaalf procent van de patiënten werd uitgesloten van behandeling op basis van bevindingen van de voorbereidingsprocedure. Bij nog eens 12% van de patiënten werd het behandelplan aangepast op basis van de bevindingen van de voorbereidingsprocedure. De belangrijkste redenen voor exclusie of aanpassing waren extrahepatische depositie van activiteit, de vasculaire anatomie en een suboptimale verdeling van de activiteit (de verdeling van de activiteit binnen de lever, in de tumoren versus het gezonde leverweefsel). Een groot deel van de patiënten (27%) had last van rugpijn na het eendaagse behandelprotocol; waarschijnlijk door de lange liggingsduur. Op basis van deze resultaten wordt behandeling met ^{166}Ho-radioembolisatie op 1 dag alleen aangeraden voor een selecte groep patiënten.

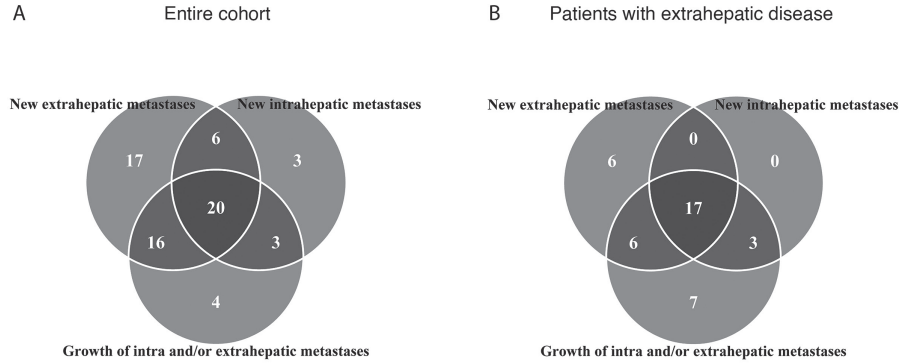

FIGUUR 4. Type progressie van het hele studiecohort (90 patiënten) (a) en specifiek voor patiënten met extrahepatische ziekte bij baseline (b).

In hoofdstuk 5 werd het type progressie 3 maanden na behandeling met radioembolisatie (met ^{166}Ho of ^{90}Y) bepaald volgens RECIST 1.1. Er werd onderscheid gemaakt tussen progressie op basis van groei van bestaande intra- of extrahepatische metastasen en progressie op basis van nieuw ontstane intra- of extrahepatische metastasen. Van de 90 patiënten uit het studiecohort hadden 69 patiënten (77%) progressieve ziekte 3 maanden na behandeling. De overgrote meerderheid (97%) van hen had nieuwe metastasen. Patiënten met extrahepatische ziekte bij baseline hadden een slechtere prognose dan patiënten zonder extrahepatische ziekte: de mediane overleving was 3.5 maanden korter en de kans op progressieve ziekte was bijna 8 keer hoger.

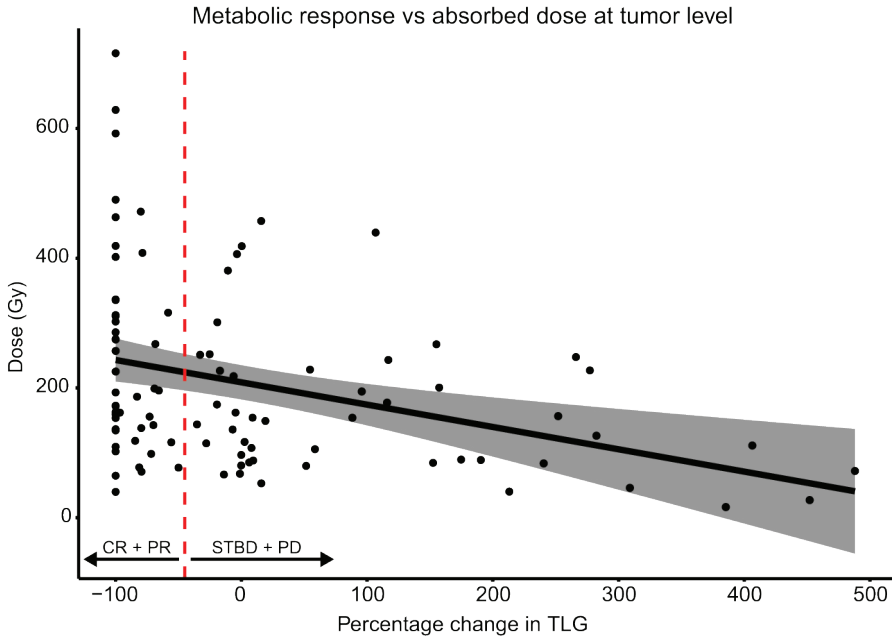

FIGUUR 5. Weergave van de relatie tussen dosis en metabole respons op tumorniveau. Een afname in total lesion glycolysis (TLG) is geassocieerd met een hogere tumordosis. De verticale stippellijn geeft de afkapwaarde voor verandering in TLG weer: links van deze lijn is er sprake van metabole respons (complete of partiele respons) en rechts van deze lijn is er progressie (stabiele ziekte of progressieve ziekte). Het grijze gebied rondom de regressielijn geeft het 95% betrouwbaarheidsinterval weer.

Hoofdstuk 6 is de eerste van twee dosis-respons studies bij ^{166}Ho-radioembolisatie. De relatie tussen dosis en metabole respons werd onderzocht bij 36 patiënten met levermetastasen van verschillende primaire tumoren. Op basis van de verandering in total lesion glycolysis (TLG, een maat voor de activiteit en het volume van een tumor) op [^{18}F]-FDG PET/CT voor en na behandeling werd de metabole respons beoordeeld. De respons werd onderverdeeld in 4 categorieën: complete respons, partiele respons, stabiele ziekte of progressieve ziekte. De dosis werd bepaald op basis van de verdeling van de activiteit op de ^{166}Ho-SPECT/CT na behandeling. Zowel op patiënt- als op tumorniveau werd een significante relatie tussen dosis en respons gevonden. Daarnaast hadden patiënten met complete of partiele respons een significant langere overleving dan patiënten zonder respons (mediane overleving 19 maanden versus 7.5 maanden).

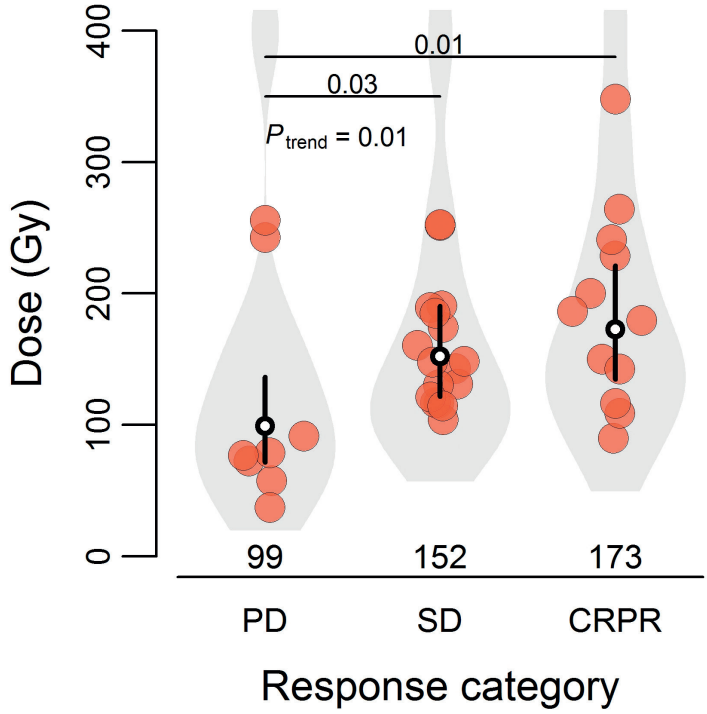

FIGUUR 6. Relatie tussen de metabole respons 3 maanden na behandeling en de gemiddelde tumordosis per patiënt. De rode bollen tonen de gemiddelde tumordosis per patiënt. De zwarte verticale lijnen met de witte stip in het midden tonen de gemiddelde dosis (met 95% betrouwbaarheidsinterval) per responscategorie, met de volgende categorieën: PD=progressieve ziekte, SD=stabiele ziekte en CRPR = complete respons of partiele respons.

In hoofdstuk 7 wordt verder ingegaan op de dosis-respons relatie bij ^{166}Ho-radioembolisatie, specifiek bij patiënten (n=40) met levermetastasen van colorectaalcarcinoom. Daarnaast werd gekeken naar de relatie tussen de dosis op het gezonde leverweefsel en de toxiciteit (zowel aan de hand van verandering in labwaarden als klinische toxiciteit op basis van symptomen). Opnieuw werd een significante dosis-respons relatie vastgesteld. Een drempelwaarde van 90 Gy als gemiddelde tumordosis werd vastgesteld. Dit kan gebruikt worden als richtlijn bij het maken van een behandelplan voor toekomstige patiënten. Daarnaast werd een relatie gevonden tussen de dosis op het gezonde leverweefsel en de toxiciteit: patiënten met een hogere leverdosis hadden meer toxiciteit (zie ook figuur 7).

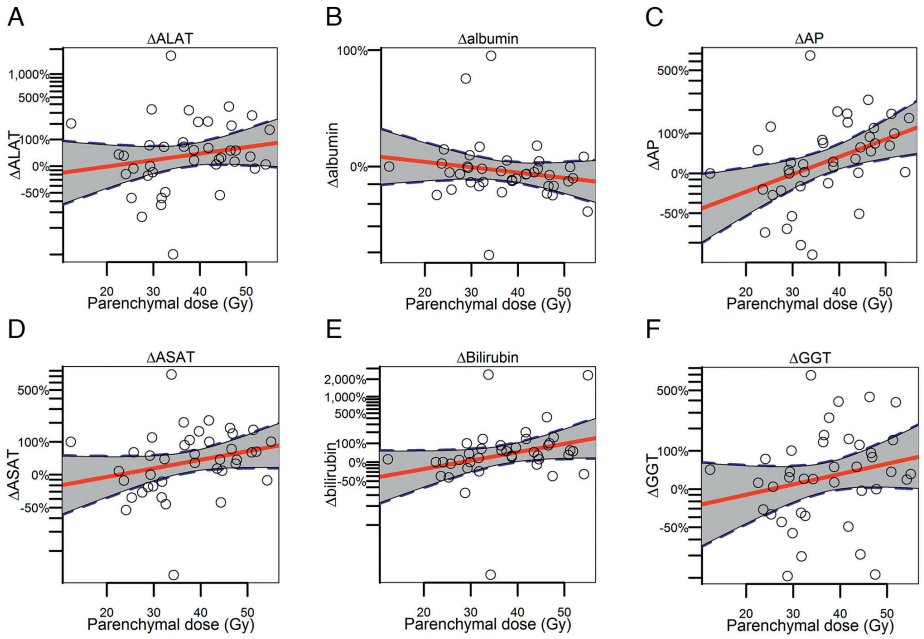

FIGUUR 7. Associatie tussen de verandering in labwaarden en de dosis op het gezonde leverweefsel. De rode lijnen zijn de regressielijnen, met de bijbehorende 95% betrouwbaarheidsintervallen getoond in grijs eromheen.

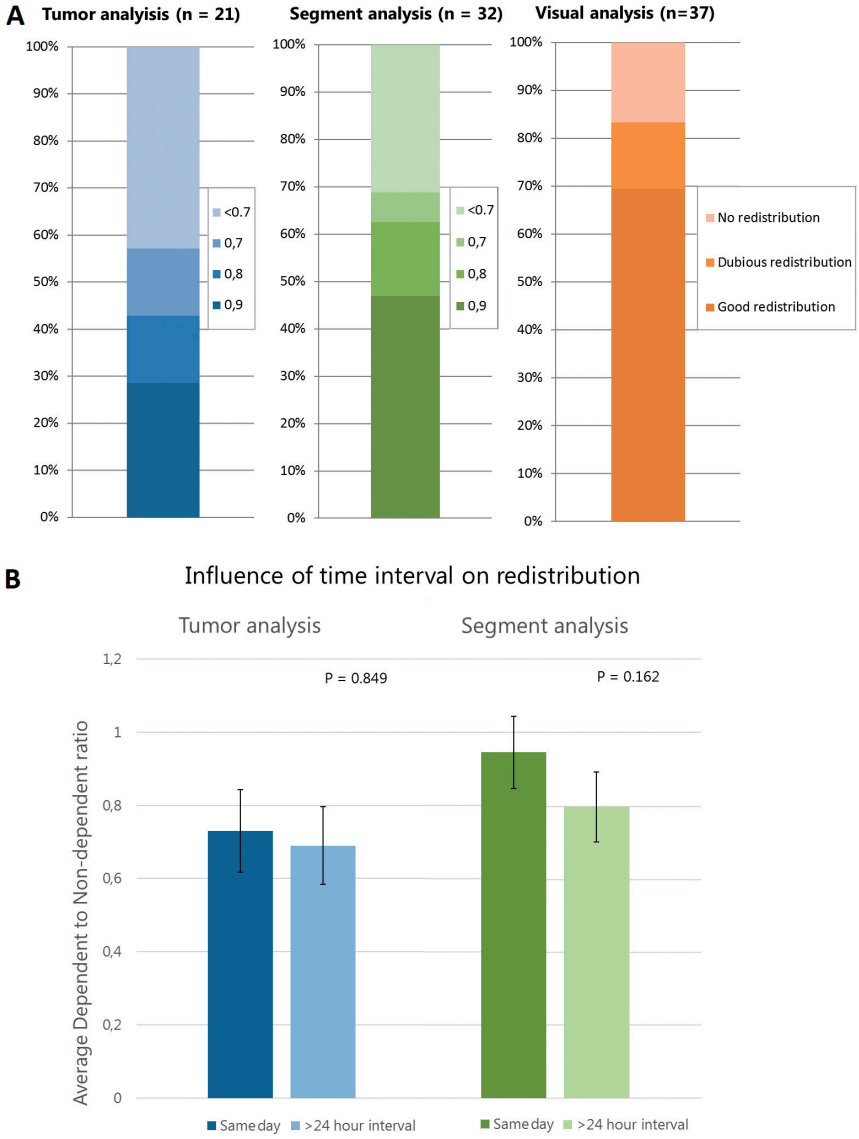

FIGUUR 8. Visuele weergave van het percentage succesvolle redistributie casus; zowel in de kwantitatieve (op tumor- en segmentniveau) als de kwalitatieve analyses. A. In de kwantitatieve analyses werd het succespercentage beoordeeld op basis van verschillende afkapwaarden voor succes: een verschil in activiteit van 10%, 20% of 30% tussen de gebieden die wel/niet afhankelijk waren van redistributie. B. Staafdiagram van de gemiddelde activiteitsratio op tumor- en segmentniveau, weergegeven voor patiënten die op dezelfde dag werden behandeld en voor patiënten waarbij er >24u tijdsverschil was tussen coil-embolisatie en behandeling.

Hoofdstuk 8 beschrijft het effect van coil-embolisatie van tumorvoedende arteriën met als doel intrahepatische redistributie te bewerkstelligen. Dit is zowel kwalitatief als kwantitatief onderzocht in 37 patienten: hierbij werd zowel een visuele schaal gebruikt als de activiteitsratio tussen de segmenten en tumoren die afhankelijk waren van redistributie na coil-embolisatie en de segmenten en tumoren die dat niet waren. In de kwalitatieve analyses werd redistributie in 70% van de casus succesvol geacht. De mediane activiteitsratio was 0.88 voor segmenten en 0.80 voor tumoren. Verschillende afkwapwaarden werden gebruikt om het percentage succesvolle casus te berekenen (zie figuur 8). Bijvoorbeeld bij een afkapwaarde van 0.8 (dus 20% minder activiteit in het leverweefsel dat afhankelijk was van redistributie) was het succespercentage 43%. Op basis van deze resultaten wordt aangeraden om het gebruik van coil-embolisatie om redistributie te bewerkstelligen alleen te gebruiken indien noodzakelijk.

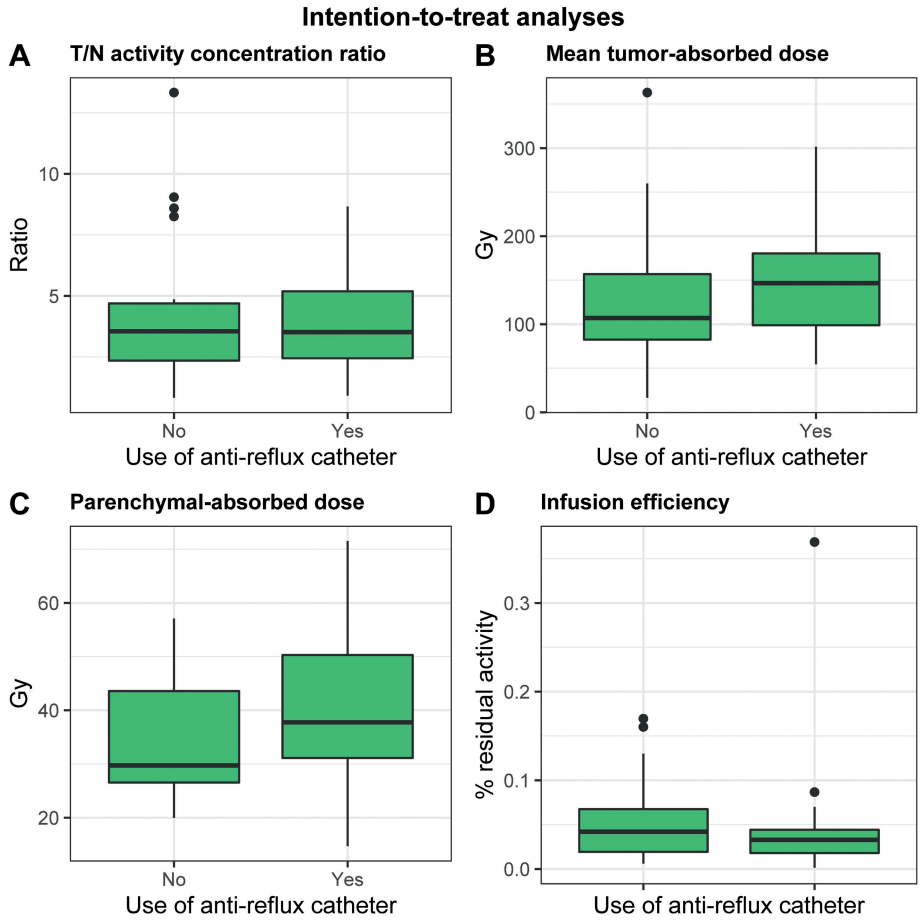

FIGUUR 9. Analyses van het effect van de anti-reflux katheter op de ratio in activiteitsconcentratie tussen tumor- en niet-tumorweefsel (a), de gemiddelde tumordosis (b), de gemiddelde parenchymdosis (c) en de infusie efficiëntie.

Hoofdstuk 9 beschrijf de resultaten van de SIM studie. In de SIM studie werd het effect van een anti-reflux katheter op de verdeling van activiteit in de lever onderzocht. In deze studie werden 21 patiënten met levermetastasen van colorectaalcarcinoom behandeld. Het gebruik van de anti-reflux katheter leidde niet tot een betere tumor targeting (hogere dosis in de tumoren versus het gezonde leverweefsel) of tot een betere infusie van activiteit. Vanwege deze bevindingen wordt het gebruik van een Surefire anti-reflux katheter met als

doel het verbeteren van de tumor targeting bij patiënten met levermetastasen van colorectaalcarcinoom afgeraden.

Addenda

Review committee
List of publications
Dankwoord
Biography

REVIEW COMMITTEE

Prof. dr. I.H.M. Borel Rinkes
Utrecht University, University Medical Center Utrecht, Cancer Center

Prof. dr. O.M. van Delden
Amsterdam University, University Medical Center Amsterdam, Interventional Radiology

Prof. dr. R. Goldschmeding
Utrecht University, University Medical Center Utrecht, Department of Pathology

Prof. dr. O.W. Kranenburg
Utrecht University, University Medical Center Utrecht, Cancer Center

Prof. dr. ir. H.W.A.M. de Jong
Utrecht University, University Medical Center Utrecht, Imaging Division, Medical Physics Group

Chair: prof. dr. I.H.M. Borel Rinkes

LIST OF PUBLICATIONS

What are the odds? Prostate metastases to ureter and peritoneum.
Caren van Roekel, Trudy G.N. Jonges, Tycho M.T.W. Lock
BMJ Case Reports 2018

Is diffusion-weighted MRI really superior to PET/CT in predicting survival after radioembolization?
Remco Bastiaannet, Caren van Roekel, Britt Kunnen, Marnix G.E.H. Lam, Hugo W.A.M. de Jong
Radiology 2018

Hepatobiliary imaging in liver-directed treatments
Caren van Roekel, Margot T.M. Reinders, Sandra van der Velden, Marnix G.E.H. Lam, Manon N.G.J.A. Braat
Semin Nucl Med 2019

Holmium-166 radioembolization of hepatic malignancies
Margot T.M. Reinders, Maarten L.J. Smits, Caren van Roekel, Arthur J.A.T. Braat
Semin Nucl Med 2019

Open epididymal spermatozoa aspiration for obstructive azoospermia
Joost M. Blok, Caren van Roekel, Ralph J.A. Oude Ophuis, Tycho M.T.W. Lock
Andrologia 2019

The efficacy of coil-embolization to obtain intrahepatic redistribution in radioembolization: qualitative and quantitative analyses
Ahmed A. Alsultan, Caren van Roekel, Maarten W. Barentsz, Arthur J.A.T. Braat, Pieter Jan van Doormaal, Marnix G.E.H. Lam, Maarten L..J. Smits
Cardiovasc Interv Radiol 2019

Use of an anti-reflux catheter to improve tumor targeting for holmium-166 radioembolization - a prospective, within-patient randomized study.
Caren van Roekel, Andor van den Hoven, Remco Bastiaannet, Rutger Bruijnen, Arthur Braat, Bart de Keizer, Marnix Lam, Maarten Smits
EJNMMI 2020

First evidence for a dose-response relationship in patients treated with holmium-166 radioembolization: a prospective study
Remco Bastiaannet, Caren van Roekel, Maarten L.J. Smits, Sjoerd G. Elias, Wouter A.C. van Amsterdam, Dan Doan, Jip F. Prince, Rutger C.G. Bruijnen, Hugo W.A.M. de Jong, Marnix G.E.H. Lam
J Nucl Med 2020

Quality of life in patients with liver tumors treated with holmium-166 radioembolization
Caren van Roekel, Maarten L.J. Smits, Jip F. Prince, Rutger C.G. Bruijnen, Maurice A.A.J. van den Bosch, Marnix G.E.H. Lam
Clin Exp Metastasis 2020

Dose-effect relationships of holmium-166 radioembolization in colorectal cancer
Caren van Roekel, Remco Bastiaannet, Maarten L.J. Smits, Rutger C. Bruijnen, Arthur J.A.T. Braat, Hugo W.A.M. de Jong, Sjoerd G. Elias, Marnix G.E.H. Lam
J Nucl Med 2020

Evaluation of the safety and feasibility of same-day holmium-166 radioembolization simulation and treatment of hepatic metastases
Caren van Roekel, Netanja I. Harlianto, Arthur J.A.T. Braat, Jip F. Prince, Andor F. van den Hoven, Rutger C.G. Bruijnen, Marnix G.E.H. Lam, Maarten L.J. Smits
J Vasc Interv Radiol 2020

Stauffer's syndrome: A true entity?
Caren van Roekel, Alexandra S. Bruins Slot, Andre C. Viddeleer, Karel J. van Erpecum, Tycho M.T.W. Lock
Clinics and Research in Hepatology and Gastroenterology 2020

Mode of progression after radioembolization in patients with colorectal cancer liver metastases
Jennifer M.J. Jongen, Caren van Roekel, Maarten L.J. Smits, Sjoerd G. Elias, Miriam Koopman, Onno Kranenburg, Inne H.M. Borel Rinkes, Marnix G.E.H. Lam
EJNMMI Research 2020

DANKWOORD

Allereerst wil ik graag alle proefpersonen en hun familieleden bedanken voor het vertrouwen in ons team. Zonder u was dit onderzoek niet mogelijk geweest.

Prof. dr. Lam, beste Marnix, ontzettend bedankt voor je steun en vertrouwen de afgelopen jaren! Als ik mijn promotie weleens somber in zag, wist je me altijd op te beuren met je immer positieve blik. Je was laagdrempelig bereikbaar voor werk-gerelateerde vragen. Wat ik ook enorm waardeer is hoe positief je reageerde op mijn zwangerschap en dat je zei dat een gezin zo belangrijk is! Ik weet ook nog goed dat je zei dat het wel 6 maanden duurt voordat je weer helemaal 'normaal' functioneert na het krijgen van een kindje. Voor de bevalling dacht ik: welnee, dat doe ik even, hup, ik ben er zo weer. Maar je had gelijk ;-) Heel erg bedankt voor de fijne samenwerking!

Prof. dr. van den Bosch, dank dat u direct uw vertrouwen in mijn kunnen uitsprak door mij na mijn coschap Radiologie aan te nemen voor deze onderzoekspositie. U vertrouwde erop dat ik ook na een aantal jaar onderzoek de radiologie nog leuk zou vinden, wat gelukkig ook zeker zo is!

Dr. Smits, beste Maarten, dankjewel voor je altijd zeer snelle, grondige en waardevolle feedback! Zo fijn dat je de tijd nam om samen stukken door te nemen. Ik bewonder je gedrevenheid en inzet enorm en ik heb heel veel van je geleerd! Leuk dat we elkaar nu weer zien op de werkvloer. Ik waardeer heel erg hoe je me (ook nu nog) begeleidt.

Dr. Braat, beste Arthur, wat fijn dat je er altijd was om ons te helpen en op te beuren. Met al onze vragen konden we bij je terecht. Je doorzettingsvermogen en altijd goede humeur zijn een voorbeeld!

Lieve Margot, wat heb ik ervan genoten om met je samen te werken! We gingen steeds samen op, deelden al veel ervaringen op werk en na onze zwangerschappen deelden we ook veel baby-vreugde ☺ Ik heb heel veel van je geleerd, qua werk maar ook van hoe je in het leven staat. Ik ben heel blij dat

we elkaar hebben leren kennen en hoop je nog veel te blijven zien. Je bent een heel lieve vriendin! Ontzettend bedankt voor alles!

Ha Frans! Wat was het gezellig met jou op de kamer! Je was altijd de rustig aanwezige, stabiele factor, en vaak ook de redder in nood met altijd goede tips qua statistiek. Heel veel succes bij de neurologie, ik ben ervan overtuigd dat je een even goede neuroloog zult worden als dat je onderzoeker was!

Remco Bastiaannet, we hebben veel samengewerkt, jouw technische kennis en mijn klinische blik vulden elkaar mooi aan. Bedankt voor al je hulp bij onze projecten! En ik hoop dat je een heel goede tijd zult hebben in de VS.

Collega's van het trialbureau, Saskia, Tjitske, Shanta, Ramona en Cees: waar was ik geweest zonder jullie. Saskia, al snel nadat ik begonnen was, kwam er monitorvisite van de SIM studie. Ik had geen idee wat te doen, zonder jou was het nooit goed gekomen. Allen heel erg bedankt voor al jullie hulp de afgelopen jaren!

Radioembolisatie team: Rutger Bruijnen, Bart de Keizer, verpleegkundigen, laboranten: bedankt voor jullie hulp bij de SIM studie! Heel fijn dat jullie altijd zo jullie best deden voor zowel de patiënten als de studie. En het was altijd gezellig om op de angiokamer te zijn!

Christiaan van Kesteren, ontzettend bedankt voor al je hulp met het maken van figuren! Je hebt veel mooie figuren gemaakt, fijn dat je ook vaak op korte termijn wilde helpen.

Dr. Elias, beste Sjoerd, zo fijn hoe je me geholpen hebt met mijn projecten en de epidemiologie master! Ondanks je enorm drukke bestaan heb je steeds tijd voor me gemaakt en gaf je altijd nuttige tips en feedback. Het was fijn om met je samen te werken, ik vond het ook leuk om je te spreken!

Dr. Lock, met u en dr. Viddeleer is het onderzoek doen ooit allemaal begonnen! Dank voor uw wijze lessen, leuke verhalen en hulp! En voor uw nimmer aflatende aanmoedigingen en vertrouwen.

Beste collega's van het stafsecretariaat: jullie ook heel erg bedankt voor jullie hulp de afgelopen jaren, vooral aan het begin met alles wat geregeld moest worden in mijn opstartfase als zeker ook nu, Carin, met alle afrondende zaken!

Lieve (ex-) collega's: Annemarie, Wieke, Josanne, Suzanne, Bianca, Wouter, Jonas, Ahmed, Esmee, Justine, Liselore, Sander, Ludwike, Marilot, Mimount, Carlo, Floor, Marcia, Sarah, Martina en Nienke: bedankt voor de gezelligheid van de afgelopen jaren, de gezamenlijke etentjes, lunchwandelingen, hulp, adviezen en spontane gezelligheid op onze kamer (met dank aan de snoeppot ;-)): ik zal jullie missen!

Lieve huidige collega's, bedankt dat jullie me zo fijn opgenomen hebben in jullie groep. Ik voelde me meteen welkom en waardeer het dat ik altijd met mijn vragen bij jullie terecht kan.

Leden van de beoordelingscommissie, prof. dr. Borel Rinkes, prof. dr. Van Delden, prof. dr. Goldschmeding, prof. dr. Kranenburg en prof. dr. De Jong, ik ben u dankbaar dat u de tijd heeft genomen om mijn proefschrift te beoordelen.

Lieve vriendinnen: Alida, Corine, Doena, Eline, Hanneke, Helma, Jola, Jolien, Josine, Martina, Mieke, Rieneke en Theodora, dank voor jullie gezelschap de afgelopen jaren! En voor jullie begrip als ik weinig tijd had. Ik ben heel blij met onze vriendschap en ik hoop dat we elkaar nog veel zullen blijven zien, ook nu we allemaal steeds meer ons eigen leven (soms heel ver van elkaar) leiden!

Hannah, lief zusje, ik ben zo blij dat we het zo leuk hebben samen! Het is altijd fijn om bij je te zijn en je bent zo lief en leuk! Ik ben heel trots op je!

Lieve papa en mama, ik ben zo dankbaar voor jullie. Jullie staan altijd voor ons klaar en helpen ons zoveel! Mama, het is zo fijn dat ik altijd bij je terecht kan, met alle grote en kleine zorgen. Bedankt ook dat je steeds zoveel oppast, Juliette en jij zijn dol op elkaar; het is heel fijn om haar bij jou achter te kunnen laten! Ik ben heel blij met ons gezin en ik ben heel trots op jullie! Ook op jullie Rens en Derk, beste broeders :-)

Jan Willem, liefste man. Bedankt voor al je geduld en hulp in de afgelopen jaren. Ik ben heel gelukkig met je! En ik vind dat je een fantastische vader bent voor onze prachtige dochter Juliette. Samen zijn we zo'n fijn gezin, ik hoop dat we dat in de komende jaren, met alle veranderingen door de opleiding etc., zullen blijven! En ik zie uit naar de komst van ons tweede kindje!

Bovenal dank aan God, Schepper en Onderhouder van het leven.

BIOGRAPHY

Caren van Roekel was born in Tiel on October 21st, 1990. After graduating from Van Lodenstein College (Amersfoort, The Netherlands), she studied French languages and culture for one year.

Afterwards, she studied Medicine at Utrecht University. In October 2016, she started her PhD with the subject of radioembolization with holmium microspheres for patients with colorectal cancer metastases under the supervision of prof. dr. Marnix Lam and dr. Maarten Smits. She also finished her post-graduate master Epidemiology. In April 2020, she started as a resident in Radiology at the University Medical Center Utrecht.